

The  
University  
Of  
Sheffield.

# Metabolic mechanisms for the evolution of stable symbiosis

Megan Elisabeth Stig Sørensen

A thesis submitted for the degree of  
Doctor of Philosophy

University of Sheffield  
Department of Animal and Plant Sciences

September 2019



# Abstract

Endosymbiosis involves the merger of once independent organisms; this evolutionary transition has defined the evolutionary history of eukaryotes and continues to underpin the function of a wide range of ecosystems. Endosymbioses are evolutionarily dynamic because the inherent conflict between the self-interest of the partners make the breakdown of the interaction ever-likely and this is exacerbated by the environmental context dependence of the benefits of symbiosis. This necessitates selection for partner switching, which can reshuffle the genetic identities of symbiotic partnerships and so rescue symbioses from cheater-induced extinction and enable rapid adaptation to environmental change. However, the mechanisms of partner-specificity, that underlie the potential for partner switching, are unknown. Here I report the metabolic mechanisms that control partner specificity within the tractable microbial photosymbiosis between *Paramecium bursaria* and *Chlorella*. I have found that metabolic function, and not genetic identity, enables partner-switching, but that genetic variation plays an important role in maintaining variation in symbiotic phenotype. In addition, I observed that symbiont stress-responses played an important role in partner specificity, and that alleviating symbiont stress responses may be an important strategy of generalist host genotypes. Furthermore, I have used experimental evolution to show that a novel, initially non-beneficial association can rapidly evolve to become a beneficial symbiosis. These results demonstrate that partner integration is defined by metabolic compatibility and that initially maladapted host-symbiont pairings can rapidly evolve to overcome their lack of co-adaptation through alterations to metabolism and symbiont regulation. Understanding the process of novel partner integration and partner switching is crucial if we are to understand how new symbioses originate and stabilise. Moreover, mechanistic knowledge of partner switching is required to mitigate the breakdown of symbioses performing important ecosystem functions driven by environmental change, such as in coral reefs.

# List of Contents

Abstract	3
List of Figures	6
List of Tables	8
Acknowledgements	9
Declaration	10
Chapter 1 – <i>Introduction</i>	11
1.1 The Organelles	12
1.2 Secondary Endosymbioses	14
1.3 The parasitism-mutualism continuum	15
1.4 Evolution of partner dependency	17
1.5 Conflict avoidance	19
1.6 Ecology and Physiology of the <i>P. bursaria</i> – <i>Chlorella</i> endosymbiosis	20
1.7 Genetics of the <i>P. bursaria</i> – <i>Chlorella</i> endosymbiosis	26
1.8 Thesis Outline	29
Chapter 2 – <i>Comparison of independent evolutionary origins reveals both convergence and divergence in the metabolic mechanisms of symbiosis</i>	31
2.1 Introduction	31
2.2 Materials and Methods	33
2.3 Results	39
2.4 Discussion	51
2.5 Supplementary Figures	56
2.6 Supplementary Results	61
Chapter 3 – <i>Light-dependent stress-responses underlie host-symbiont genotypic specificity in a photosymbiosis</i>	62
3.1 Introduction	62
3.2 Materials & Methods	65
3.3 Results	68
3.4 Discussion	81
3.5 Supplementary Figures	87
3.6 Supplementary Tables	91

Chapter 4 – <i>A novel host-symbiont interaction can rapidly evolve to become a beneficial symbiosis</i>	93
4.1 Introduction	93
4.2 Materials and Methods	95
4.3 Results	98
4.4 Discussion	105
4.5 Supplementary Tables	110
Chapter 5 – <i>Discussion</i>	114
5.1 Stress and symbiosis	115
5.2 Partner Switching	116
5.3 Rapid evolution enables the establishment of symbiosis	118
5.4 Applications of endosymbiosis research	119
5.5 Future-directions	120
5.6 In conclusion	121
Appendix A – The review paper linked to Chapter 1	123
Appendix B – Statistical outputs for Chapter 2	131
Appendix C – Statistical outputs for Chapter 3	134
Appendix D – Statistical outputs for Chapter 4	137
Bibliography	139

# List of Figures

1.1	Diagrammatic representation of the fitness interactions within endosymbioses	16
1.2	Diagrammatic representation of the <i>P. bursaria</i> - <i>Chlorella</i> endosymbiosis	22
1.3	The consequence of symbiosis for each partner	25
2.1	Correlated metabolite enrichment for the 186b and HA1 <i>P. bursaria</i> and <i>Chlorella</i> strains over time	40
2.2	Fitness of the native and non-native host-symbiont pairings relative to isogenic symbiont-free hosts	44
2.3	Difference in <i>Chlorella</i> global metabolism between strains across light conditions	45
2.4	Difference in <i>P. bursaria</i> global metabolism between strains across light conditions	48
2.5	Photophysiology measurements for the native and non-native host-symbiont pairings	51
S2.1	PCR result of the HA1 and 186b <i>Chlorella</i> strains	56
S2.2	Schematic pathways diagram of nitrogen enrichment in the arginine amino acid metabolism of the <i>Chlorella</i> metabolic fraction	57
S2.3	Schematic pathways diagram of nitrogen enrichment in other aspects of amino acid metabolism in the <i>Chlorella</i> metabolic fraction	58
S2.4	Schematic pathways diagram of nitrogen enrichment in purine metabolism in the <i>Chlorella</i> metabolic fraction	59
S2.5	The interaction of light intensity and strain identity on the $^{13}\text{C}$ enrichment profile of carbohydrate metabolites from the <i>P. bursaria</i> fraction.	60
3.1	Conceptual diagrams of potential outcomes when comparing native and non-native host-symbiont pairings	64
3.2	Initial growth rates of the host-symbiont pairings across a light gradient	69
3.3	Symbiont load of the host-symbiont pairings across a light gradient	70
3.4	The clustering of the metabolic fractions by light	72
3.5	Clustering patterns of the <i>Chlorella</i> metabolic fraction subset by host-genotype	73

3.6.	Differences in the <i>Chlorella</i> metabolism between symbiont genotypes at multiple light levels within the 186b <i>P. bursaria</i> host	75
3.7.	Relative abundances of dark-stress associated metabolites across host genotypes in the dark	80
3.8.	Relative abundances of a high-light stress associated metabolite across host genotypes and across light levels	81
S3.1.	PCR confirmation of symbiont-genotype within the reciprocal cross infections	87
S3.2.	The clustering of the metabolic fractions by light in PCA plots	88
S3.3.	Separation by symbiont-genotype within the 186b host subset of the <i>Chlorella</i> metabolic fraction	89
S3.4.	Shared response of <i>Chlorella</i> genotypes to light intensity in the <i>Chlorella</i> metabolic fraction	90
4.1.	Weekly growth rates of the native and novel symbioses across the evolution experiment	98
4.2.	Growth rate assays performed at multiple points throughout the evolution experiment	99
4.3.	Symbiont load at the start and end of the evolution experiment	100
4.4.	Fitness of the host-symbiont pairings relative to the symbiont-free host at the start and end of the evolution experiment	101
4.5.	The trajectories of the metabolic profiles from the start to the end of the evolution experiment.	103
4.6.	Metabolites of interest across the start and end of the evolution experiment within the <i>P. bursaria</i> fraction.	104
4.7.	Metabolites of interest across the start and end of the evolution experiment within the <i>Chlorella</i> fraction.	105

# List of Tables

2.1	$^{15}\text{N}$ enriched metabolites of the <i>Chlorella</i> fraction	41
2.2	$^{13}\text{C}$ enriched metabolites of the <i>P. bursaria</i> fraction	42
2.3	The identified metabolites of interest from the <i>Chlorella</i> global metabolism.	46
2.4	The identified metabolites of interest from the <i>P. bursaria</i> global metabolism.	49
3.1	Symbiont-genotype specific metabolites in the dark within the 186b <i>P. bursaria</i> host	76
3.2	Symbiont-genotype specific metabolites in the intermediate light within the 186b <i>P. bursaria</i> host	77
3.3	Symbiont-genotype specific metabolites in the high light within the 186b <i>P. bursaria</i> host	78
S3.1	Light-level associated shared <i>Chlorella</i> metabolites across the host and symbiont genotypes.	91
S4.1	Identified metabolites associated with PCA trajectories for the <i>P. bursaria</i> fraction.	110
S4.2	Identified metabolites associated with PCA trajectories for the <i>Chlorella</i> fraction	112
S4.3	Change in symbiont load for each HK1 replicate between the start and end of the evolution experiment	113

# Acknowledgements

First and foremost, I would like to thank my supervisors Michael Brockhurst, Duncan Cameron and A. Jamie Wood for making this project possible and extremely enjoyable. I have learnt a lot over the course of this PhD and it is due to their analytical guidance, which has taught me, among many things, an appreciation of the elegance of good research.

I would like to thank Ewan Minter for establishing many of the techniques used in this project and for taking the time to teach these to me. I also wish to thank Chris Lowe for his role in establishing this project and especially for his help while I conducted work in Falmouth.

I would like to thank Heather Walker for her technical expertise and help with the mass spectrometry.

I am grateful to the BBSRC White Rose DTP program for funding my PhD.

To the Brockhurst lab group, thank you for creating a culture that is scientifically exciting, supportive and fun. In particular, thank you to Ellie Harrison and Jamie Hall for your guidance and support. A special thank you to fellow officemates Cagla, Rosanna & Rachael whose friendship I value tremendously.

Lastly to my family, Mor, Far & Kim, you have been a constant source of support and inspiration, and thank you for always being willing to listen to how the algae was doing.

# Declaration

I, the author, confirm that the Thesis is my own work. I am aware of the University's Guidance on the Use of Unfair Means ([www.sheffield.ac.uk/ssid/unfair-means](http://www.sheffield.ac.uk/ssid/unfair-means)). This work has not been previously been presented for an award at this, or any other university.

The following publications have arisen from this thesis:

- Sørensen, M.E.S., Lowe, C.D., Minter, E.J.A., Wood, A.J., Cameron, D.D., and Brockhurst, M.A. (2019). The role of exploitation in the establishment of mutualistic microbial symbioses. *FEMS Microbiol Lett* *366*.
- Sørensen, M.E.S, Wood, A.J., Minter, E.J., Lowe, C.D., Cameron, D.D., and Brockhurst, M.A. (2020). Comparison of independent evolutionary origins reveals both convergence and divergence in the metabolic mechanisms of symbiosis. *Current Biology*.

Parts of chapter 1 are adapted from Sørensen et al. (2019), and the work in chapter 2 was published as Sørensen et al. (2020) following the submission of this thesis.

# Chapter 1

## Introduction

*Parts of this chapter are adapted from a publication - The role of exploitation in the establishment of mutualistic microbial symbioses (Sørensen et al., 2019) (see Appendix A).*

Endosymbiosis is the most intimate form of symbiosis, and therefore of interspecies interaction, as two unlike organisms live together with one organism residing within the cells of the other (De Bary, 1879). Endosymbioses can accelerate evolutionary innovation through the merger of once independent lineages, providing species with new ecological traits and allowing them to inhabit previously inaccessible ecological niches (Kiers and West, 2015; Wernegreen, 2012). The establishment of endosymbiosis can constitute a ‘major evolutionary transition’ (Szathmáry and Smith, 1995) in that previously autonomous entities merge, become mutually dependent, and form a new individual (Estrela et al., 2016; West et al., 2015). Endosymbiotic interactions include a vast array of diverse relationships across the three domains of life, and their formation has had extensive consequences for both the evolutionary history of life on Earth and its current ecological function. The primary endosymbiotic events that formed the mitochondria and plastids have shaped the evolution of eukaryotes and arguably enabled the emergence of complexity (Keeling, 2010; Martin et al., 2015). Ecologically, endosymbioses occur throughout the eukaryotic tree of life (Archibald, 2009) and by virtue of their adaptive evolutionary innovation, these associations often occupy keystone positions in ecosystems (Zook, 2002); for instance, plant-mycorrhizal associations form the main producers in most terrestrial ecosystems (Powell and Rillig, 2018), and coral-dinoflagellate associations form the foundation of coral reef ecosystems (Baker, 2003; Stanley and Lipps, 2011).

Transitions in individuality are, however, fraught with evolutionary conflict, and the merger of two independent organisms is rarely seamless and never selfless. Symbiosis encompasses a broad range of species interactions, including both parasitism (+/- fitness interactions) and mutualism (+/+ fitness interactions). Whilst the evolutionary rationale for parasitism is straightforwardly explained by the self-interest of the parasitic partner, explaining the origin of mutualistic symbiosis is more challenging (Frank, 1997; Sachs et al., 2004). The immediate fitness gains of cheating are expected to outweigh the potential long-term fitness benefits of cooperation, producing a ‘tragedy of the commons’ (Hardin, 1968; Rankin et al., 2007). Therefore, both in long-established associations and in the establishment of new relationships, evolutionary conflict and breakdown of mutualistic

symbiosis is ever likely, since each partner is under selection to minimise its investment in the integrated symbiotic unit (Perez and Weis, 2006; Sachs and Simms, 2006). Nevertheless, mutualistic symbiotic relationships are abundant, taxonomically widespread, ecologically important in a wide range of habitats, economically important in agricultural systems, and consequently underpin the biodiversity and function of both natural and man-made ecosystems (Bronstein, 2015; Powell and Rillig, 2018). It is the prevalence of mutualism in the face of evolutionarily conflict that fascinates researchers, and the mechanisms of mutualism maintenance continues to be a developing research area (Archetti et al., 2011; Douglas, 2008; Werner et al., 2018).

This introduction will briefly discuss the organelles as examples of the highest level of integration that endosymbionts have yet acquired, before focusing on secondary endosymbioses and their evolutionary dynamics. It then focuses on the endosymbiotic relationship between *Paramecium bursaria* and *Chlorella*, which provides a tractable experimental system for studying the evolution of endosymbiosis and is the focus of the experiments in this thesis. Finally, I outline the following data chapters and the questions they address.

### 1.1 The Organelles

The organelles, the mitochondria and plastids, arose from primary endosymbiotic events that have subsequently shaped the course of life history (Keeling, 2010; Martin et al., 2015). The bacterial ancestry of the organelles was first proposed by Konstantin Mereschkowski (1905) and later championed by Lynn Margulis (1967), but remained controversial until molecular techniques became sufficiently advanced to provide unequivocal supporting evidence (Bonen and Doolittle, 1975; Schwarz and Kössel, 1980). Crucially, Bonen and Doolittle (1975) compared rRNA sequences between algal plastids and cyanobacteria to demonstrate the prokaryotic origin of these eukaryotic organelles, and shortly after, mitochondrial rRNA was also shown to be prokaryotic (Bonen et al., 1977). These results combined with an accumulated wealth of cytological, physiological and biochemical data (Dodson, 1979; Stanier, 1970) led to the acceptance of the serial endosymbiotic theory (Gray and Doolittle, 1982). Both mitochondria and chloroplast genomes are incredibly reduced, retaining a small fraction of their original complement of genes. They represent a very rare and highly derived subset within endosymbioses (Cavalier-Smith, 2013).

Mitochondria formed from  $\alpha$ -proteobacteria endosymbionts within an archaeal host (Rivera and Lake, 2004; Spang et al., 2015), and this association led to the formation of the

eukaryotic domain of life (Martin et al., 2015). Despite forming circa 1.5 BYA, mitochondria are remarkably persistent and though they have been reduced to hydrogenosomes on multiple occasions (Allen et al., 2003), only in one instance have they ever been truly lost. This instance was facilitated by lateral gene transfer that enabled the nucleus to gain full metabolic independence (Karnkowska et al., 2016). Mitochondria are integrated with their hosts at an exquisite level of detail, to the extent that the complexes in their respiratory chain are a mosaic of proteins encoded in both the mitochondria and nucleus (Schatz and Mason, 1974).

Plastids, in comparison, are more transitory, and though stable organelles, their distribution throughout the eukaryotes is a complex mixture of acquisition, loss and replacement (Keeling, 2010). Plastids evolved from an endosymbiosis between a eukaryotic host and a cyanobacterium over a billion years ago that established photosynthesis in the eukaryotes (Dyall et al., 2004; Parfrey et al., 2011). Subsequently, multiple secondary endosymbioses, in which a eukaryotic host engulfs a plastid-bearing alga, spread plastids across the eukaryotic tree of life (Archibald, 2009; Keeling, 2013). The exact identity of these secondary endosymbioses is still being untangled, but what is certain is, unlike with mitochondria, plastid loss has happened on numerous occasions (Gornik et al., 2015). Furthermore, serial symbiont replacement appears to have occurred and the ‘shopping bag model’ hypothesises that the replaced symbiont can have transferred genes to the host leading to a complement of endosymbiont genes from mixed origins (Larkum et al., 2007; Patron et al., 2006). The complicated story of secondary gains and losses of plastids paints a far more fluid picture than that of mitochondria acquisition and is more representative of endosymbiosis as a whole; the relationship is maintained when necessary but lost when it is no longer advantageous.

Intriguingly, there has been a recent, 60-200 million years old (Berney and Pawlowski, 2006; Nowack et al., 2008), independent primary endosymbiosis — the eukaryote host *Paulinella chromatophora* acquired a cyanobacterial *Synechococcus* endosymbiont in a process that recapitulates the original evolution of the plastid (Marin et al., 2005; Nowack, 2014). The definition of an organelle currently requires protein import of a transferred gene back into the endosymbiont/organelle and this has not yet been conclusively demonstrated within the *P. chromatophore* endosymbiosis. Nonetheless, this relationship blurs the distinction between endosymbiont and organelle and has led many to question whether the current distinction between organelles and endosymbionts is meaningful. Or if, in fact, such

derived and integrated associations are already functionally equivalent to organelles (Bhattacharya and Archibald, 2006; Bodył et al., 2007; Keeling and Archibald, 2008).

### 1.2 Secondary Endosymbioses

Organellogenesis is a special case of endosymbiosis, yet endosymbiosis more generally is a common evolutionary stable strategy with important evolutionary and ecological consequences. Endosymbiosis occurs between unrelated species, including between species that belong to different domains of life, and arguably the less related the partners are the greater the potential for acquisition of novel ecological traits (Douglas, 2014; Wernegreen, 2012). Eukaryote-bacteria endosymbioses are particularly common and span a wide range of functions and environments. For example: the chemoautotrophic endosymbionts of the giant worm *Riftia pachyptila* enable life at deep sea vents (Cavanaugh et al., 1981); the defensive *Rickettsiella* endosymbionts of pea aphids decrease predation (Tsuchida et al., 2010); the *Nardonella* endosymbionts cause cuticle hardening in weevils (Anbutsu et al., 2017); and *Vibrio fischeri* within Bobtail squid produce luminescence (McFall-Ngai and Ruby, 1998). Less common, and also less studied, are eukaryote-archaea endosymbioses; the majority of which have been observed within protist hosts, in particular many anaerobic ciliates possess methanogen archaea endosymbionts (van Hoek et al., 2000). Within-domain endosymbiosis can also introduce biological innovation. Eukaryote-eukaryote endosymbioses include the secondary acquisition of plastids that had spread photosynthesis across the eukaryotic taxons (Lane and Archibald, 2008) and the many endosymbioses between algae and animals, such as corals, sponges and cnidaria (Venn et al., 2008). Prokaryote-prokaryote endosymbioses are very rare, and to date have only been documented in nested endosymbiosis, such that the prokaryote host is itself an endosymbiont of an eukaryote. For instance, the mealybug *Planococcus citri* houses  $\beta$ -Proteobacteria that in turn houses  $\gamma$ -Proteobacteria (Dohlen et al., 2001). The scarcity of prokaryote-prokaryote endosymbioses, as opposed to their many ectosymbioses and syntrophic consortiums, is believed to be because of the absence of phagocytosis in prokaryotes (López-García et al., 2017).

Endosymbioses provide a multitude of functions, including the production of antibiotics (Currie et al., 1999), luminescence (Tebo et al., 1979), photoprotection (Hörtnagl and Sommaruga, 2007), and defence against predation and parasitism (Tsuchida et al., 2010). Nutritional endosymbioses are, however, the most common and show a higher degree of dependence when compared to defensive symbioses (Fisher et al., 2017). Nutritional endosymbioses occur across a broad range of taxa and can lead to highly integrated

metabolism, in which one biochemical pathway requires the complementation of enzymes from both partners. A classic example are aphids and their obligatory endosymbiont *Buchnera aphidicola*, which share the synthesis of the essential amino acids between them (Moran et al., 2003; Wilson et al., 2010).

Photosymbioses are associations where microalgae live within a heterotrophic host and therefore enable mixotrophy (Decelle, 2013). The transition to mixotrophy represents a fundamental shift in nutritional strategy that combines the roles of producer and consumer (Esteban et al., 2010; Stoecker et al., 2009), and consequently these associations often have important roles in ecosystems (Stanley and Lipps, 2011). These relationships are based on the transfer of fixed carbon from the photosynthetic partner in exchange for nitrogen and/or phosphate. Photosymbioses are extremely common and occur in a range of organisms, including a wide range of unicellular, protist hosts (Keeling, 2013; Stoecker et al., 2009) and multicellular organisms (Venn et al., 2008). Examples include: cyanobacteria and fungi in types of lichen (Honegger, 1991), haptophytes and Acantharia protist hosts (Decelle, 2013) and dinoflagellates and cnidarian in corals (Yellowlees et al., 2008).

### *1.3 The parasitism-mutualism continuum*

The fitness outcome of a symbiosis is determined by the balance of cost and benefit for each partner (Figure 1.1). The outcomes span from parasitism (+/- fitness interactions) to mutualism (+/+ fitness interactions) and form a continuum between these two states. A given symbiotic relationship is not a stationary point on this continuum because the benefits and costs of the symbiosis are dynamic and depend upon the environmental context, the stage of development and the interacting genotypes (Thompson, 2005). Indeed, because many of the potential benefits may only be required in particular environments or at particular times, the fitness outcome of many symbioses vary on ecological scales (Heath and Tiffin, 2007; Wendling et al., 2017). As such, some organisms only engage in symbiosis when in nutrient deficient environments (Johnson, 2011; Muscatine and Porter, 1977). The nature of symbiotic relationships is, therefore, context dependent. For example, increased nitrogen or phosphate fertilisation of the soil lowers the benefit of mycorrhizal fungal symbionts for a range of plant species, leading to reduced abundance of symbiotic interactions (Treseder, 2004). One consequence of context dependent fitness outcomes is that there is likely to be no universally optimal partner, which drives symbiotic relationships to be evolutionarily dynamic (Heath and Tiffin, 2007).

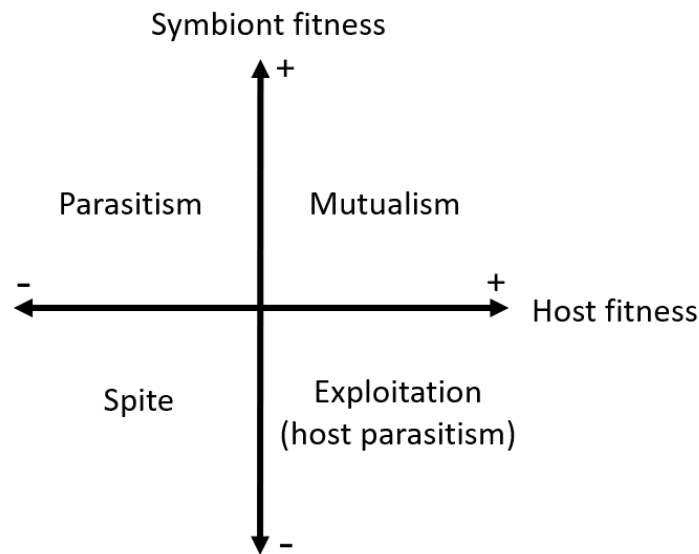


**Figure 1.1. Diagrammatic representation of the fitness interactions within endosymbioses.**

Mutualisms are defined by net positive fitness effects of interaction for both partners, but, as previously discussed, even mutualistic symbioses have an inherent potential for conflicting fitness interests among partners because of the short-term advantage of cheating. Mutualisms are, however, abundant throughout the tree of life despite their inherent evolutionary conflicts, and this disparity is considered the paradox of mutualism. Explaining the establishment of mutualistic symbioses is therefore challenging. The conditions for mutualistic symbioses to establish through mutualism alone are highly restrictive, and thus several alternative mechanisms have been proposed (Garcia and Gerardo, 2014; Keeling and McCutcheon, 2017). One of these is that mutualistic symbioses evolve from parasitisms. This transition can occur in two directions. First, the smaller parasitic partner living in or on the larger host can evolve reduced virulence to eventually become beneficial to its host (King et al., 2016; Shapiro and Turner, 2018; Tso et al., 2018). Sach et al. (2011) used phylogenetic reconstruction to predict whether bacterial symbionts originated as mutualists or parasites. For 42 beneficial bacterial symbionts, they inferred that 32 had originated as parasitic whilst only 9 had originated as mutualists (with 1 case remaining ambiguous), suggesting that parasitism is a more common route than mutualism to mutualistic symbiosis. Second, the larger host partner could capture and exploit the smaller beneficial partner, which would otherwise grow faster outside of symbiosis. This is a special case of parasitism known as host exploitation, which has been far less well-studied. This alternative route was proposed and modelled by Law & Dieckmann (1998), the model predicted that exploitative relationships can evolve into stable mutualistic symbioses with

vertical transmission simply through natural selection to increase individual fitness. The key requirement for this outcome was that the free-living symbiont pays a cost, which produces a trade-off for the symbiont. The symbiont either uses resources to overcome the cost of the free-living state or to provision the exploitative host but cannot do both. The model demonstrated that if the trade-off is sufficiently strong, the evolution of stable symbiosis can be advantageous to both partners even in an initially exploitative relationship.

To better understand the role for exploitation in the origin of mutualistic symbioses, there has been a recent call to reassess the fitness interactions of endosymbiotic relationships. Notably, Decelle (2013) has proposed that exploitation is likely to have been a common route for the origin of photosymbioses in particular. Currently there is evidence to suggest that the symbioses between scleractinian corals and the dinoflagellate algae *Symbiodinium* (Dubinsky and Berman-Frank, 2001; Smith and Muscatine, 1999; Wilkerson et al., 1988), the lichen symbiotic partners (Ahmadjian, 1993), chemosynthetic bacteria and their invertebrate hosts (Combes, 2005), and some protist-algal endosymbioses (Decelle, 2013; Lowe et al., 2016) are examples of host exploitation. Others go further, Keeling and McCutcheon (2017) state that endosymbioses are better viewed as “context dependent power struggles” or mutual exploitations, and that on evolutionary timescales conflict always remains.

#### *1.4 Evolution of partner dependency*

In nature, the degree of dependence varies extensively both within and between symbioses (Fisher et al., 2017; Minter et al., 2018). Dependence ranges from obligate associations with mutually dependent partners, through asymmetrically dependent associations where only one species is unable to survive alone, to fully facultative associations where both species can survive alone. The potential asymmetry of dependence can cause conflict as one partner relies completely upon the other, while the other partner maintains the option of a free-living lifestyle.

Comparative studies suggest that mutual dependence is more likely to evolve in vertically-inherited symbioses, where the fitness interests of both species are more aligned compared to associations with some horizontal transmission. For reproductive interests to become fully aligned, both absolute co-dispersal and reproductive synchrony are required as part of vertical transmission (Frank, 1997). If achieved, this reduces within-host competition between symbionts and stabilises the symbiosis because the reproductive success of the

symbiont is perfectly correlated to that of its host. Vertical inheritance is common in well-established, obligate symbiotic partnerships and is associated with greater dependence (Fisher et al., 2017). It is not, however, ubiquitous and there are many stable mutualisms that maintain horizontal transmission. For example, *Vibrio fischeri* and bobtail squids (Visick and Ruby, 2006), Rhizobia and legumes (Sprent et al., 1987), and *Endoriftia persephone* and tube worms (Nussbaumer et al., 2006). Consequently, it is apparent that while vertical transmission helps to promote stability of some interactions, it is neither a necessary nor sufficient condition for the evolutionary stability of mutualistic symbioses (Genkai-Kato and Yamamura, 1999).

The evolution of mutual dependence is often associated with greater integration and genetic adaptation to symbiosis because these organisms no longer need to support a free-living life stage (Bennett and Moran, 2015). As such, once dependence has evolved integration of the partners extends beyond the initial function of the symbiosis. For example, after 150 million years of evolution aphids now rely on their obligate nutritional symbiont, *Buchnera aphidicola*, for a wide range of non-nutritional functions, including development even when dietary supplements are provided (Koga et al., 2007; Wilkinson and Ishikawa, 2000). Genome reduction is commonly seen in the genomes of anciently endosymbiotic taxa because, in the absence of a free-living life-stage, many genes are redundant; the symbiont resides in a stable host environment and can rely on the host to fulfil the majority of functions (McCutcheon and Moran, 2012). The extent of genome reduction can be extreme, and the smallest bacterial genomes are those of bacterial endosymbionts, for example the circadian endosymbiont *Candidatus Hodgkinia cicadicola* has a genome of only 143,795 bps (McCutcheon et al., 2009). Host genomes will also alter, either in direct response to the symbiotic interaction, for instance the genes involved in provisioning the symbiont may be duplicated (Dahan et al., 2015), or because of endosymbiont gene transfer (EGT) the host genome may acquire new genetic material. To date there are only a few examples of EGT from non-organelle endosymbioses, including a number of *Wolbachia*-to-host-nucleus gene transfers with some of these transferred genes even being transcribed (Hotopp et al., 2007).

Although mutual dependency is associated with stable endosymbioses, in its most extreme form it can, however, cause an interaction to breakdown. For, once dependent, the host must maintain a relationship with a symbiont whose genome undergoes decay, becomes increasingly eccentric, and may lead the association to disappear down an evolutionary dead-end or “rabbit hole” (Bennett and Moran, 2015). In particular, the small effective population size and asexual nature of symbiont genomes mean they become increasing

subject to drift and so accumulate deleterious mutations. The extreme genome reduction of symbionts is likely to only be possible because the host functionally compensates for the decaying symbiont genome. The key symbiont genes, that encode the symbiotic functions upon which the host depends, normally remain under purifying and/or positive selection (Sabater-Muñoz et al., 2017). However, in the most extreme cases even these genes erode and then host compensation is not possible, in which case either the endosymbiosis goes extinct or symbiont replacement/supplementation must occur. Examples of the latter include the recurrent symbiont replacements of *Hodgekina* by entomopathogens in cicadas (Matsuura et al., 2018) and meadow spittlebugs whose ancient, highly reduced, symbiont has been replaced with a new *Sodalis*-like symbiont that has much higher genetic functionality (Koga and Moran, 2014). The new symbiont, however, faces the same evolutionary forces as the first and will likely also be subject to genome decay over evolutionary time.

### 1.5 Conflict avoidance

A range of mechanisms have been proposed to ensure the maintenance of endosymbiosis in the face of evolutionary conflict and environmental variability. There are fundamental aspects of the relationship that can reduce conflict, known as ‘conflict avoidance factors’ (Herre et al., 1999). These include vertical transmission, genetic uniformity of symbionts, and obstructions to symbionts entering alternative free-living states. In addition, active mechanisms to police cheaters have been documented within mutualistic relationships and help to prevent the breakdown of these relationships. These include, partner sanctions in the legume-rhizobium symbiosis (Kiers et al., 2003), partner choice in the yucca-yucca moth symbiosis (Bull and Rice, 1991), partner fidelity in solitary wasp-*Streptomyces* symbiosis (Kaltenpoth et al., 2014), and screening in the bobtail squid-*Vibrio fischeri* symbiosis (Archetti et al., 2011; McFall-Ngai and Ruby, 1991).

Partner switching can terminate an association if its benefit-to-cost ratio is too low, enabling the acquisition of a new, more beneficial partner. This mechanism is predicted to be particularly effective in the context of environmental change or migration and niche expansion. Symbiont-mediated resilience to environmental change has been observed in corals that have acquired novel, thermally resistant *Symbiodinium* endosymbionts following thermal bleaching events (Boulotte et al., 2016); and niche expansion in lichens was enabled by replacement of photobiont ecotypes (Rolshausen et al., 2018). Partner switching is not always beneficial, however, and although theory predicts that low-benefit partners should be out-competed, a neutral partner can in theory become fixed within a

population (Fukatsu et al., 1994). The complexity of partner switching is shown by a recent phylogenetic analysis of the nutritional endosymbionts within hemipteran insects, which found that the replacement of the primary symbiont was related to adaptive dietary transitions, but that the more frequent turnover of secondary symbionts were not correlated to diet and may have been neutral (Bell-Roberts et al., 2019). Nonetheless, in some circumstances partner switching can provide rapid adaptation through the acquisition of novel traits (Gilbert et al., 2010).

### *1.6 Ecology and Physiology of the P. bursaria – Chlorella endosymbiosis*

Empirical data on the establishment of mutualistic symbioses are rare because studying this process experimentally is challenging. The extant mutualistic symbioses we observe in nature are the products of co-evolution and are no longer in the establishment phase. Furthermore, for obligate mutualistic symbioses it may be impossible to separate the partners and therefore untangle the costs/benefits that each of the symbiotic partners derive. Nevertheless, there are several beneficial microbial symbioses that are amenable to experimental study and are emerging as model systems for the study of symbiosis. Microbial systems are particularly powerful tools because their fast generation times, ease of laboratory culturing, high fecundity, and relatively smaller and easier to manipulate genomes make experimental procedures easier (Hoang et al., 2016; Jessup et al., 2004). In addition, microbial systems are a one-to-one symbiosis, and do not have the complications of working with a multicellular host.

One of the best studied facultative mutualistic endosymbioses is that between the ciliate *Paramecium bursaria* and the green algae *Chlorella* spp. This relationship has long been known to science, with *P. bursaria* formally being described in 1836 (Focke, 1836), and the vertical nature of the endosymbiosis described in 1960 (Siegel, 1960). While the physiology and ecology of this system have been studied for several decades, only recently are the molecular details of this interaction being uncovered. The relationship is experimentally tractable because it is easily culturable, with fast generation times and multiple laboratory techniques have been established for studying this system. Crucially, this association is usually facultative and therefore the consequences of symbiosis can be assessed separately for each partner. Consequently, this system has been used to experimentally test hypotheses on the evolution on endosymbiosis (Fujishima and Kodama, 2012).

Ciliates are a very diverse group of single-celled eukaryotes and are believed to have once carried plastids but lost them and reverted to heterotrophic lifestyles for the most part

(Reyes-Prieto et al., 2008). A multitude of diverse endosymbioses occur in ciliates (Fokin, 2004; Gast et al., 2009; Nowack and Melkonian, 2010), however, within *Paramecium*, only two species form photosymbiotic endosymbioses; whereas the association between *P. bursaria* and *Chlorella* is geographically widespread, the other between *Paramecium chlorelligerum* with *Meyerella planctonica* algae is much rarer (Kreutz et al., 2012; Lanzoni et al., 2016). *P. bursaria* cells are large, ~100µm across, and covered in cilia for motility and to draw food into the cells via the oral groove (Corliss, 1961; Fenchel, 1987). These host cells vastly dwarf their symbiont, despite both being unicellular eukaryotes, and one host will house between ~100-600 algal symbiont cells (Johnson, 2011; Kadono et al., 2004).

*Chlorella* are a large genus within the green algae, though the genus phylogeny and exact taxonomic group is still currently being defined, with 'true' *Chlorella* belonging to the *Trebouxiophyceae* class (Takeda, 1988). The cells are 2-10µm in diameter, house a single chloroplast, and reproduce both asexually and sexually (Blanc et al., 2010). *Chlorella* have a cellulose-glucosamine cell wall and in symbiotic *Chlorella* the cell wall is half the thickness of free-living cells (Higuchi et al., 2018). In recent years there has been a surge of interest in *Chlorella* and its potential applications, as a nutritional product (Rodriguez-Garcia and Guil-Guerrero, 2008), biofuel producer (Demirbas, 2011) and bioreactor (Walker et al., 2005), due to their high abundance and diversity of lipids and fatty acids (Converti et al., 2009; Safi et al., 2014). Intriguingly, *Chlorella* are very common symbionts and are found within amoeba, sponges, coelenterates (including *Hydra*), molluscs, flatworms and 25 species of ciliates (Zagata et al., 2016). It is unknown whether this alga has a propensity for symbiosis or if its multiple associations are simply a consequence of its abundance.

This endosymbiosis is primarily a nutritional symbiosis, centred upon the classical photosymbiotic exchange whereby fixed carbon from the photosynthetic *Chlorella* is exchanged for organic nitrogen from the heterotrophic *P. bursaria* (Figure 1.2) (Esteban et al., 2010; Reisser, 1976). In addition to this primary nutrient exchange, gas exchange also occurs as a beneficial by-product whereby the CO<sub>2</sub> from *P. bursaria* respiration can be a substrate for photosynthesis in *Chlorella*, and the O<sub>2</sub> from *Chlorella* photosynthesis can act as substrate for *P. bursaria* respiration (Johnson, 2011). *Chlorella* endosymbionts have been estimated to release 57% of their fixed carbon to the host cell (Johnson, 2011), primarily as maltose (Ziesenisz et al., 1981). In order to provide maltose both day and night two different pathways are utilised: in the light, maltose is synthesised *de novo* from the products of the Calvin Cycle, while, in the dark, maltose is formed from starch degradation (Ziesenisz et al., 1981).

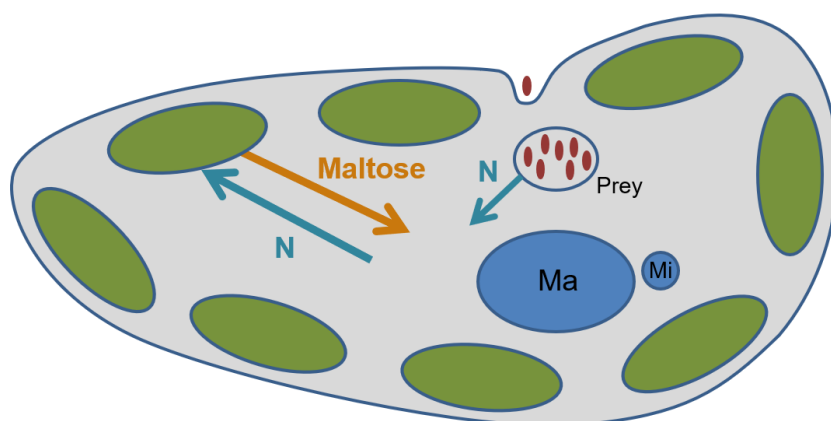


**Figure 1.2. Diagrammatic representation of the *P. bursaria* – *Chlorella* endosymbiosis.** Showing the nutrient exchange with the transfer of maltose from the *Chlorella* in exchange for organic nitrogen (denoted as ‘N’ as the identity of this compound is currently unknown). Ma = macronucleus; Mi = micronucleus.

The *P. bursaria* host acquires nitrogen from the digestion of bacteria (Johnson, 2011), and therefore must maintain its heterotrophic lifestyle even when housing autotrophic *Chlorella*. The identity of the nitrogen source provided by the host to algal symbionts is unknown, though multiple candidates have been proposed. The dominant theory is that nitrogen is provided as an amino acid; evidence supporting this comes from experiments demonstrating that the Japanese symbiotic *Chlorella* strain F36-ZK has lost its nitrate reductase activity but can utilise amino acids (Kato et al., 2006) and that symbiotic *Chlorella* strains grew better on urea or amino acids compared to inorganic nitrogen sources (Albers et al., 1982; Kessler and Huss, 1990). Furthermore, growth measurements of isolated symbiotic *Chlorella* on different nitrogen sources found that asparagine and serine supported growth in symbiotic but not free-living *Chlorella*, while other amino acids, including arginine and glutamine, could be utilised by both groups of *Chlorella* (Quispe et al., 2016). It is unclear, however, whether these patterns help to identify the exchange metabolite, because this compound need not necessarily be exclusively metabolised by symbiotic algae. In addition, results from Minaeva and Ermilova (2017) imply that arginine may be the transfer compound because the arginine concentration within symbiotic *Chlorella* matches that of isolated cells grown on arginine-supplemented medium, while much lower arginine concentrations occur in isolated cells grown on nitrate-based medium. Moreover, arginine supports growth of *Chlorella* as its sole N source (Arnow et al., 1953).

Alternatively, it has been proposed that *P. bursaria*'s nitrogen waste includes nucleic acid derivatives, such as guanine and xanthine (Soldo et al., 1978), and that these are then assimilated by *Chlorella* (Shah and Syrett, 1984). Nucleoside recycling occurs in other endosymbioses (Ramsey et al., 2010), and the utilisation of a host waste product would decrease the cost of symbiosis for *P. bursaria*. Additionally, there are conflicting results for ammonia utilisation, with some studies supporting it as a candidate nitrogen source (Albers et al., 1982) and others reporting poor *Chlorella* growth on ammonia-based media (Kato et al., 2006). The multiple, and somewhat conflicting, candidates for the nitrogen source could be explained if there is divergence among host-symbiont pairings, or if multiple nitrogen sources are provided simultaneously, alternatively further research may lead to a consensus around a single source.

The *P. bursaria* – *Chlorella* endosymbiosis utilises vertical inheritance of the symbiont, and synchronisation of their cell cycles (Kodama and Fujishima, 2012) and circadian clocks (Miwa et al., 1996). The division of the *Chlorella* is controlled by the host and occurs just prior to host cell division with a signal that is connected to the arrest of host cytoplasmic streaming (Takahashi et al., 2007). The circadian cycles of the symbiotic partners are interconnected, and the *Chlorella* sets the cycle for both partners (Miwa et al., 1996). Miwa et al. (1996) demonstrated that symbiotic *P. bursaria* have a longer clock period compared to aposymbiotic cells, that arrhythmic *P. bursaria* mutants can be rescued by symbionts, and that the host will shift in phase to match its *Chlorella* if out of sync. Furthermore, metabolic integration has occurred, and the nutrient exchange is actively regulated, for instance host  $\text{Ca}^{2+}$  inhibits serine uptake into *Chlorella* and glucose increases the uptake (Kato and Imamura, 2008a, 2008b). If the symbiont's maltose is broken down to glucose by the host, then this control process would facilitate a reward system for co-operative symbionts.

Aposymbiotic *P. bursaria* are rarely isolated from natural populations (Tonooka and Watanabe, 2002), but experimental procedures for separating the partners have been developed. The host can be cured of symbionts through treatment with herbicide chemicals, such as paraquat and cycloheximide (Kodama and Fujishima, 2008) and the symbionts can be released from the host cells by sonication, which disrupts the host membrane (Kodama et al., 2014). There is strain variation in the level of dependency (Minter et al., 2018); among five geographically diverse isolates, both partners were fully facultative in some strains, while in others they displayed mutual obligacy or host obligacy. The *P. bursaria* were more dependent on the symbiosis than the *Chlorella*, such that only one

*Chlorella* strain of the five tested was incapable of free-living growth, while three of the *P. bursaria* strains were incapable of free-living growth. This suggests asymmetry in selection for dependency between the partners, consistent with the hypothesis that this association is based upon host exploitation of the algal symbiont and not mutual benefit (Lowe et al., 2016).

The facultative nature of the relationship has allowed the re-establishment of the symbiosis to be characterised in detail by Kodama & Fujishima (Kodama and Fujishima, 2011; Kodama et al., 2016). The *Chlorella* are engulfed along with food particles and initially contained in a digestive vacuole. *Chlorella* cells selected to form endosymbionts are partitioned and individually held in perialgal vacuoles that protect against lysosomal fusion. These are repositioned to just beneath the cell cortex to maximise light harvesting, in a similar fashion to chloroplast positioning within plant cells. However, the basis upon which *Chlorella* cells are selected to become endosymbionts is unknown. One theory is that the *P. bursaria* detect carbohydrate secretion by compatible symbiotic *Chlorella*. This is supported by the observation that *Chlorella* kept in the dark prior to inoculation will be digested rather than selected (Kodama and Fujishima, 2014) and that *Chlorella* maltose release is induced by low pH (Kamako and Imamura, 2006; Shibata et al., 2016), the environment of the perialgal vesicles within which *Chlorella* are held (Schückler and Schnepf, 1992). Low-pH mediated carbohydrate secretion has also been observed in other phylogenetically distinct photosymbioses (e.g. those between Hydra and *Chlorella* (Douglas and Smith, 1984) and Dinoflagellates and coral (Tremblay et al., 2013)) suggesting perhaps that carbohydrate secretion is a commonly used cue for symbiosis-initiation. This apparently universal property may suggest that it is an ancestral physiological response of the algae that has been co-opted by the hosts as an ‘honest’ signal, rather than this being a symbiosis-specific adaptation.

The separation of the partners allows the fitness costs and benefits of symbiosis versus free-living to be directly quantified and compared. For hosts the benefit of symbiosis increased with light intensity, such that while it was costly to harbour symbiotic algae in the dark (i.e., symbiont-free hosts grow faster than symbiotic hosts), these costs were outweighed at higher light intensity such that symbiosis became highly beneficial relative to free-living for hosts in high light (Figure 1.3a) (Lowe et al., 2016). In contrast, symbiosis was never beneficial for the alga; free-living algal growth rates increased monotonically with light intensity and at all light levels exceeded those of symbiotic algae (Figure 1.3b). Furthermore, if the association is costly for an extended period of time the interaction can

breakdown, for instance complete darkness or chemical inhibitors of photosynthesis lead to the eventual loss of *Chlorella* symbionts through either digestion or egestion (Karakashian, 1963; Kodama and Fujishima, 2008). Endosymbioses are particularly susceptible to the shifts in the benefit-to-cost ratio during their establishment phase, and for the establishment to be successful it is likely that the light intensity would have to be above the no-benefit threshold regularly.

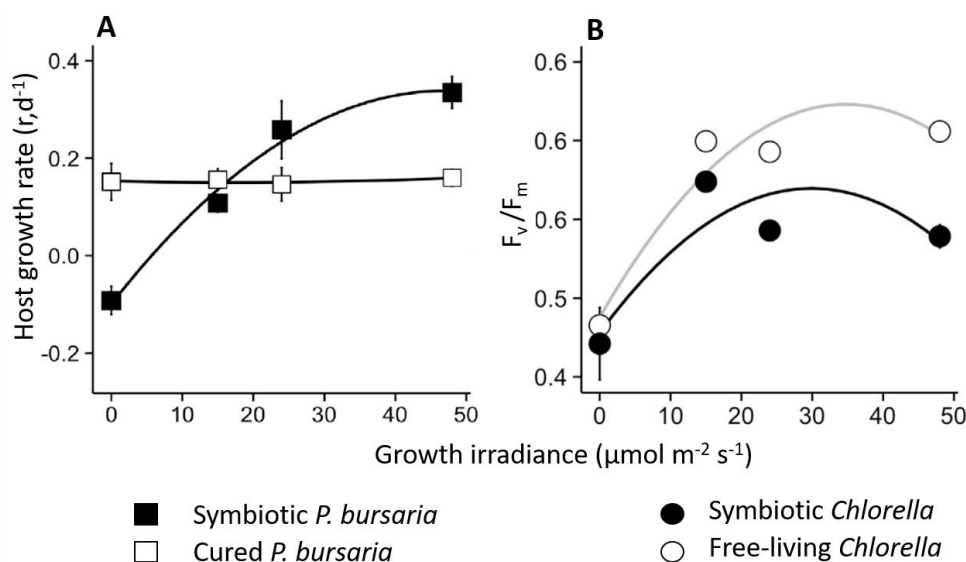


**Figure 1.3. The consequence of symbiosis for each partner.** A.) Host growth rate in response to light within symbiotic and cured *P. bursaria* (Figure 1A in the source). B.) Estimates for the photosynthetic efficiency ( $F_v/F_m$ ) between symbiotic and isolated *Chlorella* (Figure 3A in the source). Responses are presented as the mean ( $n=3$ )  $\pm$ SE. Adapted from Lowe et al., (2016) Current Biology.

Hosts manipulate the costs of symbiosis by regulating algal symbiont load (i.e. the number of algal symbionts per host cell), which consequently has a unimodal relationship with light intensity, peaking at low light, and being reduced both in the dark and at high light intensity (Lowe et al., 2016). A mathematical model of the symbiosis showed that hosts manipulate symbiont load in this way to maximise their return from nutrient trading, effectively minimising their nitrogen cost for each molecule of carbon they gain from their algal symbionts (Dean et al., 2016). Indeed, measurements of algal photosynthetic efficiency suggested that algal symbionts were more nitrogen starved than their free-living counterparts (Lowe et al., 2016). Similar patterns of benefit-to-cost ratio and host control were observed across a range of geographically diverse isolates (Minter et al., 2018). The packaging of *Chlorella* in host-derived vacuoles (Kodama and Fujishima, 2011, 2014) provides a clear mechanism of host control. Host regulation of symbiont load is believed

to arise through host-triggered symbiont division (Takahashi et al., 2007) and/or digestion/egestion of symbionts.

Taken together, the asymmetry in the benefit of the symbiosis and host-controlled regulation of symbiont load, suggest that the nutrient trading relationship between the ciliate and the alga is exploitative rather than mutualistic, benefiting the host (Lowe et al., 2016). Additional selective forces may be required therefore to explain the benefit, if any, of engaging in this symbiosis for the alga: both photoprotection and escape from viral predation have been proposed (Esteban et al., 2010; Reisser et al., 1991; Summerer et al., 2009). A cost in the free-living state, such as predation, could provide a sufficiently strong trade-off between the symbiotic and free-living state of the algae such that the evolution of stable symbiosis can be advantageous to both partners even in an exploitative relationship (Law and Dieckmann, 1998).

An important by-product of photosynthesis is photo-oxidative stress, predominantly in the form of damaging reactive oxygen species (ROS). Hundreds of photosynthesising *Chlorella* cells bring the potential for a vast increase in ROS, most of which will be contained within the *Chlorella* cells themselves, but hydrogen peroxide (H<sub>2</sub>O<sub>2</sub>) can cross membranes and may accumulate in the *P. bursaria* cytosol. Despite this potential, symbiotic *P. bursaria* have lower photo-oxidative stress and lower mortality rates than aposymbiotic cells at high UV (Hörtnagl and Sommaruga, 2007; Summerer et al., 2009). This suggests that not only do the *Chlorella* sufficiently protect the host from the ROS they produce, but that they provide additional protection for the host at high UV. The hosts nonetheless show behavioural responses to high light and will aggregate to create shading in high UV (Summerer et al., 2009). The relationship to stress within this relationship is complex, and Kawano and colleagues (Kawano et al., 2004) have hypothesised that *P. bursaria* were pre-adapted to photosymbiosis because they possessed a higher ROS tolerance than other *Paramecium* species, which allowed them to engage in this potentially lethal relationship. It is interesting to note, that ROS can play other biological roles besides causing damage: H<sub>2</sub>O<sub>2</sub> enables communication between chloroplasts and mitochondria, indicating that these compounds can be harnessed by the cell (Foyer and Noctor, 2003; Neill et al., 2002).

### 1.7 Genetics of the *P. bursaria* – *Chlorella* endosymbiosis

*Chlorella* is a well-studied taxonomic group with a reasonably well-detailed genetic annotation and multiple genome sequenced species, including a *P. busaria* symbiotic type-strain, NC64A (Blanc et al., 2010). The NC64A genome reveals adaptations to symbiosis,

including increased numbers of genes involved in amino acid transport and carbon metabolism, compared to free-living *Chlorella*, traits that both relate to the core nutrient transfer of the symbiosis. Also enriched in the symbiont genome were protein families involved in protein-protein interactions which are hypothesised to be involved in symbiosis-specific signalling (Blanc et al., 2010). The NC64A genome also revealed orthologs of plant hormones, including abscisic acid, cytokinin and auxin receptors, which is in line with the increasing evidence that phytohormones are active in microalgae (Kiseleva et al., 2012; Tarakhovskaya et al., 2007).

*P. bursaria* has been less characterised at a genetic level, owing to the challenges of its genetic architecture. It possesses two nuclei: the micro nucleus, which is the inherited copy that acts as the germline, and the macro nucleus, a polyploid version of the genome that is actively transcribed (Corliss, 1961; Wichterman, 1986). An additional difficulty arises through the epigenetic modification between the two nuclei, involving the excision of almost all the transposable elements and internal eliminated sequences from the micro nucleus when the macro nucleus forms (Preer, 2000; Singh et al., 2014). Despite these complications, recent work has started to piece together the genetics of *P. bursaria*. The transcriptome of symbiotic versus aposymbiotic *P. bursaria* was compared by Kodoma et al. (2014). They found decreased carbon metabolism and host-mediated oxidative stress responses in symbiotic *P. bursaria* cells; both of these functions are expected to be partially taken over by symbiont metabolism. In addition, increased expression of histidine kinase and HSP70 in symbiotic *P. bursaria* cells, was suggested to be related to symbiosis coordination. Recently, an almost complete *P. bursaria* genome sequence was compared to a non-symbiotic close relative, *Paramecium caudatum*, by He et al. (2019). They found that *P. bursaria* encoded more genes related to nitrogen metabolism and that these genes were more highly expressed. In particular, the glutamine synthetase gene (*glnA*) had four times higher expression in *P. bursaria* than in *P. caudatum*, suggesting that glutamine may be the amino acid transferred to the algal symbiont. Alternatively, the increased expression may be reflective of increased nitrogen demand for downstream pathways that include the synthesis of other amino acids (glutamine synthetase being the primary route through which nitrate enters central metabolism (Rigano et al., 1981)). The *P. bursaria* genome also contained more genes encoding mineral absorption than the *P. caudatum* genome, and it has been hypothesised that  $Mg^{2+}$  levels could provide a mechanism for host-mediated symbiont load control, given that the chlorophyll compound is built around a  $Mg^{2+}$  ion. Furthermore, *P. bursaria* encoded fewer genes involved in oxygen binding than *P.*

*caudatum*, which may reflect redundancy given the ready supply of oxygen produced by *Chlorella* photosynthesis.

Analysis of symbiotic *Chlorella* nuclear rDNA loci, including 18S rDNA, ITS1 and ITS2, have revealed that symbiotic and free-living *Chlorella* form polyphyletic groups (Hoshina et al., 2005). The pattern of which strongly indicates that there have been multiple, independent origins of the *P. bursaria* symbiosis that involve different *Chlorella* species, although the exact number of symbiotic originations is currently unclear. However, a consistent pattern across multiple studies is that the *P. bursaria*-symbiotic *Chlorella* form two main biogeographical clades: a ‘European’ clade and a ‘American/Japanese’ clade (Hoshina and Imamura, 2008; Hoshina et al., 2005; Summerer et al., 2008). Within either of these two clades, the rDNA loci is highly conserved, but the rDNA sequences had characteristic intron insertions between the two groups, and the ITS2 sequences differed by almost 20% (Hoshina et al., 2004, 2005). The ‘European’ *Chlorella* clade associated with *P. bursaria* is more closely related to the symbiotic *Chlorella* of *Hydra* than it is to the ‘American/Japanese’ clade of *P. bursaria*-associated *Chlorella*, according to Hoshina et al., (2005). Despite this, host-species specificity has been demonstrated such that *Chlorella* from a non-ciliate host cannot successfully infect *P. bursaria*, including *Chlorella* from *Hydra* (Summerer et al., 2007). There is one example of an artificial initiation of a *P. bursaria* endosymbiosis with the cyanobacterium *Synechocystis* (Ohkawa et al., 2011), but there has been little follow up work on this intriguing interaction.

A phagotrophic protist such as *P. bursaria* feeds continually on bacteria, and, therefore, host-bacterial interactions happen continually. Most bacteria pass through the cell quickly, either being digested or escaping. Others are encased in vesicles for longer periods before digestion and are believed to be food storage vesicles. However, a few bacterial taxa appear to interact with the host and form stable endosymbioses. One potential example is *Candidatus Sonnebornia yantaiensis*, which lengthen *P. bursaria* survival if kept in pure water and locate close to the *Chlorella* perialgal vesicles (Gong et al., 2014). However, it is still debated whether they are true symbionts or simply long-term food stores (Gong et al., 2014). Across the *Paramecium* genus, almost 60 bacterial taxa have been reported as intracellular colonisers (Fokin, 2004). Though these additional relationships are yet to be thoroughly defined, *P. bursaria* seems likely to engage in other endosymbioses besides its core symbiotic relationship with *Chlorella*.

## 1.8 Thesis Outline

This thesis compares the multiple independent evolutionary origins of the *P. bursaria* - *Chlorella* endosymbiosis to understand the underpinning metabolic mechanisms. The chapters address the following specific questions:

*Chapter 2: Comparison of independent evolutionary origins reveals both convergence and divergence in the metabolic mechanisms of symbiosis*

In this chapter I compared the metabolic mechanisms of two independent origins of the *P. bursaria* - *Chlorella* photosymbiosis using a novel reciprocal pulse-chase labelling experiment to reveal the pathways and dynamics of nutrient exchange. Predictions arising from the metabolic results were tested phenotypically with partner-switch experiments and physiological assays. These data suggest that the multiple origins of this symbiosis have a convergent mechanism of nutrient exchange, but that other important traits relevant to the host-symbiont phenotype have diverged between the independent origins of this endosymbiosis.

*Chapter 3: Light-dependent stress-responses underlie host-symbiont genotypic specificity in a photosymbiosis*

Here I investigated the genetic variation for host-symbiont specificity in the *P. bursaria* - *Chlorella* endosymbiosis using a reciprocal cross-infection experiment coupled with metabolomics. The results reveal patterns of host-symbiont genetic specificity driven by contrasting light-dependent symbiont stress-responses.

*Chapter 4: A novel host-symbiont interaction can rapidly evolve to become a beneficial symbiosis*

I experimentally evolved a novel host-symbiont pairing to test if initially non-beneficial associations formed through partner switching can evolve to become beneficial. Changes in host-symbiont growth rate, symbiont load, relative fitness, and metabolomics were quantified over time. The results show that the novel symbiosis could rapidly evolve to become equivalently beneficial to the native control through convergent metabolic mechanisms.

### *Chapter 5: Discussion*

I discuss the results of the three data chapters, synthesising the findings to provide an overall account of their implications for our understanding of the evolution of endosymbioses. In particular, I discuss the consequences of my results in the context of stress responses, partner switching and the rapid evolutionary adaptation of novel associations.

## Chapter 2

# Comparison of independent evolutionary origins reveals both convergence and divergence in the metabolic mechanisms of symbiosis

### 2.1 Introduction

Eukaryotic complexity is underpinned by endosymbiotic relationships, from the ancient mergers that led to the organelles, to the abundant and diverse secondary endosymbioses that provide novel metabolic capabilities across diverse taxa (Douglas, 2014; Moran, 2007). Many eukaryotes depend on their endosymbiotic partners for nutrition and survival (Ankrah and Douglas, 2018; Fisher et al., 2017; Johnson, 2011). The mechanisms that enable establishment of new associations have rarely been elucidated. This is partly because the origins of endosymbiotic relationships are difficult to study, but comparison of extant relationships can provide insight. In particular, where a symbiotic relationship has originated multiple times, these independent originations can be compared to determine the degree of convergence and divergence in the molecular mechanisms underpinning the symbiosis (Corsaro et al., 1999; Moran and Wernegreen, 2000; Sachs et al., 2011). Independent evolutionary origins of a beneficial symbiotic relationship suggest that a strong selective advantage has, on multiple occasions, overcome the inherent conflict between the self-interest of the partners. Independent origins of symbiosis appear to be common and have been reported for diverse symbiotic relationships, such as in lichens (Gargas et al., 1995; Muggia et al., 2011), aphids and their secondary symbionts (Sandström et al., 2001), the fungus-growing ant system (Munkacsi et al., 2004), and rhizobia-legume associations (Masson-Boivin et al., 2009).

The experimentally tractable microbial symbiosis between the ciliate host *Paramecium bursaria* and the algal endosymbiont *Chlorella* has arisen independently multiple times. This endosymbiosis relies on a classical photosymbiotic exchange between fixed carbon from the photosynthetic algae and organic nitrogen from the heterotrophic host (Johnson, 2011; Ziesenis et al., 1981). This relationship has originated on at least two independent occasions giving rise to distinct geographical clades, known as the European clade and the

American/Japanese clade (Hoshina and Imamura, 2008; Summerer et al., 2008). This relationship has been well-characterised in regards to the establishment process and the integration of the partners (Fujishima, 2009; Kato et al., 2006; Kodama and Fujishima, 2011; Miwa et al., 1996). However, less is known about the symbiotic phenotypes and the mechanisms of convergence and divergence among the clades, except for their variation in nutritional requirements (Kamako et al., 2005; Kessler and Huss, 1990). Furthermore, it is unclear whether partner-switching can occur between the two main clades; with some studies indicating that it can (Summerer et al., 2007) but others suggesting that it cannot (Weis, 1978).

In photosymbioses the nutritional exchange provides the primary benefit of the symbiotic interaction, suggesting that this exchange is the crucial mechanism enabling the establishment of new associations and partner-switching (Decelle et al., 2015; Karkar et al., 2015). In the *P. bursaria* - *Chlorella* photosymbiosis the algae symbionts release 57% of their fixed carbon to their host, primarily as maltose (Ziesenis et al., 1981). In exchange the host provides organic nitrogen, but the identity of the transferred nitrogen compound is unknown. Multiple candidates have been proposed and the dominant theory is that nitrogen is provided as an amino acid (Albers et al., 1982; Kato et al., 2006). The exact amino acid identity, however, has not been resolved because different studies have implicated different amino acids (He et al., 2019; Minaeva and Ermilova, 2017; Quispe et al., 2016). The nutritional exchange is a fundamental component of this endosymbiosis, and as such it has been found to be a critical aspect of the establishment process, with maltose secretion believed to be a cue for the initiation of this association (Douglas and Smith, 1984; Kodama and Fujishima, 2014; Tremblay et al., 2013).

Disentangling the contributions of each partner to the interlinked symbiotic metabolism is challenging. Isotopic enrichment is a valuable tool for discerning the origin of compounds transferred between the organisms. Using dual labelling the fate of multiple elements can be followed bidirectionally to track transfers between two partners; for instance,  $C^{13}$  and  $N^{15}$  isotopes can be used to track metabolic exchange in photosymbioses. Bulk isotopic enrichment has been used to detail the origin of metabolites in a number of symbioses, including sponges and their microbial communities (Achlati et al., 2018; Shih et al., 2019), a novel algal-fungal endosymbiosis (Du et al., 2019), and myco-heterotrophic orchids and fungal symbionts (Cameron et al., 2006, 2008). An extension of this is the combination of enrichment analysis with mass-spectrometry that allows fine-scale pathway resolution of enrichment. This has been successfully used to study the C flux in the cnidarian-

dinoflagellate symbiosis (Matthews et al., 2018) and to study the C and N flux in the amino acids of a legume-rhizobium association (Molero et al., 2011).

Here, I extend the current metabolic methodologies applied to endosymbioses by using a reciprocal bidirectional pulse-chase experiment on global metabolism, which allowed the transferred C and N to be simultaneously tracked at an individual metabolite level. I employed an untargeted LC-ToF method to gain an overview of the metabolism rather than isolated pathways. Prior to metabolomic analysis, the symbiotic partners were separated, allowing the host and symbiont fractions to be analysed separately, which enables metabolism of each partner and the fate of exchanged metabolites to be determined. Using this approach, I compared the metabolic mechanisms of two independent origins of the *P. bursaria* - *Chlorella* photosymbiosis. Furthermore, I tested the implications of the metabolic results with partner-switch experiments and physiological assays to build an understanding of the causes and consequences of the metabolic mechanisms in these clades. The results revealed a convergent primary nutrient exchange, which enabled partner-switching. In contrast, divergence was observed in the metabolic mechanisms of light management, leading to differences in photophysiology between the strains and phenotypic mismatches in partner-switched associations. I discuss the consequences of these results for partner-switching and the evolution of endosymbioses.

## 2.2 Materials and Methods

### *Culturing conditions*

*P. bursaria* stock cultures were maintained at 25°C under a 14:10 L:D cycle with 50  $\mu\text{E m}^{-2} \text{ s}^{-1}$  of light. The two natural strains used were: 186b (CCAP 1660/18) obtained from the Culture Collection for Algae and Protozoa (Oban, Scotland), and HA1 isolated in Japan and obtained from the Paramecium National Bio-Resource Project (Yamaguchi, Japan). The stocks were maintained by batch culture in bacterized Protozoan Pellet Media (PPM, Carolina Biological Supply), made to a concentration of 0.66  $\text{g L}^{-1}$  with Volvic natural mineral water, and inoculated approximately 20 hours prior to use with *Serratia marcescens* from frozen glycerol stocks.

To isolate *Chlorella* from the symbiosis, symbiotic cultures were first washed and concentrated with a 11 $\mu\text{m}$  nylon mesh using sterile Volvic. The suspension was then ultrasonicated using a Fisherbrand™ Q500 Sonicator (Fisher Scientific, NH, USA), at a power

setting of 20% for 10 seconds sonification to disrupt the host cells. The liquid was then spotted onto Bold Basal Media plates (BBM) (Stein, 1979), from which green colonies were streaked out and isolated over several weeks. Plate stocks were maintained by streaking out one colony to a fresh plate every 3/4 weeks.

Symbiont-free *P. bursaria* were made by treating symbiotic cultures with paraquat (10  $\mu\text{g mL}^{-1}$ ) for 3 to 7 days in high light conditions ( $>50 \mu\text{E m}^{-2} \text{ s}^{-1}$ ), until the host cells were visibly symbiont free. The cultures were then extensively washing with Volvic and closely monitored with microscopy to check that re-greening by *Chlorella* did not occur. Stock cultures of the symbiont-free cells were maintained by batch culture at 25°C under a 14:10 L:D cycle with  $3 \mu\text{E m}^{-2} \text{ s}^{-1}$  of light and were given fresh PPM weekly.

#### *Cross Infections*

Symbiont-free populations of the two *P. bursaria* strains were re-infected by adding a colony of *Chlorella* from the plate stocks derived from the appropriate strain. The re-greening process was followed by microscopy and took between 2-6 weeks. Over the process, cells were grown at the intermediate light level of  $12 \mu\text{E m}^{-2} \text{ s}^{-1}$  and were given bacterized PPM weekly.

#### *Diagnostic PCR*

The correct algae genotype within the cross-infections was confirmed using diagnostic PCR. The *Chlorella* DNA was extracted by isolating the *Chlorella* and then using a standard 6% Chelex100 resin (Bio-Rad) extraction method. A nested PCR technique with overlapping, multiplex Chlorophyta specific primers were used as described by Hoshina et al. (2005). Standard PCR reactions were performed using Go Taq Green Master Mix (Promega) and  $0.5 \mu\text{mol L}^{-1}$  of the primer. The thermocycler programme was set to: 94°C for 5min, 30 cycles of (94°C for 30sec, 55°C for 30sec, 72°C for 60sec), and 5 min at 72°C.

#### *Fitness assay*

*P. bursaria* cultures, both the symbiotic cross-infections and symbiont-free cells, were washed with Volvic and resuspended in bacterized PPM. The cultures were then split and acclimated at their treatment light level ( $0, 12, 50 \mu\text{E m}^{-2} \text{ s}^{-1}$ ) for five days. Cell densities were counted by fixing 360  $\mu\text{L}$  of each cell culture, in triplicate, in 1% v/v glutaraldehyde in 96-well flat bottomed micro-well plates. Images were taken with a plate reader (Tecan Spark 10M) and cell counts were made using an automated image analysis macro in ImageJ v1.50i (Schneider et al., 2012). The competitions were started by setting up microcosms

that each contained 50:50 populations of green and white cells (with target values of 20 green cells and 20 white cells per ml) that were in direct competition. Cells were sampled on day 0 and day 7 on a flow cytometer and the proportion of green to white cells was measured and used to calculate the selection rate. Green versus white cells were distinguished using single cell fluorescence estimated using a CytoFLEX S flow cytometer (Beckman Coulter Inc., CA, USA) by measuring the intensity of chlorophyll fluorescence (excitation 488nm, emission 690/50nm) and gating cell size using forward side scatter; a method established by Kadono et al. (2004). The measurements were calibrated against 8-peak rainbow calibration particles (BioLegend), and then presented as relative fluorescence to reduce variation across sampling sessions. The re-establishment of endosymbiosis takes between 2-4 weeks, and this method was tested to ensure that the symbiont-free cells do not re-green over the course of the experiment.

### *Fluorimetry*

The cells were washed and concentrated with a 11 $\mu$ m nylon mesh using sterile Volvic and re-suspended in bacterized PPM. The cultures were then split and acclimated to their treatment light condition (12, 24 & 50  $\mu$ E m<sup>-2</sup> s<sup>-1</sup>) for five days.  $F_v/F_m$ ,  $\Phi_{PSII}$ , and NSV values were measured by fast repetition rate fluorimetry (FastPro8, Chelsea instruments fluorometer (Oxborough et al., 2012) following the manufactures procedure. Cultures were dark acclimated for 15 minutes prior to measurements. For maximum quantum yield, measurements were repeated until  $F_v/F_m$  stabilized (typically 3-5minutes) and  $F_v/F_m$  then estimated as an average of 10 measurements.  $\Phi_{PSII}$  was measured in response to an actinic light source at sequentially increasing irradiances between 0 – 2908 PFD with 110 flashes of 1.1 $\mu$ s at 1 $\mu$ s intervals following standard green algae protocol. Peak emission wavelengths of the LED used for excitations was 450nm. Non-photochemical quenching was estimated by the normalised Stern-Volmer coefficient, defined as  $NSV = F_o'/F_v'$  (McKew et al., 2013) and corrects for differences in  $F_v/F_m$  between samples.

### *Metabolomics*

Cultures were washed and concentrated with a 11 $\mu$ m nylon mesh using Volvic and re-suspended in bacterized PPM. The cultures were first grown for three days at 50  $\mu$ E m<sup>-2</sup> s<sup>-1</sup> to increase cell densities, and then split and acclimated at their treatment light condition (6 & 50  $\mu$ E m<sup>-2</sup> s<sup>-1</sup>) for three days. For the sampling, the cultures were split into 3 treatment: the control, N<sup>15</sup> enrichment by the addition of labelled *Serratia marscesens* (100 $\mu$ l per microcosm), or C<sup>13</sup> enrichment by the addition of HC<sup>13</sup>O<sub>3</sub> (100 mg L<sup>-1</sup>). The

cultures were sampled at four time points (0,2,6,8 hrs after the enrichment event). There were three biological replicates for each sampling event.

At each sampling event, the symbiotic partners were separated in order to get *P. bursaria* and *Chlorella* metabolic fraction. The *P. bursaria* cells were concentrated with a 11 $\mu$ m nylon mesh using Volvic and then the *P. bursaria* cells were disrupted by sonication (20% power for 10 secs). 1ml of the lysate was pushed through a 1.6 $\mu$ m filter, which caught the intact *Chlorella* cells, and the run-through was collected and stored as the *P. bursaria* fraction. The 1.6 $\mu$ m filter was washed with 5ml cold deionized water, and then reversed so that the *Chlorella* cells were resuspended in 1ml of cold methanol, which was stored as the *Chlorella* fraction.

The samples were analysed with a Synapt G2-Si with Acquity UPLC, recording in positive mode over a large untargeted mass range (50 – 1000 Da). A 2.1x50mm Acquity UPLC BEH C18 column was used with acetonitrile as the solvent. The machine settings are listed in detail below:

Mass spectrometry settings:

Polarity:	positive
Capillary voltage:	2.3 kV
Sample Cone voltage:	20 V
Source Temperature:	100 $^{\circ}$ c
Desolvation temperature:	280 $^{\circ}$ c
Gas Flow:	600 L hr $^{-1}$
Injected volume:	5 $\mu$ l

Gradient information:

Time (mins)	Water (%)	Acetonitrile (%)
0	95	5
3	65	35
6	0	100
7.5	0	100
7.6	95	5

The *P. bursaria* and *Chlorella* fraction were analysed separately. The xcms R package (Benton et al., 2010; Smith et al., 2006; Tautenhahn et al., 2008) was used for automatic peak detection by extracting the spectra from the CDF data files, using a step argument of 0.01 m/z. The automatically identified peaks were grouped across samples and were used to identify and correct correlated drifts in retention time from run to run. Pareto scaling was applied to the resulting intensity matrix.

#### *Isotope analysis*

For the *P. bursaria* isotope analysis the  $^{13}\text{C}$  labelled samples were compared with the control, while for the *Chlorella* analysis the  $^{15}\text{N}$  labelled samples were compared to the control. In order to identify isotopic enrichment without user bias, I used Random Forest (RF) models to identify metabolites that associated with the isotope labelling. This is a machine-learning decision-tree based approach that produces powerful multivariate regression and is an established method for high-throughput biological data (Touw et al., 2013), including metabolomics (Hopkins et al., 2017). The isotope label was used as the response variable to regress against the metabolic profile of each sample. Each random forest model was run with 1000 iterations, and each RF analysis was run 500 times to account for uncertainty in the rank score. For each run, the rank score of the RF importance (measured as the mean decrease in Gini) was recorded for each m/z bin. The mean and standard error of the rank score was then calculated to assess the consistency of the variable importance. In total 4 RF models were analysed within each fraction, 1 per timepoint.

The rank score values were then compared between the strains. The high proportion of shared metabolites were selected and filtered to select those that had a higher relative abundance in the labelled fraction than in the control. From these, the profile of each candidate metabolite was manually checked for isotopic enrichment, and when a clear enrichment profile was present the monoisotopic mass was identified. The enrichment proportion of the isotopic masses to the monoisotopic mass was calculated, and the natural enrichment value within the control fraction was subtracted from the enrichment in the labelled fraction. Following this calculation, it was possible to determine if enrichment had occurred, and if so, the monoisotopic mass was considered a ‘mass of interest’.

#### *Unlabelled analysis*

For the unlabelled, control fraction, the data was compared between the strains by calculating the  $\log_2(\text{Fold Change})$  between the conditions (either between the strains

within each light level, or between the light levels within each strain) in a series of pairwise contrasts for each metabolite. Student T-tests were performed between the relative abundances of the paired comparisons. The Benjamini–Hochberg procedure was used to account for the high number of multiple P-value comparisons, with the false discovery rate set to 0.1 and 0.05 (Storey and Tibshirani, 2003) as highlighted in the volcano plots.

#### *Identification of significant masses*

Masses of interest were investigated using the MarVis-Suite 2.0 software (<http://marvis.gobics.de/>) (Kaefer et al., 2009), using retention time and mass to compare against KEGG (<https://www.genome.jp/kegg/>) (Kanehisa and Goto, 2000; Kanehisa et al., 2019) and MetaCyc (<https://biocyc.org/>) (Caspi et al., 2018) databases. The Metabolomics Standards Initiative requires two independent measures to confirm identity, which the combination of retention time and accurate mass achieves. This analysis therefore confirms level 1 identification.

#### *Data Analysis*

Statistical analyses were performed in R v.3.5.0 (R Core Team, 2018) and all plots were produced using package ggplot2 (Wickham, 2016). Physiology tests were analysed by both ANOVA and ANCOVA, with light, host and symbiont identity as factors.

$\Phi_{\text{PSII}}$  results were analysed with non-linear mixed effects models (nlme) with the nlme R package (Pinheiro et al., 2019). The  $\Phi_{\text{PSII}}$  data was fitted to an exponential decay function:

$$\Phi_{\text{PSII}} = a e^{(bI)}$$

Where  $a$  is a normalisation constant and  $b$  is the rate constant. The nlme model included random effects by replicate on each parameter and fixed factors of host, symbiont and light factors that interacted with  $a$  following model reduction. Model fitting entailed starting with the most complex possible model, which was then compared to simpler models, and in the case that their explanatory power were equal, the most parsimonious model was chosen. See the supplementary statistics table for further details on the statistics used.

## 2.3 Results

The *P. bursaria* - *Chlorella* endosymbiosis has originated multiple times and forms two distinct biogeographical clades, specifically, the European clade and the American/Japanese clade (Hoshina and Imamura, 2008; Summerer et al., 2008). Using a representative of each – the strain 186b originally isolated in the UK and strain HA1 originally isolated in Japan (clade identity was confirmed by diagnostic PCR (Figure S1)) – I first tested whether these clades used convergent biochemical mechanisms of carbon (from the photosynthetic endosymbiotic *Chlorella*) for nitrogen (acquired by the protist host through the ingestion and digestion of free-living bacteria) exchange. To do this, I devised a novel, reciprocal, temporally-resolved, metabolomic pulse chase experiment. Using  $^{15}\text{N}$ -labelled bacterial necromass, I traced isotopic enrichment derived from N assimilated through *P. bursaria* digestion in *Chlorella* metabolites. In parallel, using  $^{13}\text{C}$ -labelled  $\text{HCO}_3$  I traced isotopic enrichment derived from C fixed by *Chlorella* photosynthesis in *P. bursaria* metabolites. This allowed the metabolic fate of resources exchanged between symbiotic partners to be quantified over time, allowing comparison of symbiotic metabolism between the strains.

Using Random Forest models to identify *Chlorella* metabolites that co-varied with  $^{15}\text{N}$  enrichment, I observed a shared isotopic enrichment response in 46% of metabolites (i.e. had a high-ranking score in both strains), suggesting that both *Chlorella* strains directed the exchanged nitrogen through central nitrogen metabolism in similar ways (Figure 2.1a). Similarly, I observed a shared  $^{13}\text{C}$  enrichment response in 75.12 % of *P. bursaria* metabolites, suggesting a high degree of convergence between the *P. bursaria* host strains in how they utilised the C derived from their algal symbionts (Figure 2.1b). Smaller proportions of metabolites showed an asymmetric response (i.e., were high-ranked in one strain but low-ranked in the other; for  $^{15}\text{N}$  enrichment, 20.55% in 186b *Chlorella* and 9.55% in HA1 *Chlorella*; for  $^{13}\text{C}$  enrichment 13.17% in 186b *P. bursaria* and 3.42% in HA1 *P. bursaria*), and there were subtle temporal differences in enrichment patterns between strains, suggesting only limited divergence in utilisation of exchanged metabolites has occurred between these host-symbiont clades.

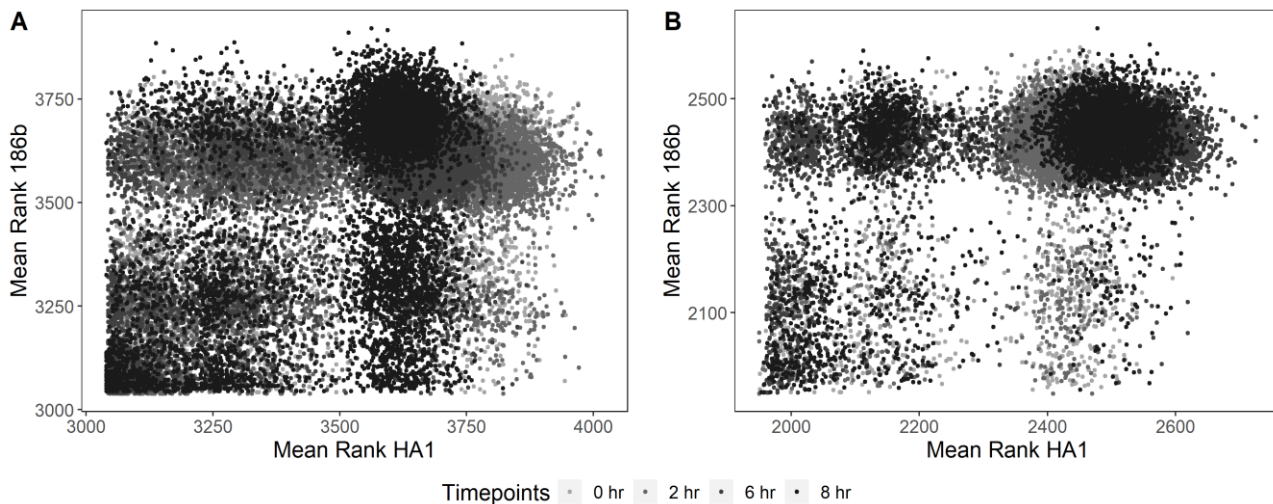


**Figure 2.1. Correlated metabolite enrichment for the 186b and HA1 *P. bursaria* and *Chlorella* strains over time.** Each data point represents a metabolite. In each scatterplot the mean Random Forest rank order of each metabolite in the HA1 strain is plotted against the mean rank order of each metabolite in the 186b strain. The rank order value is positively correlated with magnitude of the enrichment signal. Timepoint is shown by the colour of each data point. A.)  $^{15}\text{N}$  enrichment in the *Chlorella* fraction. B.)  $^{13}\text{C}$  enrichment in the *P. bursaria* fraction. For both panels, the mean rank order is derived from multiple Random Forest analyses (n=500).

Co-enriched metabolites with the strongest enrichment over time were identified using LC-ToFMS (simultaneously resolving the monoisotopic mass and chromatographic retention time for each M/Z). For  $^{15}\text{N}$  co-enrichment in *Chlorella* (Table 2.1), I identified metabolites associated with the amino acid and purine pathways, which have both previously been suggested as probable N exchange metabolites in this symbiosis. Targeted pathway analysis indicated that an amino acid (probably arginine) is the more likely N exchange metabolite from *P. bursaria* to *Chlorella* in both clades (see supplementary results and Figure S2-S4). In addition, I observed co-enrichment in larger, N-rich metabolites, including chlorophyll precursors, which most likely represent the largest N-sinks for *Chlorella*, thus becoming enriched in  $^{15}\text{N}$  as a function of N demand. For  $^{13}\text{C}$  enrichment in *P. bursaria* (Table 2.2), I identified metabolites involved in carbohydrate and lipid metabolism, suggesting that symbiont derived C was directed to carbon storage, as well as enrichment in central and amino acid metabolism, which are likely to have a high turnover of carbon and represent strong carbon sinks. For some carbohydrate storage metabolites, I observed stronger differences in  $^{13}\text{C}$  enrichment between light conditions in the 186b compared to the HA1 strain (Figure S5), indicating strain differences in the rate of flux through some of co-enriched pathways.

**Table 2.1: <sup>15</sup>N enriched metabolites of the *Chlorella* fraction.** List of the identified metabolites found to be enriched with <sup>15</sup>N in the *Chlorella* fraction in both the HA1 and 186b strain. This table includes their candidate identification, such as their detected mass and retention time as well as the main pathway the candidate compounds function within. 'RF Time' refers to the timepoint at which the metabolite was identified by the Random Forest Model.

RF Time	Detected Mass	Retention Time	Pathway	Candidate Compounds	Exact Mass	Adduct	KEGG/ MetaCyc
1	113	482	Pyrimidine/Amino acid	Uracil	112.0273	H+	C00106
				1,3-diaminopropane	74.0844	K+	C00986
1	166	478	Purine	5-Amino-4-imidazole carboxylate	127.0382	K+	C05516
1,2	237.1	286	Biotin	Dethiobiotin	214.1317	Na+	C01909
1,2,3,4	871.6	405	Chlorophyll	Pheophytin A	870.5659	H+	C05797
1,2,4	593.3	405	Chlorophyll	Pheophorbide A	592.2686	H+	C18021
				Urobilinogen	592.3261	H+	C05790
2,3	140	213	Amino acid	L-Aspartate 4-semialdehyde	117.0426	Na+	C00441
				Indole	117.0578	Na+	C00463
				1-Aminocyclopropane-carboxylate	101.0477	K+	C01234
				5-Aminopentanal	101.0841	K+	C12455
3	482.4	324	Folate biosynthesis	Dihydrofolate	443.1553	K+	C00415
3	848.6	294	Ubiquinone	Rhodoquinone-10	847.6842	H+	CPD-9613
4	227.1	460	Amino acid/Chlorophyll	Tryptophan	204.0899	Na+	C00078
				Porphobilinogen	226.0954	H+	C00931

**Table 2.2: <sup>13</sup>C enriched metabolites of the *P. bursaria* fraction.** List of the identified metabolites found to be enriched with <sup>13</sup>C in the *P. bursaria* fraction in both the HA1 and 186b strains. This table includes their candidate identification, such as their detected mass and retention time as well as the main pathway the candidate compounds function within. 'RF Time' refers to the timepoint at which the metabolite was identified by Random Forest Model.

RF Time	Detected Mass	Retention Time	Pathway	Candidate Compounds	Exact Mass	Adduct	KEGG
1	100	16	Glycerophospholipid	Ethanolamine	61.0528	K+	C00189
1	689.2	16	Carbohydrate	Glycogen	666.2219	Na+	C00182
1,2	124	15	Vitamins and Cofactors	Niacin	123.032	H+	C00253
1,2	261	14	Carbohydrate	Monosaccharide phosphate	260.0297	H+	C00092
1,2,3	251	17	Isoprenoid pathway	(R)-5-Phosphomevalonate	228.0399	Na+	C01107
1,2,3,4	190	341	Phosphonate	Demethylphosphinothricin	167.0347	Na+	C17962
1,2,3,4	441.3	310	Lipid	Hydroxycholesterol	402.3498	K+	C05500
1,2,3,4	639.2	414	Heme biosynthesis	Haem	616.1773	Na+	C00032
1,2,3,4	212.9	479	Chlorocyclohexane and chlorobenzene degradation	Chlorodienelactone	173.972	Ka+	C04706
1,2,4	109	479	Quinone	p-Benzoquinone	108.0211	H+	C00472
1,2,4	345.9	480	Amino acid metab	3-Iodo-L-tyrosine	306.9705	K+	C02515
1,3,4	169	19	Central metabolism	2-Oxoglutarate	146.0215	Na+	C00026
				2-Oxoisocaproate	130.063	K+	C00233
				3-Methyl-2-oxopentanoate	130.063	K+	C00671
				2-Dehydropantoate	146.0579	K+	C00966
				3-Phosphonopyruvate	167.9824	H+	C02798
				Phosphoenolpyruvate	167.9824	H+	C00074
2	313.2	287	Lipid	HPODE	312.2301	H+	C04717
2,3,4	519.1	400	Peptide	Nitro-hydroxy-glutathionyl-dihydronaphthalene	496.1264	Na+	C14803
2,4	71.1	373	Amino acid	Aminopropiononitrile	70.0531	H+	C05670
3	405.1	236	Isoprenoid pathway	Farnesyl diphosphate	382.131	Na+	C00448

The pulse-chase analysis suggests that these *P. bursaria* - *Chlorella* strains, representing independent origins of the symbiosis, show convergent utilisation of partner-derived nutrients, and I hypothesised therefore that partner-switched host-symbiont pairings would be functional. To test this, I performed a reciprocal cross-infection experiment whereby the *P. bursaria* host strains were cured of their native algal symbiont, and subsequently re-infected with either their native algal symbiont or the reciprocal non-native algal symbiont. I then directly competed each host-symbiont pairing against its respective symbiont-free host strain across a light gradient. I used flow cytometry to quantify the proportion of green (with symbiont) versus white (symbiont-free) host cells at the start and end of the growth cycle to calculate the selection rate, thus providing a direct measure of the fitness effect of symbiosis for hosts. As predicted, all the symbiont pairings showed a classic photosymbiotic reaction norm, such that the relative fitness of hosts with symbionts versus hosts without symbionts increased with increasing irradiance (Figure 2.2), and more steeply in the HA1 host background (host genotype \* light environment interaction, ANOVA,  $F_{3,31} = 29.34$ ,  $P < 0.001$ ). This confirms that both host genotypes could derive the benefits of symbiosis from either of the symbiont genotypes, but that the fitness effect of symbiosis varied between strains.

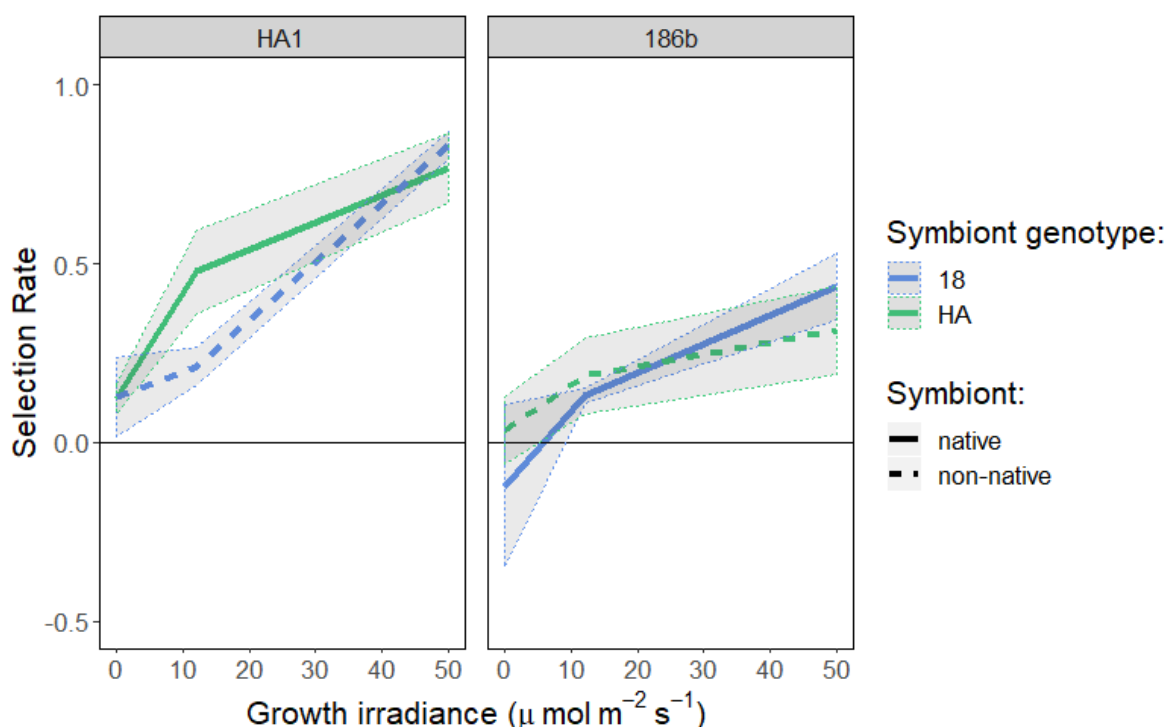


**Figure 2.2. Fitness of the native and non-native host-symbiont pairings relative to isogenic symbiont-free hosts.** Lines show mean ( $n=3$ ) competitive fitness of symbiont-containing hosts relative to their isogenic symbiont-free host genotype calculated as selection rate, and the shaded area denotes  $\pm$ SE. The left-hand panel shows data for the HA1 *P. bursaria*, the right-hand panel the data for the 186b *P. bursaria* containing either native (solid line) or non-native (dotted line) *Chlorella* symbionts. Colour denotes the *Chlorella* genotype. Selection rate = 0 represents equal fitness.

These light-dependent differences in the fitness of the host-symbiont pairings suggest that the HA1 and 186b strains may have diverged in aspects of their metabolism and physiology outside of the primary symbiotic nutrient exchange. Next, to characterise potential differences in global metabolism between the HA1 and 186b host-symbiont strains, I performed untargeted metabolomics analyses on the unlabelled metabolites from the separated *Chlorella* and *P. bursaria* fractions. Pair-wise contrasts, both between the strains and between the light levels, were used to identify masses of interest (Figure 2.3 & 2.4). I observed a range of metabolites that differentiated the 186b and HA1 *Chlorella* strains (Table 2.3), and metabolism differed more between strains than it did between light conditions within strains (Figure 2.3). Notably, the HA1 *Chlorella* strain displayed higher levels of several carotenoids than the 186b *Chlorella* strain, particularly at high irradiance, whereas the 186b *Chlorella* strain displayed higher levels of metabolites involved in chlorophyll and ubiquinol metabolism than the HA1 *Chlorella* strain at both low and high irradiance. Fewer metabolites distinguished the global metabolism of the *P. bursaria* strains (Table 2.4). In all cases these metabolites were present at higher levels in the 186b *P. bursaria* strain compared to the HA1 *P. bursaria* strain (Figure 2.4), and neither strain's metabolism varied significantly with irradiance (Figure 2.4). The identified metabolites that distinguished the strains were associated with a range of functions, including amino acid metabolism, amino sugars, and sphingolipid metabolism. Several other metabolites, although present in the host fraction, are likely to have been secreted into the host cytoplasm by the algal symbiont or be derived from the bacterial necromass. These include a zeatin candidate, which may play a role in *Chlorella* signalling, and several metabolites identified as putative antibiotics.

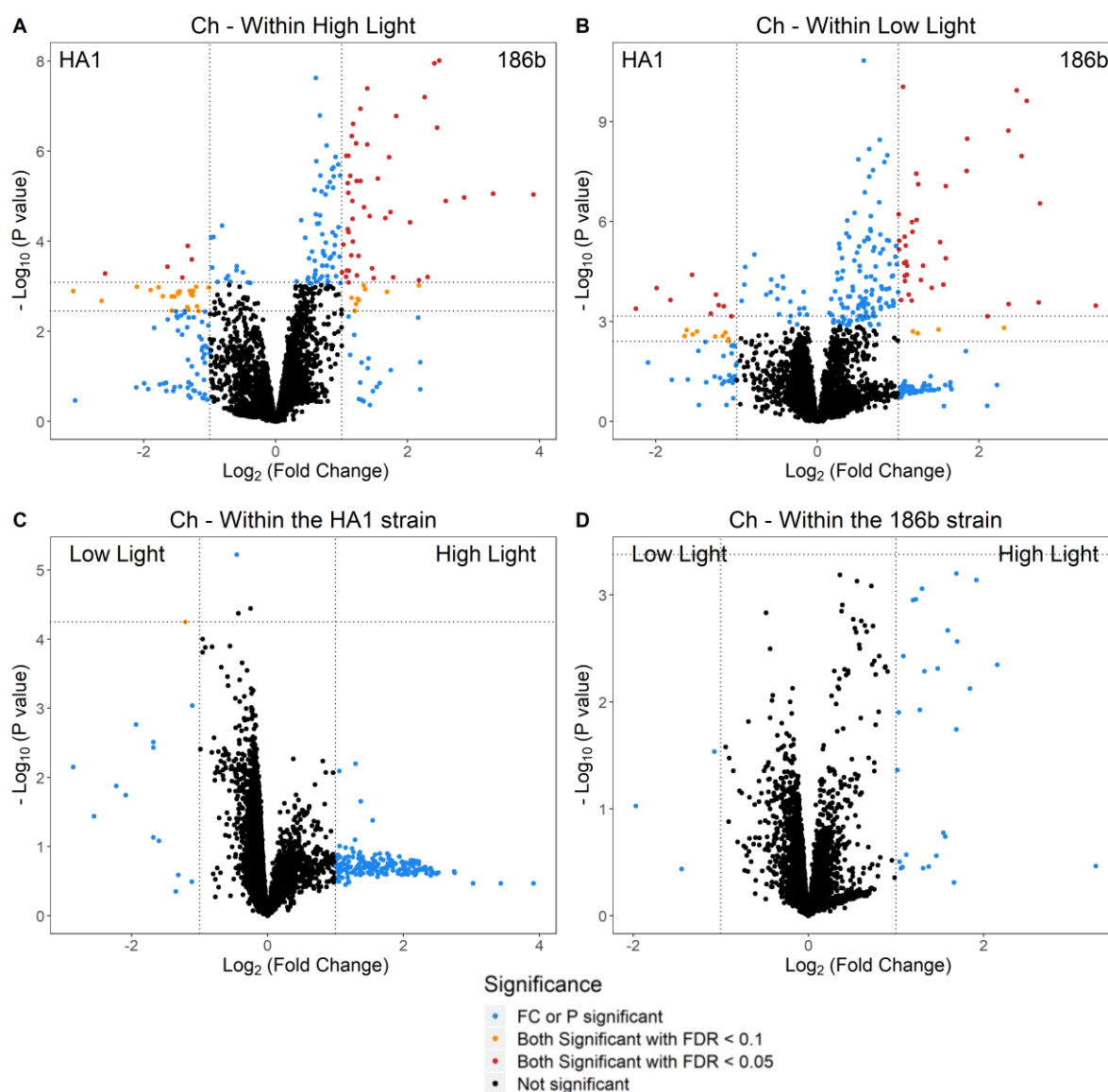


**Figure 2.3. Difference in *Chlorella* global metabolism between strains across light conditions.** Represented as volcano plots with the fold change of each metabolite against its statistical significance. The data points are highlighted at two false discovery rate (FDR) values, and if the Log<sub>2</sub>(fold change) is greater than 1 or less than -1. A.) Comparing the expression between the two strains within the high light condition. B.) Comparing the expression between the two strains within the low light condition. C.) Comparing expression between the two light levels within the HA1 strain. D.) Comparing expression between the two light levels within the 186b strain.

**Table 2.3: The identified metabolites of interest from the *Chlorella* global metabolism.** These metabolites were highlighted by the volcano plot (Figure 2.3) and had significantly higher abundances in either one of the strains or one of the light conditions within the *Chlorella* fraction.

Upregulated in	Condition	Detected Mass	Retention Time	FDR	Pathway	Candidate Compounds	Exact Mass	Adduct	Kegg / Metacyc				
HA1 strain	H & L light	247.2	336	*,**	Alkaloid/quinone	Anapheline	224.1889	Na+	C06183				
						Geranylhydroquinone	246.162	H+	C10793				
		283.3	336	*,**	Fatty acid	Oleate	282.2559	H+	C00712				
	H light	218.2	17	*	Amino acid	L-Glutamylputrescine	217.1426	H+	C15699				
						Alanyl-L-lysine	217.1426	H+	C05341				
		265.3	337	*	Fatty acid	1-Hexadecanol	242.261	Na+	C00823				
		385.2	375	*	Plant Hormone	Gibberellin A36	362.1729	Na+	C11862				
		571.5	435	*	Carotenoid	Methoxyneurosporene	570.4801	H+	C15895				
		589.4	420	*	Carotenoid	Echinenone	550.4175	K+	C08592				
						Anhydrorhodovibrin	566.4488	Na+	C15877				
						Hydroxychlorobactene	550.4175	K+	C15911				
						3-Hydroxyechinenone	566.4124	Na+	C15966				
						591.4	420	*	Carotenoid	Zeaxanthin	568.428	Na+	C06098
										Zeinoxanthin	552.4331	K+	C08590
beta-Cryptoxanthin		552.4331	K+	C08591									
Xanthophyll	568.428	Na+	C08601										
Low Light	HA1 strain	743.5	373	*	Phosphoglyceride	1-18:3-2-trans-16:1-phosphatidylglycerol	742.4785	H+	CPD-2186				
186 Strain	H & L light	105	15	*,**	Central metabolism	Hydroxypyruvate	104.011	H+	C00168				
						Allophanate	104.0222	H+	C01010				
		169	17	**	Central metabolism	2-Oxoglutarate	146.0215	Na+	C00026				
						Phosphoenolpyruvate	167.9824	H+	C00074				
						3-Phosphonopyruvate	167.9824	H+	C02798				
						2-Oxoisocaproate	130.063	K+	C00233				
						3-Methyl-2-oxopentanoate	130.063	K+	C00671				
						2-Dehydropantoate	146.0579	Na+	C00966				
						Coumarin	146.0368	Na+	C05851				
						273.2	395	**	Fatty Acid	16-Hydroxypalmitate	272.2351	H+	C18218
289.3	244	**	Diterpenoid	Kaurenol	288.2453	H+	C11872						

Table 2.3 continued

Upregulated in	Condition	Detected Mass	Retention Time	FDR	Pathway	Candidate Compounds	Exact Mass	Adduct	Kegg / Metacyc
186 Strain	H & L light	337.3	380	**	Fatty acids	13;16-Docosadienoic acid	336.3028	H+	C16533
		607.3	361	**	Chlorophyll	Protoporphyrinogen IX	568.305	K+	C01079
		781.6	471	**	Ubiquinone	3-methoxy-4-hydroxy-5-nonaprenylbenzoate	780.2	H+	CPD-9898
		925.6	359	**	Chlorophyll	Bacterio-pheophytins	888.5765	K+	C05798
	H light	262.1	248	**	Folate	Dihydrobiopterin	239.1018	Na+	C00268
						6-Lactoyl-5;6;7;8-tetrahydropterin	239.1018	Na+	C04244
		323.2	248	*	Photoreception	Vitamin A aldehyde	284.214	K+	C00376
		335.3	372	**	Isoprenoids	Phytol	296.3079	K+	C01389
		751.5	366	**	Ubiquinone	2-Octaprenyl-3-methyl-5-hydroxy-6-methoxy-1;4-benzoquinone	712.5431	K+	C05815
	L light	273.3	268	**	Diterpenoid	Ent-Kaurene	272.2504	H+	C06090

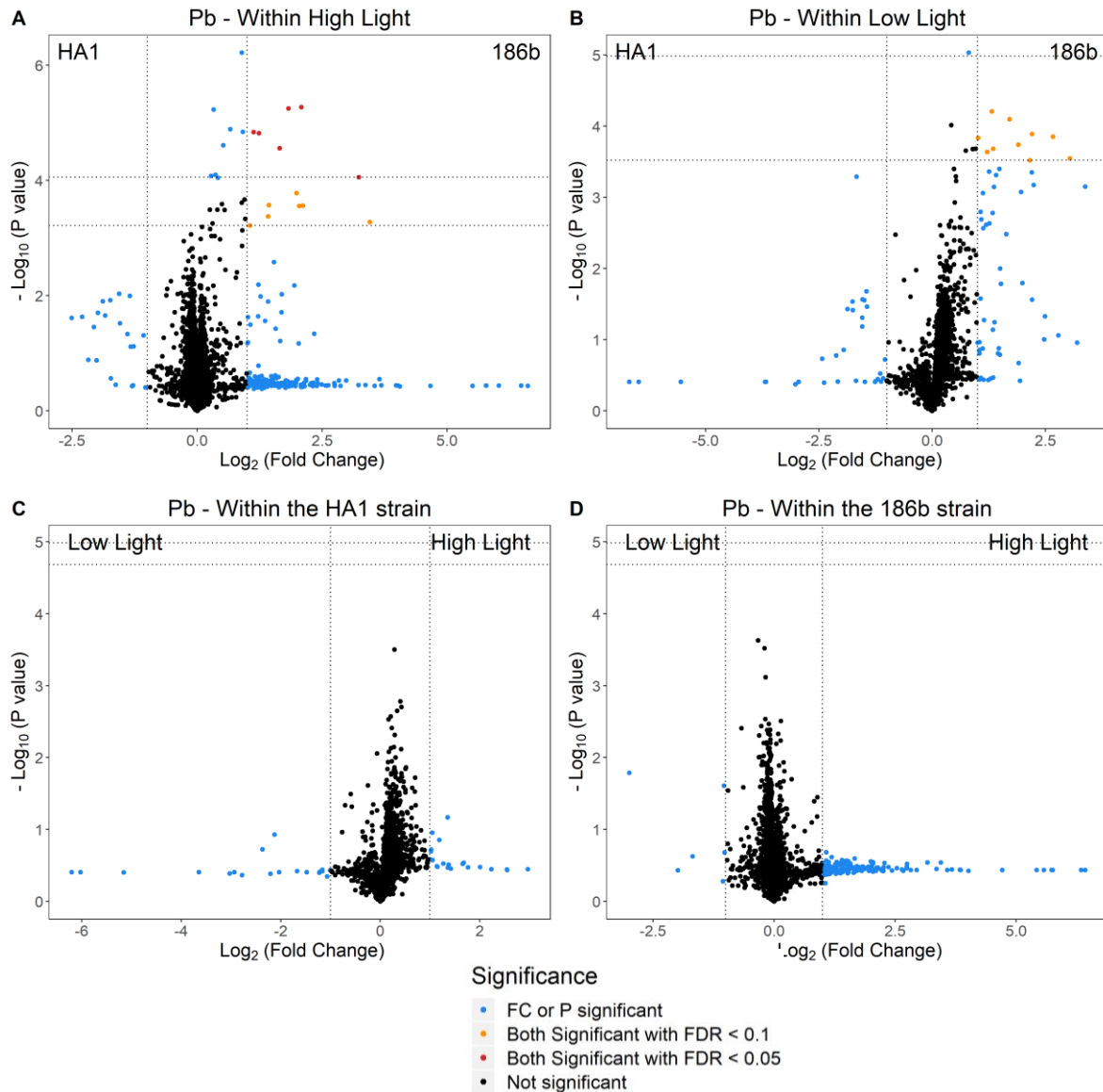


**Figure 2.4. Difference in *P. bursaria* global metabolism between strains across light conditions.** Represented as volcano plots with the fold change of each metabolite against its statistical significance. The data points are highlighted at two false discovery rate (FDR) values, and if the Log<sub>2</sub>(fold change) is greater than 1 or less than -1. A.) Comparing the expression between the two strains within the high light condition. B.) Comparing the expression between the two strains within the low light condition. C.) Comparing expression between the two light levels within the HA1 strain. D.) Comparing expression between the two light levels within the 186b strain.

**Table 2.4: The identified metabolites of interest from the *P. bursaria* global metabolism.** These metabolites were highlighted by the volcano plot (Figure 2.4) and had significantly higher abundances in either one of the strains or one of the light conditions within the *P. bursaria* fraction.

Upregulated in	Condition	Detected Mass	Retention time	FDR	Pathway	Candidate Compounds	Exact mass	Adduct	KEGG	
186 strain	H & L light	124	238	** , *	Vitamins and Cofactors	Niacin	123.032	H+	C00253	
		126	217	** , *	Sulfur metabolism	Taurine	125.0147	H+	C00245	
		170	237	** , *	Amino acid	Glutamate	147.0532	Na+	C00025	
						5-Amino-4-oxopentanoate	131.0582	K+	C00430	
						Glutamate 5-semialdehyde	131.0582	K+	C01165	
		364.2	236	* , *	Antibiotic ?	ACV	363.1464	H+	C05556	
		396.1	237	* , *	Antibiotic ?	Deacetylcephalosporin C	373.0944	Na+	C03112	
						Novobiocic acid	395.1369	H+	C12474	
		H light	352.2	237	*	Plant hormone?	trans-Zeatin riboside	351.1543	H+	C16431
			390.1	237	*	Amino and nucleotide sugar	N-Acetylneuraminate 9-phosphate	389.0723	H+	C06241
	416.1		250	**	Antibiotic ?	Cephalosporin C	415.1049	H+	C00916	
						Chlorobiocic acid	415.0823	H+	C12471	
		434.1	249	*	Antibiotic ?	Novobiocic acid	395.1369	K+	C12474	
	L light	418.2	268	*	Sphingolipid metabolism	Sphingosine 1-phosphate	379.2488	K+	C06124	

The clear differences in global metabolism between the algal strains suggests that they may vary in their photophysiology, which could, in turn, help to explain the light-dependent differences in fitness observed in the reciprocal cross-infection experiment. To test this, I measured several key photochemical parameters in the native and non-native host-symbiont pairings. For two measures of photosynthetic efficiency —  $F_v/F_m$  (the intrinsic efficiency of photosystem II [PSII], Figure 2.5a) and  $\Phi_{PSII}$  (the proportion of the light absorbed by chlorophyll associated with PSII that is used in photochemistry, Figure 2.5b) (Maxwell and Johnson, 2000) — I observed a significant host genotype by symbiont genotype by light environment interaction (for  $F_v/F_m$  ANOVA,  $F_{7,232} = 86.41$ ,  $P < 0.001$ ; for  $\Phi_{PSII}$  nlme model intercept summary ANOVA,  $F_{11,24} = 11.66$ ,  $P < 0.001$  (see Appendix B for full statistical output)). In the HA1 *P. bursaria* host, the pattern of photosynthetic efficiency across the light gradient did not vary with algal strain, whereas in the 186b *P. bursaria* host, the native 186b *Chlorella* showed lower photosynthetic efficiency than the HA1 *Chlorella* at low growth irradiance, but the pattern was reversed at high growth irradiance. Correspondingly, the HA1 *Chlorella* produced more carotenoids at high irradiance than the 186b *Chlorella*, and carotenoids perform a role in photoprotection and can therefore decrease the light energy that reaches the photosystems and thereby limit photosynthesis.

Non-photochemical quenching is used by photosynthetic organisms to safely deal with excess and potentially damaging light energy and was estimated using the normalised Stern-Volmer coefficient (NSV). The NSV response (Figure 2.5c) across the actinic light gradient was significantly affected by host genotype for the intercept value suggesting differences among the host genotypes in their ability to photo-protect algal symbionts (ANOVA,  $F_{1,34} = 4.74$ ,  $P < 0.05$ ). Meanwhile, both symbiont genotype and growth irradiance affected the first coefficient (ANOVA,  $F_{3,32} = 5.56$ ,  $P < 0.01$ ); and symbiont genotype affected the second coefficient (ANOVA,  $F_{1,34} = 8.932$ ,  $P < 0.01$ ) (see Table S2.1 for full statistical output). Higher levels of NSV and steeper NSV reaction norms for the 186b *Chlorella*, particularly in its native host background, are consistent with the greater investment in photosynthetic machinery observed in the metabolome, allowing this genotype to better dissipate excess light energy as heat whilst not compromising photosynthetic efficiency.

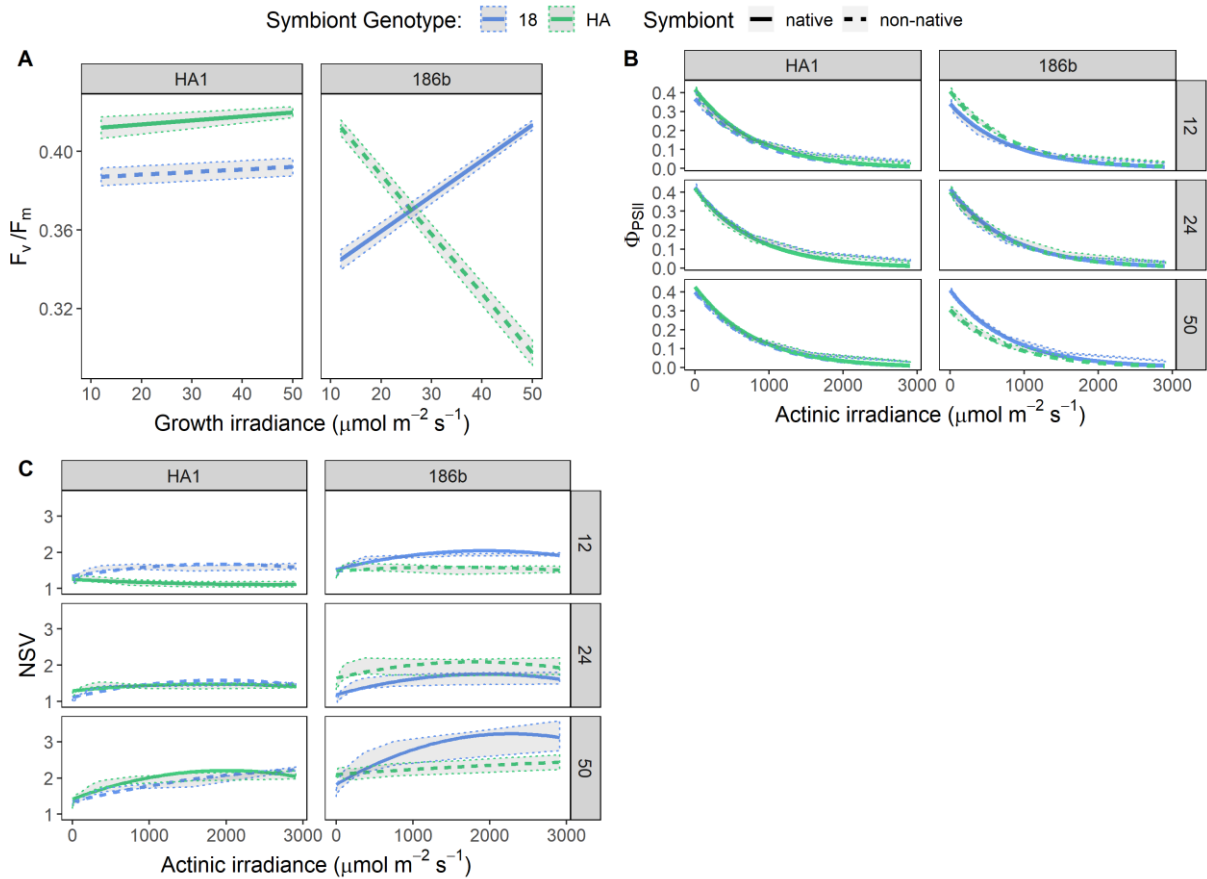


**Figure 2.5. Photophysiology measurements for the native and non-native host-symbiont pairings.** For all subplots, lines represent the mean ( $n=3$ ) and the shaded area denotes  $\pm\text{SE}$ . In each subplot the left-hand panel shows data for the HA1 *P. bursaria* host, the right-hand panel shows data for the 186b *P. bursaria* host containing either native (solid) or non-native (dashed line). Colour denotes *Chlorella* genotype (186b in blue; HA1 in green). A) Estimates of the maximum quantum yield of photosystem II ( $F_v/F_m$ ) across growth irradiances. B) Light-adapted quantum yield of photosystem II ( $\Phi_{\text{PSII}}$ ) across growth irradiances, lines represent exponential decay models using nlme package in R. C.) The normalised Stern-Volmer quenching coefficient ( $\text{NSV} = F_o'/F_v'$ ) across growth irradiances, presented at polynomial models. See Appendix B for model details.

## 2.4 Discussion

In this chapter, I have compared the metabolic mechanisms underpinning two independent origins of the *P. bursaria* - *Chlorella* photosymbiosis using a novel reciprocal metabolomic pulse-chase method. This showed highly conserved patterns of nutrient exchange and utilisation for both the host-derived N in the *Chlorella* genotypes and the symbiont-derived C in the *P. bursaria* genotypes. Consistent with a conserved primary symbiotic nutrient exchange, partner-switched host-symbiont pairings were functional. By directly competing symbiotic hosts against isogenic symbiont-free hosts, I showed that the fitness benefits of symbiosis to hosts increased with light irradiance but varied according to host genotype.

Global metabolism varied more strongly between the *Chlorella* than the *P. bursaria* genotypes and suggested divergent mechanisms of light management. Specifically, the algal symbiont genotypes either produced photo-protective carotenoid pigments at high irradiance or more chlorophyll and ubiquinol, resulting in corresponding differences in photosynthetic efficiency and non-photochemical quenching among host-symbiont pairings. These data suggest that the multiple origins of the *P. bursaria* - *Chlorella* symbiosis relied upon a conserved mechanism of nutrient exchange, whereas other traits linked to photosynthesis and thus the functioning of the photosymbiosis are divergent.

Reciprocal nutrient exchange is central to the *P. bursaria* - *Chlorella* symbiosis, however, whilst the carbon exchange metabolite has long been identified as maltose (Ziesenis et al., 1981), the identity of the nitrogen transfer compound has thus far been unknown. Previous work has reported evidence supporting a role for amino acids (Kato et al., 2006; Kessler and Huss, 1990), but with conflicting information regarding the amino acid responsible and whether there are multiple transfer compounds. For example, a recent genomic comparison found that *P. bursaria* had 4 times higher expression of a glutamine synthetase gene (*GlnA*) than the non-symbiotic *Paramecium caudatum* (He et al., 2019). In contrast, Quispe et al. (2016) found that symbiotic but not free-living *Chlorella* could utilise asparagine and serine, whereas other amino acids, including arginine and glutamine, could be utilised by both symbiotic and free-living *Chlorella*. Although it is unclear that the exchange metabolite need necessarily be one exclusively metabolised by symbiotic algae. In contrast, the metabolomics analysis presented here indicated arginine as the most likely exchange metabolite in both genotypes based on the enrichment pattern, although our first sampled time-point was too late to detect the actual exchange metabolite. Nevertheless, this matches results from Minaeva and Ermilova (2017) who found the arginine concentration within symbiotic *Chlorella* matches that of isolated cells grown on arginine-supplemented medium, while much lower arginine concentrations occur in isolated cells grown on nitrate-based medium. Moreover, arginine supports growth of *Chlorella* as its sole N source (Arnow et al., 1953). The challenge in identifying the nitrogen exchange is that the metabolism of amino acid compounds is closely connected, especially for glutamine and arginine, which makes separating the true transfer compound from up/down-stream effects difficult. Future isotope enrichment experiments will be required to measure the enrichment profile more intensively over a shorter time-period.

This chapter has demonstrated highly conserved patterns of nutrient exchange and utilisation among two independent origins of the *P. bursaria* - *Chlorella* symbiosis, and

further showed that this enables partner-switching between clades. In contrast, *Paramecium* has previously been shown to be unable to establish symbiosis with algae isolated from other host species, such as *Hydra* (Summerer et al., 2007). This suggests that other photosymbioses may use alternative nutrient exchanges, which in turn prevent between-host partner-switches. This could be tested by comparing the nutrient exchange metabolism in other photosymbioses using the methods established here. Partner switching within a host species leads to the potential of symbiont replacement if multiple symbiont strains are locally available. Hoshina et al. (2012) demonstrated that co-infection of multiple algal symbionts within the same *P. bursaria* host cell is possible, using *Chlorella variabilis* and *Micractinium reisseri* (Chlorellaceae). Partner-switching can rescue symbioses from cheater-induced extinction by restoring symbiotic function (Koga and Moran, 2014; Matsuura et al., 2018), enable rapid adaptation to environmental change (Boulotte et al., 2016; Lefèvre et al., 2004), and facilitate niche-expansion (Joy, 2013; Rolshausen et al., 2018; Sudakaran et al., 2017). Local adaptation by symbiont acquisition is likely to occur far faster than by symbiont evolution and may be a general mechanism of ecological innovation in symbioses. For instance, it is believed to have enabled diversification in insect endosymbioses (Sudakaran et al., 2017). Furthermore, symbiont replacement is thought to have been an important factor in plastid evolution (Keeling, 2010) and ‘the shopping bag model’ hypothesises that serial symbiont replacement not only altered symbiont identity, but led to a complement of endosymbiont genes and proteins from multiple origins (Larkum et al., 2007). This arises because the preceding transient symbionts can have transferred genes to the host nucleus, which entangles the lineages. (Dorrell and Smith, 2011; Patron et al., 2006; Stiller et al., 2014).

The biogeographical clades have been defined at a molecular level (Hoshina et al., 2005) but there is very little work on their phenotypic differences beyond their nutritional requirements. Previous work identified strain variation in vitamin B<sub>12</sub> requirement and inorganic nitrogen utilisation of symbiotic *Chlorella* (Kamako et al., 2005; Kessler and Huss, 1990), the latter may be due to divergent genome reduction following specialisation on host-derived organic nitrogen sources. This chapter identified significant differences between the strains across a range of relevant phenotypes, including, their global metabolism and photosynthetic responses. Our data suggest metabolic mechanisms for the observed differences in photosynthetic responses. The 186b *Chlorella* invests more than the HA1 *Chlorella* in the components of its photosystems, through chlorophyll and ubiquinol, providing 186b *Chlorella* with sufficient electron transport machinery to deal with excess light energy. This enables effective non-photochemical quenching, and high NSV values,

without compromising photosynthetic efficiency and results in high fitness of the 186b host-symbiont pairing at high light. This high photosynthetic investment strategy is likely to be costly, however, potentially explaining the higher cost of 186b *Chlorella* symbionts when in the dark. On the other hand, the HA1 *Chlorella* display higher levels of carotenoid pigments at high irradiance, which are likely to facilitate photoprotection and nonphotochemical quenching. However, this occurs at the expense of photosynthetic efficiency because these pigments decrease the amount of light energy that reaches the photosystems, and results in lower fitness of the HA1 symbiont-186b host pairing at high light. This mechanism is only expressed at high irradiance, suggesting that HA1 *Chlorella* adopts a responsive protection strategy to deal with high light intensity. Divergence in the metabolism of light management appears to provide the mechanistic basis for the variation in phenotype among strains and, therefore, may explain strain variation.

Direct measurement of the fitness effect of symbiosis is highly challenging in most associations, and consequently fitness is usually implied indirectly from growth rates or other traits believed to correlate with fitness (Heath and Tiffin, 2007). Here, I used a novel relative fitness assay that directly competes symbiotic hosts against isogenic symbiont-free hosts across a light gradient over several generations. This enables direct estimation of selection coefficients, and therefore of the fitness effects of symbiosis. The HA1 host gained a greater fitness benefit from symbiosis than the 186b host, regardless of symbiont genotype. The HA1 symbiosis is more likely, therefore, to be able to re-establish symbiosis. The 186b symbiosis is particularly costly in dark and low light conditions, and would therefore be likely to only re-establish symbiosis under high light conditions where symbiosis is beneficial. The differences between the strains, therefore, extends to their evolutionary fitness that in turn will determine when these endosymbioses can establish and under which conditions they are maintained.

Partner switching requires compatibility between host and symbiont if it is to rescue the breakdown of symbiosis (Boulotte et al., 2016; Matsuura et al., 2018), but to enable adaptation to new niches (Joy, 2013; Rolshausen et al., 2018) it requires phenotypic variation among symbiont genotypes. In this chapter I have shown that both of these characteristics exist within independent originations of the *P. bursaria* - *Chlorella* symbiosis. The results revealed the metabolic and phenotypic consequences of independent originations of symbiosis and showed that despite these differences, partner switching is possible because of evolutionary convergence to a shared nutrient-exchange. The concurrent divergence in the algae strain photophysiology altered the light-dependent

responses of the symbiosis, and similar genotype-dependent light responses have been observed in other photosymbioses (Abrego et al., 2008; Howells et al., 2012; Ye et al., 2019), suggesting that this may be an important cause of genotype by genotype interactions within photosymbiotic associations. The influence of partner identity on the symbiotic phenotype indicates that symbiont switching could potentially enable adaptation. Multiple independent originations occur in a diverse range of symbioses (Masson-Boivin et al., 2009; Muggia et al., 2011; Sandström et al., 2001) and this may be a critical input of genetic variation that enables adaptation to changing environmental conditions.

## 2.5 Supplementary Figures

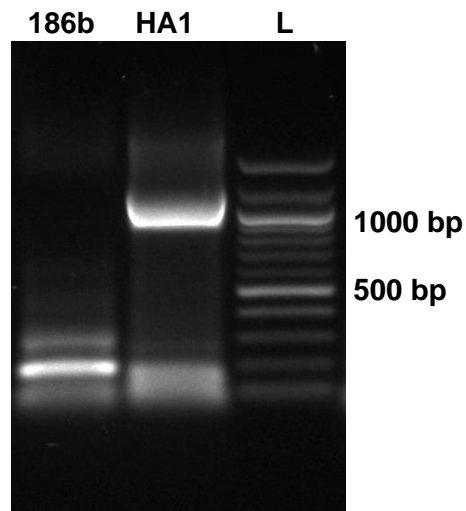


**Figure S2.1. PCR result of the HA1 and 186b *Chlorella* strains.** Overlapping, multiplex primers were used to amplify fragments within the 18S rDNA and ITS region of the *Chlorella* nuclear genome. In this region the ‘American/Japanese’ strains, such as HA1, have had three introns inserted that the ‘European’ strains, such as 186b, lack (Hoshina and Imamura, 2008; Hoshina et al., 2005). The banding patterns here match the expected pattern in that the HA1 fragment is considerably larger than the main fragment of 186b, and both have additional smaller fragments. Shown alongside a 100bp ladder.

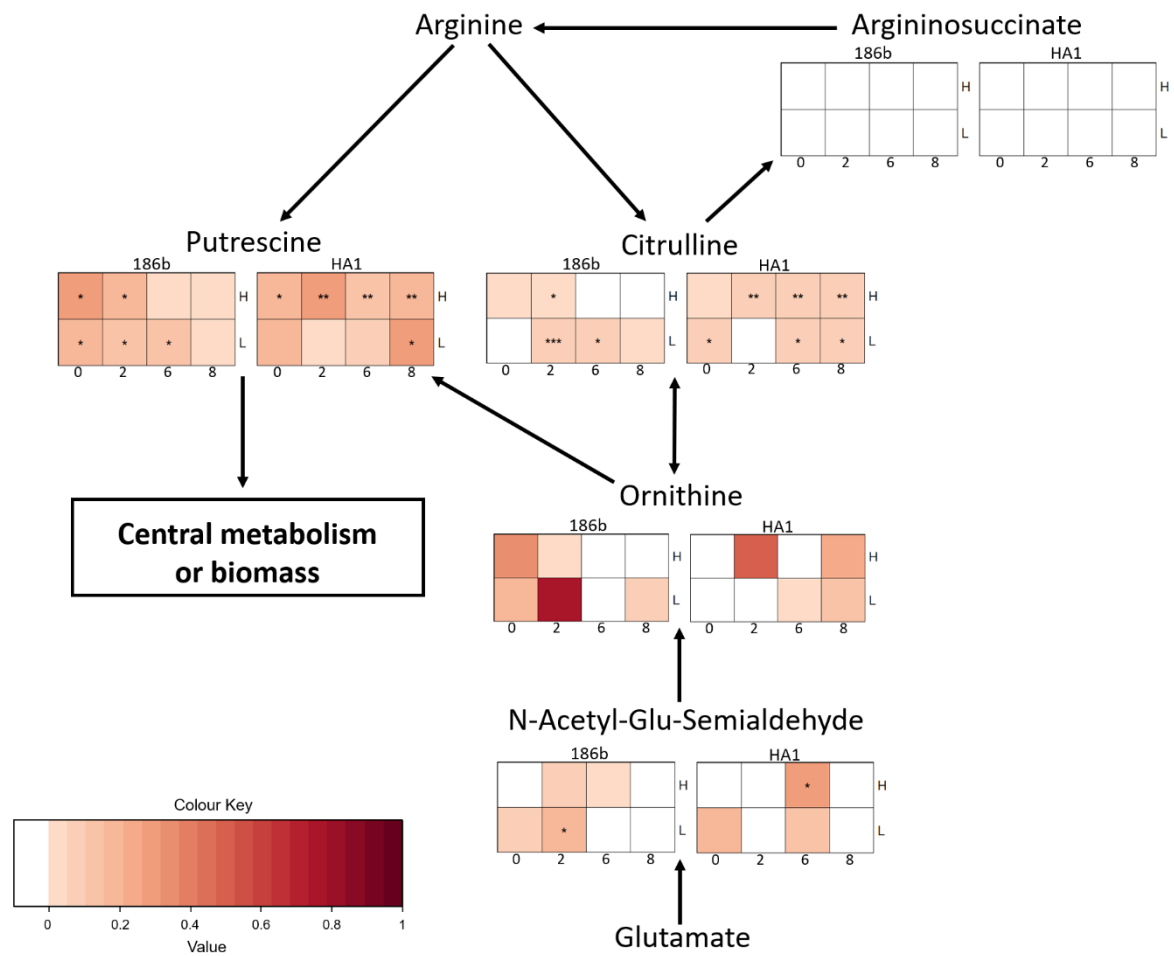


**Figure S2.2.** Schematic pathways diagram of nitrogen enrichment in the arginine amino acid metabolism of the *Chlorella* metabolic fraction. The tables show relative <sup>15</sup>N enrichment across time (hrs) in the two light conditions (H = 50  $\mu\text{E m}^{-2} \text{s}^{-1}$ , L = 6  $\mu\text{E m}^{-2} \text{s}^{-1}$ ). The colour corresponds to the fold change of the enrichment compared to the control, with significance stars indicating the statistical strength of this change. These results are further discussed in the Supplementary Results section.

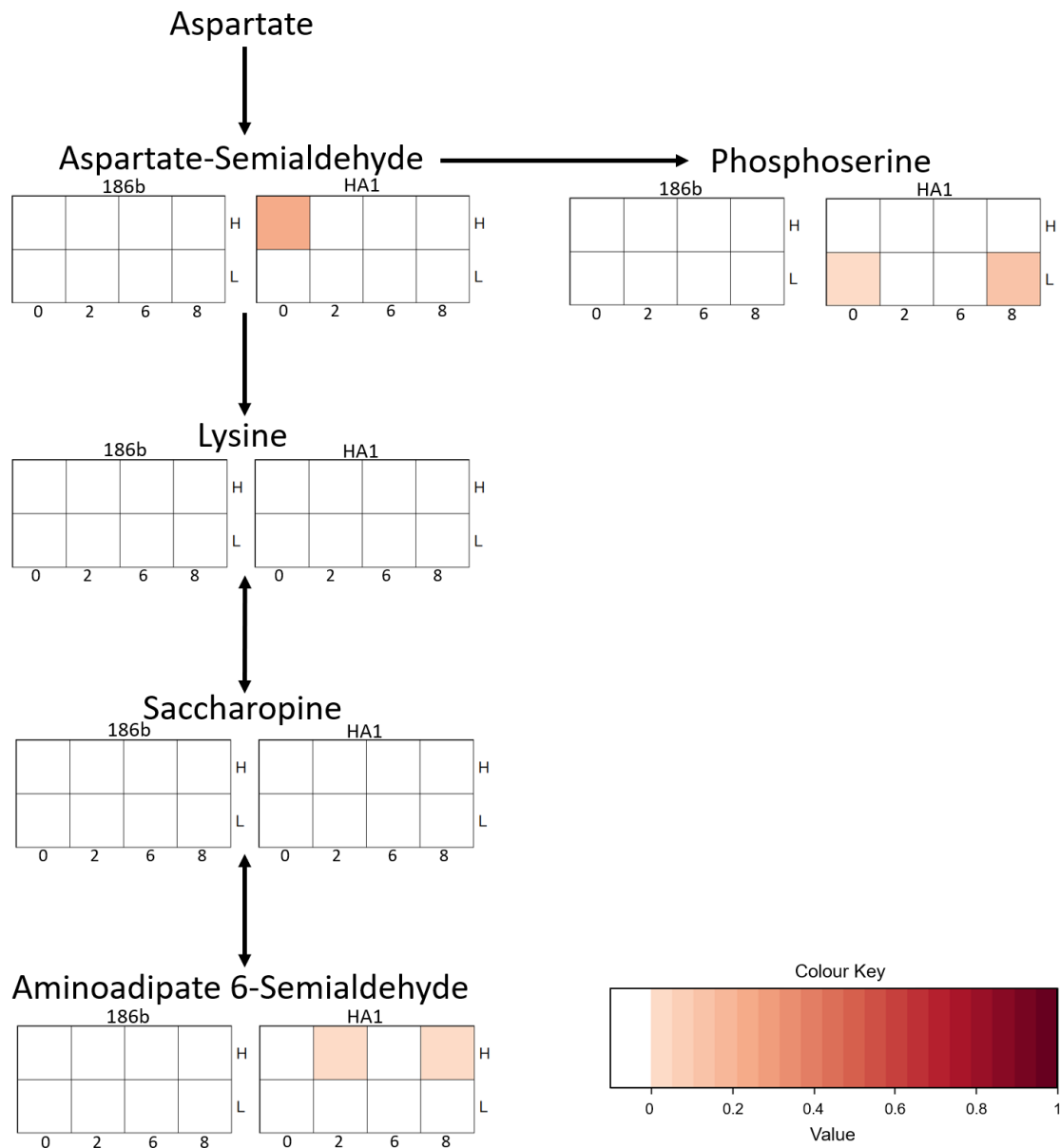


**Figure S2.3. Schematic pathways diagram of nitrogen enrichment in other aspects of amino acid metabolism in the *Chlorella* metabolic fraction.** This data shows the amino acid metabolism that includes lysine, aspartate and serine. The tables show relative  $^{15}\text{N}$  enrichment across time (hrs) in the two light conditions ( $\text{H} = 50 \mu\text{E m}^{-2} \text{s}^{-1}$ ,  $\text{L} = 6 \mu\text{E m}^{-2} \text{s}^{-1}$ ). The colour corresponds to the fold change of the enrichment compared to the control, with significance stars indicating the statistical strength of this change. These results are further discussed in the Supplementary Results section.

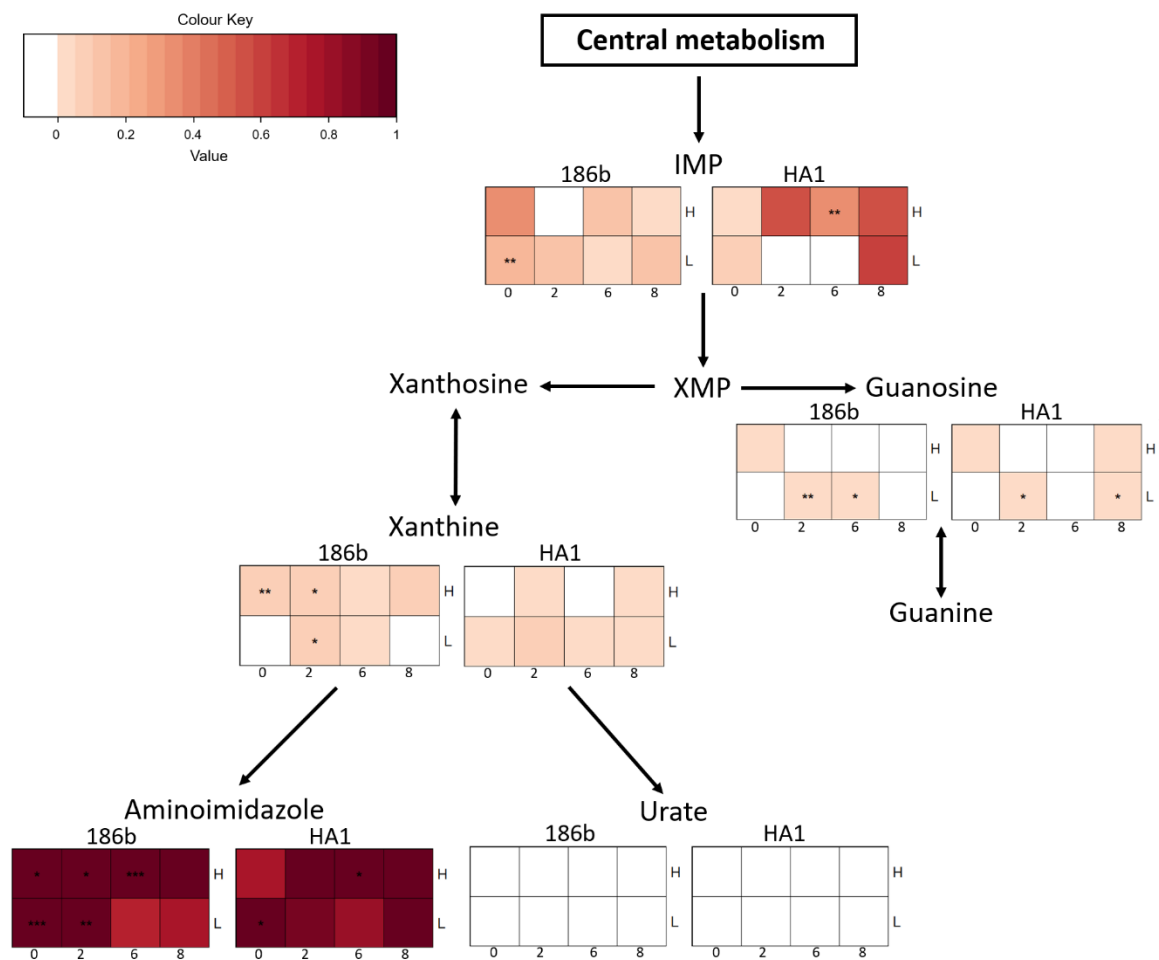


**Figure S2.4. Schematic pathways diagram of nitrogen enrichment in purine metabolism in the *Chlorella* metabolic fraction.** The tables show relative  $^{15}\text{N}$  enrichment across time (hrs) in the two light conditions ( $\text{H} = 50 \mu\text{E m}^{-2} \text{s}^{-1}$ ,  $\text{L} = 6 \mu\text{E m}^{-2} \text{s}^{-1}$ ). The colour corresponds to the fold change of the enrichment compared to the control, with significance stars indicating the statistical strength of this change. These results are further discussed in the Supplementary Results section.

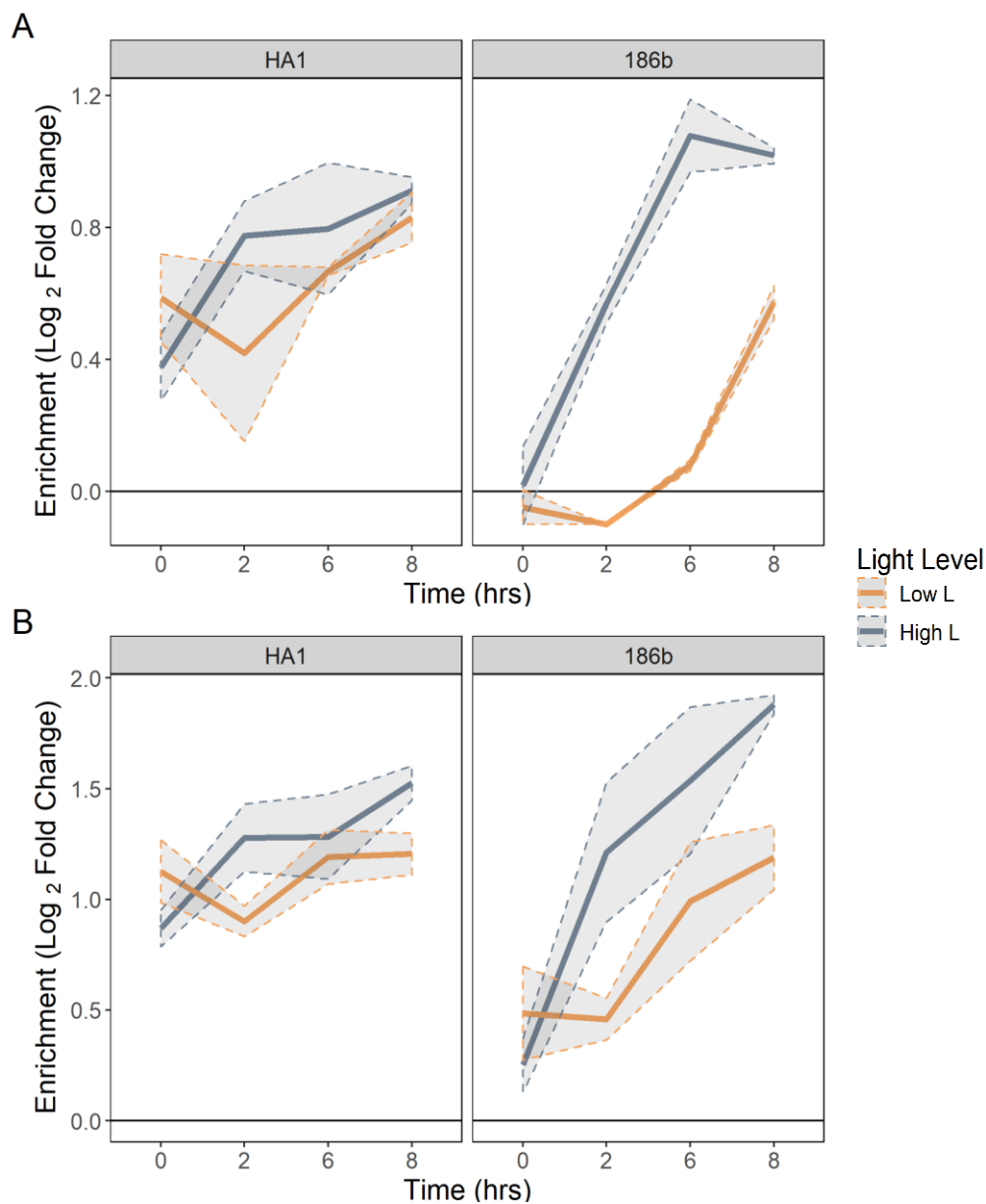


**Figure S2.5. The interaction of light intensity and strain identity on the <sup>13</sup>C enrichment profile of carbohydrate metabolites from the *P. bursaria* fraction.** For all panels, the enrichment value is the Log<sub>2</sub> of the Fold Change in enrichment of the <sup>13</sup>C labelled fraction compared to the control, presented as the mean (n=3) ±SE. The low light level refers to 6 μE m<sup>-2</sup> s<sup>-1</sup> and the high light to 50 μE m<sup>-2</sup> s<sup>-1</sup>. A) Profile of 689.2 m/z, 16 rt, Glycogen. B) Profile of 365.1 m/z, 16 rt, a disaccharide, thought to be sucrose.

## 2.6 Supplementary Results

### *Metabolic pathway analysis*

Given that the low molecular weight compounds in the results of the  $^{15}\text{N}$  co-enrichment in *Chlorella* (Table S2.1) were almost exclusively amino acid or purine related, I focused on these pathways for a further targeted approach. Key compounds of these pathways were selected and searched for in the metabolite dataset. Overall, 16 potential components of amino acid metabolism were identified and 10 potential components of purine metabolism. To follow the flow of enriched nitrogen in these pathways, the enrichment profile of these compounds was calculated, and the results plotted as heatmaps, based on the method used by Austen et al. (In Press).

Within amino acid metabolism the nitrogen enrichment is focused downstream from arginine (Figure S2.2); ornithine, putrescine and citrulline possessed clear enrichment profiles while upstream compounds such as arginosuccinate had no detectable enrichment. Furthermore, other aspects of amino acid metabolism, such as that centred around aspartate, serine or lysine (Figure S2.3), showed little and inconsistent enrichment. Unfortunately, I could not identify a candidate compound for arginine to test if it had the enrichment profile of a transfer molecule (predicted to be a very high initial enrichment that then substantially decreased over time). Such a pattern was not seen for any compound, I suggest, therefore, that our first timepoint was not early enough to capture the initial enrichment events involving the transfer compound itself.

Within purine metabolism, the nitrogen enrichment occurred both up and downstream of the purine bases (Figure S3.4). The enrichment upstream of the purine bases indicates that enriched nitrogen is entering this pathway from the amino acid of central metabolism. Based on this pattern, I believe that the purine pathway is a site of secondary enrichment and it reveals that purine-derivatives present a substantial nitrogen demand.

# Chapter 3

## Light-dependent stress-responses underlie host-symbiont genotypic specificity in a photosymbiosis

### 3.1 Introduction

Photosymbioses are mixotrophic interactions whereby a heterotrophic host is provided with carbon fixed by intracellular photosynthetic microalgae (Decelle, 2013; Esteban et al., 2010). This important energetic transition often leads to photosymbioses performing unique, keystone functional roles in ecosystems. For example, the association between *Symbiodinium* and cnidarian hosts form photosynthetic coral that are the foundation of reef ecosystems (Baker, 2003). Photosymbioses are widely distributed throughout the tree of life, and occur both within microbial hosts (Keeling, 2013; Lane and Archibald, 2008) and metazoans (Venn et al., 2008). The nutritional exchange provides the primary benefit of photosymbioses and the photosynthetic partner normally receives nitrogen and potentially other key nutrients in return for the fixed carbon they provide. As a result of this exchange photosymbioses are often assumed to be mutualistic, but detailed experimental studies have reported instances of host exploitation (Decelle, 2013; Lowe et al., 2016). Photosymbioses are hugely important, but there are many aspects of these relationships we do not fully understand. In particular, we urgently need to understand how genetic variation affects the outcome of these host-symbiont interactions, since this is the fuel for their coevolution (Heath and Stinchcombe, 2014).

Genetic variation for the outcome of symbiosis, either in symbiotic traits or fitness, can be quantified as the host genotype by symbiont genotype interaction ( $G^H \times G^S$ ), also termed intergenomic epistasis (Heath, 2010).  $G^H \times G^S$  interactions have been reported for a wide taxonomic range of symbioses. For example, the symbiont density of *Wolbachia* in its bean beetle host is affected by both host genotype and *Wolbachia* genotype (Kondo et al., 2005); transmission success of an oomycete pathogen in *Arabidopsis thaliana* depends on the specific combinations of host and parasite strain (Salvaudon et al., 2005); and aphid

performance on *Trifolium* is dependent on the genotype of its nutritional endosymbiont *Regiella insecticola* and aphid genotype (Ferrari et al., 2007).

It is well-established that the dynamics and outcomes of coevolution depend on the environmental context (the Geographic Mosaic theory) (Thompson, 2005). This is because the outcome of host-symbiont interaction is frequently environmentally context dependent, causing a host genotype by symbiont genotype by environment ( $G^H \times G^S \times E$ ) interaction. While  $G^H \times G^S \times E$  interactions are common in host-parasite relationships (e.g., Wendling et al., 2017; Zouache et al., 2014), they are of particular importance in beneficial symbioses because variation along environmental axes related to the symbiotic exchange can shift the nature of the interaction along the parasitism-mutualism continuum. In both plant-mycorrhizae (Pieulell et al., 2008) and plant-rhizobia (Heath et al. 2010; Heath & Tiffin 2007) interactions, extensive variation exists in the host-symbiont response to environmental conditions. For example, Heath et al. (2010) reported variation in nodulation between N-fixing rhizobia and legume strains in response to environmental nitrate, such that increasing nitrate led some genotype combinations to reduce nodulation, others to increase nodulation, while some were unaffected. This case illustrates that the environment is fundamental to the function of symbioses, and, in certain combinations of environment and genotypes, the rhizobia – legume symbiosis was shifted to such an extent that it was more advantageous for the plant to partially dissociate than to continue the relationship. One consequence of context dependence is that there is likely to be no universally optimal partner, and consequently symbiotic relationships are evolutionarily dynamic (Heath and Tiffin, 2007).

Stress responses play an important role in the fitness of photosymbioses due to their exposure to potentially-damaging light energy (Venn et al., 2008; Yakovleva et al., 2009). Photo-oxidative stress is a by-product of photosynthesis that can cause damage to cells through reactive oxygen species (ROS) if it is not mitigated (Murata et al., 2007). Stress tolerance is likely to show genetic variation among host-symbiont associations. In coral - *Symbiodinium* endosymbioses, the symbiont genotype primarily determines the thermal and light tolerance of the association (Abrego et al., 2008; Howells et al., 2012), although the host genotype does also influence this process (Baird et al., 2009; Loya et al., 2001). If the stress tolerance of the symbiont is exceeded, then the symbiosis breakdowns and coral bleaching occurs (Weis, 2008). It has, however, been theorised that coral bleaching may potentially be adaptive as it provides an opportunity for the host to acquire a new symbiont genotype that is better adapted and more tolerant of the prevailing environmental

conditions (Buddemeier and Fautin, 1993; Gilbert et al., 2010). In the *Hydra - Chlorella* photosymbiosis, although algal genotype had some effect, the threshold of thermal tolerance was determined by the host genotype (Ye et al., 2019). In the microbial photosymbiosis between the heterotrophic ciliate *Paramecium bursaria* and the green algae *Chlorella sp*, symbiotic hosts have been shown to have lower photo-oxidative stress and lower mortality rates than aposymbiotic cells at high UV (Hörtnagl and Sommaruga, 2007; Summerer et al., 2009). Stress tolerance can therefore be affected by both partners of the photosymbiosis to varying degrees, but host-symbiont pairings that lack sufficient combined stress tolerance are unlikely to survive and will be prone to breakdown.

Despite the high level of genetic variation within the *P. bursaria - Chlorella* association, owing to the multiple independent originations of the symbiosis (Hoshina and Imamura, 2008; Summerer et al., 2008), there have been no systematic studies of the genotype by genotype by environment interaction within this endosymbiosis. Furthermore, the photo-oxidative stress response has not been studied in detail and has not been compared across strains nor across light gradients. Metabolomics can be used to identify the metabolic markers of stress while also examining central metabolism, and therefore this technique provides a tractable experimental system with which to study genetic variation within a photosymbiosis.

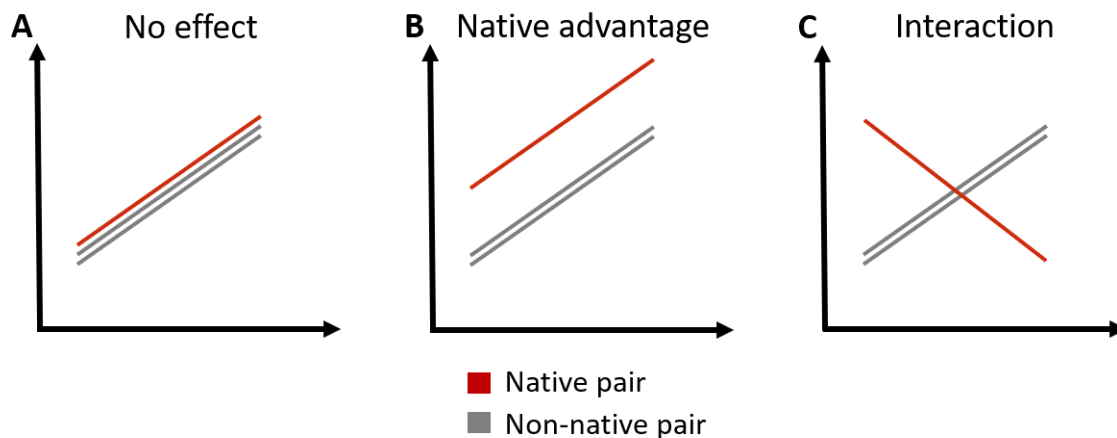


**Figure 3.1. Conceptual diagrams of potential outcomes when comparing native and non-native host-symbiont pairings.** The colour of the line denotes whether the symbiont is the native or non-native symbiont. A) Shows the ‘no effect’ outcome when there is no significant difference between native and non-native pairs. B) Shows the ‘native advantage’ outcome whereby the native pair has the advantage in all conditions. C) Shows the ‘interaction’ outcome where the native pair is advantageous in some conditions, but disadvantageous in others.

In this chapter, I investigated the genetic variation in the *P. bursaria* - *Chlorella* endosymbiosis using a reciprocal cross-infection experiment coupled with metabolomics. Potential outcomes of the cross-infections are visualised in Figure 3.1 and show how comparisons between the native and non-native host-symbiont pairs can reveal the degree of partner specificity. If, for instance, the host is a generalist then there should be no effect of symbiont identity (Figure 3.1a), while if the host is a specialist it may be that the native symbiont is always the most advantageous (Figure 3.1b) or that the benefit-to-cost ratio of the different symbionts is dependent on environmental conditions (e.g. a  $G^H \times G^S \times E$  interaction)(Figure 3.1c). I assessed the outcome of the cross-infections using phenotypic assays of host-symbiont growth rate and symbiont load, and investigated the global differences in metabolism using ESI-ToF untargeted metabolomic analysis. The results revealed a  $G^H \times G^S \times E$  interaction for the host-symbiont growth rate and the regulation of symbiont load. Moreover, I observed metabolic differences between the symbionts that offer potential mechanistic bases for host-symbiont specificity. Chiefly, that contrasting stress responses between the symbiont genotypes played an important role and may have altered the benefit-to-cost ratio of symbiosis for the host. I discuss how the differences in stress management may influence host-symbiont specificity and the implications for partner switching.

## 3.2 Materials & Methods

### *Cultures & Strains*

*P. bursaria* – *Chlorella* cultures were maintained under the conditions described in Chapter 2. The three natural strains used in this chapter were: 186b (CCAP 1660/18) obtained from the Culture Collection for Algae and Protozoa (Oban, Scotland), and HA1 and HK1 isolated in Japan and obtained from the Paramecium National Bio-Resource Project (Yamaguchi, Japan).

### *Cross infection*

The separation of symbiotic partners was achieved by the method described in Chapter 2. Once separated, the three aposymbiotic *P. bursaria* strains were re-infected by adding a colony of *Chlorella* from the plate stocks derived from the appropriate strain. This was done with all three of the isolated *Chlorella* strains to construct all possible host-symbiont genotype pairings (n=9). The re-establishment of endosymbiosis was confirmed on the

microscope and took between 2-6 weeks. Over the process, cells were grown at the intermediate light level of  $12 \mu\text{E m}^{-2} \text{ s}^{-1}$  and were given bacterized PPM weekly.

#### *Diagnostic PCR*

The correct algae genotype within the cross-infections was confirmed using diagnostic PCR. The *Chlorella* DNA was extracted by isolating the *Chlorella* and then using a standard 6% Chelex100 resin (Bio-Rad) extraction method. A nested PCR technique with overlapping, multiplex Chlorophyta specific primers were used as described by Hoshina et al. (2005). Standard PCR reactions were performed using Go Taq Green Master Mix (Promega) and  $0.5 \mu\text{mol L}^{-1}$  of the primer. The thermocycler programme was set to:  $94^\circ\text{C}$  for 5min, 30 cycles of ( $94^\circ\text{C}$  for 30sec,  $55^\circ\text{C}$  for 30sec,  $72^\circ\text{C}$  for 60sec), and 5 min at  $72^\circ\text{C}$ .

#### *Growth rate*

Growth rates of the symbioses were measured across a light gradient. The cells were washed and concentrated with a  $11 \mu\text{m}$  nylon mesh using sterile Volvic and re-suspended in bacterized PPM. The cultures were then split and acclimated to their treatment light condition (0, 12, 24, &  $50 \mu\text{E m}^{-2} \text{ s}^{-1}$ ) for five days. The cultures were then re-suspended in bacterized PPM to a target cell density of  $150 \text{ cell mL}^{-1}$ . Cell densities were measured at 0, 24, 48 and 72 hours by fixing  $360 \mu\text{L}$  of each cell culture, in triplicate, in 1% v/v glutaraldehyde in 96-well flat bottomed micro-well plates. Images were taken with a plate reader (Tecan Spark 10M) and cell counts were made using an automated image analysis macro in ImageJ v1.50i (Schneider et al., 2012).

#### *Symbiont load*

The symbiont load was measured in cultures derived from the growth rate experiment so that the data could be integrated between the two measurements. Triplicate  $300 \mu\text{l}$  samples of each cell culture were taken from 72 hour cultures for flow cytometry analysis. Host symbiont load was estimated using a CytoFLEX S flow cytometer (Beckman Coulter Inc., CA, USA) by measuring the intensity of chlorophyll fluorescence for single *P. bursaria* cells (excitation 488nm, emission 690/50nm) and gating cell size using forward side scatter; a method established by Kadono et al. (2004). The measurements were calibrated against 8-peak rainbow calibration particles (BioLegend), and then presented as relative fluorescence to reduce variation across sampling sessions.

### *Metabolomics*

Cultures of the symbiotic pairings were washed and concentrated with a 11 $\mu$ m nylon mesh using sterile Volvic and re-suspended in bacterized PPM. The cultures were then split and acclimated at their treatment light condition (0, 12 & 50  $\mu$ E m<sup>-2</sup> s<sup>-1</sup>) for seven days. The metabolomic fractions of the *P. bursaria* and *Chlorella* were separated with the method described in Chapter 2. After which the *Chlorella* fraction samples were already in methanol, but the *P. bursaria* fraction samples had then to be diluted by 50% with methanol. Metabolic profiles were recorded using ESI ToF-MS, on the Qstar Elite with automatic injection using Waters Alliance 2695 HPLC (no column used), in positive mode. This is an established high-throughput method with a large mass range (50 Da to 1000 Da).

Mass spectrometry settings:

Polarity:	positive
Ion Spray voltage:	4.2 kV
Declustering potential:	120 V
Focusing potential:	265 V
Source temperature:	200°C
Gas Flow:	40 ml min <sup>-1</sup>
Solvent:	50:50 methanol to water at flow rate 40 $\mu$ l min <sup>-1</sup>
Injected volume:	10 $\mu$ l

The processing was performed using in-house software Visual Basic macro 216 (Overy et al., 2005), which combined the spectra across the technical replicates by binning the crude m/z values into 0.2-unit bins. The relative mass abundances (% total ion count) for each bin was summed. Pareto scaling was applied to the results, and the data was then analysed by principal component analysis using SIMCA-P software (Umetrics). When treatment-based separation was observed, supervised orthogonal partial least squares discriminant analysis (OPLS-DA) separation was then performed using the discriminatory treatment with the SIMCA-P software.

For the pair-wise comparison of the metabolic profiles of interest, the log<sub>2</sub>(Fold Change) of relative abundance between the compared samples was calculated per metabolite. T-tests were performed on the relative abundance of the two samples, and the P-values were plotted against the log<sub>2</sub>(Fold Change) in the volcano plots.

### *Identification of significant masses*

Masses of interest were annotated using the initial identifications from the in-house software program and further comparisons against KEGG (<https://www.genome.jp/kegg/>) (Kanehisa and Goto, 2000; Kanehisa et al., 2019) and Metlin (<https://metlin.scripps.edu>) (Smith et al., 2005) databases. The Metabolomics Standards Initiative requires two independent measures to confirm identity, this analysis only used one measure (accurate mass) and therefore, meets only the level 2 requirements of putative annotated compounds.

### *Data Analysis*

Statistical analyses were performed in R v.3.6.1 (R Core Team, 2018) and all plots were produced using package ggplot2 (Wickham, 2016). Details of the statistical methods used are within the supplementary statistics table.

## 3.3 Results

Using three strains of the *P. bursaria* - *Chlorella* endosymbiosis representing both the ‘European’ (the 186b strain) and ‘American/Japanese’ (the HA1 and HK1 strains) clades, I constructed all possible host-symbiont genotype pairings ( $n = 9$ ) and confirmed correct algal identity by diagnostic PCR (Figure S3.1). To determine host-genotype versus symbiont-genotype contributions to host-symbiont growth performance I measured the growth reaction norm of each host-symbiont pairing across a light gradient (Figure 3.2). All host-symbiont pairings showed the classic photosymbiotic reaction norm, such that growth rate increased with irradiance, but I observed a significant host-genotype by symbiont-genotype by light environment ( $G^H \times G^S \times E$ ) interaction for host-symbiont growth rate (ANOVA,  $F_{17,162} = 18.81$ ,  $P < 0.001$ ). This was driven by contrasting effects of symbiont genotype on growth in the different host backgrounds across light environments. In the HK1 and HA1 host-backgrounds similar growth reaction norms with light were observed for each symbiont genotype, whereas in the 186b host background the growth reaction norm varied according to symbiont genotype. Interestingly, the native 186b host-symbiont pairing had both the lowest intercept and the highest slope, indicating that in the 186b host background the native symbionts were costlier in the dark yet more beneficial in high-light environments than non-native symbiont-genotypes.

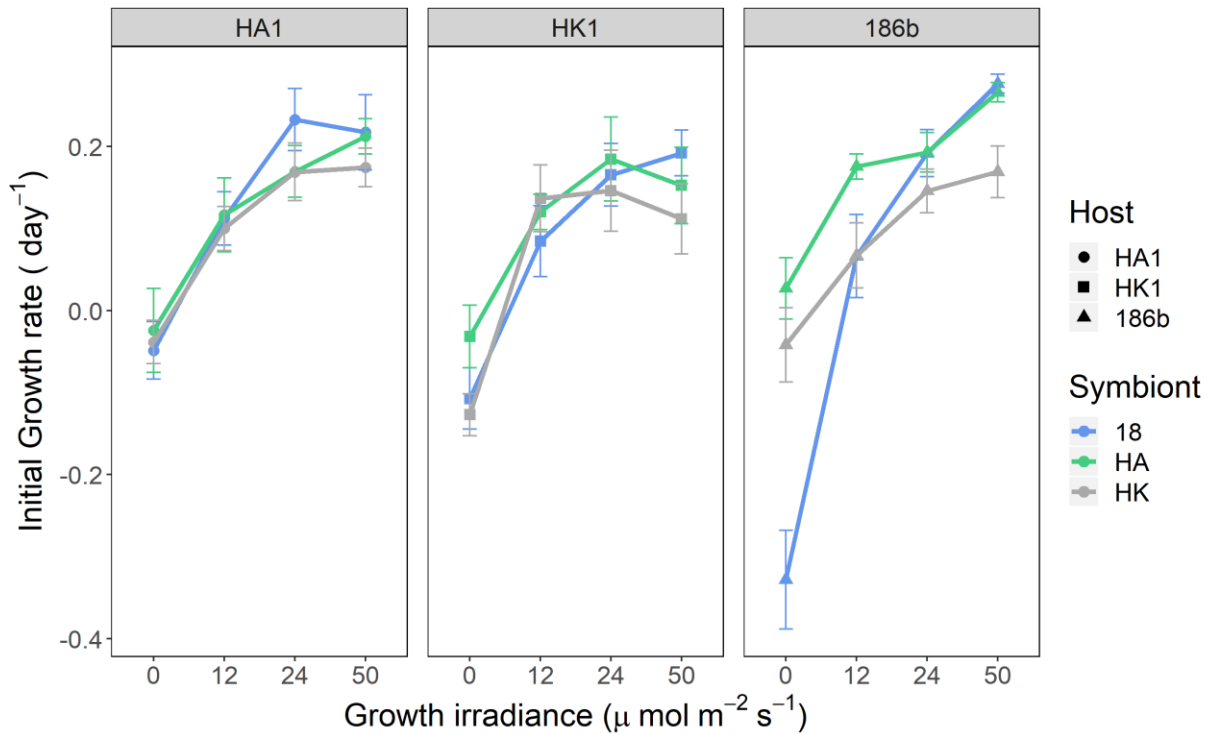


**Figure 3.2. Initial growth rates of the host-symbiont pairings across a light gradient.** The data points show the mean ( $n=3$ ) initial growth rate  $\pm$ SE. Each panel shows the data for a specific genotype of *P. bursaria* host and host genotype is also represented by the shape of the data points. The symbiont genotypes are distinguished by colour.

*P. bursaria* host cells regulate their native symbiont load according to light irradiance to maximise the benefit-to-cost ratio of symbiosis, such that symbiont load peaks at low irradiance and is reduced both in the dark and at high irradiance (Dean et al., 2016; Lowe et al., 2016). To test if regulation of symbiont load varied among host-symbiont pairings, I measured symbiont load across a light gradient as the intensity of single-cell fluorescence by flow cytometry (Figure 3.3). All host-symbiont pairings showed the expected unimodal symbiont load curve with light, but I observed a significant  $G^H \times G^S \times E$  interaction for symbiont load (ANOVA,  $F_{17,162} = 3.78$ ,  $P < 0.001$ ). Polynomial models were used to distinguish how the symbiont load curves varied among the host-symbiont pairings across the light gradient (plotted in Figure 3.3). The model coefficients showed a significant  $G^H \times G^S$  interaction (ANOVA,  $F_{8,36} = 27.22$  (the intercept); 8.58 (first coefficient); 6.09 (second coefficient),  $P < 0.001$  (see Appendix C for full statistical output)). Whereas, in the HA1 host similar symbiont load reaction norms were observed for each symbiont genotype, for the HK1 and 186b host backgrounds the form of the symbiont load reaction norms varied according to symbiont genotype. In the HK1 host the magnitude of the symbiont load (Y at maximum) varied by symbiont genotype, such that higher symbiont loads were observed

for the native compared to the non-native symbiont-genotypes. In the 186b host, peak symbiont load (X at maximum) occurred at different light levels according to symbiont genotype, such that for the native symbiont the symbiont load curve peaked at a higher light intensity when compared to the non-native symbionts. This suggests that the HK1 and 186b host-genotypes discriminate among symbiont-genotypes, and then regulate symbiont load accordingly.

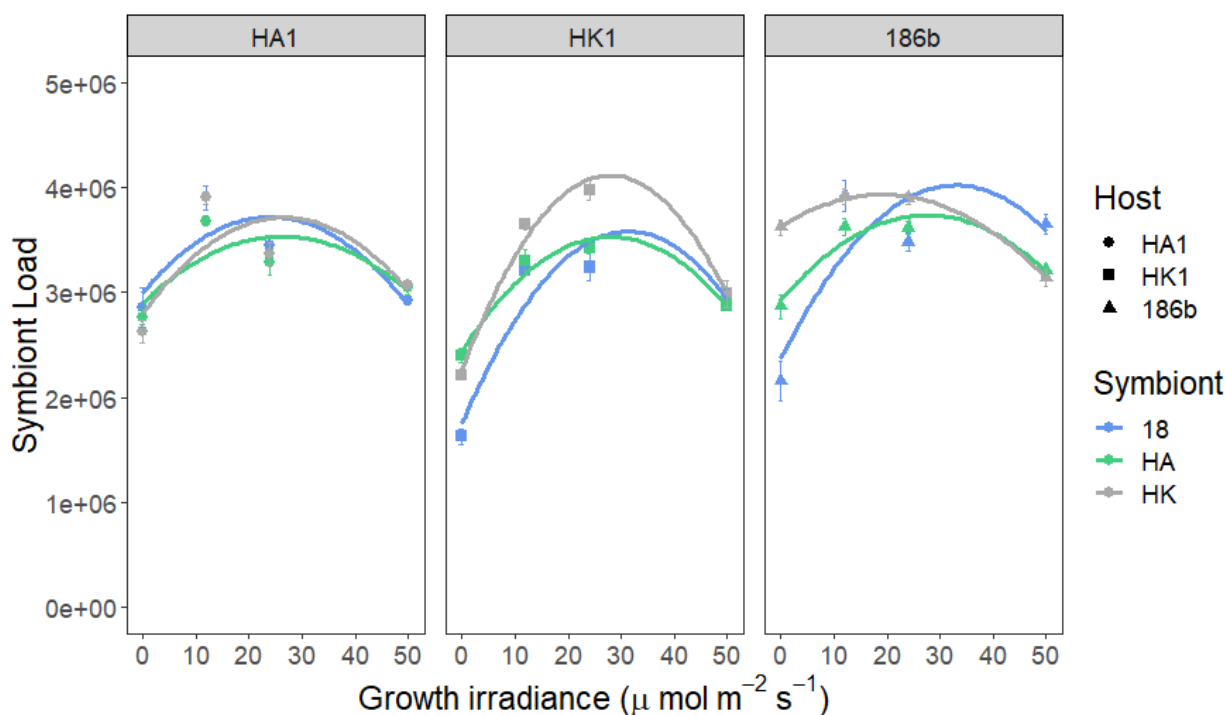


**Figure 3.3. Symbiont load of the host-symbiont pairings across a light gradient.** The data points show the mean ( $n=3$ ) symbiont load, measured as relative chlorophyll fluorescence,  $\pm$ SE. The lines show the polynomial models the data was modelled by; for full model details see Appendix C. Each panel shows the data for a specific genotype of *P. bursaria* host and host genotype is also represented by the shape of the data points. The symbiont genotypes are distinguished by colour.

To investigate the potential metabolic mechanisms underlying the observed  $G^H \times G^S \times E$  interactions for host-symbiont growth rate and symbiont load, I performed untargeted global metabolomics with ESI-ToF-MS independently for the host and symbiont metabolite fractions for each host-symbiont pairing across the light gradient. Across the entire dataset, for both the host and symbiont metabolite fractions, principal component analysis revealed an overall pattern of clustering by light level (OPLS-DA Figure 3.4, PCA Figures S3.2). This suggests that light irradiance was the primary driver of differential metabolism for both host and symbiont, with broadly similar metabolic responses to light observed across all host-symbiont pairings. This shared response to light intensity was

further investigated by identifying the metabolites associated with either the dark or high light condition within the *Chlorella* fraction (Figure S3.4 and Table S3.1). This revealed a range of candidate symbiont metabolites that varied with light intensity. Metabolomics has an inherent trade-off between the confidence of the identifications and the extent the analysis is untargeted and unbiased. To take a truly untargeted approach with this many samples I did not use chromatography separation and therefore the identifications here are putative. The putative identifications associated with the shared dark response included amino acids and components of pyruvate and glycolysis metabolism. In addition, putative fatty acid and heme synthesis compounds were identified and these are known to be aspects of the non-photosynthetic roles of plastids (Barbrook et al., 2006), which suggests the *Chlorella* symbionts may fulfil additional functions, beyond carbohydrate supply, for their host. In contrast, the putative metabolites associated with the shared high-light response included plant hormones, a purine, carotenoids, carbohydrates and chlorophyll, indicating that photosynthesis and photoprotection characterised *Chlorella* metabolism in high light.

However, host-dependent differences in the metabolism of symbiont-genotypes could be detected. For the symbiont metabolite fraction, subset by host-genotype, I observed native versus non-native clustering of symbiont metabolism only when associated with the 186b host-genotype (PCA Figures 3.5, OPLS-DA Figure S3.3). This is consistent with the greater phenotypic differences in growth and symbiont load observed among host-symbiont pairings with the 186b host-genotype compared to with either the HK1 or HA1 host-genotypes.

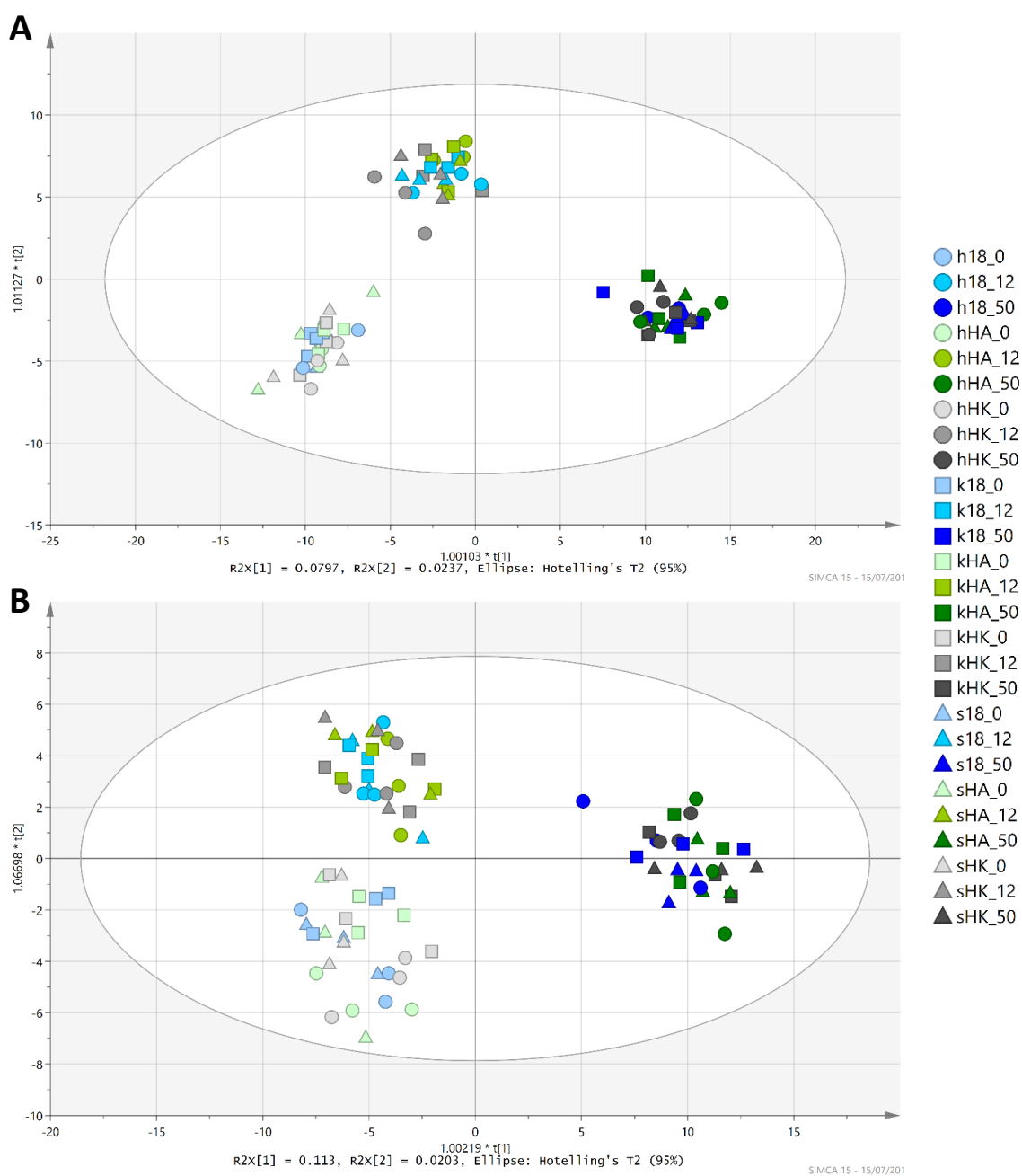


**Figure 3.4. The clustering of the metabolic fractions by light.** These OPLS-DA plots show the metabolic fractions separated by light intensity, following clear PCA clustering by light (see PCA plots S3.2). Each point represents the metabolic profile of a sample; with the shape denoting the *P. bursaria* host genotype, the colour denoting the *Chlorella* symbiont genotype and the shade of the colour denoting the light intensity. Both fractions cluster according to shade, and therefore, according to light intensity. There are 3 replicates of each combination of host, symbiont and light intensity. A) The *Chlorella* metabolic fraction. B) The *P. bursaria* metabolic fraction.

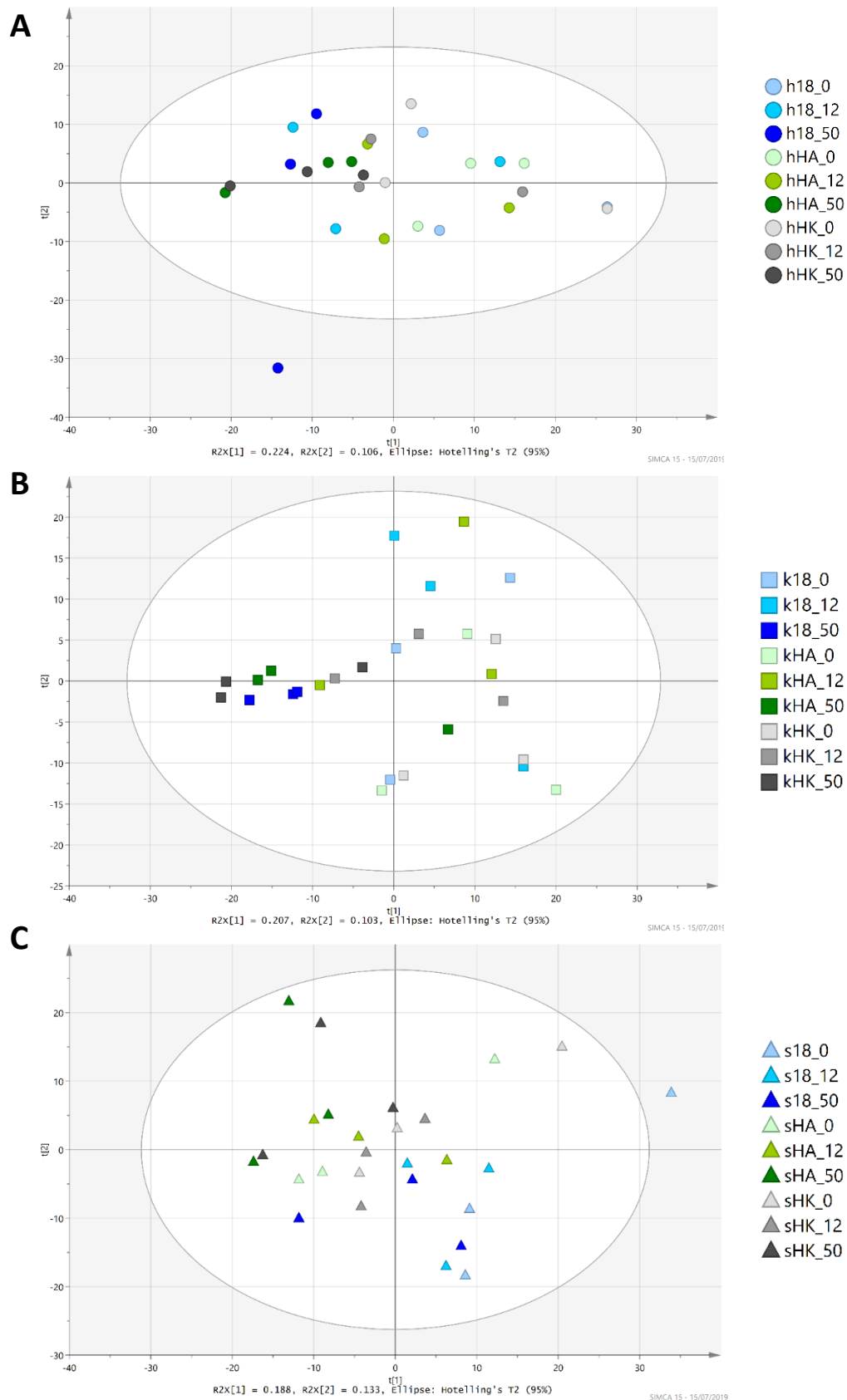


**Figure 3.5. Clustering patterns of the *Chlorella* metabolic fraction subset by host-genotype.** These PCA plots show the HA1 host (A), the HK1 host (B), and the 186b host (C). Each point represents the metabolic profile of a sample; with the shape denoting the *P. bursaria* host genotype, the colour denoting the *Chlorella* symbiont genotype and the colour shade denoting the light intensity. Only within the 186b host (C) do the samples cluster by colour, and therefore, symbiont genotype. There are 3 replicates of each combination of host, symbiont and light intensity.

To identify the metabolites driving differences in metabolism of the symbiont-genotypes in the 186b host-genotype background, I next performed pairwise contrasts using volcano plots to highlight which metabolites varied significantly according to symbiont genotype (Figure 3.6). This revealed a range of candidate symbiont metabolites that varied between the native host-symbiont pairing and either of the non-native host-symbiont pairings (Table 3.1, 3.2 and 3.3). The putative identifications included, in the dark, elevated levels of candidate metabolites associated with stress responses (stress-associated hormones, jasmonic acid and abscisic acid, and stress associated-fatty acids, such as arachidonic acid) but reduced production of vitamins and co-factors by the native symbiont, compared to the non-native symbionts (Table 3.1). At high irradiance, the native symbiont showed higher levels of candidate metabolites in central metabolism, hydrocarbon metabolism and of biotin (vitamin B7), compared to the non-native symbionts (Table 3.3). In contrast, the non-native symbionts produced elevated levels, relative to native symbionts, of a candidate glutathione derivative, and glutathione is an antioxidant involved in the ascorbate-glutathione cycle that combats high UV stress through radical oxygen scavenging.

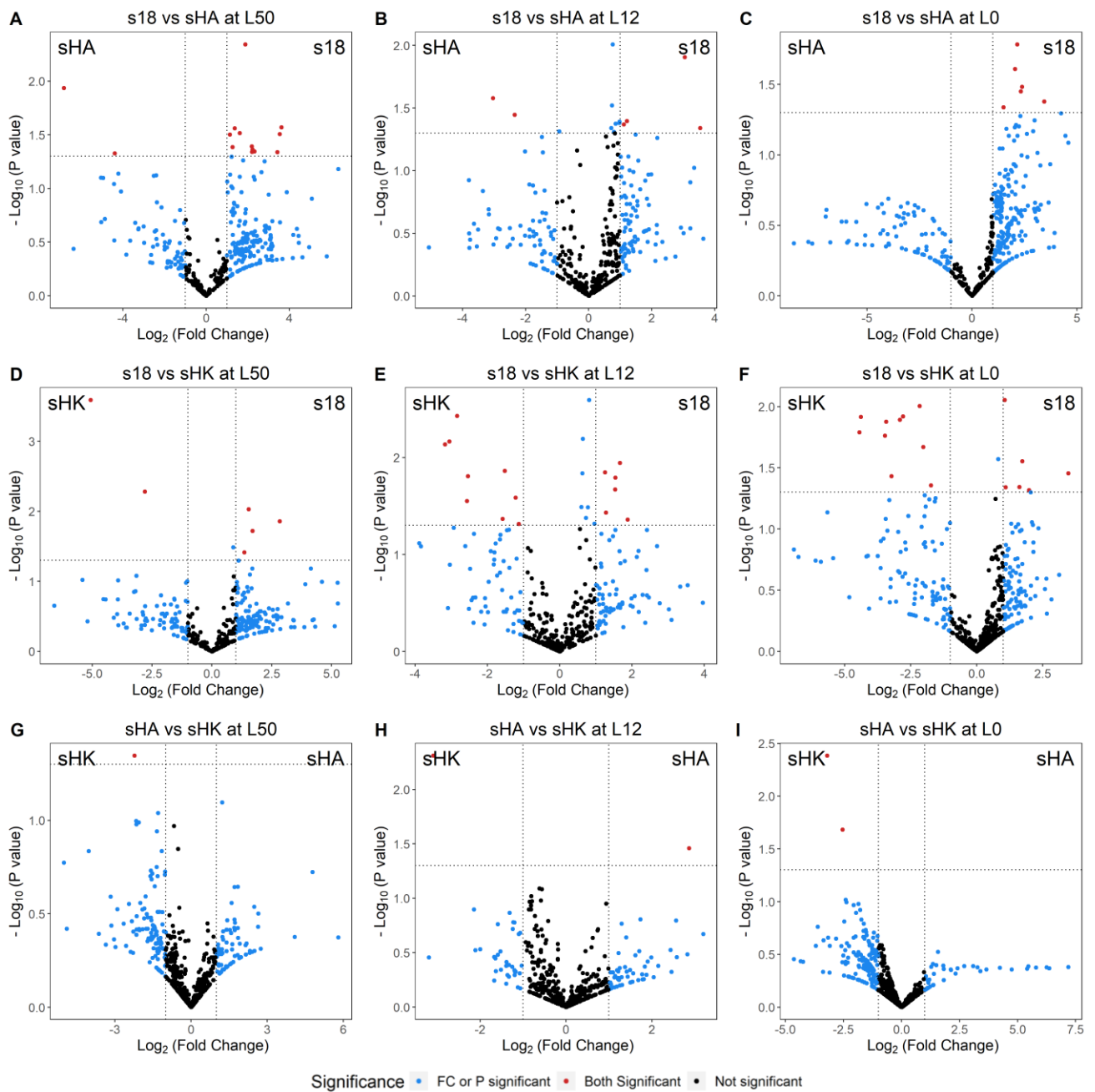


**Figure 3.6.** Differences in the *Chlorella* metabolism between symbiont genotypes at multiple light levels within the 186b *P. bursaria* host. Pairwise comparisons between symbiont genotypes are represented as volcano plots, plotting the fold change of each metabolite against its statistical significance. The data points are highlighted in red if the P value is significant and if the Log<sub>2</sub>(fold change) is greater than 1 or less than -1. Each panel compares two symbionts genotypes at one light level: A-C compare the 186b and HA1 symbionts, D-F compare the 186b and HK1 symbionts, and G-I compare the HA1 and HK1 symbionts. The first column is at the highest light level (50 $\mu$ E), the second column at the intermediate light level (12 $\mu$ E), and the third column is in the dark (0 $\mu$ E).

**Table 3.1. Symbiont-genotype specific metabolites in the dark within the 186b *P. bursaria* host.** These metabolite IDs were highlighted by the volcano plot (Figure 3.6) and were found to have significantly higher abundances in one symbiont-genotype compared to another within the 186b host subset of the *Chlorella* metabolic fraction in the dark (0 $\mu$ E). Recorded with 46ppm accuracy.

Strain Associated	Comparison	mz ID	Detected Mass	Accurate Mass	Adduct	Candidate Compound	Pathway	Stress Associated
s18	s18 vs sHA	118	117.966	117.0426	H+	Aspartate-4-semialdehyde	Amino acid	
				117.0578	H+	Indole	Amino acid + hormone	
				117.0790	H+	Glycinebetaine	Amino acid + osmolyte	
				117.0790	H+	Valine	Amino acid	
	s18 vs sHA	134.2	134.109	133.1040	H+	Aspartate	Amino acid	
	s18 vs sHA	255.2	255.104	216.1725	K+	w-hydroxydodecanoic acid	Hydroxy fatty acids	
				254.2246	H+	Palmitoleic acid	Unsaturated fatty acids	
	s18 vs sHA	343.2	343.153	342.1162	H+	Disaccharide	Carbohydrate	
				304.2402	K+	Arachidonic acid	Unsaturated fatty acids	Yes
				304.2402	K+	Kaurenoic acid	Diterpenoid (related to GA)	
	s18 vs sHK	247.2	247.117	224.1412	Na+	Methyl jasmonate	Hormone (JA)	Yes
	s18 vs sHK	267.2	267.102	228.2089	K+	Myristic acid	Saturated fatty acids	
				244.2263	Na+	N1-acetylspermine	Amino acid	
s18 vs sHK	271.2	271.167	248.1412	Na+	Abscisic acid aldehyde	Hormone (ABA)	Yes	
s18 vs sHK	686.4	686.391	663.3748	Na+	1-Palmitoyl-2-(5-keto-6-octenedioyl)-sn-glycero-3-phosphocholine	Glycerophospholipids	Yes	
sHK	s18 vs sHK	220.2	220.153	219.1107	H+	Pantothenate	Vitamin (B5)	
				219.1120	H+	Zeatin	Hormone (cytokinin)	
	s18 vs sHK	238	238.053	199.0246	K+	O-phospho-L-homoserine	Amino acid	
				215.0195	Na+	O-phospho-4-hydroxy-L-threonine	Vitamin (B6)	
				215.0807	Na+	Kinetin	Hormone (cytokinin)	
	s18 vs sHK	241.2	241.188	202.2157	K+	Spermine	Amino acid	
	s18 vs sHK	335.2	335.115	334.2144	H+	Prostaglandin	Fatty acyls	
				312.3028	Na+	Eicosanoic acid	Saturated fatty acids	
sHK	sHA vs sHK	355	355.048	354.0577	H+	5-amino-6-(5'-phosphoribosylamino)uracil	Riboflavin	

**Table 3.2. Symbiont-genotype specific metabolites in the intermediate light within the 186b *P. bursaria* host.** These metabolite IDs were highlighted by the volcano plot (Figure 3.6) and were found to have significantly higher abundances in one symbiont-genotype compared to another within the 186b host subset of the *Chlorella* metabolic fraction in the intermediate light condition (12 $\mu$ E). Recorded with 46ppm accuracy.

Strain Associated	Comparison	mz ID	Detected Mass	Exact Mass	Adduct	Candidate Compound	Pathway	Stress Associated
	s18 vs sHA	361.4	361.303	338.3185	Na+	Erucic acid	Fatty acid	
<b>s18</b>	s18 vs sHK	263.2	263.179	224.1412	K+	Methyl jasmonate	Hormone	Yes
<b>sHK</b>	s18 vs sHK	241.2	241.188	202.2157	K+	Spermine	Amino acid	
	s18 vs sHK	417.4	417.316	416.3654	H+	6-oxocampestanol	Hormone (Brassinosteroid)	
		417.4	417.316	416.3654	H+	Gamma-tocopherol	Ubiquinone	
	s18 vs sHK	451.2	451.12	450.1936	H+	Geranylgeranyl-PP	Ubiquinone + Chlorophyll	
<b>sHA</b>	SHA vs sHK	365	365.083	364.0420	H+	Xanthosine-5'-phosphate	Purine	
		365	365.083	326.1226	K+	6,7-dimethyl-8-(1-D-ribityl)lumazine	Riboflavin	

**Table 3.3. Symbiont-genotype specific metabolites in the high light within the 186b *P. bursaria* host.** These metabolite IDs were highlighted by the volcano plot (Figure 3.6) and were found to have significantly higher abundances in one symbiont-genotype compared to another within the 186b host subset of the *Chlorella* metabolic fraction in the highest light condition (50 $\mu$ E). Recorded with 46ppm accuracy.

Strain Associated	Comparison	mz ID	Detected Mass	Accurate Mass	Adduct	Compound	Pathway	Stress Associated			
s18	s18 vs sHA	171	171.088	132.0059	K+	Oxalacetic acid	TCA /central				
				169.9980	H+	Glycerone phosphate	Glycolysis / central				
				169.9980	H+	Glyceraldehyde-3-phosphate	Glycolysis / central				
				132.0423	K+	3-hydroxy-3-methyl-2-oxobutanoate	Amino acid				
				132.0423	K+	2-acetolactate	Amino acid				
				132.0423	K+	Glutarate	Amino acid				
				132.0535	K+	Asparagine	Amino acid				
				148.0372	Na+	Citramalate	C5-Branched dibasic acid				
				132.0899	K+	Ornithine	Amino acid				
				148.0736	Na+	Mevalonic acid	Mevalonate pathway				
				148.0736	Na+	Pantoate	Pantothenate biosynthesis				
				s18 vs sHA	237.2	237.181	214.1317	Na+	Dethiobiotin	Vitamin (B7)	
				s18 vs sHA	239.2	239.145	200.1776	K+	Lauric acid	Saturated fatty acids	
							216.1725	Na+	w-hydroxydodecanoic acid	Hydroxy fatty acids	
s18 vs sHA	251.2	251.146	228.2089	Na+	Myristic acid	Saturated fatty acids					
			212.2504	K+	Pentadecane	Hydrocarbon					
s18 vs sHA	537.4	537.356	536.4382	H+	$\alpha/\beta/\gamma/\delta$ carotene	Carotenoid					
			536.4382	H+	Lycopene (all-trans or tetra cis)	Carotenoid					
s18 vs sHK + sHA	213	213.097	174.0164	K+	Aconitic acid	TCA cycle / central					
			190.0114	Na+	Oxalosuccinate	TCA cycle / central					
			174.0528	K+	3-Carboxy-4-methyl-2-oxopentanoate	Amino acid					
			174.0528	K+	Shikimic acid	Shikimate pathway					
			190.0477	Na+	3-dehydroquininate	Shikimate pathway					
			174.0793	K+	Indole-3-acetamide	Amino acid + hormone					
			174.0892	K+	Suberic acid	Fatty acid					
			174.1004	K+	N2-acetyl-L-ornithine	Amino acid					
			190.1066	Na+	$\gamma$ -hydroxy-l-arginine	Arginine-nitric oxide					
			212.0896	H+	Volemitol	Carbohydrate					

Table 3.3 continued

Strain Associated	Comparison	mz ID	Detected mass	Accurate mass	Adduct	Compound	Pathway	Stress Associated
	s18 vs sHK + sHA	257.2	257.123	256.2402	H+	palmitic acid	saturated fatty acid	
				256.1172	H+	2-(3-Carboxy-3-aminopropyl)-L-histidine	unusual amino acid	
	s18 vs sHK	235.2	235.131	212.2504	Na+	pentadecane	Hydrocarbon - metabolite	
<b>sHK</b>	s18 vs sHK	220.2	220.153	219.1120	H+	Zeatin	Hormone	
				219.1107	H+	Pantothenate	Vitamin B5	
<b>sHK + sHA</b>	s18 vs sHK + sHK	465	465.096	426.0879	K+	S-Glutathionyl-L-cysteine	Cysteine + methionine	Yes
<b>sHK</b>	sHA vs sHK	329.2	329.1783	328.2402	H+	Docosahexaenoic acid	Unsaturated fatty acids	

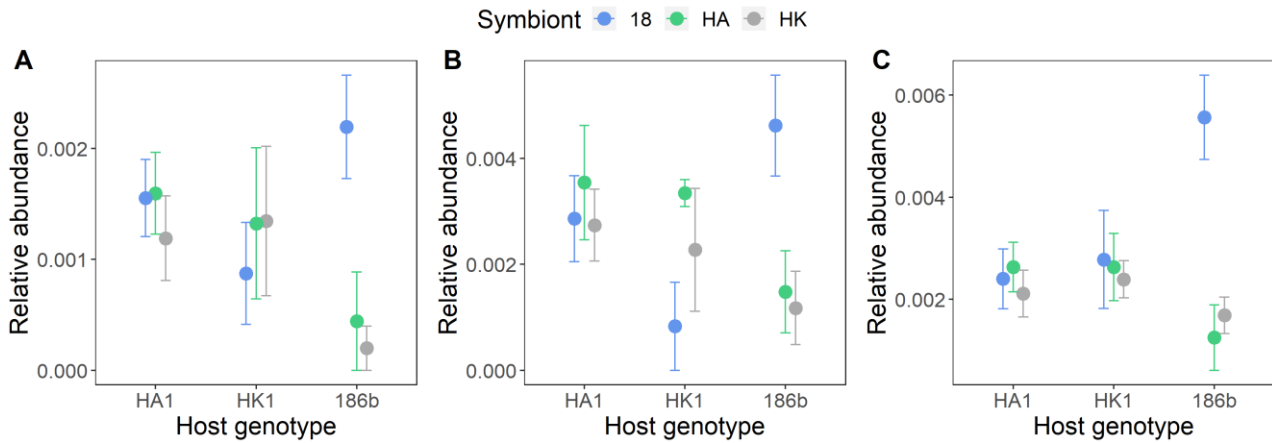


**Figure 3.7. Relative abundances of dark-stress associated metabolites across host genotypes in the dark.** The data points show the mean ( $n=3$ ) relative abundance  $\pm$  SE. Each panel shows the data for one metabolite, with the colour distinguishing the symbiont-genotype. The three metabolites were associated with a prolonged darkness stress response for the native symbiont within the 186b host and are listed in Table 3.1. A) The  $mz$  bin 247.2, candidate compound: methyl jasmonate. B) The  $mz$  bin 271.2, candidate compound: Abscisic acid aldehyde. C) The  $mz$  bin 686.4.2, candidate compound: a Glycerophospholipid.

To test whether the 186b *Chlorella* underwent similar stress-responses when in the other host-genotype backgrounds, I next examined levels of the identified stress-associated candidate metabolites for 186b *Chlorella* across all host-genotypes. For dark-associated candidate stress metabolites, higher abundances were observed for 186b *Chlorella* in the 186b host-genotype background than in the HA1 or HK1 host-genotype backgrounds (Figure 3.7). These metabolite abundances were similar across all symbiont-genotypes in the HA1 or HK1 host-genotype backgrounds, suggesting that the dark-associated stress response of the 186b *Chlorella* is limited to its native host background and that dark-associated algal symbiont stress was ameliorated by the other host genotypes. In addition, the uniformity of the high-light stress response was tested by examining the abundance of the high-light candidate stress metabolites for the HA1 and HK1 *Chlorella* across all host-genotypes. As a group, these high-light stress associated metabolites did not have an overall clear pattern, although one metabolite had high abundances in the HA1 and HK1 *Chlorella* across all the host-genotype backgrounds (Figure 3.8). This implies that the high-light stress may therefore be independent of host-genotype.

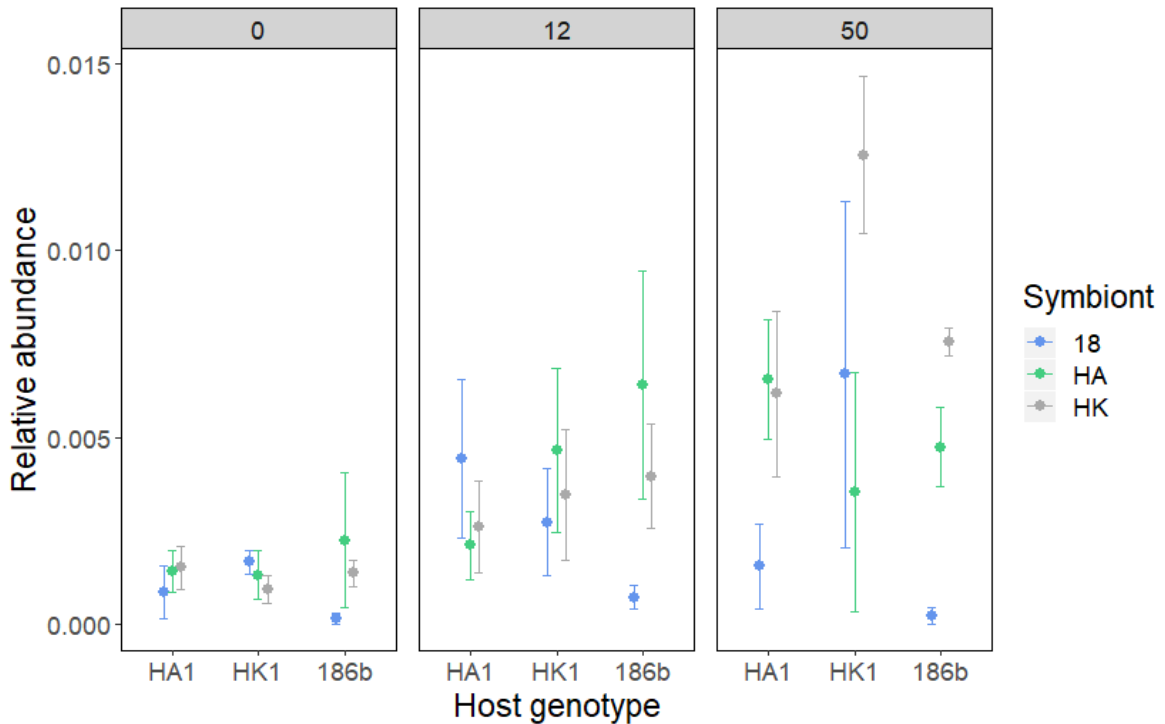


**Figure 3.8. Relative abundances of a high-light stress associated metabolite across host genotypes and across light levels.** The data points show the mean (n=3) relative abundance  $\pm$  SE. Each panel shows the data for a light level (0, 12 or 50  $\mu\text{E m}^{-2} \text{s}^{-1}$ ) with the *P. bursaria* host-genotype on the X-axis and the symbiont-genotype shown by the colour. The metabolite is mz 465, candidate compound: S-Glutathionyl-L-cysteine (see Table 3.3). The metabolite was identified associated with a high-light stress response for the HA1 and HK1 symbionts within the 186b host.

### 3.4 Discussion

In this chapter, I investigated genetic variation for host-symbiont specificity in the *P. bursaria* - *Chlorella* endosymbiosis using a reciprocal cross-infection experiment coupled with metabolomics. I observed a significant  $G^H \times G^S \times E$  interaction for the host-symbiont growth rate that was predominately driven by the differential effects of symbiont-genotypes on host-symbiont growth rate within the 186b host, while in the other host-genotype backgrounds symbiont genotype did not affect growth rate. The regulation of symbiont load also displayed a  $G^H \times G^S \times E$  interaction driven by symbiont-genotype-specific responses in the 186b and HK1 host-genotypes. Consistent with the phenotype data, the metabolic profile of the *Chlorella* fraction varied when isolated from pairings with the 186b host genotype, but not with the other host-genotypes. The metabolic differences between symbionts in the 186b host potentially provides the mechanistic basis for the  $G^H \times G^S \times E$  interaction, and suggests that contrasting stress responses played an important role and

may have altered the benefit-to-cost ratio of symbiosis for this host. Specifically, whereas the 186b *Chlorella* showed a dark-associated stress response, producing stress-associated hormones and fatty acids, the HA1 and HK1 *Chlorella* showed a high-light-associated stress response, producing compounds to combat radical oxygen species. These data suggest that differences in light management among algal symbionts may underlie host-symbiont specificity, with implications for the likely success of partner switching.

The  $G^H \times G^S \times E$  interaction in the host-symbiont growth reaction norm reveals a striking asymmetry in specialisation among host genotypes. The growth rate reaction norm varied by symbiont genotype for the 186b host genotype, whereby the native symbiont was costlier in the dark but more beneficial in the high light environment compared to the non-native symbionts. This shows that the symbiont genotype affected the interaction between the benefit-to-cost ratio and light within the 186b host. In contrast, within the HK1 and HA1 host-backgrounds host-symbiont growth rate reaction norms did not vary according to symbiont genotype. Thus, whereas the HA1 and HK1 host-genotypes appear to be symbiont generalists, the performance of the 186b host genotype is far more dependent upon the genetic identity of its algal symbiont. The native 186b host-symbiont pairing appears to be specialised to high-light environments, showing high performance only within a limited range of high irradiances. Light specialism is common among photosynthetic organisms, such as the light ecotypes of the cyanobacteria *Prochlorococcus* (Rocap et al., 2003) and green alga *Ostreococcus* (Rodríguez et al., 2005), but this is the first time it has been shown in the *P. bursaria* – *Chlorella* endosymbiosis. The variation in host specialisation has implications for symbiont replacement via partner switching. Generalist hosts are likely to be more able to integrate novel symbiont-genotypes than more specialist hosts. Conversely, because diverse symbiont-genotypes result in similar growth reaction norms in generalist host genotypes, these host genotypes are probably less able to shift their ecological niche through partner switching. Nonetheless, variation in specialisation suggests that host-genotypes may vary extensively in the immediate fitness consequences of partner switching.

A previous mathematical model of the *P. bursaria* - *Chlorella* interaction suggested that symbiont load is host controlled and regulated to maximise the benefit-to-cost ratio of symbiosis (Dean et al., 2016; Lowe et al., 2016), offering a framework to understand the observed variation in the symbiont load reaction norms. Host regulation is believed to alter symbiont load through altering the balance of symbiont division/ingestion and symbiont digestion/egestion (Kodama and Fujishima, 2012; Takahashi et al., 2007). I observed a  $G^H$

$\times G^S \times E$  interaction in symbiont load data that is consistent with patterns of genotype-specific symbiont loads measured in other symbioses (Chong and Moran, 2016; Kondo et al., 2005), and is the first-time genotype-specific symbiont loads have been observed for the *P. bursaria* - *Chlorella* symbiosis. Whereas the HA1 host genotype regulated all symbiont genotypes in a similar manner, regulation varied according to symbiont genotype in the 186b and HK1 host-genotype backgrounds. In the HK1 host-genotype background the magnitude of the symbiont load altered according to symbiont genotype and the native symbiont had the highest symbiont load throughout — a ‘native advantage’ outcome. In the 186b host-genotype background, the light intensity of the maximal symbiont load altered with symbiont genotype, specifically the symbiont load of the native symbiont peaked at a higher light intensity than the non-native symbionts. A change in the irradiance level at which the symbiont load curve peaks suggests fundamental differences in the benefit-to-cost ratio of these symbiont genotypes in response to light. The maximal symbiont load represents the point at which the benefit of the symbionts outweighs their cost. Symbiont loads that peak at a high irradiance imply that greater irradiance is required for the benefit per-symbiont to outweigh its cost (Dean et al., 2016). After the maximum load, symbiont load decreases with increasing irradiance because the energetic output per symbiont increases (Hoogenboom et al., 2010), and as such fewer symbiont are required to meet the demand (Dean et al., 2016; Lowe et al., 2016).

These phenotypic responses can be compared to the potential outcomes discussed in the chapter introduction (Figure 3.1). Within the HA1 host, symbiont genotype had no effect on growth rate or symbiont load, and therefore, HA1 appears to be a partner-generalist (similar to Figure 3.1a). Within the HK1 host the results were mixed; for growth rate, symbiont genotype had no effect, but symbiont load displayed a ‘native advantage’ outcome (similar to Figure 3.1b). A higher symbiont load, however, is not necessarily an advantage, and the discrepancy between the unaffected growth rate and increased symbiont load implies that the HK1 native symbiont is both less beneficial and less costly than the non-native symbionts. This is because the higher number of symbionts led to the same growth rate, suggesting that both the benefit and cost of symbioses was affected, but not the relationship between benefit and cost. In contrast, within the 186b host the growth rate and symbiont load depended on the interaction between symbiont genotype and the environment (similar to Figure 3.1c). Such that the relationship between the benefit-to-cost ratio and light differed according to symbiont-genotype, and this drives the  $G^H \times G^S \times E$  interaction.

The metabolomics data suggested that the native versus non-native symbiont-genotypes displayed contrasting stress-responses when inhabiting the 186b host-genotype background. In the dark, the 186b native symbiont-genotype had multiple candidate stress-response indicators, including stress-associated hormones and fatty acids. Prolonged darkness can trigger a stress response because the absence of photosynthesis can starve photosynthetic organisms of both fixed carbon and energy (Zhang et al., 2007); in plants and algae it has been demonstrated that the starch reserves are almost exhausted after one night (Graf et al., 2010; Ral et al., 2006). Starvation stress-responses are coordinated by signalling hormones and lipids such as those I have identified, especially abscisic acid (Lu et al., 2014), and arachidonic acid (Merzlyak et al., 2007). These signals can lead to downstream effects that try to negate the stress by mobilising alternative compounds for energy/carbon (Manoharan et al., 1999) or by triggering a resting state where metabolism and growth are reduced (Peters, 1996). The starvation stress response suggests that the symbiotic nutrient exchange has broken down within the 186b native symbiosis, and that neither partner is provisioning the other adequately. Consistent with these patterns, the 186b symbiont was costly and its load tightly regulated by the host in the dark when it was most stressed. Interestingly, in the other host backgrounds the 186b native symbiont did not display elevated dark-stress associated metabolites, and was not costly in these backgrounds. This suggests that the other hosts were perhaps more generous in provisioning their symbionts in the dark, and so prevented the starvation-based dark-associated stress response. Greater symbiont compatibility appears, therefore, partially due to the ability of hosts to prevent and ameliorate the stress response, and therefore, the cost of their symbionts.

In contrast, the HA1 and HK1 symbiont-genotypes in the 186b host-genotype background did not show dark-associated stress-responses, which, I hypothesise, is connected to their higher levels of candidate vitamins and cofactors that may help to stabilise cellular metabolism and therefore delay or prevent a full stress response (Abdel-Rahman et al., 2005; Asensi-Fabado and Munné-Bosch, 2010). At high irradiance, however, the pattern of stress-responses was reversed. Whilst the native 186b symbiont-genotype had no indicators of stress, the HA1 and HK1 non-native symbiont-genotypes showed indicators of high-light-mediated stress. Specifically, the HA1 and HK1 symbiont genotypes showed elevated levels of a candidate glutathione derivative; glutathione is an antioxidant involved in the ascorbate-glutathione cycle that scavenges reactive oxygen species to counteract the damaging consequences of excess light (Mallick, 2004; Shiu and Lee, 2005). It is well documented that increased antioxidant production is indicative of increased oxidative damage due to thermal or light stress (Bartosz, 1997; Lesser, 2006); in particular, the

consequences of this in symbiosis have been studied in coral, where oxidative stress causes the breakdown of symbiosis and coral bleaching (Lesser, 2011). The abundance profile of this candidate antioxidant revealed the HK1 and HA1 symbionts had high abundances across the host-backgrounds. Implying that while the dark-stress response is dependent on an interaction between symbiont-genotype and host-genotype, the high-light stress response is primarily dependent on symbiont-genotype. The consequences for host-symbiont growth vary between the symbiont genotypes, with the HA1 symbiont apparently capable of counteracting the stress without limiting growth rate, whereas for the HK1 symbiont stress from the high light intensity becomes excessive and its host-symbiont growth plateaus. This is supported by the candidate unsaturated fatty acid that had higher abundances in the HK1 symbiont compared to the HA1 symbiont in the high light environment. Unsaturated fatty acids are typically associated with higher stress (Klyachko-Gurvich et al., 1999; Thompson, 1996). Genetic variation in stress tolerance is observed in multiple photosymbioses, for example *Symbiodinium*-genotypes have different tolerance levels to high temperature stress (Cunning et al., 2015; Howells et al., 2012).

Surprisingly, I did not observe symbiont-genotype effects on the host metabolism. The absence of detectable genotype separation within the *P. bursaria* fraction could be a result of the differences being subtler than those of the *Chlorella* metabolism or alternatively due to biases in our detection methodology. Untargeted metabolomics attempts to be as unbiased as possible, but nonetheless extraction methods and machine settings will bias detection to metabolites with certain physiochemical properties (Ortmayr et al., 2016). For instance, there is often a trade-off between recording polar versus nonpolar metabolites and between sensitivity and dalton range of detection. Currently, the lack of host metabolic genotype separation precludes the investigation of how the HA1 and HK1 hosts compensates the 186b symbiont's costliness in the dark and derive similar benefits of symbiosis from the different symbiont genotypes. This compensation could take the form of a metabolite that helps to ameliorate the stress response in the dark, or could be increased nutrient transfer to prevent starvation, perhaps the amino acid nitrogen compound which also contains fixed carbon. If the latter is true, then a pulse-chase metabolic experiment may be required to measure the transfer rates. This question remains open and hopefully future work will be able to investigate *P. bursaria* metabolomics in detail and untangle the host side of this interaction.

Stress is known to lead to the breakdown of symbioses (Abrego et al., 2008; Weis, 2008) and occurs in numerous environmental conditions, for example coral bleaching can be

caused by the stress of high temperature, high irradiance, prolonged darkness, or chemical pollution (DeSalvo et al., 2012; Douglas, 2003). In the *Hydra – Chlorella* endosymbiosis, the older, more stable origin of this association possesses greater oxidative stress tolerance compared to the more recent origin (Ishikawa et al., 2016). Stress tolerance and stress prevention are therefore likely to be crucial aspects of symbioses, and particularly so in photosymbioses that cannot escape the potentially damaging consequences of light. This chapter has shown how contrasting light-dependent symbiont stress-responses drive host-symbiont genetic specificity by altering the benefit-to-cost ratio of the symbiosis. A result that corresponds with the role of symbiont-stress tolerance in determining the performance of other photosymbioses (Abrego et al., 2008; Howells et al., 2012; Ye et al., 2019), providing evidence that this interaction may be a common feature of photosymbioses. Furthermore, the comparison of stress metabolites across the host-genotypes suggested that generalist host profiles occur in genotypes that alleviate stress in their partners, leading to similar benefit-to-cost ratios across their symbionts. The alleviation of stress, therefore, may not only affect the fitness outcome of a symbiosis but also the likelihood of novel symbiont integration, and thus partner switching. It would be interesting to examine whether this holds true for other photosymbioses, as the role of stress in partner integration could be consequence of genotype-driven stress tolerance playing such a pivotal role in photosymbioses. Photosymbioses are inherently tied to photo-oxidative stress, and it appears that the evolution of these endosymbioses is driven by their adaptation to, and tolerances of, stress.

### 3.5 Supplementary Figures

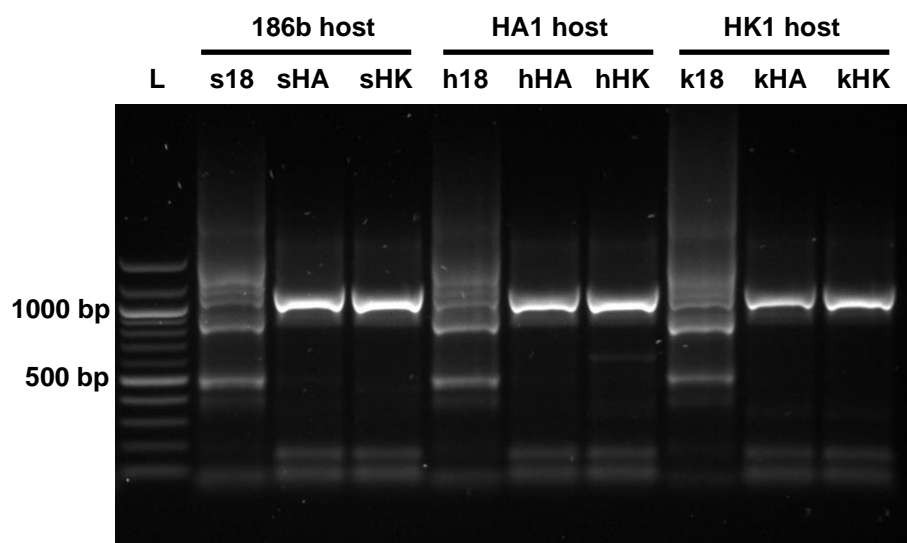


**Figure S3.1. PCR confirmation of symbiont-genotype within the reciprocal cross infections.** Overlapping, multiplex primers were used to amplify fragments within the 18S rDNA and ITS region of the *Chlorella* nuclear genome. In this region the ‘American/Japanese’ strains, such as HA1 and HK1, have had three introns inserted that the ‘European’ strains, such as 186b, lack (Hoshina and Imamura, 2008; Hoshina et al., 2005). The main fragment of HA1/HK1 is, therefore, considerably larger than the main fragments of 186b, and both have additional smaller fragments. The banding pattern results here confirm that the cross-infections were successful and contain the correct *Chlorella* genotype, specifically that the distinct banding pattern of 186b was present when expected. This PCR method can distinguish between ‘American/Japanese’ and ‘European’ strains, but not between strains that come from the same biogeographical clade. Host genotype has been shortened to a letter (‘s’ = 186b host, ‘h’ = HA1 host, ‘k’ = HK1 host); symbiont genotype is shown by two capitals (‘18’ = 186b symbiont, ‘HA’ = HA1 symbiont, ‘HK’ = HK1 symbiont). Shown alongside a 100bp ladder.

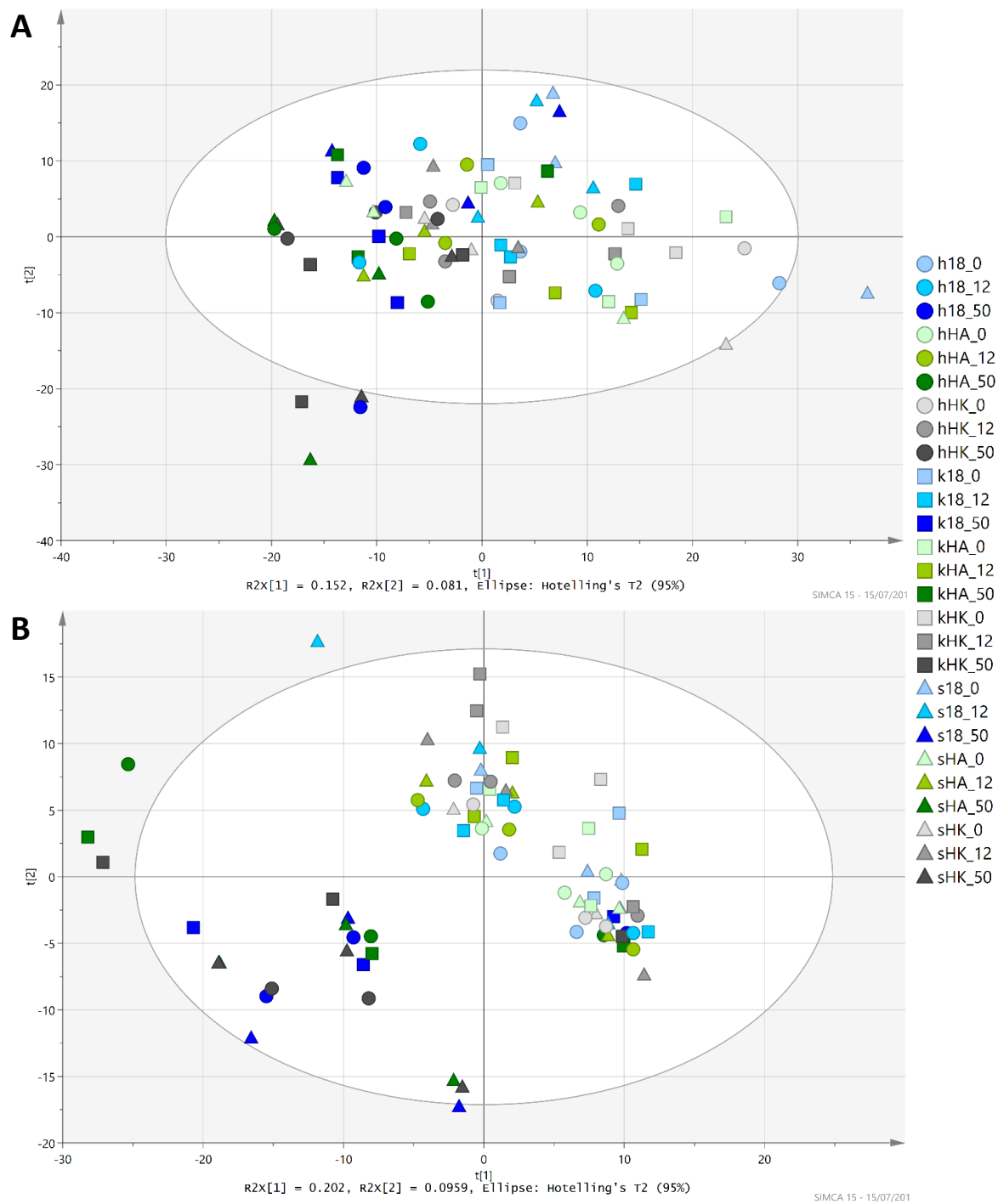


**Figure S3.2. The clustering of the metabolic fractions by light in PCA plots.** These PCA plots show the initial clustering of the metabolic fractions by light, which was then shown by OPLS-DA plots (Figure 3.3). Each point represents the metabolic profile of a sample; with the shape denoting the *P. bursaria* host genotype, the colour denoting the *Chlorella* symbiont genotype and the shade of the colour denoting the light intensity. There are 3 replicates of each combination of host, symbiont and light intensity. A) The *Chlorella* metabolic fraction. B) The *P. bursaria* metabolic fraction.

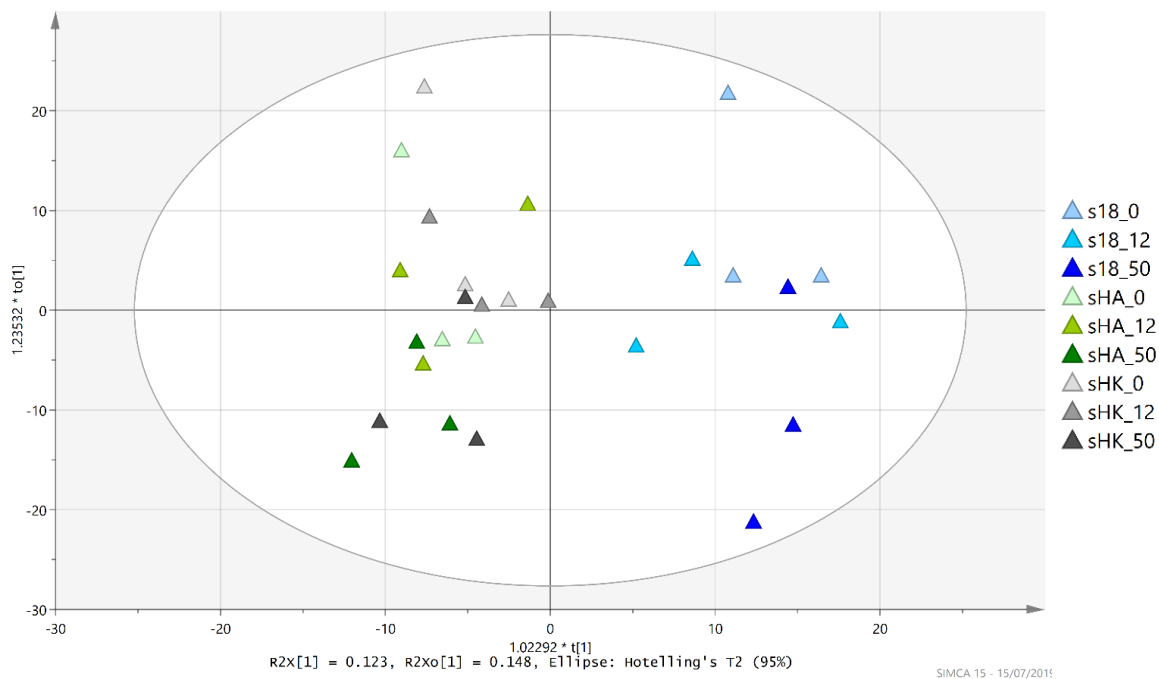


**Figure S3.3. Separation by symbiont-genotype within the 186b host subset of the *Chlorella* metabolic fraction.** This OPLS-DA plot follows the initial clustering by symbiont-genotype within the 186b host subset in the PCA plot (Figure 3.4C). Each point represents the metabolic profile of a sample; with the colour denoting the *Chlorella* symbiont genotype and the shade of the colour denoting the light intensity. The samples separate between the ‘blue’ samples (186b symbiont-genotype) and the ‘green’ and ‘grey’ samples (HA1 and HK1 symbiont genotypes). There are 3 replicates of each combination of host, symbiont and light intensity.

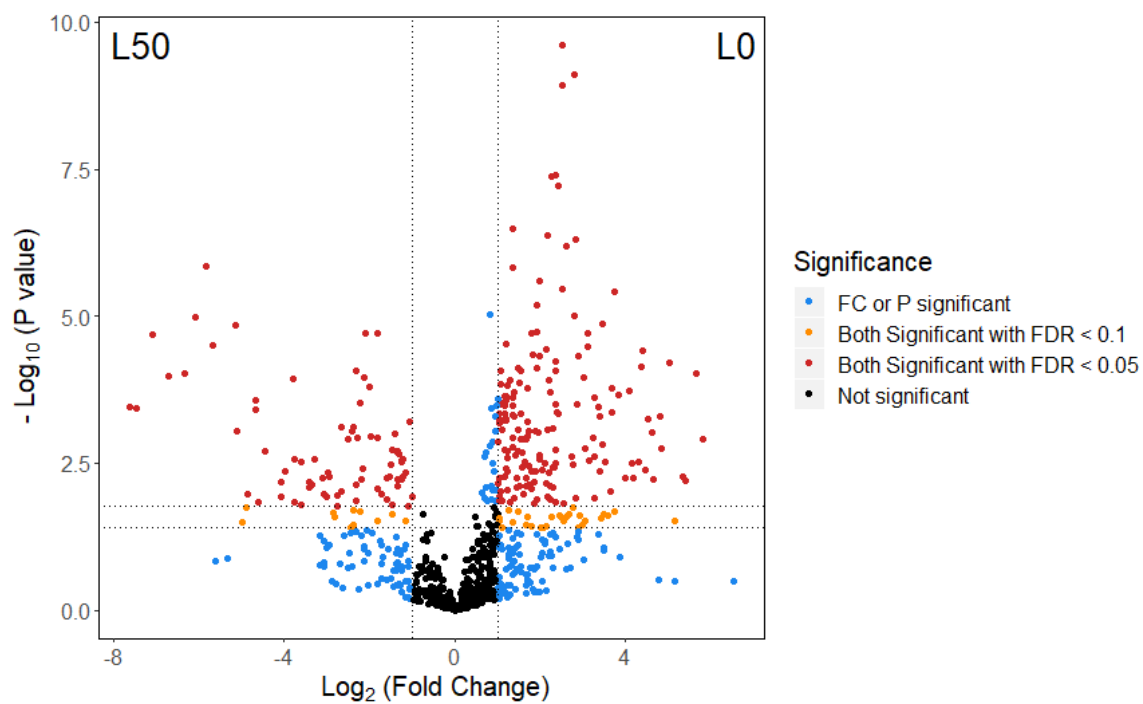


**Figure S3.4. Shared response of *Chlorella* genotypes to light intensity in the *Chlorella* metabolic fraction.** Pairwise comparison between the dark (L0 = 0 $\mu$ E) and high light level (L50 = 50 $\mu$ E) across genotypes represented as a volcano plot, plotting the fold change of each metabolite against its statistical significance. The data includes *Chlorella* data from all nine of the cross-infections, and therefore indicates the shared response, irrespective of host or symbiont genotype. The data points are highlighted at two false discovery rate (FDR) values, and if the  $\text{Log}_2(\text{fold change})$  is greater than 1 or less than -1.

### 3.6 Supplementary Tables

**Table S3.1. Light-level associated shared *Chlorella* metabolites across the host and symbiont genotypes.** These metabolite IDs were identified from the top compounds highlighted in the volcano plot Figure S3.4. They have, therefore, statistically significantly higher abundances in either the dark or high light, within the *Chlorella* metabolic fraction.

Light Association	mz ID	Detected Mass	Accurate + Adduct	Accurate Mass	Adduct	Candidate Compound	KEGG ID	Pathway
0μE	69	69.031	68.974	30.011	K+	Formaldehyde	C00067	Methane
	69	69.031	68.983	45.993	Na+	Nitrite	C00088	Nitrogen
	69	69.031	68.995	46.005	Na+	Formate	C00058	Pyruvate + Methane
	69	69.031	69.032	46.042	Na+	Ethanol	C00469	Glycolysis
	73	73.009	73.02838	72.021	H+	Methylglyoxal	C00546	Pyruvate
	75	75.023	75.008	74.000	H+	Glyoxylic acid	C00048	Central (Glyoxylate cycle)
	75	75.023	75.045	74.037	H+	Lactaldehyde	C00424	Carbohydrate + Pyruvate
	75	75.023	75.045	74.037	H+	Propanoic acid	C00163	Propanoate (lipid)
	75	75.023	75.044	74.037	H+	Hydroxyacetone	C05235	Propanoate (lipid)
	105	105.033	105.019	104.011	H+	Hydroxypyruvic acid	C00168	Amino acid + Photorespiration
	105	105.033	105.019	104.011	H+	Malonate	C00383	Fatty acid
	105	105.033	105.030	104.022	H+	Urea-1-carboxylate	C01010	Urea degradation
	154	153.993	154.011	131.022	Na+	Iminoaspartate	C05840	Nicotinate
	154	153.993	154.027	115.063	K+	Proline	C00148	Amino acid
	154	153.993	154.048	131.058	Na+	5-Aminolevulinate	C00430	Heme Biosynthesis
	154	153.993	154.048	131.058	Na+	Glutamate-5-Semialdehyde	C01165	Amino acid
	154	153.993	154.048	131.058	Na+	4-Hydroxy-proline	C01157	Amino acid
	154	153.993	154.050	153.043	H+	3-Hydroxyanthranilate	C00632	Amino acid
	154	153.993	154.059	131.069	Na+	Creatine	C00300	Amino acid
	154	153.993	154.084	131.095	Na+	B-Alaninebetaine	C08263	Osmoprotectant/stress
154	153.993	154.084	131.095	Na+	Isoleucine	C00407	Amino acid + Cyanoamino	
154	153.993	154.084	131.095	Na+	Leucine	C00123	Amino acid	
154	153.993	154.087	153.079	H+	Dopamine	C03758	Alkaloid + Amino acid	
154	153.993	154.096	131.106	Na+	N-Carbamoylputrescine	C00436	Amino acid	

Table S3.1 continued

Light Association	mz ID	Detected Mass	Accurate + Adduct	Accurate Mass	Adduct	Candidate Compound	KEGG ID	Pathway
0µE	212	212.022	212.033	173.069	K+	N-Acetyl-glutamate-semialdehyde	C01250	Amino acid
	212	212.022	212.053	189.064	Na+	N-Acetyl-glutamate	C00624	Amino acid
	425.2	425.176	425.100	386.137	K+	Pteryxin	C09307	Coumarins
	425.2	425.176	425.100	386.137	K+	Samidin	C09310	Coumarins
	425.2	425.176	425.135	424.127	H+	Adifoline	C09020	Indole alkaloid
	521.4	521.386	521.311	520.304	H+	Cyasterone	C08816	Sterol Lipid + Terpenoid
	651.2	651.241	651.196	612.232	K+	Novobiocin	C05080	Antibiotic
50µE	242.2	242.193	242.100	219.111	Na+	Pantothenate	C00864	Pantothenate + CoA
	242.2	242.193	242.102	219.112	Na+	Zeatin	C15545/C00371	Plant hormone
	242.2	242.193	242.125	241.118	H+	Tetrahydrobiopterin	C00272	Folate biosynthesis
	300.2	300.186	300.160	299.152	H+	Codeine	C06174	Isoquinoline alkaloid
	300.2	300.186	300.107	277.118	Na+	Queuine	C01449	Nucleobase + Purine
	365	365.08	365.050	364.042	H+	Xanthosine-5-phosphate	C00655	Purine
	365	365.08	365.085	326.121	K+	Neohesperidose	C08244	Carbohydrate
	365	365.08	365.085	326.121	K+	Robinobiose	C08246	Carbohydrate
	365	365.08	365.086	326.123	K+	6,7-dimethyl-8-(D-ribityl)lumazine	C04332	Riboflavin
	448.2	448.117	448.122	409.158	K+	Linustatin	C08333	Cyanogenic glucosides
	531.4	531.367	531.454	492.491	K+	Tritriacontane-16,18-dione	C08394	Alkane
	569.4	569.338	569.313	568.305	H+	Protoporphyrinogen IX	C01079	Chlorophyll
	569.4	569.338	569.436	568.428	H+	Xanthrophyll	C08601	Carotenoid
	569.4	569.338	569.436	568.428	H+	Zeaxanthin	C06098	Carotenoid + Hormone (ABA)
	585.4	585.329	585.431	584.423	H+	Antheraxanthin	C08570	Carotenoid
	664.2	664.196	664.267	625.303	K+	Leukotriene C4	C02166	Lipid - Arachidonic acid

## Chapter 4

### A novel host-symbiont interaction can rapidly evolve to become a beneficial symbiosis

#### 4.1 Introduction

Endosymbioses are evolutionarily dynamic. Their environmental context dependence (Thompson, 2005) generates inherent potential for conflicting fitness interests among the symbiotic partners (Sachs and Simms, 2006). This can lead to the breakdown of symbiosis if environmental conditions change faster than symbionts can adapt or where pursuit of individual fitness interests lead to the emergence of cheating. Both situations can create selection for partner switching to recombine novel symbiotic partnerships (Boulotte et al., 2016). Partner switching can restore symbiont function following breakdown (Koga and Moran, 2014; Matsuura et al., 2018) or where the current symbiotic phenotype is maladapted to prevailing environmental context (Lefèvre et al., 2004). As such, partner-switching can enable niche-expansion by hosts (Joy, 2013; Sudakaran et al., 2017) and provide a mechanism by which host-symbiont local adaptation can arise faster than by adaptation of the current symbiont (Jaenike et al., 2010; Jiggins and Hurst, 2011). For example, corals acquire thermally-tolerant *Symbiodinium* endosymbionts following thermal bleaching events (Boulotte et al., 2016), and replacement of the photobiont with an alternative ecotype is believed to have enabled symbiont-mediated niche expansion in lichens (Rolshausen et al., 2018). A greater understanding of partner switching is also required if we are to understand life-history patterns; specifically, serial symbiont replacements have occurred in plastid evolution and have entangled the eukaryotic lineages (Patron et al., 2006; Stiller et al., 2014). The frequency of partner switching in natural populations suggests that new host-symbiont genotype pairings must arise regularly in a wide range of symbioses.

Despite the widespread occurrence of partner-switching, however, new host-symbiont pairings may have low fitness because the genotypes are unlikely to be co-adapted due to a lack of recent coevolutionary history. This has been observed in a range of symbiotic interactions: for example, a newly acquired *Symbiodinium* endosymbiont was found to

translocate less fixed carbon than the native symbiont to its cnidarian host (Matthews et al., 2018); novel bacterial endosymbionts had reduced vertical transmission rates in aphid hosts (Russell and Moran, 2005); and novel *Wolbachia* endosymbionts reduced the reproductive fitness of *Drosophila simulans* (McGraw et al., 2002). How then are these newly-formed, poorly co-adapted host-symbiont pairings stabilised? Experimental studies suggest that initially low fitness host-symbiont associations can rapidly ameliorate their initial fitness costs: For example, the higher fitness cost of novel *Spiroplasma* endosymbiont genotypes could be rapidly alleviated in *Drosophila melanogaster* (Nakayama et al., 2015). I hypothesised, therefore, that this process could be enabled by rapid evolution, to create a beneficial, co-adapted association from a low fitness starting point.

Experimental evolution provides a powerful tool to study the dynamics of symbiotic interactions as it allows evolutionary processes to be studied in real time and in controlled laboratory conditions (Hoang et al., 2016). Previous applications of experimental evolution to symbiosis have studied the evolution of entirely *de novo* associations (Jeon, 1987; Nakajima et al., 2009, 2015), as well as the transition between parasitism and mutualism (King et al., 2016; Sachs and Wilcox, 2006; Shapiro and Turner, 2018; Tso et al., 2018). Rarely, however, has experimental evolution been used to study beneficial endosymbioses (Hoang et al., 2016). To test the role of rapid evolution in the establishment of new host-symbiont associations, I recapitulated the process of partner-switching by creating a novel *Paramecium bursaria* - *Chlorella* association which had initially low fitness, and then experimentally evolving replicate populations. The *P. bursaria* - *Chlorella* symbiosis is primarily based on a nutrient exchange between fixed carbon from the photosynthetic alga and organic nitrogen from the heterotrophic host (Johnson, 2011; Ziesenisz et al., 1981). It is highly experimentally tractable and amenable to experimental evolution: symbiotic *P. bursaria* have fast generation times and replicate populations can easily be cultured in the laboratory. To my knowledge, the *Paramecium bursaria* - *Chlorella* endosymbiosis has not been used previously for experimental evolution, although an evolution experiment using another member of the *Paramecium* genus has been published. Lohse et al. (2006) coevolved *Paramecium caudatum* with a bacterial parasite for 130-260 host-generations, reporting that hosts evolved greater resistance against their coevolved parasites. In addition, *Chlorella vulgaris* was shown to rapidly adapt to predation within a few generations (Yoshida et al., 2004). These demonstrate that both *Paramecium* and *Chlorella* are capable of rapid evolutionary responses to selection.

I used the results from Chapter 3 to choose a newly-formed *P. bursaria* - *Chlorella* association that was less-beneficial than the native association. I chose the 186b host and HK1 symbiont pairing, which had lower growth rate than the native 186b pairing at high light (Figure 3.2). Furthermore, this novel association had lower symbiont load than the native pair at high light (Figure 3.3), which offered a potential mechanism for selection to act upon. I predicted, therefore, that the novel symbiosis would evolve upregulation of its symbiont load to increase the benefit to the host and so increase its growth rate. Replicate populations of the novel 186b-HK1 association were experimentally evolved by serial transfer for ~50 host generations and compared to control populations of the native association that were evolved under identical conditions. I tracked changes in host-symbiont growth rate and per host symbiont load over the course of the experiment, and quantified change in fitness between the start and end of the experiment. To determine the mechanisms of adaptation, and distinguish host versus symbiont contributions, I performed untargeted metabolomics separately on the host and symbiont at the start and end of the experiment. I observed that the initially non-beneficial novel host-symbiont association rapidly evolved to become as beneficial as the native host-symbiont pairing. The data further suggest that this was driven by changes in symbiont load and metabolism. These data confirm that rapid evolution can indeed enable non-beneficial host-symbiont pairings arising from partner-switching to become highly beneficial in fewer than 50 host generations.

## 4.2 Materials and Methods

### *Cultures & Strains*

*P. bursaria* - *Chlorella* cultures were maintained under the conditions described in Chapter 2. The two symbiotic partnerships used in this chapter were: the 186b host-genotype with its native symbiont and the 186b host-genotype with the non-native, HK1, symbiont. These were created from the cross-infections in Chapter 3.

### *Evolution Experiment*

The populations used derive from the cross-infections in Chapter 3, and, therefore, the symbiotic partnerships come from the same cured 186b ancestor that was then re-infected with either its native (186b) or novel (HK1) symbionts. The two symbiotic partnerships were split into six replicate populations that were used as the starting populations. The 200ml populations were propagated by weekly serial transfer for 25 transfers at a high light

(50  $\mu\text{E m}^{-2} \text{ s}^{-1}$ ) 14:10 L:D cycle. At every transfer, cell-density was equalised to 100 cells  $\text{ml}^{-1}$  and the transferred cells were washed with a 11 $\mu\text{m}$  nylon mesh using Volvic before being re-suspended in bacterized PPM. Cell density was measured before and after each transfer by fixing 360  $\mu\text{L}$  of each cell culture, in triplicate, in 1% v/v glutaraldehyde in 96-well flat bottomed micro-well plates. Images were taken with a plate reader (Tecan Spark 10M) and cell counts were made using an automated image analysis macro in ImageJ v1.50i (Schneider et al., 2012). Fitness assays were conducted at the start and end of the experiment as described in Chapter 2. Growth rate and symbiont load assays were conducted at the start, T10, T20 and end of the experiment described in Chapter 3.

### *Metabolomics*

The cultures were sampled at the start and end of the evolution experiment. Cultures were washed and concentrated with a 11 $\mu\text{m}$  nylon mesh using Volvic and re-suspended in bacterized PPM. The cultures were acclimated at their treatment light condition (50  $\mu\text{E m}^{-2} \text{ s}^{-1}$ ) for seven days. For the start point, the six experimental replicates were used as replicates for the metabolomics. For the end point, three replicates of each of the six experimental replicates were used for the metabolomics because divergence may have occurred over the course of the experiment.

At each sampling event, the symbiotic partners were separated in order to get *P. bursaria* and *Chlorella* metabolic fraction using the extraction method described in Chapter 2. Samples were freeze-dried for storage, and then resuspended in 50:50 methanol to water prior to mass spectrometry.

The samples were analysed with a Synapt G2-Si with Acuity UPLC, recording in positive mode over a large untargeted mass range (50 – 1000 Da). A 2.1x50mm Acuity UPLC BEH C18 column was used with acetonitrile as the solvent. The machine settings are listed in detail below:

Mass spectrometry settings:

Polarity:	positive
Capillary voltage:	2.3 kV
Sample Cone voltage:	20 V
Source Temperature:	100 $^{\circ}\text{C}$
Desolvation temperature:	280 $^{\circ}\text{C}$
Gas Flow:	600 L $\text{hr}^{-1}$
Injected volume:	5 $\mu\text{l}$
Column temperature:	45 $^{\circ}\text{C}$

Gradient information:

Time (mins)	Water (%)	Acetonitrile (%)
0	95	5
3	65	35
6	0	100
7.5	0	100
7.6	95	5

The *P. bursaria* and *Chlorella* fraction were analysed separately. The xcms R package (Benton et al., 2010; Smith et al., 2006; Tautenhahn et al., 2008) was used to extract the spectra from the CDF data files, using a step argument of 0.01 m/z. Peaks were identified, and then grouped across samples. These aligned peaks were used to identify and correct correlated drifts in retention time from run to run. Pareto scaling was applied to the resulting intensity matrix.

#### *Metabolomics Analysis*

The metabolic profiles from the start and end of the experiment were compared using principal component analysis (PCA) with the `prcomp()` function in Base R (<https://www.r-project.org/>). For both fractions the first three components were considered, this accounted for >88% of the variance. The top 1% of the loadings were selected using the absolute magnitude of the loadings. These top loadings were identified where possible, and the identified loadings were then depicted in their associated component space. The relative abundance of these top loadings was visualised using heatmaps drawn with the `heatmap.2()` function from the `gplot` package (Warnes et al., 2009). The phylogenies were based on UPGMA clustering of the PCA coordinates of the samples using the `hclust()` function.

#### *Identification of significant masses*

Masses of interest were investigated using the MarVis-Suite 2.0 software (<http://marvis.gobics.de/>) (Kaefer et al., 2009), using retention time and mass to compare against KEGG (<https://www.genome.jp/kegg/>) (Kanehisa and Goto, 2000; Kanehisa et al., 2019) and MetaCyc (<https://biocyc.org/>) (Caspi et al., 2018) databases. The Metabolomics Standards Initiative requires two independent measures to confirm identity, which the combination of retention time and accurate mass achieves.

#### *Data Analysis*

Statistical analyses were performed in Rv.3.5.0 (R Core Team, 2018) and all plots were produced using package `ggplot2` (Wickham, 2016) unless otherwise stated. Physiology tests

were analysed by both ANOVA and ANCOVA, with transfer time, host and symbiont identity as factors. A linear mixed effect model was used to analysis the growth rate per transfer using `lm()` function from the `nlme` package (Pinheiro et al., 2019). The `lm` model included fixed effects of symbiont genotype and transfer number, and random effects of transfer number given sample ID.

### 4.3 Results

Replicate experimental populations of either the novel host-symbiont pairing or the native host-symbiont pairing were established. Specifically, the 186b *P. bursaria* - *Chlorella* strain was cured of its native algal symbiont and subsequently re-infected with either its native algal symbiont or the novel HK1 algal symbiont. Six replicate populations of each of these two symbiotic partnerships were then propagated by weekly serial transfer for 25 transfers at a high light (50 $\mu$ E) 14:10 L:D regime. At every transfer cell-density was equalised to 100 cells ml<sup>-1</sup> among populations to prevent extinctions. The growth rate per transfer was higher for the native pairing than the novel pairing (Figure 4.1) (linear mixed effect model, HK1 symbiont fixed effect of  $-0.08 \pm 0.006$ , T-value =  $-14.126$ , see Appendix D for full statistical output), but increased over time for both pairings (transfer number fixed effect  $0.001 \pm 0.0004$ , T-value =  $3.088$ ).

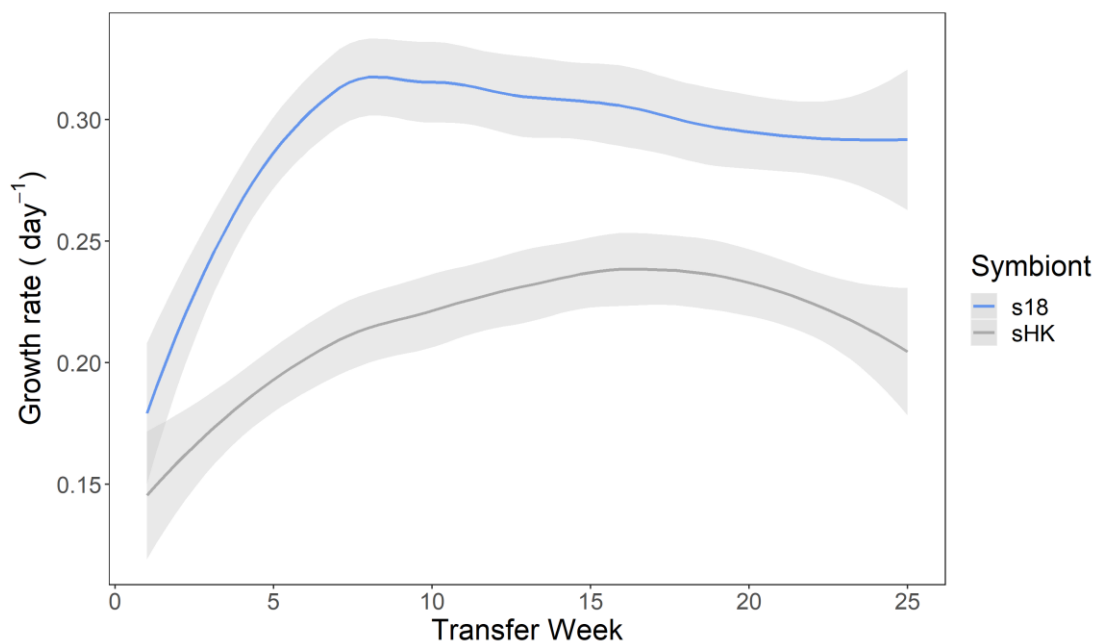


**Figure 4.1. Weekly growth rates of the native and novel symbioses across the evolution experiment.** The lines show the smoothed mean ( $n=6$ ) growth rates  $\pm$  SE and colour denotes the symbiont genotype (blue = s18 = native symbiont; grey = sHK = novel symbiont). The smoothing function used was the loess method.

To test for change in symbiotic performance I quantified the host-symbiont growth rate reaction norm across a light gradient at multiple points during the experiment (Figure 4.2). At the beginning of the experiment, the growth rate of the native pairing increased more steeply with irradiance than the novel pairing, suggesting that the host derived greater symbiotic benefit at higher light intensity from its native symbiont. This difference was reduced over time, such that both the native and the novel pairings showed equivalent growth rate responses with light irradiance by the endpoint of the experiment (ANOVA,  $F_{13,178} = 56.14$ ,  $P < 0.001$ ). This compensation for the initially poor performance of the novel symbiont at high irradiance occurred rapidly, such that the host-symbiont growth rate reaction norms of the native and novel pairings already appeared similar by transfer 10. These data suggest that newly established symbioses can rapidly achieve similar growth performance as the native host-symbiont pairing.

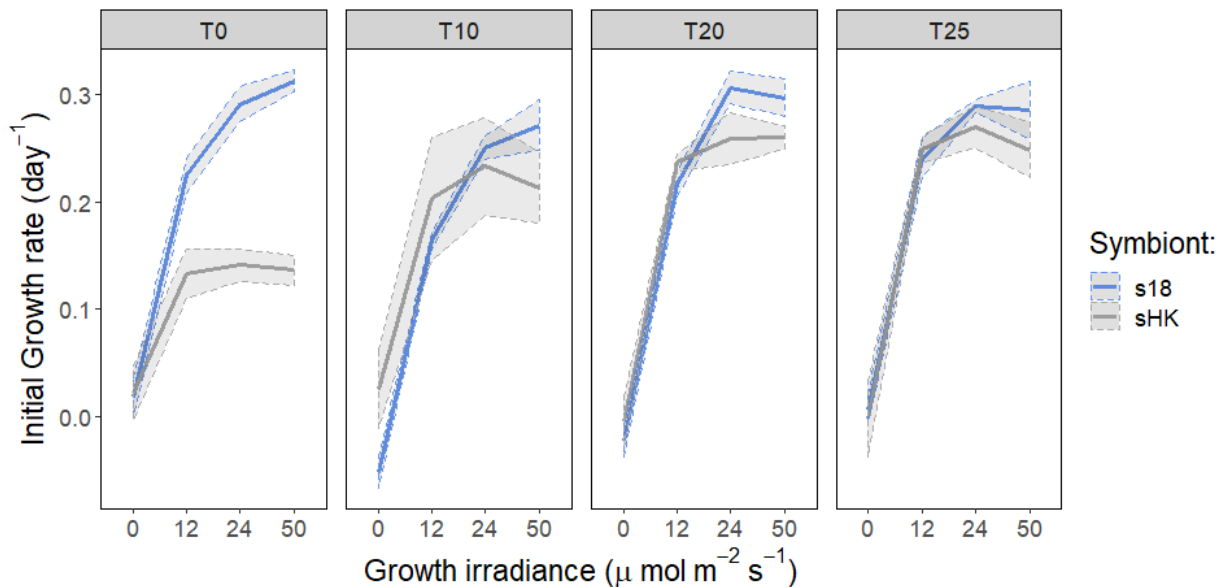


**Figure 4.2. Growth rate assays performed at multiple points throughout the evolution experiment.** Each panel shows the mean ( $n=6$ ) initial growth rate across a light gradient and the shaded area denotes  $\pm$  SE. The panels represent the transfer week within the evolution experiment at which the growth assay was performed (T0 = week 0, T10 = week 10, T20 = week 20 & T25 = week 25). The symbiont-genotype is denoted by colour.

In this symbiosis, hosts are known to regulate the cost-to-benefit ratio of symbiosis by altering symbiont load. To determine if regulation of symbiont load changed during the transfer experiment, symbiont load was measured as the intensity of single-cell fluorescence using a flow cytometer following growth across a light gradient (Figure 4.3). At the start of the experiment both host-symbiont pairings showed the expected unimodal symbiont load curve with light, albeit with higher symbiont loads for the native compared to the

novel pairing at the highest light level,  $50 \mu\text{E m}^{-2} \text{s}^{-1}$ , which was the irradiance used in the transfer experiment. By the end of the transfer experiment, the functional forms of the symbiont load reaction norms had changed in both host-symbiont pairings (symbiont genotype\*light\*transfer interaction, ANOVA,  $F_{19,76} = 34.15$ ,  $P < 0.001$ ). Most notably, while the novel pairing had increased symbiont load at  $50 \mu\text{E m}^{-2} \text{s}^{-1}$ , symbiont load had decreased in the native pairing at this irradiance, such that symbiont load was now higher in the novel pairing at  $50 \mu\text{E m}^{-2} \text{s}^{-1}$  irradiance. This increase in novel symbiont load at high irradiance may explain the improved growth performance observed at high light in the novel pairing. Interestingly, whilst the novel pairing retained the characteristic unimodal relationship between symbiont load and irradiance during the transfer experiment, this appears to have been lost in the native pairing, suggesting that altered symbiont load regulation can arise when evolved in a consistent light-dark environment.

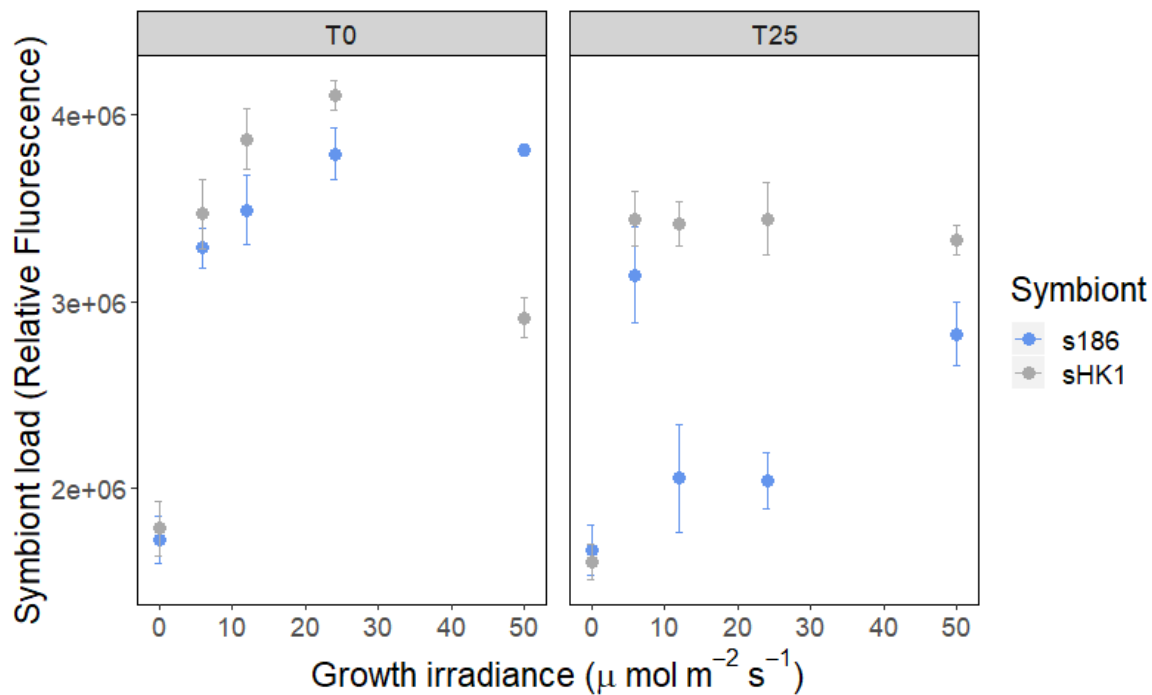


**Figure 4.3. Symbiont load at the start and end of the evolution experiment.**

Symbiont load was measured across a light gradient. The left-hand panel shows data measured at the start of the evolution experiment and the right-hand panel shows data measured at the end. The points show the mean ( $n=6$ ) relative chlorophyll fluorescence  $\pm$  SE and symbiont-genotype is denoted by colour.

To compare the fitness effect of symbiosis for the host before and after evolution, I directly competed the native and novel symbiotic pairings against the ancestral symbiont-free host strain across a light gradient at the beginning and end of the transfer experiment. Specifically, I used flow cytometry to quantify the proportion of symbiotic versus non-symbiotic cells at the start and end of competitive growth and calculated the selection rate, providing a direct measure of the fitness effects of symbiosis. At the beginning of the transfer experiment, the fitness of symbiotic relative to non-symbiotic hosts increased more steeply with irradiance for the native than the novel pairing (Figure 4.4). Following evolution, this difference had disappeared such that both the native and novel symbiotic pairings showed increasing fitness relative to non-symbiotic hosts with increasing irradiance (ANOVA,  $F_{11,41} = 8.87$ ,  $P < 0.001$ ). Indeed, at  $50 \mu\text{E m}^{-2} \text{s}^{-1}$ , the light level used in the selection experiment, the large fitness deficit observed between the novel and native pairing at the beginning of the experiment had been completely compensated following evolution.

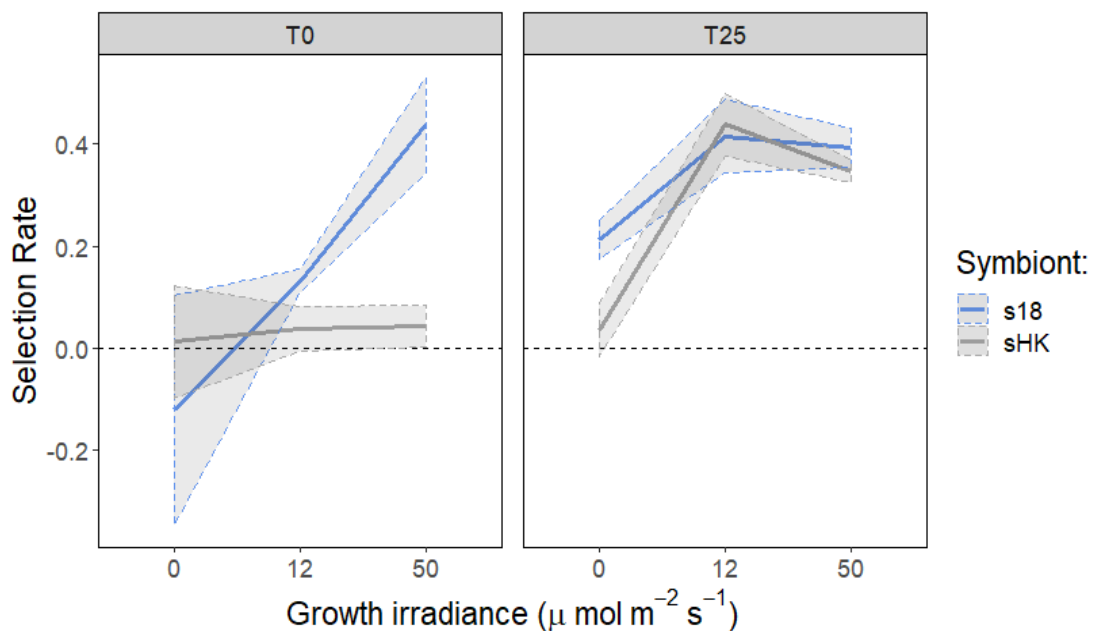


**Figure 4.4. Fitness of the host-symbiont pairings relative to the symbiont-free host at the start and end of the evolution experiment.** Lines show mean ( $n=6$ ) competitive fitness of symbiont-containing hosts relative to the symbiont free 186b host calculated as selection rate, the shaded area denotes  $\pm$  SE. The left-hand panel shows data measured at the start of the evolution experiment and the right-hand panel shows data measured at the end. Symbiont-genotype is denoted by colour. A selection rate above 0 indicates greater fitness in comparison to the symbiont-free host.

It was no longer possible to cure the evolved host-symbiont pairings of their symbionts, and so to estimate the contribution of host versus symbiont evolution to the observed convergence in host-symbiont fitness I used metabolomics. Specifically, I performed untargeted metabolomics analyses on the separated *Chlorella* and *P. bursaria* fractions from samples taken the start and end of the transfer experiment grown at  $50 \mu\text{E m}^{-2} \text{s}^{-1}$ . The ancestral *P. bursaria* and *Chlorella* metabolic profiles of both host-symbiont pairings could be clearly distinguished. Following evolution, *P. bursaria* metabolism displayed a high degree of convergence between hosts evolved with the native versus the novel symbionts (Figure 4.5 a,c). This was driven by decreased levels of compounds of central metabolism (such as pyruvate and TCA cycle intermediates, antioxidants, lipids, and some amino acids) (Table S4.1), suggesting either increased pathway completion or a reduced metabolic rate, both of which can lead to increased efficiency. In addition, there were increased levels of the amino acid cysteine and a shikimate pathway component (Figure 4.6). I also observed increased levels of algae-cell degradation components, such as cell-wall degradation product chitotriose, in some replicates with either symbiont, potentially suggesting increased digestion of *Chlorella* (Figure 4.6). In contrast, the metabolic profiles of the symbiont genotypes were less consistent (Figure 4.5 b,d). Whereas all replicates of the native 186b *Chlorella* evolved in a similar direction, the replicates of the novel HK1 *Chlorella* split into two different directions. Two of the HK1 replicates took a similar trajectory to the 186b symbionts, while the remaining four replicates followed an opposing evolutionary trajectory. The group of four HK1 replicates that diverged during the experiment, had lower production of metabolites within core aspects of metabolism, such as lipids, amino acids and carbohydrates. The second group including the remaining two HK1 replicates and all the 186b replicates had higher production within primary metabolism pathways, particularly within lipids and carbohydrates, as well as a key chlorophyll compound, a photo-protective carotenoid, and secondary metabolites with potential antioxidant properties (Figure 4.7, Table S4.2). This greater investment into photosynthesis and photo-protection may improve carbon transfer to the host and decrease light stress, which aligns with the decrease in host antioxidants.

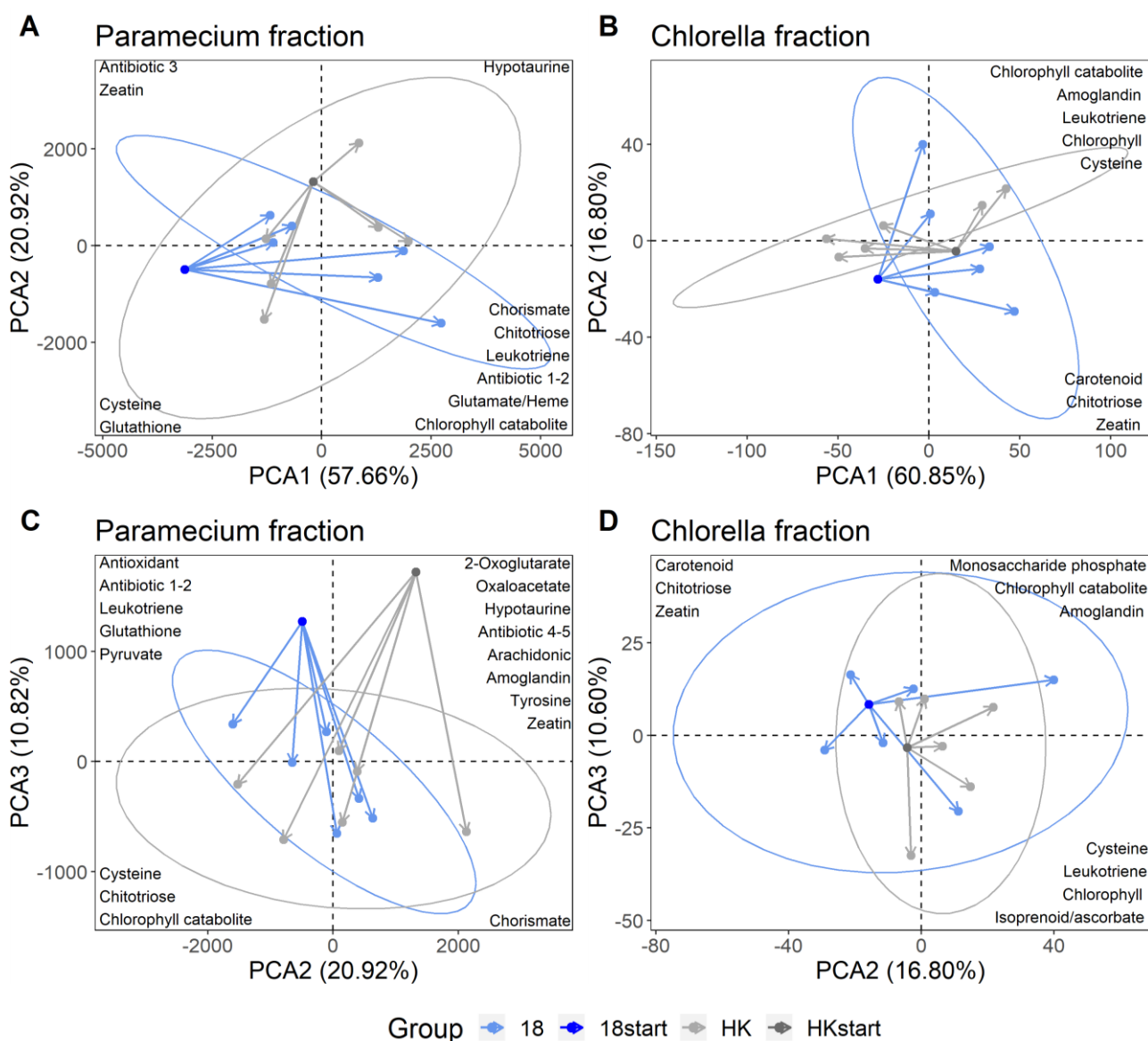


**Figure 4.5. The trajectories of the metabolic profiles from the start to the end of the evolution experiment.** These trajectories are shown within PCA plots and the arrows represent the movement in principal component space over the course of the experiment, with 95% confidence ellipses drawn for the evolved profiles. The metabolite identifications for the top loadings are shown in their corresponding location. Colour denotes the symbiont-genotype and shade represents whether the samples are from the start or end of the experiment. A and C show the results for the *P. bursaria* fraction, B and D the *Chlorella* fraction. The top row (A and B) plot PCA 1 versus PCA 2. The bottom row (C and D) plot PCA 2 versus PCA 3. The data here presents the biological replicates, which have been averaged over their technical replicates.

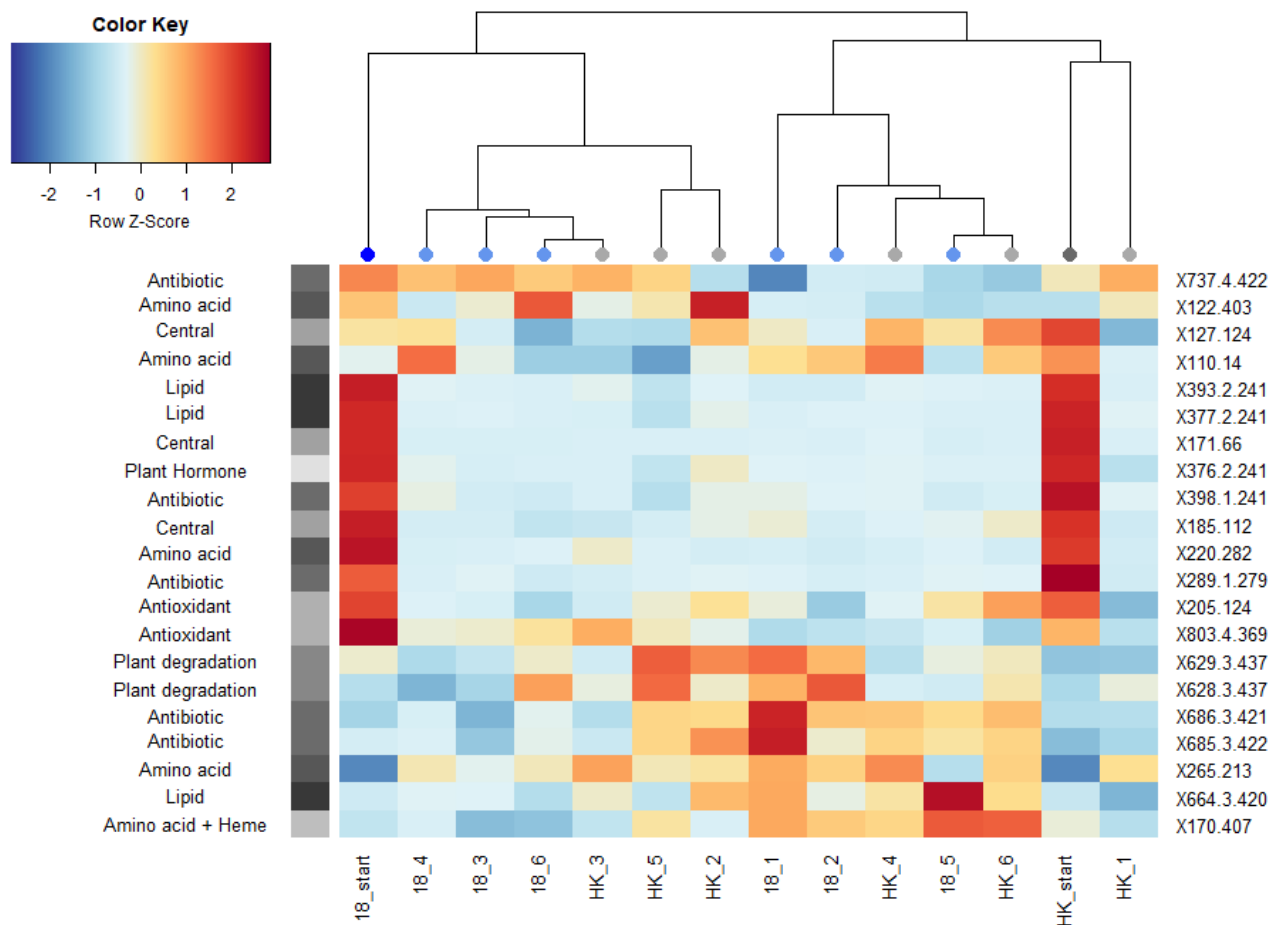


**Figure 4.6. Metabolites of interest across the start and end of the evolution experiment within the *P. bursaria* fraction.** The data is shown as a heatmap with the colour representing the relative abundance of the metabolites. The metabolites depicted were identified from the top loadings of the PCA plots. The columns in the heatmap correspond to sample; these are labelled with their symbiont-genotype (18 = 186b; HK = HK1) and with the replicate number if from the end of the experiment or ‘start’ if from the start. The column on the left of the heatmap indicates the function of the metabolites and the column on the right indicates the loading ID, which corresponds to the identification Table S4.1. The phylogeny of the samples was calculated with their principal component coordinates using UPGMA clustering, and the order of the rows was assigned by UPGMA clustering performed on the rows’ distance measures (based on the Pearson correlation co-efficient).

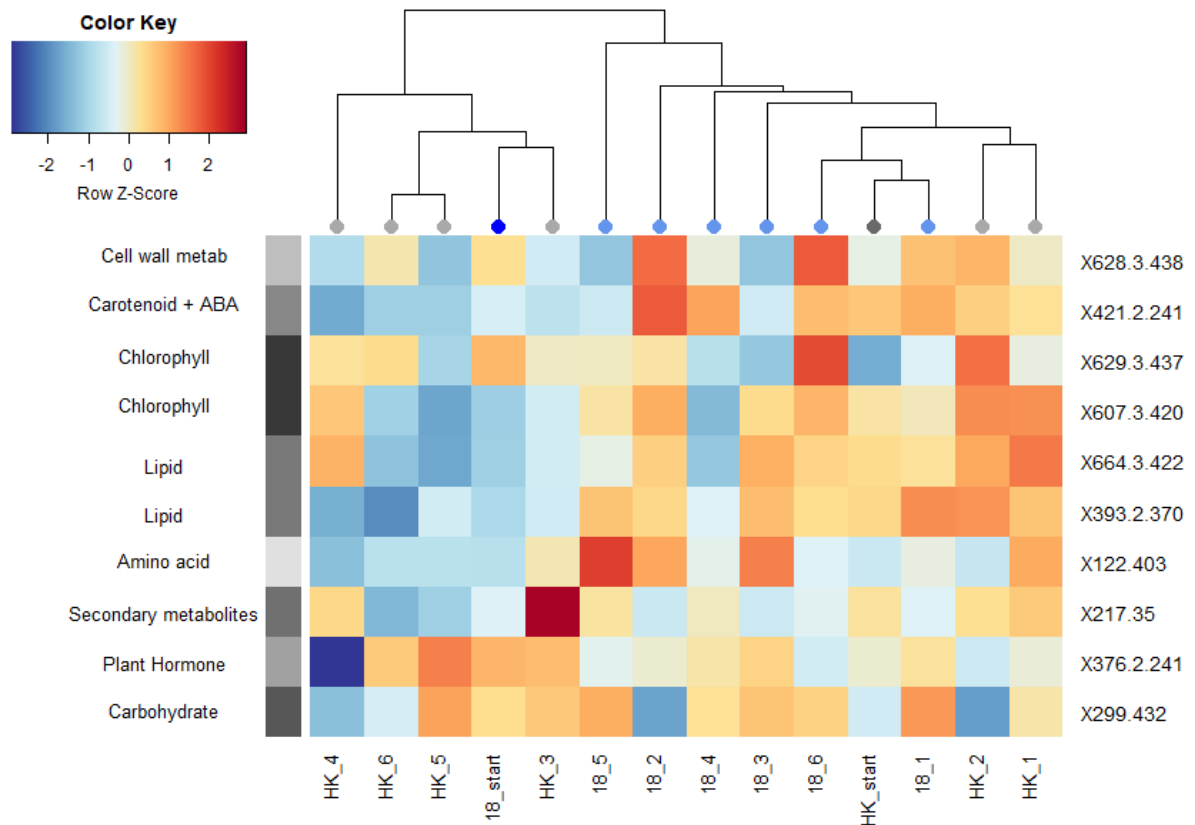


**Figure 4.7. Metabolites of interest across the start and end of the evolution experiment within the *Chlorella* fraction.** The data is shown as a heatmap with the colour representing the relative abundance of the metabolites. The metabolites depicted were identified from the top loadings of the PCA plots. The columns in the heatmap correspond to the sample; these are labelled with their symbiont-genotype (18 = 186b; HK = HK1) and with the replicate number if from the end of the experiment or ‘start’ if from the start. The column on the left of the heatmap indicates the function of the metabolites and the column on the right indicates the loading ID, which corresponds to the identification Table S4.2. The phylogeny of the samples was calculated on their principal component coordinates using UPGMA clustering, and the order of rows was assigned by UPGMA clustering performed on the rows’ distance measures (based on the Pearson correlation co-efficient).

## 4.4 Discussion

In this chapter, I show that an initially non-beneficial, novel host-symbiont pairing evolved to become as beneficial as the native host-symbiont pairing in fewer than 50 host generations. This increase in the fitness benefit of symbiosis to hosts was accompanied by increased symbiont load following evolution in the novel, but not the native, host-symbiont pairing at the irradiance level in which they had evolved. I observed convergence of *P. bursaria* metabolism between the native and novel host-symbiont pairings following

evolution. Specifically, decreased levels of the intermediates of central metabolism, antioxidants and lipids, were observed following evolution compared to samples from the start of the experiment. Multiple trajectories of metabolic evolution were observed in *Chlorella* among the replicates of the novel host-symbiont pairing, two of which increased their investment into metabolites associated with photosynthesis and photo-protection. Together these data suggest that newly-formed host-symbiont pairings can rapidly evolve higher fitness through changes in symbiont load regulation and metabolism.

Consistent with findings from other symbioses (Matthews et al., 2018; Nakayama et al., 2015), I observed initially low fitness of the newly-formed host-symbiont pairing, suggesting poor co-adaptation arising from a lack of coevolutionary history. This initial lack of co-adaptation is likely a consequence of the novel symbiont belonging to a different clade than the native symbiont, and therefore these symbiont genotypes arise from independent origins of this symbiosis (Hoshina and Imamura, 2008; Summerer et al., 2008). The *Chlorella* clades are biogeographical and it is highly unlikely these symbiont-genotypes co-occur (Hoshina et al., 2005) and, therefore, the partners of the novel association have probably never encountered one another before. Furthermore, the previous chapters of this thesis have shown that the symbiont clades are associated with different photophysiology traits and stress tolerances that affect the light-dependent fitness outcome of this association. Trait variation between the clades could explain the initially mis-matched symbiotic phenotype that caused low fitness of the novel host-symbiont pairing.

Following evolution, the initially low fitness novel host-symbiont pairing acquired high fitness benefits equivalent to the native host-symbiont association. Phylogenetic reconstruction has predicted that many beneficial bacterial symbionts originated as parasites (Sachs et al., 2011), which demonstrates that the evolution of benefit also occurs in nature and can lead to stable mutualisms. In addition, the evolution of benefit has been documented within evolution experiments (King et al., 2016; Nakayama et al., 2015; Shapiro and Turner, 2018; Tso et al., 2018). My findings, therefore, align with previous results and extend the evidence to include the evolution of benefit from a novel, non-beneficial symbiosis.

The evolution of increased benefit within the novel association was partially mediated by increased symbiont load, which could directly affect the benefit-to-cost ratio of the symbiosis (Holland et al., 2002, 2004). Corals are known to adjust the per host load of *Symbiodinium* endosymbionts according to environmental conditions and symbiont

genotype to maximise the benefit of the symbiosis (Cunning et al., 2015). Similar regulation of symbiont load with light intensity has been observed in the *P. bursaria* - *Chlorella* association (Dean et al., 2016; Lowe et al., 2016). Such that the symbiont load peaks in the low light, when the benefit of the symbionts outweighs their cost, and then the symbiont load decreases with increasing irradiance as the benefit-per-symbiont increases (Hoogenboom et al., 2010) and fewer symbionts are required to meet the demand. Changes to symbiont load can occur by hosts either triggering symbiont cell division or by the digestion/egestion of symbionts (Kodama and Fujishima, 2008; Takahashi et al., 2007). The evolution of increased symbiont load in the novel host-symbiont pairing implies that, initially, hosts had too few symbionts to meet their demand for fixed carbon. Accordingly hosts upregulated symbiont load during the course of the experiment, leading to a higher host-symbiont growth rate. In contrast, in the control native host-symbiont pairing, symbiont load at the light level at which the populations had evolved declined following evolution without any reduction in host-symbiont growth rate. This implies that the benefit-per-symbiont accrued to the host may have increased during evolution in the native but not in the newly formed association, suggesting that evolution can further fine-tune even established host-symbiont associations.

The difference between the evolved symbiont loads may be explained by the metabolic adaptation of the symbionts, which affects their benefit to the host. The native symbiont evolved higher production of several key metabolites, including chlorophyll, lipids and carbohydrates. These metabolites imply that increased symbiont investment into photosynthesis may have increased the carbon transferred to the host; a correlation that has been observed in other photosymbioses (Cantin et al., 2009; Freeman et al., 2013). In turn, the increased translocated carbon could have driven the increased benefit-per-symbiont and, therefore, led to the observed reduced symbiont load of the native symbiont. On the other hand, the metabolic profiles of the novel symbiont evolved in two directions. Two of the HK1 replicates converged with the 186b symbionts, having higher production of the same key metabolites. The remaining HK1 replicates, however, did not evolve increased photosynthetic investment or carbon transfer but decreased the metabolic intensity of some of these key compounds, and therefore did not converge with the metabolism of the native symbiont. To test whether the alternative metabolic trajectories affected the benefit of the symbionts, I examined the per-replicate symbiont load, on the premise that a higher symbiont load should be associated with a lower benefit-per-symbiont. Within this data (Table S3), the two HK1 replicates that converged metabolically with the native symbionts had a lower increase in symbiont load compared

to the replicates that metabolically diverged. This implies that while a few of the novel symbionts evolved in a similar manner to the native symbionts and increased their benefit to the host, the majority of the novel symbiont replicates did not.

Over the course of the experiment, the *P. bursaria* metabolism converged between hosts harbouring the native and novel symbiont. The convergence in metabolic profile of the evolved hosts was largely associated with a decrease in intermediates of central metabolism. A decrease in the accumulation of intermediates can be potentially explained by two alternative mechanisms. First, a higher metabolic flux rate can increase pathway completion, which means that the abundance of pathway intermediates decreases but the production of end-products will increase (Ferea et al., 1999; Maharjan et al., 2007; Pfeiffer et al., 2001). Alternatively, a reduction of overall metabolic rate would reduce the abundance of both pathway end-products and intermediates (Ibarra et al., 2002; Lewis et al., 2010). Both of these can be indicative of increased metabolic efficiency if performance is not compromised (Ratcliffe and Shachar-Hill, 2006; Rees and Hill, 1994), which is the case here. In addition, the shared metabolic profile of the evolved hosts had decreased in antioxidant production. A reduction of antioxidants has been documented as an adaptation to stable photosymbioses in a number of cases, including in the *Hydra* - *Chlorella* symbioses (Ishikawa et al., 2016), and a similar decrease in host oxidative stress responses was observed through transcriptome comparisons of symbiotic compared to symbiotic-free *P. bursaria* (Kodama et al., 2014). This reduction in antioxidants is indicative of less oxidative stress within the hosts and is believed to be because symbionts take over the oxidative stress response resulting in a more tightly integrated symbiosis (Hörtnagl and Sommaruga, 2007; Summerer et al., 2009). In line with this, the reduction in host antioxidants was accompanied by an increase in symbiont oxidative stress protection in most of the symbiont replicates, specifically a photo-protective carotenoid and secondary metabolites with potential antioxidant properties.

In addition, in the evolved host metabolism of some replicates, I observed increased levels of algae-cell degradation components that could be indicative of increased *Chlorella* digestion. Symbiont digestion is an important element of symbiont load control that also provides nutrition for the host (Kodama and Fujishima, 2008; Titlyanov et al., 1996). Host digestion in response to a changing benefit-to-cost ratio has been documented in the cereal weevil whose digestion of its *Sodalis* endosymbiont changes with its benefit, and therefore alters throughout the developmental stages (Vigneron et al., 2014); and in corals that digest their dinoflagellate symbionts when starved (Titlyanov et al., 1996). Increased

digestion was observed in host replicates with either symbiont genotype and, therefore, was not specific to either a decrease or increase in symbiont load. Instead, symbiont digestion appears to be a general mechanism by which hosts can derive additional benefit from their symbionts.

Partner switching is a crucial aspect of endosymbioses that is known to rescue endosymbioses where the symbiont has lost key functionality or is mis-matched to new environmental conditions (Joy, 2013; Koga and Moran, 2014; Lefèvre et al., 2004; Matsuura et al., 2018). Due to a lack of prior coadaptation, successful partner switching may often require for an initial period of low fitness to be overcome. In this chapter I have used a powerful combination of physiological, metabolic and evolutionary methodologies to study the processes that underlie symbiosis integration. With this approach, I have demonstrated that a novel, initially non-beneficial symbiosis rapidly evolved to be beneficial, primarily through adaptations in host metabolism and symbiont load regulation. The host adapted to the novel symbionts by converging metabolically to the hosts with the native symbiont, but the symbiont load regulation between the hosts remained different, possibly connected to the alternative metabolic profile in the majority of the novel symbionts. Interestingly, the fitness of the novel pairings increased in all of the replicates despite the potentially different degrees of symbiont benefit. This could be because there are two alternative strategies regarding symbiont metabolism and symbiont load, and both strategies lead to higher fitness. Alternatively, it could reveal asymmetry between the contribution of the partners to adaptation, and that host adaptation is the primary driver in this endosymbiosis. Asymmetry between the contribution of host and symbiont to adaptation has been documented within other endosymbioses (Koch et al., 2017), and is theorised to be an aspect of their unequal control (Frank, 1997). The control within this endosymbiosis is thought to be especially one-sided since this photosymbiosis is believed to be an instance of host exploitation (Decelle, 2013; Lowe et al., 2016). Overall, these results support the hypothesis that rapid evolution of benefit can stabilise novel associations and so enables partner switching to occur with a broader range of partners than initial compatibility tests would reveal.

## 4.5 Supplementary Tables

**Table S4.1. Identified metabolites associated with PCA trajectories for the *P. bursaria* fraction.** These were identified from the top 1% of loadings when using the first three principal components. The metabolite ID is that referred to in Figure 4.6.

PC of loading	ID	Detected mass	Accurate mass	Adduct	Function	Pathway	Compound	Kegg / Metacyc
PC1, PC3	X110.14	110	109.0197	H+	Amino acid	Taurine metab	Hypotaurine	C00519
PC1	X170.407	170	131.0582	K+	Amino acid + Heme	Heme biosynthesis	5-Amino-4-oxopentanoate	C00430
			147.0532	Na+		Amino acid/Central	Glutamate	C00025
			131.0582	K+		Amino acid	Glutamate 5-semialdehyde	C01165
PC1, PC2, PC3	X265.213	265	226.0477	K+	Amino acid	Shikimate pathway	Chorismate	C00251
			226.0477	K+		Shikimate pathway	Prephenate	C00254
			242.0192	Na+		Shikimate pathway	Deoxy-ketofructose-phosphate	C16848
PC1, PC2, PC3	X376.2.241	376.2	353.1699	Na+	Plant hormone	Plant hormone (zeatin)	Dihydrozeatin riboside	C16447
PC1, PC2, PC3	X628.3.437	628.3	627.2487	H+	Plant degradation	Chitin degradation	Chitotriose	CPD-13227
PC1, PC2	X629.3.437	629.3	628.2897	H+	Plant degradation	Chlorophyll degradation	Chlorophyll catabolite	C18098
PC1, PC2	X664.3.420	664.3	625.3033	K+	Lipid	Lipid - Arachidonic acid	Leukotriene C4	C02166
PC1, PC2, PC3	X685.3.422	685.3	684.3178	H+	Antibiotic	Antibiotic	gamma-L-Glutamyl-butirosin B	C18005
PC1, PC2	X686.3.421	686.3	685.3256	H+	Antibiotic	Antibiotic	Viomycin	C01540
PC1	X737.4.422	737.4	714.3979	Na+	Antibiotic	Antibiotic	Avermectin B1b monosaccharide	C11965
PC1, PC3	X803.4.369	803.4	780.3622	Na+	Antioxidant	Glutathione metabolite	Bis(glutathionyl)spermine	C16563
PC2	X122.403	122	121.0197	H+	Amino acid	Amino acid	Cysteine	C00736
PC3	X127.124	127	88.0160	K+	Central	TCA/Glycolysis	Pyruvate	C00022
			104.0110	Na+		Amino acid	Hydroxypyruvate	C00168
PC3	X171.66	171	132.0059	K+	Central	Central/TCA/Glycolysis	Oxaloacetate	C00036
			169.9980	H+		Glycolysis/Carbohydrate	Glycerone phosphate	C00111
			169.9980	H+		Glycolysis/Carbohydrate	Glyceraldehyde 3-phosphate	C00118
			132.0535	K+		Amino acid	L-Asparagine	C00152
PC3	X185.112	185	146.0215	K+	Central	Central/TCA/amino acids	2-Oxoglutarate	C00026
			146.0579	K+		Pantothenate + CoA	2-Dehydropantoate	C00966
			146.0579	K+		Amino acid	2-Aceto-2-hydroxybutanoate	C06006
PC3	X205.124	205	182.0579	Na+	Antioxidant	Amino acid/antioxidant	4-Hydroxyphenyllactate	C03672
			182.0215	Na+		Antibiotic	3;5-Dihydroxyphenylglyoxylate	C12325
			166.0491	K+		Purine alkaloid	Methylxanthine	C16353

Table S4.1 continued

PC of loading	ID	Detected mass	Accurate mass	Adduct	Function	Pathway	Compound	Kegg / Metacyc
PC3	X220.282	220	181.0739	K+	Amino acid	Amino acid	Tyrosine	C00082
			181.0739	K+		Amino acid	N-Hydroxy-L-phenylalanine	C19712
PC3	X289.1.279	289.1	288.0998	H+	Antibiotic	Antibiotic	6-Deoxydihydrokalafungin	C12435
PC3	X377.2.241	377.2	354.2406	Na+	Lipid	Lipid - Arachidonic acid	Amoglandin	C00639
PC3	X393.2.241	393.2	354.2406	K+	Lipid	Lipid - Arachidonic acid	Amoglandin	C00639
			370.2355	Na+		Lipid - Arachidonic acid	6-Keto-prostaglandin F1alpha	C05961
			370.2355	Na+		Lipid - Arachidonic acid	Thromboxane B2	C05963
PC3	X398.1.241	398.1	359.1151	K+	Antibiotic	Antibiotic	Penicillin N	C06564
			397.0798	K+		Antibiotic	4-Ketoanhydrotetracycline	C06627

**Table S4.2. Identified metabolites associated with PCA trajectories for the *Chlorella* fraction.** These were identified from the top 1% of loadings when using the first three principal components. The metabolite ID is that referred to in Figure 4.7.

PC of loading	ID	Detected mass	Accurate mass	Adduct	Function	Pathway	Compound	Kegg / Metacyc
PC1, PC2, PC3	X122.403	122	121.0197	H+	Amino acid	Amino acid	Cysteine	C00097
PC1, PC3	X393.2.370	393.2	354.2406	K+	Lipid	Arachidonic acid	Amoglandin	C00639
			370.2355	Na+		Arachidonic acid	6-Keto-PGF1a	C05961
			370.2355	Na+		Arachidonic acid	Thromboxane B2	C05963
PC1, PC2	X421.2.241	421.2	382.2508	K+	Carotenoid + ABA	Carotenoid + ABA synthesis	C25-Allenic-apo-aldehyde	C14044
PC1, PC3	X628.3.438	628.3	627.2487	H+	Cell wall metab	Chitin degradation	Chitotriose	CPD-13227
PC1, PC3	X629.3.437	629.3	628.2897	H+	Chlorophyll degradation	Chlorophyll degradation	Chlorophyll catabolite	C18098
PC1, PC2, PC3	X664.3.422	664.3	625.3033	K+	Lipid	Arachidonic acid	Leukotriene C4	C02166
PC2, PC3	X376.2.241	376.2	353.1699	Na+	Plant hormone	Plant hormone (Zeatin)	Dihydrozeatin riboside	C16447
PC2	X607.3.420	607.3	568.305	K+	Chlorophyll	Chlorophyll metabolism	Protoporphyrinogen IX	C01079
			584.2635	Na+		Chlorophyll metabolism	Bilirubin	C00486
PC3	X217.35	217	178.0477	K+	Secondary metabolite	Ascorbate/Vitamin C	L-Galactono-1;4-lactone	C01115
			194.0579	Na+		Phenylpropanoid/cell walls	Ferulate	C01494
			216.0399	H+		Isoprenoid biosynthesis	2-C-Methyl-D-erythritol 4-phosphate	C11434
			178.063	K+		Phenylpropanoid/cell wall	Coniferaldehyde	C02666
PC3	X299.432	299	260.0297	K+	Monosaccharide phosphate	Starch + sucrose	Glucose 6-phosphate	C00092
			260.0297	K+		Glycolysis	Glucose 1-phosphate	C00103
			260.0297	K+		Fructose and mannose	Mannose 6-phosphate	C00275
			276.0246	Na+		Pentose phosphate pathway	6-Phospho-D-gluconate	C00345
			260.0297	K+		Galactose	Galactose 1-phosphate	C00446
260.0297	K+	Fructose and mannose	Mannose 1-phosphate	C00636				

**Table S4.3. Change in symbiont load for each HK1 replicate between the start and end of the evolution experiment.** The metabolic group column denotes whether the replicate’s metabolic profile converged with the profile of the native 186b symbionts or diverged. From these two groups (‘converge’ or ‘diverge’) a group mean difference in symbiont load was calculated.

<b>HK1 replicate</b>	<b>Difference in symbiont load</b>	<b>Metabolic group</b>	<b>Group mean difference</b>
1	145404.2	converge	
2	337137.9	converge	241271
3	745804.2	diverge	
4	426775.4	diverge	
5	490066.7	diverge	500951.4
6	341159.3	diverge	

# Chapter 5

## Discussion

Endosymbiosis is an important evolutionary process underpinning a major evolutionary transition that has had a profound effect on the evolution of complex life (Keeling, 2010; Martin et al., 2015) and continues to impact the functioning of modern ecosystems (Baker, 2003; Powell and Rillig, 2018; Zook, 2002). The merger of two organisms can drive biological innovation (Wernegreen, 2012) and fundamental shifts in nutritional strategy, such as the transition to mixotrophy in photosymbioses (Esteban et al., 2010). Despite their importance our knowledge of these relationships remains limited, although there is increasing interest in this research area (Raina et al., 2018). In this thesis I have used experiments with the tractable microbial photosymbiosis between *P. bursaria* and *Chlorella* to study the mechanisms of host-symbiont specificity and partner switching.

First, I used a novel metabolic approach to compare the metabolic mechanism of two independent origins of the *P. bursaria* - *Chlorella* endosymbiosis. I found that convergence had occurred for the primary nutrient exchange, but that the metabolic mechanisms of light management had diverged and that these differences led to phenotypic variation. Next, I investigated the genetic variation in greater detail using a reciprocal cross-infection experiment coupled with metabolomics. I found that the differences in light-dependent symbiont stress responses affected the outcome of the interaction between host and symbiont genotypes, and thus underlies host-symbiont specificity. Finally, using an evolution experiment I found that host-symbiont specificity could be overcome as a novel association, initially lacking benefit, evolved to become a beneficial symbiosis. This data suggest that newly formed host-symbiont pairings can rapidly evolve higher fitness through changes in symbiont load regulation and metabolism. The capability for rapid partner amelioration and integration demonstrates the potential scope and flexibility for partner identity within partner switching.

In this general thesis discussion, I will explore some of the key themes emerging from my results, discuss potential applications of endosymbiosis research, and suggest future directions that could expand on my findings.

### 5.1 Stress and symbiosis

Light is a key factor mediating the fitness effects of photosymbiosis, and its dual role as both the source of energy and of potentially damaging agent of oxidative stress is well documented (Decelle et al., 2015; Venn et al., 2008; Yakovleva et al., 2009). Across this thesis, my findings have shown how critical light management is for the *P. bursaria* - *Chlorella* endosymbiosis, and that variation in light management affects both the fitness and compatibility of host-symbiont pairings. In Chapter 2, I found that the *Chlorella* strains from the two independent originations of the symbiosis had diverged in their light stress tolerance; the HA1 genotype increased production of photoprotective compounds in response to high light, while the 186b genotype instead invested more in photosynthetic machinery enabling high irradiance levels to be used effectively in photosynthesis. Further differences in light-associated stress responses among the clades were discovered in Chapter 3. Whereas the 186b *Chlorella* displayed a dark-associated stress-response, the HA1 and HK1 *Chlorella* displayed high-light-associated stress responses. These responses translated into higher costs of symbiosis in the dark for the 186b host-symbiont pairing, but lower benefits of symbiosis in high light for the HA1 host-symbiont pairing. Together these results suggest a key role of light-associated stress tolerance in the context dependent fitness effects of symbiosis and as a cause of divergence among the independent originations of this symbiosis. This aligns with other photosymbioses, particularly studies in the coral - *Symbiodinium* and *Hydra* - *Chlorella* endosymbioses, where thermal and light stress tolerance determine the fitness outcome of the symbiosis (Abrego et al., 2008; Ye et al., 2019).

Light stress tolerance is a product of the host-symbiont interaction. For example, in Chapter 3 I show that the dark-associated stress response induced in the 186b *Chlorella* in their native background is alleviated when 186b *Chlorella* are residing in the HA1 host genotype background. This suggests a hitherto unknown mechanism of host-mediated amelioration that could possibly be linked to greater provisioning preventing symbiont starvation. In addition, in Chapter 4 I show that an initially non-beneficial novel host-symbiont association could rapidly evolve to become beneficial in part due to changes in expression of stress-related metabolites in both the host and the symbiont. These results have implications for the hypothesis of Kawano et al. (2004) who theorised that *P. bursaria*, in contrast to other *Paramecium* species, acquired symbionts because of their pre-adaptations to oxidative stress. The results of this thesis support this idea but show that different *P. bursaria* genotypes vary in their ability to tolerate and ameliorate stress with consequences for host-symbiont specificity. In particular, it is notable that host genotype

backgrounds, such as HA1, that appear capable of alleviating symbiont stress are better able to establish beneficial symbioses with a wider range of symbiont genotypes, i.e., they are generalists in terms of specificity.

### 5.2 Partner Switching

Partner switching can rescue symbioses by restoring symbiont function (Koga and Moran, 2014; Matsuura et al., 2018), enable rapid adaptation to environmental change (Boulotte et al., 2016; Lefèvre et al., 2004), and facilitate niche-expansion (Joy, 2013; Rolshausen et al., 2018; Sudakaran et al., 2017). In particular, local adaptation by symbiont acquisition is likely to occur far faster than by symbiont evolution and may therefore be an important mode of host adaptation. In the majority of systems, however, the mechanisms that enable and restrict partner-switching have rarely been elucidated.

The *Chlorella* clades associated with the European and Japanese/American originations of the *P. bursaria-Chlorella* symbiosis are highly diverged, indeed, the European *Chlorella* clade is more closely related to the *Hydra*-symbiotic *Chlorella* than the *Chlorella* from the Japanese/American clade of the *P. bursaria-Chlorella* symbiosis (Hoshina et al., 2005). Nevertheless, while algal symbiont switching between *Hydra* and European clade *P. bursaria* is not possible (Summerer et al., 2007), I show that partner-switching between the European and Japanese/American clades of the *P. bursaria - Chlorella* symbiosis results in functional host-symbiont pairings. This partner-switching is enabled by a convergent nutrient exchange between these two originations of the *P. bursaria - Chlorella* endosymbiosis (Chapter 2). Both *Chlorella* from *Hydra* and *P. bursaria* are thought to supply their hosts with maltose (Mews, 1980; Ziesenisz et al., 1981), but it appears likely that the nitrogen source they receive in return differs. In *Hydra*, *Chlorella* appear to receive glutamine from their host (Hamada et al., 2018), while in *P. bursaria* my results in Chapter 2 suggest that the nitrogen source is arginine. This divergence in N-exchange metabolite could drive the observed between-species incompatibility (Summerer et al., 2007). Many endosymbioses have multiple independent origins, and convergence upon shared symbiotic exchanges despite genetic differences appears to be a common theme (Gargas et al., 1995; Masson-Boivin et al., 2009; Sandström et al., 2001). This suggests that metabolic function, and not simple genetic identity, may underlie successful partner-switching, which in turn will determine which novel combinations of host and symbiont can establish new associations.

I have shown that the *P. bursaria* host genotypes vary in their degree of partner-generalism, seen by the symbiotic fitness of novel associations (Chapters 2 & 3). Specifically, my findings show that genotypes varied such that one host genotype appeared to be a generalist (HA1), another a specialist (186b), and the third was intermediate (HK1) for partner specificity. The influence of host-symbiont genotype interactions on the outcome and fitness effects of symbiosis is a core component of co-evolutionary theory (Thompson, 2005). Coexistence of generalist and specialist strategies for partner specificity suggests that each strategy may confer fitness benefits (Wilson and Yoshimura, 1994). This is typically explained by the “Jack-of-all trades is a master of none” hypothesis, wherein although generalists occupy a wider range of niches, specialists have higher fitness in their chosen niche (Futuyma and Moreno, 1988; Straub et al., 2011). Generalist-specialist coexistence is seen across diverse symbioses. For example variation in the degree of host generalism has been reported in legume and rhizobia associations (Wilkinson and Parker, 1996), ectomycorrhiza and conifer symbioses (Molina and Trappe, 1982), and *Symbiodinium*-hosting corals, with absolute partner specificity being rarely observed (Silverstein et al., 2012). Indeed, some host species possess a remarkable degree of partner-generalism, for instance western hemlock forms associations with over 100 fungal symbiont species (Kropp and Trappe, 1982). In contrast to the “Jack-of-all trades” hypothesis, the *P. bursaria* – *Chlorella* specialist host examined here did not have higher fitness than the generalist host when tested with its conspecific symbiont. This implies that this specialist strain does not represent an alternative evolutionary optimum, but rather would be outcompeted if the strains co-occurred naturally. Furthermore, generalist host genotypes are more likely to successfully integrate new symbiotic partners. However, interestingly host generalism was associated with a consistent symbiotic phenotype across diverse algal symbionts, suggesting that such hosts may be less able shift their ecological niche through partner switching. On the other hand, specialism can preclude adaptation and absolute dependency on partner genotype can prevent partner switching entirely (Moran and Wernegreen, 2000). My results provide evidence that host genotype has a large influence determining the compatibility of new symbiotic partners and therefore the potential for partner switching.

This thesis has increased the understanding of the metabolic mechanisms underlying partner switching, which are important to understand from both an evolutionary and ecological perspective. For the former, a greater understanding of partner switching is required if we are to understand life-history patterns and establish an accurate understanding of the eukaryotic tree of life (Keeling, 2010). Specifically, the spread of

plastids has involved serial symbiont replacement that has entangled lineages (Delwiche, 1999; Dorrell and Smith, 2011; Stiller et al., 2014). The ‘shopping bag model’ hypothesises that the replaced symbiont can have transferred genes to the host nucleus, leading to a complement of endosymbiont genes and proteins from mixed origins (Larkum et al., 2007; Patron et al., 2006). These replacements have involved significant transitions between red and green plastids, but we do not currently know the number of these replacements and whether they were functionally equivalent or endowed novel traits (Archibald and Keeling, 2002). For ecological systems, partner-switching will affect ecosystems by potentially enabling migration and adaptation to environmental change, and because endosymbioses are often keystone organisms, changes in these relationships will have knock-on effects (Zook, 2002). For instance, partner-switching has been an important factor in insect endosymbioses diversification (Sudakaran et al., 2017) and in some instances symbiont replacement has been associated with nutritional transitions (Bell-Roberts et al., 2019) that have had large effects on the plants the insects feed on and their many predators and competitors (Frago et al., 2012; Sugio et al., 2015).

### *5.3 Rapid evolution enables the establishment of symbiosis*

A key finding of this thesis is that initially non-beneficial novel symbiotic pairings can rapidly evolve to become beneficial (Chapter 4). This suggests that following partner-switching a period of adaptation may often be required to allow for the novel symbiont to be integrated. There are multiple examples that have documented the rapid evolution of the fitness outcome of a symbiosis, though most of the previous examples have focused on transitions between parasitism and mutualism (King et al., 2016; Sachs and Wilcox, 2006; Shapiro and Turner, 2018; Tso et al., 2018). For instance, the opportunistic fungal pathogen *Candida albicans* was found to quickly evolve to protect its mouse host from systemic infections (Tso et al., 2018), demonstrating that initially costly symbionts could evolve to be beneficial. In my results the evolution of benefit appeared to be predominately driven by the evolution of host metabolism and symbiont-load regulation, suggesting asymmetry in the contribution of the partners to this adaptation. The relative contribution of host versus symbiont adaptation to the evolution of a symbiosis varies (Hill, 2009; Koch et al., 2017), and is partially determined by the relative level of control each partner exerts (Frank, 1997; Johnstone and Bshary, 2002) as well as other factors such as a relative generation time. In a parasitism, like the starting condition used by Tso and colleagues, the symbiont initiates the interaction and has more control. The symbiont is predicted, therefore, to have the dominant contribution to adaptation, and it was the evolution of the fungus that drove the transition from parasitism to mutualism in the example above

(Tso et al., 2018). In contrast, the *P. bursaria* - *Chlorella* symbiosis is an example of host exploitation (Decelle, 2013; Lowe et al., 2016) and therefore, the host initiates the interaction and has more control. This could explain why host adaptation was the primary driver in the evolution experiment of Chapter 4.

#### 5.4 Applications of endosymbiosis research

Endosymbioses have keystone roles in ecosystems, and as such knowledge of these associations can have implications for conservation and agriculture (Anthony et al., 2017; Monika et al., 2019). It is becoming increasingly urgent that we understand how symbiotic interactions respond to climate change, which alters the environmental context and therefore potentially the fitness outcome and stability of symbiotic associations (Kikuchi et al., 2016; Stat et al., 2006; Thompson, 2005). In response to rapid environmental change endosymbioses must either adapt to the new conditions, switch to partners better adapted to the new conditions, or otherwise they may face extinction. A particular focus has been on the breakdown of the coral-*Symbiodinium* endosymbiosis with increased ocean temperature that leads to coral bleaching (Douglas, 2003; Weis, 2008), which in turn can lead to coral mortality that has already caused catastrophic loss of coral reefs (Hughes et al., 2017; Sully et al., 2019). Investigations have found that the survival of this key endosymbiosis can be increased through the survival of partner-generalist hosts and increased levels of symbiont diversity (Fabina et al., 2013). Crucially, partner switching to more thermally tolerant symbionts can enable survival of the corals (Berkelmans and van Oppen, 2006; Rowan, 2004), and there are hopes that this will prevent the complete loss of these habitats (Coles et al., 2018; Hughes et al., 2003). Furthermore, there have been recent calls to use directed evolution to introduce more tolerant symbionts and induce beneficial partner switching in order to promote the survival of this keystone endosymbiosis (Anthony et al., 2017; van Oppen et al., 2015, 2017). My results have shown similar symbiont-genotype variation in stress tolerance within the *P. bursaria* - *Chlorella* symbiosis, and, importantly, show that benefit can rapidly evolve in novel associations. The implication of which is that testing novel coral - *Symbiodinium* associations should include sufficient time for these novel pairings to co-adapt, because an initial lack of co-adaptation may prevent new phenotypic properties being immediately evident.

Endosymbiotic research has also recently been applied to agriculture and health management. Specifically, the potential for using plant-microbe interactions to improve crop yield has received a lot of interest; both in terms of manipulating mycorrhizal fungi endosymbioses to act as biofertilizers (Monika et al., 2019) and for using a broader range

of rhizobacteria to increase plant protection against pathogens and pests (Kour et al., 2019). In addition, the disruption of key endosymbiotic associations of insects is being considered for a symbiosis-based method of pest control (Hosokawa et al., 2007; Nobre, 2019). Finally, endosymbiotic research is already being used in parasite control and *Wolbachia* infected mosquitos have been released into the wild in Brazil, Florida and Australia (O'Neill, 2018). The *Wolbachia* endosymbionts are used to inhibit the infection of human-disease causing viruses or parasites to stop the spread of mosquito-borne diseases such as dengue, Zika and malaria (Bourtzis et al., 2014; Caragata et al., 2016; Werren et al., 2008). My results have shown that metabolic function underlies the basis of partner compatibility, and this may be a useful consideration when designing artificial symbiotic partnerships for these applications.

The manipulation of endosymbioses for conservation, health or agriculture requires a detailed understanding of the mechanistic basis of these interactions in order that our alterations can have the desired effect. Understanding these systems requires the combination of controlled laboratory-based research to study the underlying mechanisms and large-scale *in-situ* studies that can examine the role of complex multi-species interactions within their ecosystems. The *P. bursaria* - *Chlorella* photosymbiosis is analogous in many ways to the coral - *Symbiodinium* endosymbiosis, and this thesis has demonstrated how stress response and genotype variation interactions can be understood at a mechanistic level in this simpler, microbial endosymbiosis. Future work could develop the *P. bursaria* - *Chlorella* association as a model for the less tractable coral - *Symbiodinium* relationship and use the tractable microbial system to explicitly test hypotheses that cannot currently be tested in the more complex system.

### 5.5 Future-directions

Following on from the work in this thesis on the mechanisms that underlie host-symbiont specificity, I believe the next logical step would be to directly test partner switching within this system. Re-infection experiments with a diverse group of symbiont genotypes could determine whether *P. bursaria* displays active partner choice, and if so whether the conspecific symbiont is chosen or if the most beneficial symbiont for the local conditions is selected.

Future work could also use a greater variety of genotypes to establish whether the mechanistic patterns observed here are representative. Specifically, it would be necessary to include other European clade strains to separate clade versus strain effects. This data

could test whether generalist and specialist strategies for partner specificity co-exist within the main biogeographical clades. In addition, strain natural habitat data could be incorporated and tested for correlations with symbiosis specificity or light ecotype traits.

The potential presence of bacterial endosymbionts within *P. bursaria* was not considered within this thesis, though it is highly likely that they are present (Fokin, 2004; Gong et al., 2014). Future work could build on the current candidate bacterial symbionts and identify which species are stably present within these systems and whether the bacterial community differs between symbiont-free and symbiotic *P. bursaria*. It may be that we need to view the *P. bursaria* - *Chlorella* relationship as one component of a complex multi-partner consortium.

Furthermore, greater molecular knowledge is required, particularly *Paramecium* specific metabolomic, transcriptome and genomic data should be increased and integrated to produce curated databases. Further integration of genomic data is needed for both partners, and it would be interesting to compare full genome sequences of the two symbiont clades to uncover the genetic differences that underpin their metabolic variation. Moreover, increased molecular knowledge of this system would allow the development of genetically transformed partners that would allow specific hypotheses to be tested.

### *5.6 In conclusion*

Independent origins of symbiosis is common (Masson-Boivin et al., 2009; Muggia et al., 2011; Sandström et al., 2001) and I have found that these provide important standing variation that enables phenotypic diversity, but that metabolic compatibility, not genetic identity, defines the limits of partner integration. This suggests that efforts to study the diversity of symbiotic interactions need to include metabolic function. Although the use of metabolomics within symbiosis is growing (Achlati et al., 2018; Chavez-Dozal and Nishiguchi, 2016; Padfield et al., 2016), there is an over-reliance on isolated sequence studies. This holds particularly true for microbiome research's tendency to use 18S and 16S rRNA sequencing results without integration of metabolites, transcripts and proteins (Knight et al., 2019; Poretsky et al., 2014).

Stress is known to be a critical factor for partner integration within photosymbioses (Howells et al., 2012; Venn et al., 2008; Ye et al., 2019). My results add to this knowledge by showing that light-dependent symbiont stress-responses drive host-symbiont genetic specificity within the *P. bursaria* - *Chlorella* association. This reveals that this microbial

symbiosis could be used as a model photosymbiosis to investigate the role of stress further, which is of particular relevance to the coral - *Symbiodinium* association. In addition, this thesis explicitly links stress tolerance and partner specificity, suggesting that host genotypes best able to alleviate stress in their symbionts are the most generalist in terms of the fitness of their associations with non-native symbiont genotypes. Typically, these two factors are considered separately and a potential link between the two needs to be investigated to test if it is common within photosymbioses. If true, this would imply stress tolerance is one of the critical factors in the establishment of these relationships and would build on Kawano et al.'s (2004) hypothesis that it is a necessary pre-adaptation. This would then become an important consideration in the transition to endosymbiosis and might have implications for our understanding of plastid acquisition (Lesser, 2006).

This thesis has shown that a novel association can rapidly evolve to be beneficial and so overcome an initial lack of co-adaptation and benefit common to novel associations (Matthews et al., 2018; McGraw et al., 2002; Russell and Moran, 2005). This is an important finding for understanding the dynamics of partner switching and reveals that partner integration can occur in a broader range of circumstances than initial compatibility tests would reveal. This has ramifications in the growing field of endosymbiosis manipulation (Anthony et al., 2017; Monika et al., 2019), because it shows that new phenotypes may only become visible once a novel association has had time to co-adapt. This is particularly salient for the current efforts to rescue the coral - *Symbiodinium* symbiosis through symbiont replacement to more thermally-tolerant symbiont genotypes (van Oppen et al., 2015, 2017).

Endosymbiosis requires experimental research to fully understand the diversity and complexity of these intimate symbiotic interactions. This work highlights the power of metabolomics to characterise the mechanistic basis of partner specificity and partner switching. Endosymbiotic relationships involve the integration of two organism at every level of their biology, from their ecology, metabolism, genetics and evolution, and if we are to understand these complex interactions in their entirety, we must integrate our levels of study as we move forward.

Appendix A – The review paper from which extracts were taken for the Introduction (Chapter 1)

MINIREVIEW – Incubator

# The role of exploitation in the establishment of mutualistic microbial symbioses

Megan E. S. Sørensen<sup>1,\*</sup>, Chris D. Lowe<sup>2</sup>, Ewan J. A. Minter<sup>1</sup>, A. Jamie Wood<sup>3,4</sup>, Duncan D. Cameron<sup>1</sup> and Michael A. Brockhurst<sup>1,‡</sup>

<sup>1</sup>Department of Animal and Plant Sciences, University of Sheffield, Sheffield S10 2TN, UK, <sup>2</sup>Centre for Ecology and Conservation, University of Exeter, Penryn Campus, Cornwall TR10 9FE, UK, <sup>3</sup>Department of Biology, University of York, York YO10 5DD, UK and <sup>4</sup>Department of Mathematics, University of York, York YO10 5DD, UK

\*Corresponding author: Department of Animal and Plant Sciences, University of Sheffield, Sheffield, S10 2TN, UK. Tel: +0114 222 0140; E-mail: [messorensen1@sheffield.ac.uk](mailto:messorensen1@sheffield.ac.uk)

**One sentence summary:** The authors review the theoretical and experimental evidence supporting exploitation as an alternative route to the evolution of mutualistic symbioses.

Editor: Daniel Tamarit

<sup>†</sup>Megan E. S. Sørensen, <http://orcid.org/0000-0001-8983-2943>

<sup>‡</sup>Michael A. Brockhurst, <http://orcid.org/0000-0003-0362-820X>

## ABSTRACT

Evolutionary theory suggests that the conditions required for the establishment of mutualistic symbioses through mutualism alone are highly restrictive, often requiring the evolution of complex stabilising mechanisms. Exploitation, whereby initially the host benefits at the expense of its symbiotic partner and mutual benefits evolve subsequently through trade-offs, offers an arguably simpler route to the establishment of mutualistic symbiosis. In this review, we discuss the theoretical and experimental evidence supporting a role for host exploitation in the establishment and evolution of mutualistic microbial symbioses, including data from both extant and experimentally evolved symbioses. We conclude that exploitation rather than mutualism may often explain the origin of mutualistic microbial symbioses.

**Keywords:** microbiology; experimental evolution; microbial symbioses

## INTRODUCTION

Symbiosis – ‘the living together of unlike organisms’ (De Bary 1879) – encompasses a broad range of species interactions, including both parasitism (+/- fitness interactions) and mutualism (+/+ fitness interactions). Whilst the evolutionary rationale for parasitism is straightforwardly explained by the self-interest of the parasitic partner, explaining the origin of mutualistic symbiosis is more challenging. The immediate fitness gains

of cheating are expected to outweigh the potential long-term fitness benefits of cooperation, producing a ‘tragedy of the commons’ (Hardin 1968; Rankin, Bargum and Kokko 2007). Therefore, both in long-established associations and in the establishment of new relationships, evolutionary conflict and breakdown of mutualistic symbiosis is ever likely, since each partner is under selection to minimise its investment in the integrated symbiotic unit (Perez and Weis 2006; Sachs and Simms 2006). Nevertheless, mutualistic symbiotic relationships are abundant, taxonomically widespread, ecologically important in a wide range of

Received: 21 February 2019; Accepted: 1 July 2019

© FEMS 2019. This is an Open Access article distributed under the terms of the Creative Commons Attribution License (<http://creativecommons.org/licenses/by/4.0/>), which permits unrestricted reuse, distribution, and reproduction in any medium, provided the original work is properly cited.

habitats, economically important in agricultural systems and, consequently, underpin the biodiversity and function of both natural and man-made ecosystems (Bronstein 2015; Powell and Rillig 2018).

Mutualistic symbiosis can accelerate evolutionary innovation through the merger of once independent lineages, providing species with new ecological traits and allowing them to inhabit previously inaccessible ecological niches (Wernegreen 2004; Kiers and West 2015). A classic example of this is nutrient trading, where the partners exchange compounds that are otherwise difficult or impossible for them to acquire. These include aphids with their obligate endosymbiont *Buchnera aphidicola* that exchange essential amino acids (Moran et al. 2003), and land plants with arbuscular mycorrhizal fungi where fixed carbon is exchanged for phosphate and organic nitrogen (Pfeffer et al. 1999). Besides exchanging nutrients, mutualistic symbioses can involve a wide range of benefits, including the production of antibiotics (Currie et al. 1999), luminescence (Tebo, Scott Linthicum and Neelson 1979), photoprotection (Hörtnagl and Sommaruga 2007) and protection from predation (Tsuchida et al. 2010). Since many of these potential benefits may only be required in particular environments or at particular times, many symbioses vary ecologically across a continuum from mutualism to parasitism (Heath and Tiffin 2007; Wendling, Fabritzek and Wegner 2017). Indeed, some organisms may only engage in symbiosis when in nutrient-deficient environments (Muscatine and Porter 1977; Johnson 2011).

Mutualistic symbiosis involves a shift in individuality as two unrelated species evolve inter-dependence and transition to function as a single organism (Szathmáry and Smith 1995; Estrela, Kerr and Morris 2016). In nature, the degree of dependence varies extensively both within and between symbioses (Minter et al. 2018). Dependence can range from obligate associations with mutually dependent partners, through asymmetrically dependent associations where only one species is unable to survive alone, to fully facultative associations where both species can survive alone. Comparative studies suggest that mutual dependence is more likely to evolve in vertically inherited symbioses, where the fitness interests of both species become aligned (Fisher et al., 2017). Transitions in individuality are, however, fraught with evolutionary conflict, and the merger of two independent organisms is rarely seamless and never selfless. Conflict is likely to be greatest during the establishment of new symbioses, before the partners have been able to evolve complex mechanisms required to align their fitness interests.

Explaining the establishment of mutualistic symbioses is therefore challenging, and this is the focus of our review. As we shall explain in the subsequent section, the conditions for mutualistic symbioses to establish through mutualism alone are highly restrictive, and thus several alternative mechanisms have been proposed (Garcia and Gerardo 2014; Keeling and McCutcheon 2017). One of these is that mutualistic symbioses evolve from parasitisms. This transition can occur in two directions. First, the smaller parasitic partner living in or on the larger host can evolve reduced virulence to eventually become beneficial to its host (King et al. 2016; Shapiro and Turner 2018; Tso et al. 2018). Sach et al. (2011) used phylogenetic reconstruction to predict whether bacterial symbionts originated as mutualists or parasites. For 42 beneficial bacterial symbionts, they inferred that 32 had originated as parasitic whilst only 9 had originated as mutualists (with 1 case remaining ambiguous), suggesting that parasitism is a more common route than mutualism to mutualistic symbiosis. Second, the larger host partner could capture and exploit the smaller beneficial partner, which would

otherwise grow faster outside of symbiosis. This is a special case of parasitism known as host exploitation, which has been far less well-studied. In this review, we gather together the evidence supporting a role for host exploitation in the establishment of mutualistic microbial symbiosis.

## THEORETICAL STUDIES OF SYMBIOSIS: MUTUALISM VERSUS EXPLOITATION

### The paradox of mutualism

Mutualisms are abundant throughout the tree of life despite their inherent evolutionary conflicts, and this disparity is considered the paradox of mutualism. The paradox of mutualism has been well explored using theoretical models that aim to discover the evolutionary stable strategies of mutualistic symbiosis. The reciprocal exchange of services/goods within mutualisms make them a specific form of group cooperation. There are two primary evolutionary explanations for group cooperation. Within a species, kin selection explains that helping related individuals provides inclusive fitness benefits to the actor (following Hamilton's rule (Hamilton 1964)). Alternately for non-relatives, game theory has provided the strategic alliance model, which is based around reciprocity and includes the Tit-for-Tat strategy (Axelrod 1984). Frank (1996), however, highlighted that the evolution of interspecific symbiosis cannot be explained by either of these models; kin selection is not applicable because the interaction is between unrelated individuals from different species, and the strategic alliance model fails because it requires memory of past interactions, the recognition of individuals and is dissipated by forms of mixing. The traditional explanations for cooperation are, therefore, insufficient to explain the evolutionary stability of symbioses.

Theoretical work has consequently focused on mutualism-specific explanations, and a key process underlying much of this work is finding mechanisms that align the partners' fitness interests. Herre et al. (1999) proposed that this alignment could be achieved by 'conflict avoidance factors', which include vertical transmission, genetic uniformity of symbionts, population spatial structure and obstructions to alternative free-living states. The influence of these factors has been explored by theoretical models, particularly vertical transmission that aligns the reproductive interests of the partners (Yamaura (1993)). For reproductive interests to be fully aligned, both absolute co-dispersal and reproductive synchrony are required as part of vertical transmission (Frank 1997). If achieved, this reduces within-host competition between symbionts and stabilises the mutualism because the reproductive success of the symbiont is perfectly aligned to that of its host. Vertical inheritance is common in well-established, obligate symbiotic partnerships and is associated with greater dependence (Fisher et al. 2017). It is not, however, ubiquitous and there are many stable mutualisms that maintain horizontal transmission. For example, *Vibrio fischeri* and bobtail squids (Visick and Ruby 2006), Rhizobia and legumes (Sprent, Sutherland and Faria 1987), and *Endoriftia persephone* and tube worms (Nussbaumer, Fisher and Bright 2006). Consequently, it is clear that while conflict avoidance factors help to promote stability of some interactions, they are neither necessary nor sufficient for the evolutionary stability of mutualistic symbioses (Genkai-Kato and Yamamura 1999).

Frank (1995) provided a solution to the paradox of mutualism by developing a model centred on policing strategies, which repressed competition and reduced the benefits of cheating to ensure the fair distribution of resources. Furthermore, the

results of the extended policing model (Frank 1996) showed that variation in individual resources altered the degree of investment in policing, with well-supplied individuals doubling their policing investment and poorly supplied individuals not investing at all. The theoretical prediction for the role of policing in maintaining mutualistic symbioses has been supported by numerous occurrences in a wide-range of natural systems. For example, partner sanctions in the legume–rhizobium symbiosis (Kiers et al. 2003), partner choice in the yucca–yucca moth symbiosis (Bull and Rice 1991), partner fidelity in solitary wasp–*Streptomyces* symbiosis (Kaltenpoth et al. 2014) and screening in the bobtail squid–*Vibrio fischeri* symbiosis (McFall-Ngai and Ruby 1991; Archetti et al. 2011).

Following Frank's first policing models, there has been extensive development of theory exploring the evolution of mutualism. The current consensus is that stabilising mechanisms, such as the various policing strategies, vertical transmission and other conflict avoidance factors, provide solutions to the paradox of mutualism (for extensive reviews of the topic, see Sachs et al. (2004); Leigh (2010) and Archetti et al. (2011)). However, while it is clear that these complex adaptations play a crucial role in the maintenance of extant mutualistic symbioses, it is unlikely that they can explain the origin of new symbioses because here there is little time for such complex stabilising mechanisms to evolve. The pre-existence of such traits, allowing for their co-option for the purpose of stabilising symbiosis, may be a prerequisite for the establishment of symbiosis. For instance, one can imagine that partner-choice could evolve from pre-existing feedback mechanisms and may even provide the selective environment from which the symbiosis establishes (Frederickson 2013). However, given that complex stabilising mechanisms are not ubiquitous this seems unlikely to be a general explanation. Moreover, elaborate host–symbiont interactions, such as the bobtail squid–*Vibrio fischeri* multistage screening process, must have evolved subsequent to establishment, even if the fundamental aspects were pre-adaptations. It is more parsimonious therefore to assume that important limitations exist as to the conditions where mutualism can act as an establishment mechanism for mutualistic symbiosis.

### Exploitation as an alternative route to symbiosis

An alternative route to the establishment of mutualistic symbiosis was proposed by Law and Dieckmann (1998). This model predicted that exploitative relationships wherein a host exploits a 'victim' species which it acquires by horizontal transmission can evolve into stable mutualistic symbioses with vertical transmission simply through natural selection to increase individual fitness. The key requirement for this outcome was that the free-living victim pays a cost to defend itself from being captured by the host. In this scenario, there is a trade-off for the victim, who either uses resources to defend itself or to provision the exploitative host. Depending on the relative magnitude of these trade-offs, it is possible that the victim has higher fitness in symbiosis. In this case, the evolution of vertical transmission is advantageous to both partners as the victim has a higher reproductive rate in symbiosis than when free-living, where it must pay a high cost of defence. However, it remains the case that the victim's optimal state would be to be free-living with no interaction with the exploiter and thus paying neither of these costs. The model demonstrated that if the trade-off is sufficiently strong, the evolution of stable symbiosis can be advantageous to both partners even in an exploitative relationship. Furthermore, once vertical transmission has evolved it becomes much harder for the victim

to escape the host, and the victim can become trapped in the symbiotic state. It is important to note that this interaction has now become a mutualistic symbiosis; the victim provisions the host to the host's benefit, whilst the victim's reproductive rate in symbiosis now exceeds that which is achievable in free-living environments containing the host.

Because host exploitation does not require symmetric mutual benefits at the outset nor complex stabilising mechanisms to allow establishment, it offers a simpler explanation for the emergence of mutualistic symbiosis. Once mutualistic symbiosis is established, further stabilising mechanisms could evolve to prevent its breakdown. Thus mutualism-stabilising mechanisms may often be a secondary phenomenon, arising to further enforce originally exploitative but now mutualistic symbioses.

## EXPLOITATION IN ACTION

Empirical data on the establishment of mutualistic symbioses are rare because studying this process experimentally is challenging. The extant mutualistic symbioses we observe in nature are the products of co-evolution and no longer in the establishment phase. Furthermore, for obligate mutualistic symbioses it may be impossible to separate the partners and therefore untangle the costs/benefits that each of the symbiotic partners derive. Nonetheless, there are several mutualistic microbial symbioses that are amenable to experimental study, and two main experimental approaches. The first approach is to study extant facultative associations that remain experimentally tractable and allow the direct measurement of the relative costs and benefits of both the free-living and symbiotic states. The second approach is to experimentally evolve newly formed symbioses in the laboratory to explore the environmental conditions that promote their establishment and stability (Hoang, Morran and Gerardo 2016). We review the data from both approaches in the following section.

### Experiments with extant facultative mutualistic microbial symbioses

One of the best studied facultative mutualistic microbial symbioses is that between the single-celled ciliate host *Paramecium bursaria* and its green alga symbiont, *Chlorella*. This classical photosymbiosis is founded upon the exchange of fixed carbon from the photosynthetic algae in return for organic nitrogen from the host (Fig. 1). It has been estimated that the *Chlorella* endosymbionts release 57% of their fixed carbon to the host (Johnson 2011), primarily as maltose (Ziesenisz, Reisser and Wiessner 1981). The nitrogen source is not yet verified; current candidates include amino acids (Kato, Ueno and Imamura 2006; Kato and Imamura 2008b), nucleic acid derivatives (Soldo, Godoy and Larin 1978; Shah and Syrett 1984) and ammonia (Albers, Reisser and Wiessner 1982).

Crucially, while the symbionts are inherited vertically with tight cell cycle synchrony, the partners can be separated by sonication/chemical treatment (Kodama and Fujishima 2008, 2011, 2012) allowing the costs and benefits of symbiosis versus free-living to be directly compared. For hosts, the benefit of symbiosis increases with light intensity, such that while it is costly to harbour symbiotic algae in the dark (i.e. symbiont-free hosts grow faster than symbiotic hosts), these costs are outweighed at higher light intensity such that symbiosis is highly beneficial for hosts in high light. In contrast, symbiosis is never beneficial

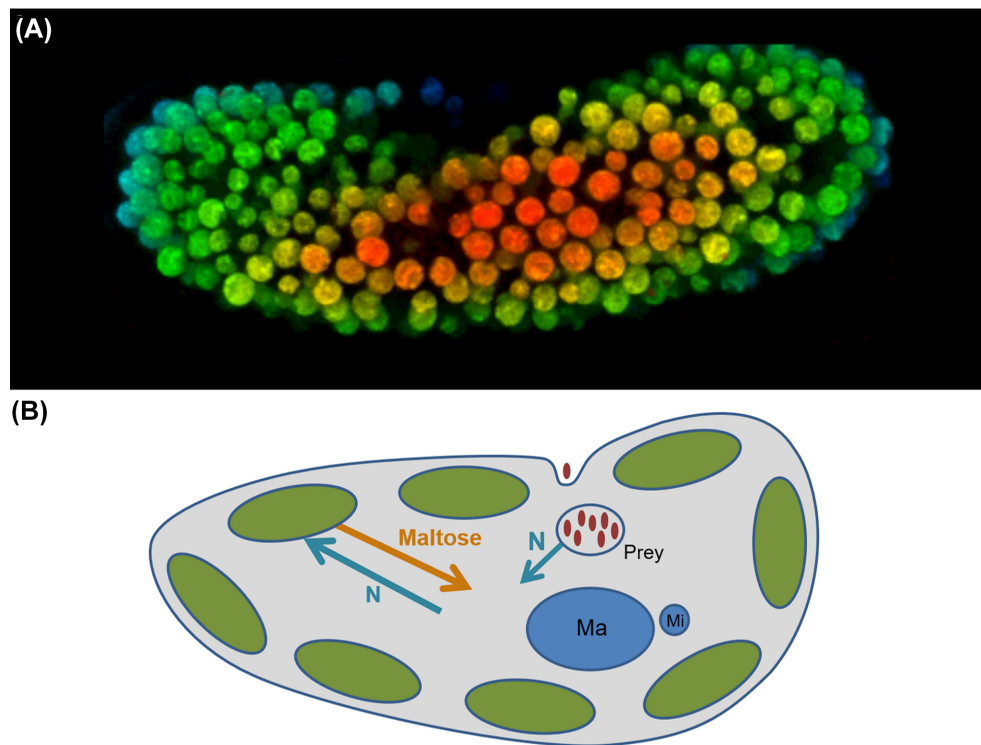


**Figure 1.** *Paramecium bursaria* and *Chlorella* endosymbiosis. A. Z-stack of confocal sections of the chlorophyll autofluorescence of *Chlorella* endosymbionts within one *Paramecium bursaria* cell. With colour representing the intensity of fluorescence and therefore the position of the *Chlorella* in the Z-plane. B. Diagram of the relationship, showing the nutrient exchange with the transfer of maltose from the *Chlorella* in exchange for organic nitrogen (denoted as 'N' as the identity of this compound is currently unknown). Ma = macronucleus; Mi = micronucleus.

for the alga: free-living algal growth rates increase monotonically with light intensity and at all light levels exceed those of symbiotic algae. Moreover, hosts impose tight control on algal symbiont load (i.e. the number of algal symbionts per host cell) which peaks at low light, and is reduced both in the dark and at high light intensity (Lowe *et al.* 2016). A mathematical model of the symbiosis showed that hosts manipulate symbiont load in this way to maximise their return from nutrient trading, effectively minimising their nitrogen cost for each molecule of carbon they gain from their algal symbionts (Dean *et al.* 2016). Indeed, measurements of algal photosynthetic efficiency suggested that algal symbionts were more nitrogen-starved than their free-living counterparts (Lowe *et al.* 2016). Similar patterns of cost:benefit and host control were observed across a range of geographically diverse isolates (Minter *et al.* 2018).

The mechanism of the control in this relationship is likely to be multifaceted, but in large part is thought to be due to host digestion. Host selection in the establishment of the symbiosis specifies which *Chlorella* are packaged into vacuoles and re-located, while all others are digested (Kodama and Fujishima 2011, 2014). Even once established, complete darkness or chemical inhibitors, both of which prevent *Chlorella* photosynthesis and therefore stop the carbon supply to the host, lead to the eventual loss of *Chlorella* symbionts, through either digestion or egestion (Karakashian 1963; Kodama and Fujishima 2008). In addition, cell division of symbiotic *Chlorella* is tightly regulated and has been linked to host cytoplasmic streaming (Takahashi *et al.* 2007). Furthermore, metabolic processes are believed to actively influence the exchange process, for instance host  $\text{Ca}^{2+}$  inhibits serine uptake into *Chlorella* and glucose increases the

uptake (Kato and Imamura 2008a, 2008b). If the symbiont's maltose is broken down to glucose by the host, then this control process would facilitate a reward system for more co-operative symbionts. The multiple control processes identified to date are all host-derived, supporting the idea that this symbiosis was founded upon exploitation.

Phylogenetic analysis shows that symbiotic and free-living *Chlorella* form polyphyletic groups (Hoshina and Imamura 2008; Summerer, Sonntag and Sommaruga 2008), indicating multiple transitions to and from symbiosis. Moreover, diverse isolates of *P. bursaria-Chlorella* vary in their degree of dependence; from completely facultative associations to obligate mutual dependence, via asymmetric dependence where hosts depend on symbionts but not vice versa (Minter *et al.* 2018). Taken together, these experimental data suggest that the nutrient trading relationship between the ciliate and the alga is exploitative rather than mutualistic, benefiting the host (Lowe *et al.* 2016). Additional selective forces may be required therefore to explain the benefit of symbiosis for the alga, and while several have been proposed, including photoprotection and escape from viral predation (Reisser *et al.* 1991; Summerer *et al.* 2009; Esteban, Fenchel and Finlay 2010), this interaction proves that a stable, even sometimes obligate, symbiosis can evolve from exploitation.

Other similar symbioses also appear to be founded upon exploitation. For example, for scleractinian corals and the dinoflagellate algae *Symbiodinium* there is evidence of asymmetry in the fitness effects of symbiosis upon the partners. The algal growth rate is reduced from a free-living doubling time of 3 days to a symbiotic doubling time of between 70 and 100 days (Wilkerson, Kobayashi and Muscatine 1988). Whereas hosts experience increased growth rates in symbiosis. Further support

for the idea that this association is exploitative is provided by the asymmetry of the nutrient exchange: whilst the algal symbiont provides ~95% of its photosynthate to the host, in return they are kept in a nitrogen-starved state by the host (Smith and Muscatine 1999; Dubinsky and Berman-Frank 2001). Similarly, studies on lichen symbioses and the partnership between chemosynthetic bacteria and their invertebrate hosts have also reported reduced symbiont growth rates in symbiosis compared to free-living (Ahmadjian 1993; Combes 2005). Additionally, the association of *Acantharia* marine protists with haptophyte algae is also believed to be a form of farming, whereby only the host benefits (Decelle 2013). What these interactions have in common is that they feature a producer living within a consumer. In both the coral and *P. bursaria* symbioses, the algal symbionts are 'engulfed' during establishment and therefore do not actively enter symbiosis. In symbiosis, the algae are contained within a host membrane, enabling the host to control provisioning of resources. This inequality of control may be a defining feature of apparently mutualistic symbioses founded upon exploitation.

### Experimental evolution of microbial symbioses

Experimental evolution provides an unparalleled window into evolutionary processes by allowing their observation in real time from defined genetic and phenotypic starting points under controlled conditions in the laboratory. While simplified lab environments preclude direct comparisons to nature, they allow key variables to be separated from the myriad of confounding variables in the field, providing a way to unambiguously separate the proximate and ultimate causes of symbiosis (Mazancourt, Loreau and Dieckmann 2005).

To date there are only few examples of experimentally evolved establishments of novel symbiotic relationships. Jeon (1972) reported the first instance of an intracellular obligate parasite evolving to become a mutualistic symbiont. The experiment used *Amoeba discoides* that had become spontaneously infected with rod-shaped bacteria and these were then cultured together, without any selection for symbiosis, for five years. At first, the bacteria were harmful; the infected amoebae grew slower, were more sensitive to starvation, were smaller and some hosts cells were killed upon infection. However, after five years, the infected amoebae grew normally despite carrying the same number of bacteria cells. Crucially, this was not due simply to the evolution of reduced virulence by the bacterium. Nuclear transfer experiments swapped the evolved nucleus and cytoplasm with that of the ancestor and demonstrated that the evolved nucleus could now not survive without the coevolved bacterial symbiont. Thus, a mutualistic and obligate symbiosis had evolved from a parasitism.

More recently, Nakajima et al. (2009, 2015) established long-term microcosms containing a green alga (*Micractinium* sp., formally *Chlorella vulgaris*), a bacterium (*Escherichia coli*), and a ciliate (*Tetrahymena thermophila*). The experiment was maintained without external addition of resources and without transfer to fresh medium for over five years and therefore formed a self-sustaining ecosystem. Over the course of the experiment the free-living algae diversified into two distinct forms. One of these was a non-aggregating type that formed an endosymbiotic association with *Tetrahymena* as its host, whereas an aggregate forming type lived outside of *Tetrahymena* cells but formed a symbiotic association with the *E. coli*. The algal aggregation phenotype was negatively correlated with *Tetrahymena* longevity in coculture, suggesting that only non-aggregating algae improved host fitness. Potentially underpinning this host benefit, the evolved

endosymbiotic algae excreted more glycerol and sucrose, and contained more photopigments than the ancestral clone (Germond et al. 2013). The evolved free-living algae adapted to the free-living environment and outcompeted any endosymbiotic algae that escaped symbiosis. This suggests that a trade-off between adaptation to the free-living versus the symbiotic environment may frequently enforce interspecific cooperation and thus stabilise symbiosis, and is conceptually similar to the trade-off proposed by Law and Dieckmann (1998).

Although additional experimental evolution studies are clearly needed, it is intriguing that both studies to date support the role for exploitation in the establishment of symbioses that evolve become mutualistic. Both experiments suggest a key role for trade-offs between symbiotic and free-living environments in driving the emergence of mutualistic symbiosis, as predicted by Law and Dieckmann (1998). These experiments were essentially observational in design, lacking treatments to compare the effects of environmental variables. Experiments manipulating key environmental parameters likely to affect symbiosis, such as the potential for horizontal transmission or the free-living mortality rate, will be an important next step towards understanding the environmental drivers of the establishment of symbiosis.

### CONCLUSION

Both the theoretical and empirical evidence support the role for parasitism or exploitation in the establishment of symbioses, and the later evolution of mutual benefit. Establishment through exploitation provides a simple explanation for the establishment of symbiosis because it does not require complex stabilising mechanisms to repress conflict. Exploitation may be especially prevalent among associations where the smaller partner is engulfed by a larger host and enclosed in the host membrane. In such associations, it is clear from the available experimental data that the core nutrient exchange between partners does not in itself provide mutual benefits. It is likely that fitness trade-offs between the symbiotic and free-living environments play a key role in enforcing exploitative symbioses, and may lead to the eventual emergence of dependence and mutual benefit through the loss of fitness in the free-living state.

### ACKNOWLEDGEMENTS

AJW is grateful to Thorunn Helgason and Elva Robinson for stimulating discussions.

### FUNDING

This work was funded by grant NE/K011774/2 from the Natural Environment Research Council, UK to MAB, CDL, DDC, and AJW, and a White Rose DTP studentship from the Biotechnology and Biological Sciences Research Council, UK to MESS (BB/M011151/1). The funders had no role in the design of the study, the collection, analysis and interpretation of data, or the writing of the manuscript.

**Conflicts of interest.** None declared

### REFERENCES

- Ahmadjian V. *The Lichen Symbiosis*. John Wiley & Sons, 1993.
- Albers D, Reisser W, Wiessner W. Studies on the nitrogen supply of endosymbiotic chlorellae in green paramecium *bursaria*. *Plant Sci Lett* 1982;25:85–90.

- Archetti M, Scheuring I, Hoffman M *et al*. Economic game theory for mutualism and cooperation. *Ecol Lett* 2011;**14**:1300–12.
- Axelrod R. *The Evolution of Cooperation*. Basic Books, 1984.
- Bronstein JL ed. *Mutualism*. Oxford, New York: Oxford University Press, 2015
- Bull JJ, Rice WR. Distinguishing mechanisms for the evolution of Co-Operation. *J Theor Biol* 1991;**149**:63–74.
- Combes C. *The Art of Being a Parasite*. University of Chicago Press, 2005.
- Currie CR, Scott JA, Summerbell RC *et al*. Fungus-growing ants use antibiotic-producing bacteria to control garden parasites. *Nature* 1999;**398**:701–4.
- Dean AD, Minter EJA, Sørensen MES *et al*. Host control and nutrient trading in a photosynthetic symbiosis. *J Theor Biol* 2016;**405**:82–93.
- De Bary A. *The phenomenon of symbiosis*. Strasbourg, Germany: Karl J. Trubner, 1879.
- Decelle J. New perspectives on the functioning and evolution of photosymbiosis in plankton. *Commun Integr Biol* 2013;**6**:e24560.
- Dubinsky Z, Berman-Frank I. Uncoupling primary production from population growth in photosynthesizing organisms in aquatic ecosystems. *Aquat Sci* 2001;**63**:4–17.
- Esteban GF, Fenchel T, Finlay BJ. Mixotrophy in ciliates. *Protist* 2010;**161**: 621–41.
- Estrela S, Kerr B, Morris JJ. Transitions in individuality through symbiosis. *Curr Opin Microbiol* 2016;**31**:191–8.
- Fisher RM, Henry LM, Cornwallis CK *et al*. The evolution of host-symbiont dependence. *Nature Commun* 2017;**8**:ncomms15973.
- Frank SA. Models of symbiosis. *Am Nat* 1997;**150**: S80–99.
- Frank SA. Policing and group cohesion when resources vary. *Anim Behav* 1996;**52**:1163–9.
- Frank SA. The origin of synergistic symbiosis. *J Theor Biol* 1995;**176**:403–10.
- Frederickson ME. Rethinking mutualism stability: cheaters and the evolution of sanctions. *Q Rev Biol* 2013;**88**:269–95.
- Garcia JR, Gerardo NM. The symbiont side of symbiosis: do microbes really benefit? *Front Microbiol* 2014;**5**:510.
- Genkai-Kato M, Yamamura N. Evolution of mutualistic symbiosis without vertical transmission. *Theor Popul Biol* 1999;**55**:309–23.
- Germond A, Kunihiro T, Inouhe M *et al*. Physiological changes of a green alga (*Micractinium* Sp.) involved in an early-stage of association with *tetrahymena thermophila* during 5-Year microcosm culture. *Biosystems* 2013;**114**:164–71.
- Hamilton WD. The genetical evolution of social behaviour. II. *J Theor Biol* 1964;**7**:17–52.
- Hardin G. The tragedy of the commons. *Science* 1968;**162**:1243–8.
- Heath KD, Tiffin P. Context dependence in the coevolution of plant and rhizobial mutualists. *Proc Royal Soc Lond B: Biol Sci* 2007;**274**:1905–12.
- Herre EA, Knowlton N, Mueller UG *et al*. The Evolution of Mutualisms: Exploring the Paths between Conflict and Cooperation." *Trends Ecol Evol* 1999;**14**:49–53.
- Hoang KL, Morran LT, Gerardo NM. Experimental evolution as an underutilized tool for studying beneficial animal–microbe interactions. *Front Microbiol* 2016;**7**:1444.
- Hoshina R, Imamura N. Multiple origins of the symbioses in *paramecium bursaria*. *Protist* 2008;**159**:53–63.
- Hörtnagl PH, Sommaruga R. Photo-oxidative stress in symbiotic and aposymbiotic strains of the ciliate *paramecium bursaria*. *Photochem Photobiol Sci* 2007;**6**:842.
- Jeon KW. Development of cellular dependence on infective organisms: micrurgical studies in amoebas. *Science* 1972;**176**:1122–3.
- Johnson MD. The acquisition of phototrophy: adaptive strategies of hosting endosymbionts and organelles. *Photosynth Res* 2011;**107**:117–32.
- Kaltenpoth M, Roeser-Mueller K, Koehler S *et al*. Partner choice and fidelity stabilize coevolution in a cretaceous-age defensive symbiosis. *Proc Natl Acad Sci* 2014;**111**:6359–64.
- Karakashian SJ. Growth of *paramecium bursaria* as influenced by the presence of algal symbionts. *Physiol Zool* 1963;**36**:52–68.
- Kato Y, Imamura N. Effect of calcium ion on uptake of amino acids by symbiotic *chlorella* F36-ZK isolated from Japanese *paramecium bursaria*. *Plant Sci* 2008a;**174**:88–96.
- Kato Y, Imamura N. Effect of sugars on amino acid transport by symbiotic *chlorella*. *Plant Physiol Biochem* 2008b;**46**:911–7.
- Kato Y, Ueno S, Imamura N. Studies on the nitrogen utilization of endosymbiotic algae isolated from Japanese *paramecium bursaria*. *Plant Sci* 2006;**170**:481–6.
- Keeling PJ, McCutcheon JP. Endosymbiosis: The feeling is not mutual. *J Theor Biol* 2017;**434**:75–9.
- Kiers ET, Rousseau RA, West SA *et al*. Host sanctions and the legume–rhizobium mutualism. *Nature* 2003;**425**:78–81.
- Kiers ET, West SA. Evolving new organisms via symbiosis. *Science* 2015;**348**:392–4.
- King KC, Brockhurst MA, Vasieva O *et al*. Rapid evolution of microbe-mediated protection against pathogens in a worm host. *ISME J* 2016;**10**:1915–24.
- Kodama Y, Fujishima M. Cell division and density of symbiotic *chlorella variabilis* of the ciliate *paramecium bursaria* is controlled by the host's nutritional conditions during early infection process. *Environ Microbiol* 2012;**14**:2800–11.
- Kodama Y, Fujishima M. Cycloheximide induces synchronous swelling of perialgal vacuoles enclosing symbiotic *chlorella vulgaris* and digestion of the algae in the ciliate *paramecium bursaria*. *Protist* 2008;**159**:483–94.
- Kodama Y, Fujishima M. Four important cytological events needed to establish endosymbiosis of symbiotic *Chlorella* Sp. to the alga-free *paramecium bursaria*. *Japan. J Protozool* 2011;**44**:1–20.
- Kodama Y, Fujishima M. Symbiotic *chlorella variabilis* incubated under constant dark conditions for 24 hours loses the ability to avoid digestion by host lysosomal enzymes in digestive vacuoles of host ciliate *paramecium bursaria*. *FEMS Microbiol Ecol* 2014;**90**:946–55.
- Law R, Dieckmann U. Symbiosis through exploitation and the merger of lineages in evolution. *Proc Roy Soc Lon B: Biol Sci* 1998;**265**:1245–53.
- Leigh EG, Jr. The evolution of mutualism. *J Evol Biol* 2010;**23**:2507–28.
- Lowe CD, Minter EJ, Cameron DD *et al*. Shining a light on exploitative host control in a photosynthetic endosymbiosis. *Curr Biol* 2016;**26**:207–11.
- Mazancourt CD, Loreau M, Dieckmann U. Understanding mutualism when there is adaptation to the partner. *J Ecol* 2005;**93**:305–14.
- McFall-Ngai MJ, Ruby EG. Symbiont recognition and subsequent morphogenesis as early events in an animal-bacterial mutualism. *Science* 1991;**254**:1491–4.
- Minter EJA, Lowe CD, Sørensen MES *et al*. Variation and asymmetry in host-symbiont dependence in a microbial symbiosis. *BMC Evol Biol* 2018;**18**:108.

- Moran NA, Plague GR, Sandström JP et al. A genomic perspective on nutrient provisioning by bacterial symbionts of insects. *Proc Natl Acad Sci* 2003;100:14543–8.
- Muscatine L, Porter JW. Reef corals: Mutualistic symbioses adapted to nutrient-poor environments. *Bioscience* 1977;27:454–60.
- Nakajima T, Fujikawa Y, Matsubara T et al. Differentiation of a free-living alga into forms with ecto- and endosymbiotic associations with heterotrophic organisms in a 5-year microcosm culture. *Biosystems* 2015;131:9–21.
- Nakajima T, Sano A, Matsuoka H. Auto-/Heterotrophic endosymbiosis evolves in a mature stage of ecosystem development in a microcosm composed of an alga, a bacterium and a ciliate. *Biosystems* 2009;96:127–35.
- Nussbaumer AD, Fisher CR, Bright M. Horizontal endosymbiont transmission in hydrothermal vent tubeworms. *Nature* 2006;441:345–8.
- Perez S, Weis V. Nitric oxide and cnidarian bleaching: An eviction notice mediates breakdown of a symbiosis. *J Exp Biol* 2006;209:2804–10.
- Pfeffer PE, Douds DD, Bécard G et al. Carbon uptake and the metabolism and transport of lipids in an arbuscular mycorrhiza. *Plant Physiol* 1999;120:587–98.
- Powell JR, Rillig MC. Biodiversity of arbuscular mycorrhizal fungi and ecosystem function. *New Phytol* 2018;220:1059–75.
- Rankin DJ, Bargum K, Kokko H. The tragedy of the commons in evolutionary biology. *Trends Ecol Evol* 2007;22:643–51.
- Reisser W, Burbank D, Meints R et al. Viruses distinguish symbiotic *Chlorella* spp of *Paramecium-bursaria*. *Endocytobiosis Cell Res* 1991;7:245–51.
- Sachs JL, Mueller UG, Wilcox TP et al. The evolution of cooperation. *Q Rev Biol* 2004;79:135–60.
- Sachs JL, Simms EL. Pathways to mutualism breakdown. *Trends Ecol Evol* 2006;21:585–92.
- Sachs JL, Skophammer RG, Regus JU. Evolutionary transitions in bacterial symbiosis. *Proc Natl Acad Sci* 2011;108:10800–807.
- Shah N, Syrett PJ. The uptake of guanine and hypoxanthine by marine microalgae. *J Mar Biol Assoc UK* 1984;64:545–56.
- Shapiro JW, Turner PE. Evolution of mutualism from parasitism in experimental virus populations. *Evolution* 2018;72:707–12.
- Smith GJ, Muscatine L. Cell cycle of symbiotic dinoflagellates: Variation in G1 phase-duration with anemone nutritional status and macronutrient supply in the *Aiptasia pulchella*-*Symbiodinium pulchrum* symbiosis. *Mar Biol* 1999;134:405–18.
- Soldo AT, Godoy GA, Larin F. Purine-Excretory nature of refractile bodies in the marine ciliate *Parauronema acutum*\*. *J Protozool* 1978;25:416–8.
- Sprent JI, Sutherland JM, De Faria SM. Some aspects of the biology of nitrogen-fixing organisms. *Phil Trans R Soc Lond B* 1987;317:111–29.
- Summerer M, Sonntag B, Hörtnagl P et al. Symbiotic ciliates receive protection against UV damage from their algae: A test with *Paramecium bursaria* and *Chlorella*. *Protist* 2009;160:233–43.
- Summerer M, Sonntag B, Sommaruga R. Ciliate-symbiont specificity of freshwater endosymbiotic *Chlorella* (Trebouxiophyceae, Chlorophyta)1. *Journal of Phycology* 2008;44:77–84.
- Szathmáry E, Smith JM. The major evolutionary transitions. *Nature* 1995;374:227–32.
- Takahashi T, Shirai Y, Kosaka T et al. Arrest of cytoplasmic streaming induces algal proliferation in green *Paramecia*. *PLoS One* 2007;2:e1352.
- Tebo BM, Linthicum DS, Neelson KH. Luminous bacteria and light emitting fish: ultrastructure of the symbiosis. *Biosystems* 1979;11:269–80.
- Tso GHW, Reales-Calderon JA, Tan ASM et al. Experimental evolution of a fungal pathogen into a gut symbiont. *Science* 2018;362:589–95.
- Tsuchida T, Koga R, Horikawa M et al. Symbiotic bacterium modifies aphid body color. *Science* 2010;330:1102–4.
- Visick KL, Ruby EG. *Vibrio fischeri* and its host: it takes two to tango. *Curr Opin Microbiol* 2006;9:632–8.
- Wendling CC, Fabritzek AG, Wegner KM. Population-specific genotype x genotype x environment interactions in bacterial disease of early life stages of pacific oyster larvae. *Evol Appl* 2017;10:338–47.
- Wernegreen JJ. Endosymbiosis: Lessons in conflict resolution. *PLOS Biol* 2004;2:e68.
- Wilkerson FP, Kobayashi D, Muscatine L. Mitotic index and size of symbiotic algae in caribbean reef corals. *Coral Reefs* 1988;7:29–36.
- Yamamura N. Vertical transmission and evolution of mutualism from parasitism. *Theor Popul Biol* 1993;44:95–109.
- Ziesenisz E, Reisser W, Wiessner W. Evidence of de novo synthesis of maltose excreted by the endosymbiotic *Chlorella* from *Paramecium bursaria*. *Planta* 1981;153:481–5.

## Appendix B

Statistical outputs for Chapter 2. The analyses associated with Figures 2.2 and 2.5. In the majority of cases, responses were analysed as ANOVA models. For  $\Phi$ PSII responses reported in Figure 2.5b, a non-linear mixed effects model was used.

### Relating to Figure 2.2

ANOVA model for selection rate in response to growth irradiance analysed by host genotype (following model reduction)

Factor	DF	SS	MSS	F value	p value
Host	1	0.516	0.516	19.387	<0.001
Growth irradiance	1	1.6963	1.6963	63.731	<0.001
Host:Growth irradiance	1	0.1308	0.1308	4.915	0.034088
Residuals	31	0.8251	0.0266		

**F-statistic: 29.34 on 3 and 31 DF, p-value: 3.469e-09, Adjusted R2: 0.7144**

### Relating to Figure 2.5a

ANOVA model for FvFm estimates in response to light analysed by host and symbiont genotype

Factor	DF	SS	MSS	F value	p value
Host	1	0.07719	0.07719	121.099	<0.001
Symbiont	1	0.00006	0.00006	0.088	0.767
Light	1	0.00418	0.00418	6.563	0.011
Host:Symbiont	1	0.03891	0.03891	61.052	<0.001
Host:Light	1	0.01305	0.01305	20.481	<0.001
Symbiont:Light	1	0.12213	0.12213	191.616	<0.001
Host:Symbiont:Light	1	0.13001	0.13001	203.984	<0.001
Residuals	232	0.14787	0.00064		

**F-statistic: 86.41 on 7 and 232 DF, p-value: < 2.2e-16, Adjusted R2: 0.7144**

Tukey HSD posthoc test, showing the result for symbiont comparison (18-HA):

Host	Light	Difference	P adj
	186	12	0.067
		50	0.000
HA1	12	0.025	0.004
	50	0.028	0.001

### Relating to Figure 2.5b

Non-linear mixed effects model (assuming exponential decay of the form  $y = a \times e(\text{light} \times b)$ ) for the response of steady-state quantum yield ( $\Phi$ PSII) to actinic light analysed by growth irradiance, host genotype and symbiont genotype. Replicates within treatments were treated as random effects; growth irradiance, host identity and symbiont identity were treated as fixed effects.

Model	DF	AIC	BIC	logLik	Test	L.Ratio	p-value
1)Host*Symbiont*Light	17	-11478.35	-11382.7	5756.176			
2)Host*Symbiont	9	-11446.53	-11395.9	5732.268	1vs2	47.81662	<.0001
3)Host*Light	11	-11449.02	-11387.1	5735.508	1vs3	41.33577	<.0001
4)Symbiont*Light	11	-11452.35	-11390.5	5737.174	1v4	38.00399	<.0001

Estimates of coefficients

Host	Symbiont	Light	Intercept	SE	exponent	SE
186	18	12	0.342515	0.01121	-0.001247	0.0000229
		24	0.419108	0.011165	-0.001247	0.0000229
		50	0.409108	0.011069	-0.001247	0.0000229
	HA	12	0.407578	0.011079	-0.001247	0.0000229
		24	0.40278	0.011093	-0.001247	0.0000229
		50	0.304538	0.011219	-0.001247	0.0000229
HA1	18	12	0.368342	0.011084	-0.001247	0.0000229
		24	0.427061	0.011054	-0.001247	0.0000229
		50	0.39956	0.011122	-0.001247	0.0000229
	HA	12	0.416999	0.011122	-0.001247	0.0000229
		24	0.421092	0.0111	-0.001247	0.0000229
		50	0.426505	0.011084	-0.001247	0.0000229

ANOVA on the summary statistics - the response of the nlme predicted intercept to experimental group (a single factor that combines host genotype, symbiont genotype and growth irradiance). Computed by aovSufficient (HH package)

Factor	DF	SS	MSS	F value	p value
Group	11	0.04755	0.004323	11.66	<0.001
Residuals	24	0.0089	0.000371		

**F-statistic: 11.66 on 11 and 24 DF, p-value: 2.28e-07**

Tukey HSD posthoc test, showing the results for the symbiont comparison (18-HA):

Group				
Host	Light	Difference	P adj	
186	12	0.065	0.015	
	24	-0.016	0.995	
	50	-0.105	0.000	
HA1	12	0.049	0.142	
	24	-0.006	1.000	
	50	0.027	0.845	

**Relating to Figure 2.5c**

NSV values are modelled by polynomial models in the form  $Y = ax^2 + bx + c$ . Each coefficient was then evaluated by ANOVA models to test which factors significantly affect them.

Coefficient c (the intercept) - linear model for its response to host genotype (following model reduction)

Factor	DF	SS	MSS	F value	p value
Host	1	1.15	1.15	4.739	0.0365
Residuals	34	8.251	0.2427		

**F-statistic: 4.739 on 1 and 34 DF, p-value: 0.03653, Adjusted R2: 0.09651**

Coefficient b - linear model for its response to symbiont genotype and growth irradiance (following model reduction)

<b>Factor</b>	<b>DF</b>	<b>SS</b>	<b>MSS</b>	<b>F value</b>	<b>p value</b>
Symbiont	1	1.52E-06	1.52E-06	9.485	<0.01
Growth Irradiance	2	1.16E-06	5.78E-07	3.6	0.03888
Residuals	32	5.14E-06	1.61E-07		

**F-statistic: 5.562 on 3 and 32 DF, p-value: 0.003456, Adjusted R2: 0.2811**

Coefficient a - linear model for its response to symbiont genotype (following model reduction)

<b>Factor</b>	<b>DF</b>	<b>SS</b>	<b>MSS</b>	<b>F value</b>	<b>p value</b>
Symbiont	1	1.07E-13	1.07E-13	8.932	<0.01
Residuals	34	4.08E-13	1.20E-14		

**F-statistic: 8.932 on 1 and 34 DF, p-value: 0.005176, Adjusted R2: 0.1847**

## Appendix C

Statistical outputs for Chapter 3. The analyses associated with Figures 3.2,3.3,3.8. In most cases, the responses were analysed with ANOVA models.

### Relating to Figure 3.2

ANOVA on growth rates in response to growth irradiance analysed by host and symbiont genotype

Factor	DF	SS	MSS	F value	p value
Host	2	2.79E-02	1.39E-02	2.262	0.10738
Symbiont	2	7.76E-02	3.88E-02	6.297	<0.01
Light	1	1.49E+00	1.49E+00	242.246	<0.001
Host:Symbiont	4	8.24E-02	2.06E-02	3.345	0.0116
Host:Light	2	6.26E-02	3.13E-02	5.084	<0.01
Symbiont:Light	2	1.38E-01	6.91E-02	11.215	<0.001
Host:Symbionts:Light	4	8.87E-02	2.22E-02	3.6	<0.01
Residuals	162	9.98E-01	6.20E-03		

**F-statistic: 18.81 on 17 and 162 DF, p-value: <0.001, Adjusted R<sup>2</sup>: 0.63**

### Relating to Figure 3.3

ANOVA on symbiont load in response to growth irradiance analysed by host and symbiont genotype

Factor	DF	SS	MSS	F value	p value
Host	2	5.75E+12	2.87E+12	10.869	<0.001
Symbiont	2	2.00E+12	1.00E+12	3.787	0.0247
Light	1	1.56E+12	1.56E+12	5.911	0.0161
Host:Symbiont	4	1.47E+12	3.67E+11	1.388	0.2404
Host:Light	2	1.64E+12	8.20E+11	3.101	0.0477
Symbiont:Light	2	1.65E+12	8.25E+11	3.12	0.0468
Host:Symbiont:Light	4	2.94E+12	7.35E+11	2.78	0.0287
Residuals	162	4.28E+13	2.64E+11		

**F-statistic: 3.784 on 17 and 162 DF, p-value: <0.001, Adjusted R<sup>2</sup>: 0.2091**

Symbiont load values were modelled by polynomial models in the form  $Y = ax^2 + bx + c$ . Each coefficient was then evaluated by linear models to test which factors (host and symbiont genotype) significantly affect them.

Coefficient c (the intercept) - linear model for its response to host and symbiont genotype

Factor	DF	SS	MSS	F value	p value
host	2	6.18E+12	3.09E+12	58.47	<0.001
symbiont	2	2.20E+12	1.10E+12	20.82	<0.001
host:symbiont	4	3.13E+12	7.81E+11	14.79	<0.001
Residuals	36	1.90E+12	5.28E+10		

**F-statistic: 27.22 on 8 and 36 DF, p-value: <0.001, Adjusted R<sup>2</sup>: 0.83**

Coefficient b (first coefficient) - linear model for its response to host and symbiont genotype

Factor	DF	SS	MSS	F value	p value
host	2	2.26E+10	1.13E+10	17.987	<0.001
symbiont	2	6.92E+09	3.46E+09	5.503	<0.01
host:symbiont	4	1.36E+10	3.41E+09	5.413	<0.01
Residuals	36	2.26E+10	6.29E+08		

**F-statistic: 8.58 on 8 and 36 DF, p-value: <0.001 , Adjusted R<sup>2</sup>: 0.58**

Coefficient a (second coefficient) - linear model for its response to host and symbiont genotype

Factor	DF	SS	MSS	F value	p value
host	2	1.56E+12	7.78E+11	13.836	<0.001
symbiont	2	4.57E+11	2.28E+11	4.063	0.0257
host:symbiont	4	7.28E+11	1.82E+11	3.236	0.0229
Residuals	36	2.02E+12	5.62E+10		

**F-statistic: 6.09 on 8 and 36 DF, p-value: <0.001 , Adjusted R<sup>2</sup>: 0.48**

The polynomial models were used to calculate predictive values for the coordinates at the peak maximum.

X max - ANOVA on the predicted X values at the peak maximum in response to host and symbiont genotype

Factor	DF	SS	MSS	F value	p value
host	2	165.9	82.96	9.634	<0.001
symbiont	2	192.8	96.42	11.197	<0.001
host:symbiont	4	474	118.49	13.759	<0.001
Residuals	36	310	8.61		

**F-statistic: 12.09 on 8 and 36 DF, p-value: <0.001 , Adjusted R<sup>2</sup>: 0.67**

Y max - ANOVA on the predicted Y values at the peak maximum in response to host and symbiont genotype

Factor	DF	SS	MSS	F value	p value
host	2	4.42E+11	2.21E+11	5.596	<0.01
symbiont	2	7.88E+11	3.94E+11	9.97	<0.001
host:symbiont	4	6.03E+11	1.51E+11	3.812	0.011
Residuals	36	1.42E+12	3.95E+10		

**F-statistic: 5.80 on 8 and 36 DF, p-value: <0.001 , Adjusted R<sup>2</sup>: 0.47**

Tukey HSD posthoc tests summary table for the intercept, X maximum and Y maximum values. Showing the result for symbiont comparisons:

Host	Pairwise Tests	Intercept		X-max		Y-max	
		Difference	P adj	Difference	P adj	Difference	P adj
HA1	h:HA - h:18	-98859	0.999	4.429	0.322	-197462	0.814
	h:HK - h:18	-192634	0.917	3.529	0.617	-13529	1.000
	h:HK - h:HA	-93775	0.999	-0.900	1.000	183933	0.865
HK1	k:HA - k:18	690394	<b>0.001</b>	-3.335	0.684	-52652	1.000
	k:HK - k:18	512444	<b>0.028</b>	-3.379	0.669	534623	<b>0.004</b>
	k:HK - k:HA	-177949	0.946	-0.044	1.000	587275	<b>0.001</b>
186	s:HA - s:18	546447	<b>0.016</b>	-5.764	0.078	-284314	0.391
	s:HK - s:18	1253004	<b>0.000</b>	-15.023	<b>0.000</b>	-84741	0.999
	s:HK - s:HA	706557	<b>0.001</b>	-9.259	<b>0.000</b>	199573	0.805

### Relating to Figure 3.8

ANOVA on the mz 686.4 relative abundance in response to host and symbiont genotype

Factor	DF	SS	MSS	F value	p value
host	2	9.24E-07	4.62E-07	0.396	0.67852
symbiont	2	1.29E-05	6.47E-06	5.55	0.01326
host:symbiont	4	2.16E-05	5.40E-06	4.632	<0.01
Residuals	18	2.10E-05	1.17E-06		

**F-statistic: 13.802 on 8 and 18 DF, p-value: 0.008859 , Adjusted R<sup>2</sup>: 0.463**

ANOVA on the mz 271.2 relative abundance in response to host and symbiont genotype

Factor	DF	SS	MSS	F value	p value
host	2	3.81E-06	1.91E-06	0.901	0.4237
symbiont	2	3.08E-06	1.54E-06	0.728	0.4966
host:symbiont	4	2.94E-05	7.34E-06	3.468	0.0287
Residuals	18	3.81E-05	2.12E-06		

**F-statistic: 2.141 on 8 and 18 DF, p-value: 0.08574 , Adjusted R<sup>2</sup>: 0.2599**

ANOVA on the mz 247.2 relative abundance in response to host and symbiont genotype

Factor	DF	SS	MSS	F value	p value
host	2	1.13E-06	5.64E-07	0.852	0.443
symbiont	2	1.85E-06	9.24E-07	1.394	0.274
host:symbiont	4	6.00E-06	1.50E-06	2.264	0.102
Residuals	18	1.19E-05	6.63E-07		

**F-statistic: 1.693 on 8 and 18 DF, p-value: 0.1681 , Adjusted R<sup>2</sup>: 0.1758**

## Appendix D

Statistical outputs for Chapter 4. Analyses associated with Figures 4.1 - 4.4. In most cases responses were analysed as ANOVA models. For the growth rate per transfer (Fig 4.1), a linear mixed effects model was used.

### Relating to Figure 4.1

Linear mixed effect model for the response of growth rate to transfer week analysed by symbiont genotype. Transfer week within treatment ID were treated as random effects; symbiont genotype and transfer week were treated as fixed effects.

Model	DF	AIC	BIC	logLik	Test	L.Ratio	p-value
1) Symbiont + Transfer	7	-1123.768	-1098.13	568.8839			
2) Symbiont	6	-1118.694	-1096.72	565.3468	1v2	7.074102	0.0078
3) Transfer	6	-1094.306	-1072.33	553.1531	1v3	31.46149	<.0001

Fixed effects	Estimate	SE	DF	T-value
Intercept	0.281	0.007	275	42.266
SymbiontSHK	-0.080	0.006	10	-14.126
transfer	0.001	0.000	275	3.088

Random effects	SD	Correlation
Intercept	0.015	
Transfer	0.001	-0.878
Residual	0.033	

### Relating to Figure 4.2

ANOVA for growth assay in response to light analysed by symbiont genotype and transfer number

Factor	DF	SS	MSS	F value	p value
Light	3	2.133	0.711	216.332	<0.001
Symbiont	1	0.0424	0.0424	12.911	<0.001
Transfer	3	0.0568	0.0189	5.766	<0.001
Light:Symbiont	3	0.0758	0.0253	7.688	<0.001
Symbiont:Transfer	3	0.0908	0.0303	9.204	<0.001
Residuals	178	0.585	0.0033		

F-statistic: 56.14 on 13 and 178 DF, p-value: < 2.2e-16, Adjusted R2: 0.7896

### Relating to Figure 4.3

ANOVA for symbiont-load in response to light analysed by symbiont genotype and transfer number

Factor	DF	SS	MSS	F value	p value
Symbiont	1	1.85E+12	1.85E+12	18.167	<0.001
Light	4	4.47E+13	1.12E+13	109.564	<0.001
Transfer	1	5.37E+12	5.37E+12	52.578	<0.001
Symbiont:Light	4	4.55E+12	1.14E+12	11.158	<0.001
Symbiont:Transfer	1	2.79E+12	2.79E+12	27.366	<0.001
Light:Transfer	4	4.60E+12	1.15E+12	11.257	<0.001
Symbiont:Light:Transfer	4	2.32E+12	5.81E+11	5.693	<0.001
Residuals	76	7.76E+12	1.02E+11		

F-statistic: 34.15 on 19 and 76 DF, p-value: < 2.2e-16, Adjusted R2: 0.8689

#### Relating to Figure 4.4

ANOVA for selection rate in response to light analysed by symbiont genotype and transfer number

<b>Factor</b>	<b>DF</b>	<b>SS</b>	<b>MSS</b>	<b>F value</b>	<b>p value</b>
Symbiont	1	0.1293	0.1293	7.484	<0.01
Light	2	0.6747	0.3373	19.527	<0.001
Transfer	1	0.511	0.511	29.58	<0.001
Symbiont:Light	2	0.0484	0.0242	1.401	0.258
Symbiont:Transfer	1	0.0117	0.0117	0.679	0.415
Light:Transfer	2	0.1075	0.0537	3.111	0.055
Symbiont:Light:Transfer	2	0.2032	0.1016	5.882	<0.01
Residuals	41				

F-statistic: 8.871 on 11 and 41 DF, p-value: 8.663e-08, Adjusted R2: 0.6248

Tukey HSD posthoc test, showing the result for symbiont comparison (18-HK):

<b>Transfer</b>	<b>Light</b>	<b>Difference</b>	<b>P adj</b>
T0	0	0.134	0.992
	12	-0.092	0.999
	<b>50</b>	<b>-0.395</b>	<b>0.029</b>
T25	0	-0.176	0.483
	12	0.022	1.000
	50	-0.046	1.000

## Bibliography

- Abdel-Rahman, M.H.M., Ali, R.M., and Said, H.A. (2005). Alleviation of NaCl-induced effects on *Chlorella vulgaris* and *Chlorococcum humicola* by riboflavin application. *International Journal of Agriculture and Biology (Pakistan)*.
- Abrego, D., Ulstrup, K.E., Willis, B.L., and van Oppen, M.J.H. (2008). Species-specific interactions between algal endosymbionts and coral hosts define their bleaching response to heat and light stress. *Proceedings of the Royal Society B: Biological Sciences* 275, 2273–2282.
- Achlatis, M., Pernice, M., Green, K., Guagliardo, P., Kilburn, M.R., Hoegh-Guldberg, O., and Dove, S. (2018). Single-cell measurement of ammonium and bicarbonate uptake within a photosymbiotic bioeroding sponge. *ISME J* 12, 1308–1318.
- Ahmadjian, V. (1993). *The Lichen Symbiosis* (John Wiley & Sons).
- Albers, D., Reisser, W., and Wiessner, W. (1982). Studies on the nitrogen supply of endosymbiotic chlorellae in green paramecium bursaria. *Plant Science Letters* 25, 85–90.
- Allen, J.F., Raven, J.A., Embley, T.M., der Giezen Mark van, Horner David S., Dyal Patricia L., and Foster Peter (2003). Mitochondria and hydrogenosomes are two forms of the same fundamental organelle. *Philosophical Transactions of the Royal Society of London. Series B: Biological Sciences* 358, 191–203.
- Anbutsu, H., Moriyama, M., Nikoh, N., Hosokawa, T., Futahashi, R., Tanahashi, M., Meng, X.-Y., Kuriwada, T., Mori, N., Oshima, K., et al. (2017). Small genome symbiont underlies cuticle hardness in beetles. *PNAS* 114, E8382–E8391.
- Ankrah, N.Y.D., and Douglas, A.E. (2018). Nutrient factories: metabolic function of beneficial microorganisms associated with insects. *Environmental Microbiology* 20, 2002–2011.
- Anthony, K., Bay, L.K., Costanza, R., Firn, J., Gunn, J., Harrison, P., Heyward, A., Lundgren, P., Mead, D., Moore, T., et al. (2017). New interventions are needed to save coral reefs. *Nat Ecol Evol* 1, 1420–1422.
- Archetti, M., Scheuring, I., Hoffman, M., Frederickson, M.E., Pierce, N.E., and Yu, D.W. (2011). Economic game theory for mutualism and cooperation. *Ecology Letters* 14, 1300–1312.
- Archibald, J.M. (2009). The Puzzle of Plastid Evolution. *Current Biology* 19, R81–R88.
- Archibald, J.M., and Keeling, P.J. (2002). Recycled plastids: a ‘green movement’ in eukaryotic evolution. *Trends in Genetics* 18, 577–584.
- Arnou, P., Oleson, J.J., and Williams, J.H. (1953). The Effect of Arginine on the Nutrition of *Chlorella vulgaris*. *American Journal of Botany* 40, 100–104.
- Asensi-Fabado, M.A., and Munné-Bosch, S. (2010). Vitamins in plants: occurrence, biosynthesis and antioxidant function. *Trends in Plant Science* 15, 582–592.

- Baird, A.H., Bhagooli, R., Ralph, P.J., and Takahashi, S. (2009). Coral bleaching: the role of the host. *Trends in Ecology & Evolution* 24, 16–20.
- Baker, A.C. (2003). Flexibility and Specificity in Coral-Algal Symbiosis: Diversity, Ecology, and Biogeography of Symbiodinium. *Annual Review of Ecology, Evolution, and Systematics* 34, 661–689.
- Barbrook, A.C., Howe, C.J., and Purton, S. (2006). Why are plastid genomes retained in non-photosynthetic organisms? *11*, 101–108.
- Bartosz, G. (1997). Oxidative stress in plants. *Acta Physiol Plant* 19, 47–64.
- Bell-Roberts, L., Douglas, A.E., and Werner, G.D.A. (2019). Match and mismatch between dietary switches and microbial partners in plant sap-feeding insects. *Proceedings of the Royal Society B: Biological Sciences* 286, 20190065.
- Bennett, G.M., and Moran, N.A. (2015). Heritable symbiosis: The advantages and perils of an evolutionary rabbit hole. *PNAS* 112, 10169–10176.
- Benton, H.P., Want, E.J., and Ebbels, T.M.D. (2010). Correction of mass calibration gaps in liquid chromatography-mass spectrometry metabolomics data. *Bioinformatics* 26, 2488–2489.
- Berkelmans, R., and van Oppen, M.J.H. (2006). The role of zooxanthellae in the thermal tolerance of corals: a ‘nugget of hope’ for coral reefs in an era of climate change. *Proceedings of the Royal Society B: Biological Sciences* 273, 2305–2312.
- Berney, C., and Pawlowski, J. (2006). A molecular time-scale for eukaryote evolution recalibrated with the continuous microfossil record. *Proceedings of the Royal Society B: Biological Sciences* 273, 1867–1872.
- Bhattacharya, D., and Archibald, J.M. (2006). Response to theissen and martin. *Current Biology* 16, R1017–R1018.
- Blanc, G., Duncan, G., Agarkova, I., Borodovsky, M., Gurnon, J., Kuo, A., Lindquist, E., Lucas, S., Pangilinan, J., Polle, J., et al. (2010). The *Chlorella variabilis* NC64A Genome Reveals Adaptation to Photosymbiosis, Coevolution with Viruses, and Cryptic Sex. *Plant Cell* 22, 2943–2955.
- Bodył, A., Mackiewicz, P., and Stiller, J.W. (2007). The intracellular cyanobacteria of *Paulinella chromatophora*: endosymbionts or organelles? *Trends in Microbiology* 15, 295–296.
- Bonen, L., and Doolittle, W.F. (1975). On the prokaryotic nature of red algal chloroplasts. *PNAS* 72, 2310–2314.
- Bonen, L., Cunningham, R.S., Gray, M.W., and Doolittle, W.F. (1977). Wheat embryo mitochondrial 18S ribosomal RNA: evidence for its prokaryotic nature. *Nucleic Acids Res* 4, 663–671.
- Boulotte, N.M., Dalton, S.J., Carroll, A.G., Harrison, P.L., Putnam, H.M., Peplow, L.M., and van Oppen, M.J. (2016). Exploring the *Symbiodinium* rare biosphere provides

evidence for symbiont switching in reef-building corals. *The ISME Journal* 10, 2693–2701.

Bourtzis, K., Dobson, S.L., Xi, Z., Rasgon, J.L., Calvitti, M., Moreira, L.A., Bossin, H.C., Moretti, R., Baton, L.A., Hughes, G.L., et al. (2014). Harnessing mosquito–Wolbachia symbiosis for vector and disease control. *Acta Tropica* 132, S150–S163.

Bronstein, J.L. (2015). *Mutualism* (Oxford University Press).

Buddemeier, R.W., and Fautin, D.G. (1993). Coral Bleaching as an Adaptive Mechanism. *BioScience* 43, 320–326.

Bull, J.J., and Rice, W.R. (1991). Distinguishing mechanisms for the evolution of co-operation. *Journal of Theoretical Biology* 149, 63–74.

Cameron, D.D., Leake, J.R., and Read, D.J. (2006). Mutualistic mycorrhiza in orchids: evidence from plant–fungus carbon and nitrogen transfers in the green-leaved terrestrial orchid *Goodyera repens*. *New Phytologist* 171, 405–416.

Cameron, D.D., Geniez, J.-M., Seel, W.E., and Irving, L.J. (2008). Suppression of Host Photosynthesis by the Parasitic Plant *Rhinanthus minor*. *Ann Bot* 101, 573–578.

Cantin, N.E., van Oppen, M.J.H., Willis, B.L., Mieog, J.C., and Negri, A.P. (2009). Juvenile corals can acquire more carbon from high-performance algal symbionts. *Coral Reefs* 28, 405.

Caragata, E.P., Dutra, H.L.C., and Moreira, L.A. (2016). Exploiting Intimate Relationships: Controlling Mosquito-Transmitted Disease with Wolbachia. *Trends in Parasitology* 32, 207–218.

Caspi, R., Billington, R., Fulcher, C.A., Keseler, I.M., Kothari, A., Krummenacker, M., Latendresse, M., Midford, P.E., Ong, Q., Ong, W.K., et al. (2018). The MetaCyc database of metabolic pathways and enzymes. *Nucleic Acids Res* 46, D633–D639.

Cavalier-Smith, T. (2013). Symbiogenesis: Mechanisms, Evolutionary Consequences, and Systematic Implications. *Annual Review of Ecology, Evolution, and Systematics* 44, 145–172.

Cavanaugh, C.M., Gardiner, S.L., Jones, M.L., Jannasch, H.W., and Waterbury, J.B. (1981). Prokaryotic Cells in the Hydrothermal Vent Tube Worm *Riftia pachyptila* Jones: Possible Chemoautotrophic Symbionts. *Science* 213, 340–342.

Chavez-Dozal, A., and Nishiguchi, M.K. (2016). Impact of Metabolomics in Symbiosis Research. *Metabolomics: Fundamentals and Applications* 139.

Chong, R.A., and Moran, N.A. (2016). Intraspecific genetic variation in hosts affects regulation of obligate heritable symbionts. *PNAS* 113, 13114–13119.

Coles, S.L., Bahr, K.D., Rodgers, K.S., May, S.L., McGowan, A.E., Tsang, A., Bumgarner, J., and Han, J.H. (2018). Evidence of acclimatization or adaptation in Hawaiian corals to higher ocean temperatures. *PeerJ* 6, e5347.

- Combes, C. (2005). *The Art of Being a Parasite* (University of Chicago Press).
- Converti, A., Casazza, A.A., Ortiz, E.Y., Perego, P., and Del Borghi, M. (2009). Effect of temperature and nitrogen concentration on the growth and lipid content of *Nannochloropsis oculata* and *Chlorella vulgaris* for biodiesel production. *Chemical Engineering and Processing: Process Intensification* 48, 1146–1151.
- Corliss, J.O. (1961). *The Ciliated Protozoa: Characterization, Classification and Guide to the Literature* (Elsevier).
- Corsaro, D., Venditti, D., Padula, M., and Valassina, M. (1999). Intracellular Life. *Critical Reviews in Microbiology* 25, 39–79.
- Cunning, R., Vaughan, N., Gillette, P., Capo, T.R., Maté, J.L., and Baker, A.C. (2015). Dynamic regulation of partner abundance mediates response of reef coral symbioses to environmental change. *Ecology* 96, 1411–1420.
- Currie, C.R., Scott, J.A., Summerbell, R.C., and Malloch, D. (1999). Fungus-growing ants use antibiotic-producing bacteria to control garden parasites. *Nature* 398, 701–704.
- Dahan, R.A., Duncan, R.P., Wilson, A.C., and Dávalos, L.M. (2015). Amino acid transporter expansions associated with the evolution of obligate endosymbiosis in sap-feeding insects (Hemiptera: Sternorrhyncha). *BMC Evolutionary Biology* 15, 52.
- De Bary, A. (1879). *The phenomenon of symbiosis*. Karl J. Trubner, Strasbourg, Germany.
- Dean, A.D., Minter, E.J.A., Sørensen, M.E.S., Lowe, C.D., Cameron, D.D., Brockhurst, M.A., and Jamie Wood, A. (2016). Host control and nutrient trading in a photosynthetic symbiosis. *Journal of Theoretical Biology* 405, 82–93.
- Decelle, J. (2013). New perspectives on the functioning and evolution of photosymbiosis in plankton. *Communicative & Integrative Biology* 6, e24560.
- Decelle, J., Colin, S., and Foster, R.A. (2015). Photosymbiosis in Marine Planktonic Protists. In *Marine Protists*, (Springer, Tokyo), pp. 465–500.
- Delwiche, C.F. (1999). Tracing the Thread of Plastid Diversity through the Tapestry of Life. *The American Naturalist* 154, S164–S177.
- Demirbas, M.F. (2011). Biofuels from algae for sustainable development. *Applied Energy* 88, 3473–3480.
- DeSalvo, M.K., Estrada, A., Sunagawa, S., and Medina, M. (2012). Transcriptomic responses to darkness stress point to common coral bleaching mechanisms. *Coral Reefs* 31, 215–228.
- Dodson, E.O. (1979). Crossing the prokaryote–eucaryote border: endosymbiosis or continuous development? *Canadian Journal of Microbiology* 25, 651–674.
- Dohlen, C.D. von, Kohler, S., Alsop, S.T., and McManus, W.R. (2001). Mealybug  $\beta$ -proteobacterial endosymbionts contain  $\gamma$ -proteobacterial symbionts. *Nature* 412, 433.

- Dorrell, R.G., and Smith, A.G. (2011). Do Red and Green Make Brown?: Perspectives on Plastid Acquisitions within Chromalveolates. *Eukaryotic Cell* 10, 856–868.
- Douglas, A.E. (2003). Coral bleaching—how and why? *Marine Pollution Bulletin* 46, 385–392.
- Douglas, A.E. (2008). Conflict, cheats and the persistence of symbioses. *New Phytologist* 177, 849–858.
- Douglas, A.E. (2014). Symbiosis as a General Principle in Eukaryotic Evolution. *Cold Spring Harb Perspect Biol* 6, a016113.
- Douglas, A., and Smith, D.C. (1984). The green hydra symbiosis. VIII. Mechanisms in symbiont regulation. *Proceedings of the Royal Society of London. Series B. Biological Sciences* 221, 291–319.
- Du, Z.-Y., Zienkiewicz, K., Vande Pol, N., Ostrom, N.E., Benning, C., and Bonito, G.M. (2019). Algal-fungal symbiosis leads to photosynthetic mycelium. *ELife* 8, e47815.
- Dubinsky, Z., and Berman-Frank, I. (2001). Uncoupling primary production from population growth in photosynthesizing organisms in aquatic ecosystems. *Aquat. Sci.* 63, 4–17.
- Dyall, S.D., Brown, M.T., and Johnson, P.J. (2004). Ancient Invasions: From Endosymbionts to Organelles. *Science* 304, 253–257.
- Esteban, G.F., Fenchel, T., and Finlay, B.J. (2010). Mixotrophy in Ciliates. *Protist* 161, 621–641.
- Estrela, S., Kerr, B., and Morris, J.J. (2016). Transitions in individuality through symbiosis. *Current Opinion in Microbiology* 31, 191–198.
- Fabina, N.S., Putnam, H.M., Franklin, E.C., Stat, M., and Gates, R.D. (2013). Symbiotic specificity, association patterns, and function determine community responses to global changes: defining critical research areas for coral-Symbiodinium symbioses. *Global Change Biology* 19, 3306–3316.
- Fenchel, T. (1987). *Ecology of Protozoa: The Biology of Free-living Phagotropic Protists* (Springer-Verlag).
- Ferea, T.L., Botstein, D., Brown, P.O., and Rosenzweig, R.F. (1999). Systematic changes in gene expression patterns following adaptive evolution in yeast. *PNAS* 96, 9721–9726.
- Ferrari, J., Scarborough, C.L., and Godfray, H.C.J. (2007). Genetic variation in the effect of a facultative symbiont on host-plant use by pea aphids. *Oecologia* 153, 323–329.
- Fisher, R.M., Henry, L.M., Cornwallis, C.K., Kiers, E.T., and West, S.A. (2017). The evolution of host-symbiont dependence. *Nature Communications* 8, ncomms15973.
- Focke, G.W. (1836). Ueber einige Organisation-sverhältnisse bei polygastrischen Infusorien, “Oken. Isis,.”

- Fokin, S.I. (2004). Bacterial Endocytobionts of Ciliophora and Their Interactions with the Host Cell. In *International Review of Cytology*, (Academic Press), pp. 181–249.
- Foyer, C.H., and Noctor, G. (2003). Redox sensing and signalling associated with reactive oxygen in chloroplasts, peroxisomes and mitochondria. *Physiologia Plantarum* *119*, 355–364.
- Frago, E., Dicke, M., and Godfray, H.C.J. (2012). Insect symbionts as hidden players in insect–plant interactions. *Trends in Ecology & Evolution* *27*, 705–711.
- Frank, S.A. (1997). Models of Symbiosis. *The American Naturalist* *150*, S80–S99.
- Freeman, C.J., Thacker, R.W., Baker, D.M., and Fogel, M.L. (2013). Quality or quantity: is nutrient transfer driven more by symbiont identity and productivity than by symbiont abundance? *The ISME Journal* *7*, 1116–1125.
- Fujishima, M. (2009). *Endosymbionts in Paramecium* (Springer Science & Business Media).
- Fujishima, M., and Kodama, Y. (2012). Endosymbionts in Paramecium. *European Journal of Protistology* *48*, 124–137.
- Fukatsu, T., Aoki, S., Kurosu, U., and Ishikawa, H. (1994). Phylogeny of Cerataphidini Aphids Revealed by Their Symbiotic Microorganisms and Basic Structure of Their Galls—Implications for Host-Symbiont Coevolution and Evolution of Sterile Soldier Castes. *Zoological Science* *11*, p613-623.
- Futuyma, D.J., and Moreno, G. (1988). The Evolution of Ecological Specialization. *Annual Review of Ecology and Systematics* *19*, 207–233.
- Garcia, J.R., and Gerardo, N.M. (2014). The symbiont side of symbiosis: do microbes really benefit? *Front. Microbiol.* *5*.
- Gargas, A., DePriest, P.T., Grube, M., and Tehler, A. (1995). Multiple origins of lichen symbioses in fungi suggested by SSU rDNA phylogeny. *Science* *268*, 1492–1495.
- Gast, R.J., Sanders, R.W., and Caron, D.A. (2009). Ecological strategies of protists and their symbiotic relationships with prokaryotic microbes. *Trends Microbiol.* *17*, 563–569.
- Genkai-Kato, M., and Yamamura, N. (1999). Evolution of Mutualistic Symbiosis without Vertical Transmission. *Theoretical Population Biology* *55*, 309–323.
- Gilbert, S.F., McDonald, E., Boyle, N., Buttino, N., Gyi, L., Mai, M., Neelakantan, P., and James, R. (2010). Symbiosis as a source of selectable epigenetic variation: taking the heat for the big guy. *Philosophical Transactions of the Royal Society B: Biological Sciences* *365*, 671–678.
- Gong, J., Qing, Y., Guo, X., and Warren, A. (2014). “Candidatus *Sonnebornia yantaiensis*”, a member of candidate division OD1, as intracellular bacteria of the ciliated protist *Paramecium bursaria* (Ciliophora, Oligohymenophorea). *Systematic and Applied Microbiology* *37*, 35–41.

- Gornik, S.G., Febrimarsa, Cassin, A.M., MacRae, J.I., Ramaprasad, A., Rchiad, Z., McConville, M.J., Bacic, A., McFadden, G.I., Pain, A., et al. (2015). Endosymbiosis undone by stepwise elimination of the plastid in a parasitic dinoflagellate. *PNAS* *112*, 5767–5772.
- Graf, A., Schlereth, A., Stitt, M., and Smith, A.M. (2010). Circadian control of carbohydrate availability for growth in *Arabidopsis* plants at night. *PNAS* *107*, 9458–9463.
- Gray, M.W., and Doolittle, W.F. (1982). Has the endosymbiont hypothesis been proven? *Microbiol Rev* *46*, 1–42.
- Hamada, M., Schröder, K., Bathia, J., Kürn, U., Fraune, S., Khalturina, M., Khalturin, K., Shinzato, C., Satoh, N., and Bosch, T.C. (2018). Metabolic co-dependence drives the evolutionarily ancient Hydra–*Chlorella* symbiosis. *ELife Sciences* *7*, e35122.
- Hardin, G. (1968). The Tragedy of the Commons. *Science* *162*, 1243–1248.
- He, M., Wang, J., Fan, X., Liu, X., Shi, W., Huang, N., Zhao, F., and Miao, M. (2019). Genetic basis for the establishment of endosymbiosis in *Paramecium*. *The ISME Journal* *13*, 1360.
- Heath, K.D. (2010). Intergenomic Epistasis and Coevolutionary Constraint in Plants and Rhizobia. *Evolution* *64*, 1446–1458.
- Heath, K.D., and Tiffin, P. (2007). Context dependence in the coevolution of plant and rhizobial mutualists. *Proceedings of the Royal Society of London B: Biological Sciences* *274*, 1905–1912.
- Heath, K.D., Stock, A.J., and Stinchcombe, J.R. (2010). Mutualism variation in the nodulation response to nitrate. *Journal of Evolutionary Biology* *23*, 2494–2500.
- Herre, E.A., Knowlton, N., Mueller, U.G., and Rehner, S.A. (1999). The evolution of mutualisms: exploring the paths between conflict and cooperation. *Trends in Ecology & Evolution* *14*, 49–53.
- Higuchi, R., Song, C., Hoshina, R., and Suzaki, T. (2018). Endosymbiosis-related changes in ultrastructure and chemical composition of *Chlorella variabilis* (Archaeplastida, Chlorophyta) cell wall in *Paramecium bursaria* (Ciliophora, Oligohymenophorea). *European Journal of Protistology* *66*, 149–155.
- Hill, D.J. (2009). Asymmetric Co-evolution in the Lichen Symbiosis Caused by a Limited Capacity for Adaptation in the Photobiont. *Bot. Rev.* *75*, 326–338.
- Hoang, K.L., Morran, L.T., and Gerardo, N.M. (2016). Experimental Evolution as an Underutilized Tool for Studying Beneficial Animal–Microbe Interactions. *Front. Microbiol.* *7*.
- van Hoek, A.H.A.M., van Alen, T.A., Sprakel, V.S.I., Leunissen, J.A.M., Brigge, T., Vogels, G.D., and Hackstein, J.H.P. (2000). Multiple Acquisition of Methanogenic Archaeal Symbionts by Anaerobic Ciliates. *Mol Biol Evol* *17*, 251–258.

- Holland, J.N., DeAngelis, D.L., and Bronstein, J.L. (2002). Population Dynamics and Mutualism: Functional Responses of Benefits and Costs. *The American Naturalist* 159, 231–244.
- Holland, J.N., DeAngelis, D.L., and Schultz, S.T. (2004). Evolutionary stability of mutualism: interspecific population regulation as an evolutionarily stable strategy. *Proceedings of the Royal Society of London. Series B: Biological Sciences* 271, 1807–1814.
- Honegger, R. (1991). Functional Aspects of the Lichen Symbiosis. *Annual Review of Plant Physiology and Plant Molecular Biology* 42, 553–578.
- Hoogenboom, M., Beraud, E., and Ferrier-Pagès, C. (2010). Relationship between symbiont density and photosynthetic carbon acquisition in the temperate coral *Cladocora caespitosa*. *Coral Reefs* 29, 21–29.
- Hopkins, D.P., Cameron, D.D., and Butlin, R.K. (2017). The chemical signatures underlying host plant discrimination by aphids. *Scientific Reports* 7, 8498.
- Hörtnagl, P.H., and Sommaruga, R. (2007). Photo-oxidative stress in symbiotic and aposymbiotic strains of the ciliate *Paramecium bursaria*. *Photochemical & Photobiological Sciences* 6, 842.
- Hoshina, R., and Fujiwara, Y. (2012). Photobiont Flexibility in *Paramecium bursaria*: Double and Triple Photobiont Co-Habitation. *Advances in Microbiology* 2, 227–233.
- Hoshina, R., and Imamura, N. (2008). Multiple Origins of the Symbioses in *Paramecium bursaria*. *Protist* 159, 53–63.
- Hoshina, R., Kamako, S., and Imamura, N. (2004). Phylogenetic Position of Endosymbiotic Green Algae in *Paramecium bursaria* Ehrenberg from Japan. *Plant Biol (Stuttg)* 6, 447–453.
- Hoshina, R., Kato, Y., Kamako, S., and Imamura, N. (2005). Genetic Evidence of “American” and “European” Type Symbiotic Algae of *Paramecium bursaria* Ehrenberg. *Plant Biol (Stuttg)* 7, 526–532.
- Hosokawa, T., Kikuchi, Y., Shimada, M., and Fukatsu, T. (2007). Obligate symbiont involved in pest status of host insect. *Proceedings of the Royal Society B: Biological Sciences* 274, 1979–1984.
- Hotopp, J.C.D., Clark, M.E., Oliveira, D.C.S.G., Foster, J.M., Fischer, P., Torres, M.C.M., Giebel, J.D., Kumar, N., Ishmael, N., Wang, S., et al. (2007). Widespread Lateral Gene Transfer from Intracellular Bacteria to Multicellular Eukaryotes. *Science* 317, 1753–1756.
- Howells, E.J., Beltran, V.H., Larsen, N.W., Bay, L.K., Willis, B.L., and van Oppen, M.J.H. (2012). Coral thermal tolerance shaped by local adaptation of photosymbionts. *Nature Climate Change* 2, 116–120.

- Hughes, T.P., Baird, A.H., Bellwood, D.R., Card, M., Connolly, S.R., Folke, C., Grosberg, R., Hoegh-Guldberg, O., Jackson, J.B.C., Kleypas, J., et al. (2003). Climate Change, Human Impacts, and the Resilience of Coral Reefs. *Science* 301, 929–933.
- Hughes, T.P., Kerry, J.T., Álvarez-Noriega, M., Álvarez-Romero, J.G., Anderson, K.D., Baird, A.H., Babcock, R.C., Beger, M., Bellwood, D.R., Berkelmans, R., et al. (2017). Global warming and recurrent mass bleaching of corals. *Nature* 543, 373–377.
- Ibarra, R.U., Edwards, J.S., and Palsson, B.O. (2002). *Escherichia coli* K-12 undergoes adaptive evolution to achieve in silico predicted optimal growth. *Nature* 420, 186–189.
- Ishikawa, M., Yuyama, I., Shimizu, H., Nozawa, M., Ikeo, K., and Gojobori, T. (2016). Different Endosymbiotic Interactions in Two Hydra Species Reflect the Evolutionary History of Endosymbiosis. *Genome Biol Evol* 8, 2155–2163.
- Jaenike, J., Unckless, R., Cockburn, S.N., Boelio, L.M., and Perlman, S.J. (2010). Adaptation via Symbiosis: Recent Spread of a *Drosophila* Defensive Symbiont. *Science* 329, 212–215.
- Jeon, K.W. (1987). Change of Cellular “Pathogens” into Required Cell Components. *Annals of the New York Academy of Sciences* 503, 359–371.
- Jessup, C.M., Kassen, R., Forde, S.E., Kerr, B., Buckling, A., Rainey, P.B., and Bohannan, B.J.M. (2004). Big questions, small worlds: microbial model systems in ecology. *Trends in Ecology & Evolution* 19, 189–197.
- Jiggins, F.M., and Hurst, G.D.D. (2011). Rapid Insect Evolution by Symbiont Transfer. *Science* 332, 185–186.
- Johnson, M.D. (2011). The acquisition of phototrophy: adaptive strategies of hosting endosymbionts and organelles. *Photosynth Res* 107, 117–132.
- Johnstone, R.A., and Bshary, R. (2002). From parasitism to mutualism: partner control in asymmetric interactions. *Ecology Letters* 5, 634–639.
- Joy, J.B. (2013). Symbiosis catalyses niche expansion and diversification. *Proceedings of the Royal Society B: Biological Sciences* 280, 20122820.
- Kadono, T., Kawano, T., Hosoya, H., and Kosaka, T. (2004). Flow cytometric studies of the host-regulated cell cycle in algae symbiotic with green paramecium. *Protoplasma* 223, 133–141.
- Kaeber, A., Lingner, T., Feussner, K., Göbel, C., Feussner, I., and Meinicke, P. (2009). MarVis: a tool for clustering and visualization of metabolic biomarkers. *BMC Bioinformatics* 10, 92.
- Kaltenpoth, M., Roeser-Mueller, K., Koehler, S., Peterson, A., Nechitaylo, T.Y., Stubblefield, J.W., Herzner, G., Seger, J., and Strohm, E. (2014). Partner choice and fidelity stabilize coevolution in a Cretaceous-age defensive symbiosis. *PNAS* 111, 6359–6364.

Kamako, S.-I., and Imamura, N. (2006). Effect of Japanese *Paramecium bursaria* Extract on Photosynthetic Carbon Fixation of Symbiotic Algae. *Journal of Eukaryotic Microbiology* 53, 136–141.

Kamako, S., Hoshina, R., Ueno, S., and Imamura, N. (2005). Establishment of axenic endosymbiotic strains of Japanese *Paramecium bursaria* and the utilization of carbohydrate and nitrogen compounds by the isolated algae. *European Journal of Protistology* 41, 193–202.

Kanehisa, M., and Goto, S. (2000). KEGG: kyoto encyclopedia of genes and genomes. *Nucleic Acids Res.* 28, 27–30.

Kanehisa, M., Sato, Y., Furumichi, M., Morishima, K., and Tanabe, M. (2019). New approach for understanding genome variations in KEGG. *Nucleic Acids Res.* 47, D590–D595.

Karakashian, S.J. (1963). Growth of *Paramecium bursaria* as Influenced by the Presence of Algal Symbionts. *Physiological Zoology* 36, 52–68.

Karkar, S., Facchinelli, F., Price, D.C., Weber, A.P.M., and Bhattacharya, D. (2015). Metabolic connectivity as a driver of host and endosymbiont integration. *PNAS* 112, 10208–10215.

Karnkowska, A., Vacek, V., Zubáčová, Z., Treitli, S.C., Petrželková, R., Eme, L., Novák, L., Žárský, V., Barlow, L.D., Herman, E.K., et al. (2016). A Eukaryote without a Mitochondrial Organelle. *Current Biology* 26, 1274–1284.

Kato, Y., and Imamura, N. (2008a). Effect of calcium ion on uptake of amino acids by symbiotic *Chlorella* F36-ZK isolated from Japanese *Paramecium bursaria*. *Plant Science* 174, 88–96.

Kato, Y., and Imamura, N. (2008b). Effect of sugars on amino acid transport by symbiotic *Chlorella*. *Plant Physiol. Biochem.* 46, 911–917.

Kato, Y., Ueno, S., and Imamura, N. (2006). Studies on the nitrogen utilization of endosymbiotic algae isolated from Japanese *Paramecium bursaria*. *Plant Science* 170, 481–486.

Kawano, T., Kadono, T., Kosaka, T., and Hosoya, H. (2004). Green *Paramecia* as an Evolutionary Winner of Oxidative Symbiosis: A Hypothesis and Supportive Data. *Zeitschrift Für Naturforschung C* 59, 538–542.

Keeling, P.J. (2010). The endosymbiotic origin, diversification and fate of plastids. *Philosophical Transactions of the Royal Society B: Biological Sciences* 365, 729–748.

Keeling, P.J. (2013). The number, speed, and impact of plastid endosymbioses in eukaryotic evolution. *Annu Rev Plant Biol* 64, 583–607.

Keeling, P.J., and Archibald, J.M. (2008). Organelle Evolution: What's in a Name? *Current Biology* 18, R345–R347.

- Keeling, P.J., and McCutcheon, J.P. (2017). Endosymbiosis: The feeling is not mutual. *J. Theor. Biol.* *434*, 75–79.
- Kessler, E., and Huss, V. a. R. (1990). Biochemical Taxonomy of Symbiotic *Chlorella* Strains from *Paramecium* and *Acanthocystis*\*. *Botanica Acta* *103*, 140–142.
- Kiers, E.T., and West, S.A. (2015). Evolving new organisms via symbiosis. *Science* *348*, 392–394.
- Kiers, E.T., Rousseau, R.A., West, S.A., and Denison, R.F. (2003). Host sanctions and the legume–rhizobium mutualism. *Nature* *425*, 78–81.
- Kikuchi, Y., Tada, A., Musolin, D.L., Hari, N., Hosokawa, T., Fujisaki, K., and Fukatsu, T. (2016). Collapse of Insect Gut Symbiosis under Simulated Climate Change. *MBio* *7*, e01578-16.
- King, K.C., Brockhurst, M.A., Vasieva, O., Paterson, S., Betts, A., Ford, S.A., Frost, C.L., Horsburgh, M.J., Haldenby, S., and Hurst, G.D. (2016). Rapid evolution of microbe-mediated protection against pathogens in a worm host. *The ISME Journal* *10*, 1915–1924.
- Kiseleva, A.A., Tarachovskaya, E.R., and Shishova, M.F. (2012). Biosynthesis of phytohormones in algae. *Russ J Plant Physiol* *59*, 595–610.
- Klyachko-Gurvich, G.L., Tsoglin, L.N., Doucha, J., Kopetskii, J., Shebalina (ryabykh), I.B., and Semenenko, V.E. (1999). Desaturation of fatty acids as an adaptive response to shifts in light intensity. *Physiologia Plantarum* *107*, 240–249.
- Knight, R., Ley, R.E., Raes, J., and Grice, E.A. (2019). Expanding the scope and scale of microbiome research. *Genome Biology* *20*, 191.
- Koch, A.M., Antunes, P.M., Maherali, H., Hart, M.M., and Klironomos, J.N. (2017). Evolutionary asymmetry in the arbuscular mycorrhizal symbiosis: conservatism in fungal morphology does not predict host plant growth. *New Phytologist* *214*, 1330–1337.
- Kodama, Y., and Fujishima, M. (2008). Cycloheximide Induces Synchronous Swelling of Perialgal Vacuoles Enclosing Symbiotic *Chlorella vulgaris* and Digestion of the Algae in the Ciliate *Paramecium bursaria*. *Protist* *159*, 483–494.
- Kodama, Y., and Fujishima, M. (2011). Four important cytological events needed to establish endosymbiosis of symbiotic *Chlorella* sp. to the alga-free *Paramecium bursaria*. *Jpn. J. Protozool.* Vol *44*, 1.
- Kodama, Y., and Fujishima, M. (2012). Cell division and density of symbiotic *Chlorella variabilis* of the ciliate *Paramecium bursaria* is controlled by the host's nutritional conditions during early infection process. *Environmental Microbiology* *14*, 2800–2811.
- Kodama, Y., and Fujishima, M. (2014). Symbiotic *Chlorella variabilis* incubated under constant dark conditions for 24 hours loses the ability to avoid digestion by host lysosomal enzymes in digestive vacuoles of host ciliate *Paramecium bursaria*. *FEMS Microbiol Ecol* *90*, 946–955.

- Kodama, Y., Suzuki, H., Dohra, H., Sugii, M., Kitazume, T., Yamaguchi, K., Shigenobu, S., and Fujishima, M. (2014). Comparison of gene expression of *Paramecium bursaria* with and without *Chlorella variabilis* symbionts. *BMC Genomics* *15*, 183.
- Kodama, Y., Nagase, M., and Takahama, A. (2016). Symbiotic *Chlorella variabilis* strain, 1 N, can influence the digestive process in the host *Paramecium bursaria* during early infection. *Symbiosis* 1–9.
- Koga, R., and Moran, N.A. (2014). Swapping symbionts in spittlebugs: evolutionary replacement of a reduced genome symbiont. *The ISME Journal* *8*, 1237–1246.
- Koga, R., Tsuchida, T., Sakurai, M., and Fukatsu, T. (2007). Selective elimination of aphid endosymbionts: effects of antibiotic dose and host genotype, and fitness consequences. *FEMS Microbiol Ecol* *60*, 229–239.
- Kondo, N., Shimada, M., and Fukatsu, T. (2005). Infection density of *Wolbachia* endosymbiont affected by co-infection and host genotype. *Biology Letters* *1*, 488–491.
- Kour, D., Rana, K.L., Yadav, N., Yadav, A.N., Kumar, A., Meena, V.S., Singh, B., Chauhan, V.S., Dhaliwal, H.S., and Saxena, A.K. (2019). Rhizospheric Microbiomes: Biodiversity, Mechanisms of Plant Growth Promotion, and Biotechnological Applications for Sustainable Agriculture. In *Plant Growth Promoting Rhizobacteria for Agricultural Sustainability : From Theory to Practices*, A. Kumar, and V.S. Meena, eds. (Singapore: Springer Singapore), pp. 19–65.
- Kreutz, M., Stoeck, T., and Foissner, W. (2012). Morphological and Molecular Characterization of *Paramecium* (*Viridoparamecium* nov. subgen.) *chlorelligerum* Kahl (Ciliophora). *Journal of Eukaryotic Microbiology* *59*, 548–563.
- Kropp, B.R., and Trappe, J.M. (1982). Ectomycorrhizal Fungi of *Tsuga heterophylla*. *Mycologia* *74*, 479–488.
- Lane, C.E., and Archibald, J.M. (2008). The eukaryotic tree of life: endosymbiosis takes its TOL. *Trends in Ecology & Evolution* *23*, 268–275.
- Lanzoni, O., Fokin, S.I., Lebedeva, N., Migunova, A., Petroni, G., and Potekhin, A. (2016). Rare Freshwater Ciliate *Paramecium chlorelligerum* Kahl, 1935 and Its Macronuclear Symbiotic Bacterium “*Candidatus Holospora parva*.” *PLOS ONE* *11*, e0167928.
- Larkum, A.W.D., Lockhart, P.J., and Howe, C.J. (2007). Shopping for plastids. *Trends in Plant Science* *12*, 189–195.
- Law, R., and Dieckmann, U. (1998). Symbiosis through exploitation and the merger of lineages in evolution. *Proceedings of the Royal Society of London B: Biological Sciences* *265*, 1245–1253.
- Lefèvre, C., Charles, H., Vallier, A., Delobel, B., Farrell, B., and Heddi, A. (2004). Endosymbiont Phylogenesis in the Dryophthoridae Weevils: Evidence for Bacterial Replacement. *Mol Biol Evol* *21*, 965–973.

- Lesser, M.P. (2006). OXIDATIVE STRESS IN MARINE ENVIRONMENTS: Biochemistry and Physiological Ecology. *Annual Review of Physiology* 68, 253–278.
- Lesser, M.P. (2011). Coral Bleaching: Causes and Mechanisms. In *Coral Reefs: An Ecosystem in Transition*, Z. Dubinsky, and N. Stambler, eds. (Dordrecht: Springer Netherlands), pp. 405–419.
- Lewis, N.E., Hixson, K.K., Conrad, T.M., Lerman, J.A., Charusanti, P., Polpitiya, A.D., Adkins, J.N., Schramm, G., Purvine, S.O., Lopez-Ferrer, D., et al. (2010). Omic data from evolved *E. coli* are consistent with computed optimal growth from genome-scale models. *Molecular Systems Biology* 6, 390.
- Lohse, K., Gutierrez, A., Kaltz, O., and Koella, J. (2006). Experimental evolution of resistance in *paramecium caudatum* against the bacterial parasite *holospora undulata*. *Evolution* 60, 1177–1186.
- López-García, P., Eme, L., and Moreira, D. (2017). Symbiosis in eukaryotic evolution. *Journal of Theoretical Biology* 434, 20–33.
- Lowe, C.D., Minter, E.J., Cameron, D.D., and Brockhurst, M.A. (2016). Shining a Light on Exploitative Host Control in a Photosynthetic Endosymbiosis. *Current Biology* 26, 207–211.
- Loya, Y., Sakai, K., Yamazato, K., Nakano, Y., Sambali, H., and Woesik, R. van (2001). Coral bleaching: the winners and the losers. *Ecology Letters* 4, 122–131.
- Lu, Y., Tarkowská, D., Turečková, V., Luo, T., Xin, Y., Li, J., Wang, Q., Jiao, N., Strnad, M., and Xu, J. (2014). Antagonistic roles of abscisic acid and cytokinin during response to nitrogen depletion in oleaginous microalga *Nannochloropsis oceanica* expand the evolutionary breadth of phytohormone function. *The Plant Journal* 80, 52–68.
- Maharjan, R.P., Seeto, S., and Ferenci, T. (2007). Divergence and Redundancy of Transport and Metabolic Rate-Yield Strategies in a Single *Escherichia coli* Population. *Journal of Bacteriology* 189, 2350–2358.
- Mallick, N. (2004). Copper-induced oxidative stress in the chlorophycean microalga *Chlorella vulgaris*: response of the antioxidant system. *Journal of Plant Physiology* 161, 591–597.
- Manoharan, K., Lee, T.K., Cha, J.M., Kim, J.H., Lee, W.S., Chang, M., Park, C.W., and Cho, J.H. (1999). Acclimation of *Prorocentrum Minimum* (dinophyceae) to Prolonged Darkness by Use of an Alternative Carbon Source from Triacylglycerides and Galactolipids. *Journal of Phycology* 35, 287–292.
- Marin, B., M. Nowack, E.C., and Melkonian, M. (2005). A Plastid in the Making: Evidence for a Second Primary Endosymbiosis. *Protist* 156, 425–432.
- Martin, W.F., Garg, S., and Zimorski, V. (2015). Endosymbiotic theories for eukaryote origin. *Philosophical Transactions of the Royal Society B: Biological Sciences* 370, 20140330.

- Masson-Boivin, C., Giraud, E., Perret, X., and Batut, J. (2009). Establishing nitrogen-fixing symbiosis with legumes: how many rhizobium recipes? *Trends in Microbiology* *17*, 458–466.
- Matsuura, Y., Moriyama, M., Łukasik, P., Vanderpool, D., Tanahashi, M., Meng, X.-Y., McCutcheon, J.P., and Fukatsu, T. (2018). Recurrent symbiont recruitment from fungal parasites in cicadas. *PNAS* *115*, E5970–E5979.
- Matthews, J.L., Oakley, C.A., Lutz, A., Hillyer, K.E., Roessner, U., Grossman, A.R., Weis, V.M., and Davy, S.K. (2018). Partner switching and metabolic flux in a model cnidarian–dinoflagellate symbiosis. *Proceedings of the Royal Society B: Biological Sciences* *285*, 20182336.
- Maxwell, K., and Johnson, G.N. (2000). Chlorophyll fluorescence—a practical guide. *J Exp Bot* *51*, 659–668.
- McCutcheon, J.P., and Moran, N.A. (2012). Extreme genome reduction in symbiotic bacteria. *Nature Reviews Microbiology* *10*, 13–26.
- McCutcheon, J.P., McDonald, B.R., and Moran, N.A. (2009). Origin of an Alternative Genetic Code in the Extremely Small and GC–Rich Genome of a Bacterial Symbiont. *PLOS Genetics* *5*, e1000565.
- McFall-Ngai, M.J., and Ruby, E.G. (1991). Symbiont recognition and subsequent morphogenesis as early events in an animal-bacterial mutualism. *Science* *254*, 1491–1494.
- McFall-Ngai, M.J., and Ruby, E.G. (1998). Sepiolid and Vibrios: When First They Meet. *BioScience* *48*, 257–265.
- McGraw, E.A., Merritt, D.J., Droller, J.N., and O’Neill, S.L. (2002). *Wolbachia* density and virulence attenuation after transfer into a novel host. *PNAS* *99*, 2918–2923.
- McKew, B.A., Davey, P., Finch, S.J., Hopkins, J., Lefebvre, S.C., Metodiev, M.V., Oxborough, K., Raines, C.A., Lawson, T., and Geider, R.J. (2013). The trade-off between the light-harvesting and photoprotective functions of fucoxanthin-chlorophyll proteins dominates light acclimation in *Emiliana huxleyi* (clone CCMP 1516). *New Phytologist* *200*, 74–85.
- Mereschkowsky, C. (1905). Über Natur und Ursprung der Chromatophoren im Pflanzenreiche. *Biologisches Centralblatt* *25/18*: 38–604, ed. J. Rosenthal.
- Merzlyak, M.N., Chivkunova, O.B., Gorelova, O.A., Reshetnikova, I.V., Solovchenko, A.E., Khozin-Goldberg, I., and Cohen, Z. (2007). Effect of Nitrogen Starvation on Optical Properties, Pigments, and Arachidonic Acid Content of the Unicellular Green Alga *Parietochloris incisa* (trebouxiophyceae, Chlorophyta)1. *Journal of Phycology* *43*, 833–843.
- Mews, L.K. (1980). The green hydra symbiosis. III. The biotrophic transport of carbohydrate from alga to animal. *Proceedings of the Royal Society of London. Series B. Biological Sciences* *209*, 377–401.

- Minaeva, E., and Ermilova, E. (2017). Responses triggered in chloroplast of *Chlorella variabilis* NC64A by long-term association with *Paramecium bursaria*. *Protoplasma* 254, 1769–1776.
- Minter, E.J.A., Lowe, C.D., Sørensen, M.E.S., Wood, A.J., Cameron, D.D., and Brockhurst, M.A. (2018). Variation and asymmetry in host-symbiont dependence in a microbial symbiosis. *BMC Evolutionary Biology* 18, 108.
- Miwa, I., Fujimori, N., and Tanaka, M. (1996). Effects of symbiotic *Chlorella* on the period length and the phase shift of circadian rhythms in *Paramecium bursaria*. *European Journal of Protistology* 32, 102–107.
- Molero, G., Aranjuelo, I., Teixidor, P., Araus, J.L., and Nogués, S. (2011). Measurement of <sup>13</sup>C and <sup>15</sup>N isotope labeling by gas chromatography/combustion/isotope ratio mass spectrometry to study amino acid fluxes in a plant–microbe symbiotic association. *Rapid Communications in Mass Spectrometry* 25, 599–607.
- Molina, R., and Trappe, J.M. (1982). Patterns of Ectomycorrhizal Host Specificity and Potential among Pacific Northwest Conifers and Fungi. *For Sci* 28, 423–458.
- Monika, Devi, S., Arya, S.S., Kumar, N., and Kumar, S. (2019). Mycorrhizal Fungi: Potential Candidate for Sustainable Agriculture. In *Mycorrhizosphere and Pedogenesis*, A. Varma, and D.K. Choudhary, eds. (Singapore: Springer Singapore), pp. 339–353.
- Moran, N.A. (2007). Symbiosis as an adaptive process and source of phenotypic complexity. *PNAS* 104, 8627–8633.
- Moran, N.A., and Wernegreen, J.J. (2000). Lifestyle evolution in symbiotic bacteria: insights from genomics. *Trends in Ecology & Evolution* 15, 321–326.
- Moran, N.A., Plague, G.R., Sandström, J.P., and Wilcox, J.L. (2003). A genomic perspective on nutrient provisioning by bacterial symbionts of insects. *PNAS* 100, 14543–14548.
- Muggia, L., Nelson, P., Wheeler, T., Yakovchenko, L.S., Tønsberg, T., and Spribille, T. (2011). Convergent evolution of a symbiotic duet: The case of the lichen genus *Polychidium* (Peltigerales, Ascomycota). *American Journal of Botany* 98, 1647–1656.
- Munkacsi, A.B., Pan J. J., Villesen P., Mueller U. G., Blackwell M., and McLaughlin D. J. (2004). Convergent coevolution in the domestication of coral mushrooms by fungus–growing ants. *Proceedings of the Royal Society of London. Series B: Biological Sciences* 271, 1777–1782.
- Murata, N., Takahashi, S., Nishiyama, Y., and Allakhverdiev, S.I. (2007). Photoinhibition of photosystem II under environmental stress. *Biochimica et Biophysica Acta (BBA) - Bioenergetics* 1767, 414–421.
- Muscattine, L., and Porter, J.W. (1977). Reef Corals: Mutualistic Symbioses Adapted to Nutrient-Poor Environments. *BioScience* 27, 454–460.

- Nakajima, T., Sano, A., and Matsuoka, H. (2009). Auto-/heterotrophic endosymbiosis evolves in a mature stage of ecosystem development in a microcosm composed of an alga, a bacterium and a ciliate. *Biosystems* 96, 127–135.
- Nakajima, T., Fujikawa, Y., Matsubara, T., Karita, M., and Sano, A. (2015). Differentiation of a free-living alga into forms with ecto- and endosymbiotic associations with heterotrophic organisms in a 5-year microcosm culture. *Biosystems* 131, 9–21.
- Nakayama, S., Parratt, S.R., Hutchence, K.J., Lewis, Z., Price, T. a. R., and Hurst, G.D.D. (2015). Can maternally inherited endosymbionts adapt to a novel host? Direct costs of *Spiroplasma* infection, but not vertical transmission efficiency, evolve rapidly after horizontal transfer into *D. melanogaster*. *Heredity* 114, 539–543.
- Neill, S., Desikan, R., and Hancock, J. (2002). Hydrogen peroxide signalling. *Current Opinion in Plant Biology* 5, 388–395.
- Nobre, T. (2019). Symbiosis in Sustainable Agriculture: Can Olive Fruit Fly Bacterial Microbiome Be Useful in Pest Management? *Microorganisms* 7, 238.
- Nowack, E.C. (2014). Paulinella chromatophora - rethinking the transition from endosymbiont to organelle. *Acta Societatis Botanicorum Poloniae* 83.
- Nowack, E.C., and Melkonian, M. (2010). Endosymbiotic associations within protists. *Philosophical Transactions of the Royal Society B: Biological Sciences* 365, 699–712.
- Nowack, E.C.M., Melkonian, M., and Glöckner, G. (2008). Chromatophore Genome Sequence of Paulinella Sheds Light on Acquisition of Photosynthesis by Eukaryotes. *Current Biology* 18, 410–418.
- Nussbaumer, A.D., Fisher, C.R., and Bright, M. (2006). Horizontal endosymbiont transmission in hydrothermal vent tubeworms. *Nature* 441, 345–348.
- Ohkawa, H., Hashimoto, N., Furukawa, S., Kadono, T., and Kawano, T. (2011). Forced symbiosis between *Synechocystis* spp. PCC 6803 and apo-symbiotic *Paramecium bursaria* as an experimental model for evolutionary emergence of primitive photosynthetic eukaryotes. *Plant Signaling & Behavior* 6, 773–776.
- O’Neill, S.L. (2018). The Use of Wolbachia by the World Mosquito Program to Interrupt Transmission of *Aedes aegypti* Transmitted Viruses. *Adv. Exp. Med. Biol.* 1062, 355–360.
- van Oppen, M.J.H., Oliver, J.K., Putnam, H.M., and Gates, R.D. (2015). Building coral reef resilience through assisted evolution. *PNAS* 112, 2307–2313.
- van Oppen, M.J.H., Gates, R.D., Blackall, L.L., Cantin, N., Chakravarti, L.J., Chan, W.Y., Cormick, C., Crean, A., Damjanovic, K., Epstein, H., et al. (2017). Shifting paradigms in restoration of the world’s coral reefs. *Global Change Biology* 23, 3437–3448.
- Ortmayr, K., Causon, T.J., Hann, S., and Koellensperger, G. (2016). Increasing selectivity and coverage in LC-MS based metabolome analysis. *TrAC Trends in Analytical Chemistry* 82, 358–366.

- Overy, S.A., Walker, H.J., Malone, S., Howard, T.P., Baxter, C.J., Sweetlove, L.J., Hill, S.A., and Quick, W.P. (2005). Application of metabolite profiling to the identification of traits in a population of tomato introgression lines. *J Exp Bot* 56, 287–296.
- Oxborough, K., Moore, C.M., Suggett, D.J., Lawson, T., Chan, H.G., and Geider, R.J. (2012). Direct estimation of functional PSII reaction center concentration and PSII electron flux on a volume basis: a new approach to the analysis of Fast Repetition Rate fluorometry (FRRf) data. *Limnology and Oceanography: Methods* 10, 142–154.
- Padfield, D., Yvon-Durocher, G., Buckling, A., Jennings, S., and Yvon-Durocher, G. (2016). Rapid evolution of metabolic traits explains thermal adaptation in phytoplankton. *Ecology Letters* 19, 133–142.
- Parfrey, L.W., Lahr, D.J.G., Knoll, A.H., and Katz, L.A. (2011). Estimating the timing of early eukaryotic diversification with multigene molecular clocks. *PNAS* 108, 13624–13629.
- Patron, N.J., Waller, R.F., and Keeling, P.J. (2006). A tertiary plastid uses genes from two endosymbionts. *J. Mol. Biol.* 357, 1373–1382.
- Perez, S., and Weis, V. (2006). Nitric oxide and cnidarian bleaching: an eviction notice mediates breakdown of a symbiosis. *Journal of Experimental Biology* 209, 2804–2810.
- Peters, E. (1996). Prolonged darkness and diatom mortality: II. Marine temperate species. *Journal of Experimental Marine Biology and Ecology* 207, 43–58.
- Pfeiffer, T., Schuster, S., and Bonhoeffer, S. (2001). Cooperation and Competition in the Evolution of ATP-Producing Pathways. *Science* 292, 504–507.
- Pinheiro, J., Bates, D., DebRoy, S., Sarkar, D., and R core Team (2019) (2019). nlme: Linear and Nonlinear Mixed Effects Models.
- Poretsky, R., Rodriguez-R, L.M., Luo, C., Tsementzi, D., and Konstantinidis, K.T. (2014). Strengths and Limitations of 16S rRNA Gene Amplicon Sequencing in Revealing Temporal Microbial Community Dynamics. *PLOS ONE* 9, e93827.
- Powell, J.R., and Rillig, M.C. (2018). Biodiversity of arbuscular mycorrhizal fungi and ecosystem function. *New Phytol.*
- Preer, J.R. (2000). Epigenetic Mechanisms Affecting Macronuclear Development in Paramecium and Tetrahymena. *Journal of Eukaryotic Microbiology* 47, 515–524.
- Quispe, C.F., Sonderman, O., Khasin, M., Riekhof, W.R., Van Etten, J.L., and Nickerson, K.W. (2016). Comparative genomics, transcriptomics, and physiology distinguish symbiotic from free-living *Chlorella* strains. *Algal Research* 18, 332–340.
- R Core Team (2018). R: A Language and Environment for Statistical Computing.
- Raina, J.-B., Eme, L., Pollock, F.J., Spang, A., Archibald, J.M., and Williams, T.A. (2018). Symbiosis in the microbial world: from ecology to genome evolution. *Biology Open* 7, bio032524.

Ral, J.-P., Colleoni, C., Wattebled, F., Dauvillée, D., Nempont, C., Deschamps, P., Li, Z., Morell, M.K., Chibbar, R., Purton, S., et al. (2006). Circadian Clock Regulation of Starch Metabolism Establishes GBSSI as a Major Contributor to Amylopectin Synthesis in *Chlamydomonas reinhardtii*. *Plant Physiology* *142*, 305–317.

Ramsey, J.S., MacDonald, S.J., Jander, G., Nakabachi, A., Thomas, G.H., and Douglas, A.E. (2010). Genomic evidence for complementary purine metabolism in the pea aphid, *Acyrtosiphon pisum*, and its symbiotic bacterium *Buchnera aphidicola*. *Insect Molecular Biology* *19*, 241–248.

Rankin, D.J., Bargum, K., and Kokko, H. (2007). The tragedy of the commons in evolutionary biology. *Trends in Ecology & Evolution* *22*, 643–651.

Ratcliffe, R.G., and Shachar-Hill, Y. (2006). Measuring multiple fluxes through plant metabolic networks. *The Plant Journal* *45*, 490–511.

Rees, T.A., and Hill, S.A. (1994). Metabolic control analysis of plant metabolism. *Plant, Cell & Environment* *17*, 587–599.

Reisser, W. (1976). [The metabolic interactions between *Paramecium bursaria* Ehrbg. and *Chlorella spec.* in the *Paramecium bursaria*-symbiosis. II. Symbiosis-specific properties of the physiology and the cytology of the symbiotic unit and their regulation (author's transl)]. *Arch Microbiol* *111*, 161–170.

Reisser, W., Burbank, D., Meints, R., Becker, B., and Vanetten, J. (1991). Viruses Distinguish Symbiotic *Chlorella Spp* of *Paramecium-Bursaria*. *Endocytobiosis Cell Res.* *7*, 245–251.

Reyes-Prieto, A., Moustafa, A., and Bhattacharya, D. (2008). Multiple Genes of Apparent Algal Origin Suggest Ciliates May Once Have Been Photosynthetic. *Current Biology* *18*, 956–962.

Rigano, C., Di Martino Rigano, V., Vona, V., and Fuggi, A. (1981). Nitrate reductase and glutamine synthetase activities, nitrate and ammonia assimilation, in the unicellular alga *Cyanidium caldarium*. *Arch. Microbiol.* *129*, 110–114.

Rivera, M.C., and Lake, J.A. (2004). The ring of life provides evidence for a genome fusion origin of eukaryotes. *Nature* *431*, 152–155.

Rocap, G., Larimer, F.W., Lamerdin, J., Malfatti, S., Chain, P., Ahlgren, N.A., Arellano, A., Coleman, M., Hauser, L., Hess, W.R., et al. (2003). Genome divergence in two *Prochlorococcus* ecotypes reflects oceanic niche differentiation. *Nature* *424*, 1042–1047.

Rodríguez, F., Derelle, E., Guillou, L., Gall, F.L., Vaulot, D., and Moreau, H. (2005). Ecotype diversity in the marine picoeukaryote *Ostreococcus* (Chlorophyta, Prasinophyceae). *Environmental Microbiology* *7*, 853–859.

Rodriguez-Garcia, I., and Guil-Guerrero, J.L. (2008). Evaluation of the antioxidant activity of three microalgal species for use as dietary supplements and in the preservation of foods. *Food Chemistry* *108*, 1023–1026.

- Rolshausen, G., Grande, F.D., Sadowska-Deś, A.D., Otte, J., and Schmitt, I. (2018). Quantifying the climatic niche of symbiont partners in a lichen symbiosis indicates mutualist-mediated niche expansions. *Ecography* *41*, 1380–1392.
- Rowan, R. (2004). Thermal adaptation in reef coral symbionts. *Nature* *430*, 742–742.
- Russell, J.A., and Moran, N.A. (2005). Horizontal Transfer of Bacterial Symbionts: Heritability and Fitness Effects in a Novel Aphid Host. *Appl. Environ. Microbiol.* *71*, 7987–7994.
- Sabater-Muñoz, B., Toft, C., Alvarez-Ponce, D., and Fares, M.A. (2017). Chance and necessity in the genome evolution of endosymbiotic bacteria of insects. *ISME J.*
- Sachs, J.L., and Simms, E.L. (2006). Pathways to mutualism breakdown. *Trends in Ecology & Evolution* *21*, 585–592.
- Sachs, J.L., and Wilcox, T.P. (2006). A shift to parasitism in the jellyfish symbiont *Symbiodinium microadriaticum*. *Proceedings of the Royal Society B: Biological Sciences* *273*, 425–429.
- Sachs, J.L., Mueller, U.G., Wilcox, T.P., and Bull, J.J. (2004). The Evolution of Cooperation. *The Quarterly Review of Biology* *79*, 135–160.
- Sachs, J.L., Skophammer, R.G., and Regus, J.U. (2011). Evolutionary transitions in bacterial symbiosis. *PNAS* *108*, 10800–10807.
- Safi, C., Zebib, B., Merah, O., Pontalier, P.-Y., and Vaca-Garcia, C. (2014). Morphology, composition, production, processing and applications of *Chlorella vulgaris*: A review. *Renewable and Sustainable Energy Reviews* *35*, 265–278.
- Sagan, L. (1967). On the origin of mitosing cells. *J. Theor. Biol.* *14*, 255–274.
- Salvaudon, L., Héraudet, V., Shykoff, J.A., and Koella, J. (2005). Parasite-host fitness trade-offs change with parasite identity: genotype-specific interactions in a plant-pathogen system. *Evolution* *59*, 2518–2524.
- Sandström, J.P., Russell, J.A., White, J.P., and Moran, N.A. (2001). Independent origins and horizontal transfer of bacterial symbionts of aphids. *Molecular Ecology* *10*, 217–228.
- Schatz, G., and Mason, T.L. (1974). The Biosynthesis of Mitochondrial Proteins. *Annual Review of Biochemistry* *43*, 51–87.
- Schneider, C.A., Rasband, W.S., and Eliceiri, K.W. (2012). NIH Image to ImageJ: 25 years of image analysis.
- Schüßler, A., and Schnepf, E. (1992). Photosynthesis dependent acidification of perialgal vacuoles in the *Paramecium bursaria/Chlorella* symbiosis: Visualization by monensin. *Protoplasma* *166*, 218–222.
- Schwarz, Zs., and Kössel, H. (1980). The primary structure of 16S rDNA from *Zea mays* chloroplast is homologous to *E. coli* 16S rRNA. *Nature* *283*, 739–742.

- Shah, N., and Syrett, P.J. (1984). The uptake of guanine and hypoxanthine by marine microalgae. *Journal of the Marine Biological Association of the United Kingdom* *64*, 545–556.
- Shapiro, J.W., and Turner, P.E. (2018). Evolution of mutualism from parasitism in experimental virus populations. *Evolution* *72*, 707–712.
- Shibata, A., Takahashi, F., Kasahara, M., and Imamura, N. (2016). Induction of Maltose Release by Light in the Endosymbiont *Chlorella variabilis* of *Paramecium bursaria*. *Protist*.
- Shih, J.L., Selph, K.E., Wall, C.B., Wallsgrove, N.J., Lesser, M.P., and Popp, B.N. (2019). Trophic Ecology of the Tropical Pacific Sponge *Mycale grandis* Inferred from Amino Acid Compound-Specific Isotopic Analyses. *Microb Ecol*.
- Shiu, C.-T., and Lee, T.-M. (2005). Ultraviolet-B-induced oxidative stress and responses of the ascorbate–glutathione cycle in a marine macroalga *Ulva fasciata*. *J Exp Bot* *56*, 2851–2865.
- Siegel, R.W. (1960). Hereditary endosymbiosis in *Paramecium bursaria*. *Experimental Cell Research* *19*, 239–252.
- Silverstein, R.N., Correa, A.M.S., and Baker, A.C. (2012). Specificity is rarely absolute in coral–algal symbiosis: implications for coral response to climate change. *Proceedings of the Royal Society B: Biological Sciences* *279*, 2609–2618.
- Singh, D.P., Saudemont, B., Guglielmi, G., Arnaiz, O., Goût, J.-F., Prajer, M., Potekhin, A., Przybòs, E., Aubusson-Fleury, A., Bhullar, S., et al. (2014). Genome-defence small RNAs exapted for epigenetic mating-type inheritance. *Nature* *509*, 447–452.
- Smith, G.J., and Muscatine, L. (1999). Cell cycle of symbiotic dinoflagellates: variation in G1 phase-duration with anemone nutritional status and macronutrient supply in the *Aiptasia pulchella*–*Symbiodinium pulchrorum* symbiosis. *Marine Biology* *134*, 405–418.
- Smith, C.A., O’Maille, G., Want, E.J., Qin, C., Trauger, S.A., Brandon, T.R., Custodio, D.E., Abagyan, R., and Siuzdak, G. (2005). METLIN: a metabolite mass spectral database. *Ther Drug Monit* *27*, 747–751.
- Smith, C.A., Want, E.J., O’Maille, G., Abagyan, R., and Siuzdak, G. (2006). XCMS: Processing Mass Spectrometry Data for Metabolite Profiling Using Nonlinear Peak Alignment, Matching, and Identification. *Anal. Chem.* *78*, 779–787.
- Soldo, A.T., Godoy, G.A., and Larin, F. (1978). Purine-Excretory Nature of Refractile Bodies in the Marine Ciliate *Paraurena acutum*\*. *The Journal of Protozoology* *25*, 416–418.
- Sørensen, M.E., Wood, A.J., Minter, E.J., Lowe, C.D., Cameron, D.D., and Brockhurst, M.A. (2020). Comparison of independent evolutionary origins reveals both convergence and divergence in the metabolic mechanisms of symbiosis. *Current Biology*.

- Sørensen, M.E.S., Lowe, C.D., Minter, E.J.A., Wood, A.J., Cameron, D.D., and Brockhurst, M.A. (2019). The role of exploitation in the establishment of mutualistic microbial symbioses. *FEMS Microbiol Lett* 366.
- Spang, A., Saw, J.H., Jørgensen, S.L., Zaremba-Niedzwiedzka, K., Martijn, J., Lind, A.E., van Eijk, R., Schleper, C., Guy, L., and Ettema, T.J.G. (2015). Complex archaea that bridge the gap between prokaryotes and eukaryotes. *Nature* 521, 173–179.
- Sprent, J.I., Sutherland, J.M., and Faria, S.M.D. (1987). Some aspects of the biology of nitrogen-fixing organisms. *Phil. Trans. R. Soc. Lond. B* 317, 111–129.
- Stanier, R.Y. (1970). Some aspects of the biology of cells and their possible evolutionary significance. In *Symp Soc Gen Microbiol*, pp. 1–38.
- Stanley, G.D., and Lipps, J.H. (2011). Photosymbiosis: The Driving Force for Reef Success and Failure. *The Paleontological Society Papers* 17, 33–59.
- Stat, M., Carter, D., and Hoegh-Guldberg, O. (2006). The evolutionary history of Symbiodinium and scleractinian hosts—Symbiosis, diversity, and the effect of climate change. *Perspectives in Plant Ecology, Evolution and Systematics* 8, 23–43.
- Stein, J.R. (1979). (ED.) *Handbook of Phycological Methods: Culture Methods and Growth Measurements* (Cambridge University Press).
- Stiller, J.W., Schreiber, J., Yue, J., Guo, H., Ding, Q., and Huang, J. (2014). The evolution of photosynthesis in chromist algae through serial endosymbioses. *Nature Communications* 5, 5764.
- Stoecker, D.K., Johnson, M.D., Vargas, C. de, and Not, F. (2009). Acquired phototrophy in aquatic protists. *Aquat Microb Ecol* 57, 279–310.
- Storey, J.D., and Tibshirani, R. (2003). Statistical significance for genomewide studies. *PNAS* 100, 9440–9445.
- Straub, C.S., Ives, A.R., and Gratton, C. (2011). Evidence for a Trade-Off between Host-Range Breadth and Host-Use Efficiency in Aphid Parasitoids. *The American Naturalist* 177, 389–395.
- Sudakaran, S., Kost, C., and Kaltenpoth, M. (2017). Symbiont Acquisition and Replacement as a Source of Ecological Innovation. *Trends in Microbiology* 25, 375–390.
- Sugio, A., Dubreuil, G., Giron, D., and Simon, J.-C. (2015). Plant–insect interactions under bacterial influence: ecological implications and underlying mechanisms. *J Exp Bot* 66, 467–478.
- Sully, S., Burkepille, D.E., Donovan, M.K., Hodgson, G., and Woesik, R. van (2019). A global analysis of coral bleaching over the past two decades. *Nat Commun* 10, 1–5.
- Summerer, M., Sonntag, B., and Sommaruga, R. (2007). An experimental test of the symbiosis specificity between the ciliate *Paramecium bursaria* and strains of the unicellular green alga *Chlorella*. *Environmental Microbiology* 9, 2117–2122.

- Summerer, M., Sonntag, B., and Sommaruga, R. (2008). Ciliate-Symbiont Specificity of Freshwater Endosymbiotic *Chlorella* (trebouxiophyceae, Chlorophyta)1. *Journal of Phycology* 44, 77–84.
- Summerer, M., Sonntag, B., Hörtnagl, P., and Sommaruga, R. (2009). Symbiotic Ciliates Receive Protection Against UV Damage from their Algae: A Test with *Paramecium bursaria* and *Chlorella*. *Protist* 160, 233–243.
- Szathmáry, E., and Smith, J.M. (1995). The major evolutionary transitions. *Nature* 374, 227–232.
- Takahashi, T., Shirai, Y., Kosaka, T., and Hosoya, H. (2007). Arrest of Cytoplasmic Streaming Induces Algal Proliferation in Green *Paramecia*. *PLOS ONE* 2, e1352.
- Takeda, H. (1988). Classification of *Chlorella* strains by cell wall sugar composition. *Phytochemistry* 27, 3823–3826.
- Tarakhovskaya, E.R., Maslov, Yu.I., and Shishova, M.F. (2007). Phytohormones in algae. *Russ J Plant Physiol* 54, 163–170.
- Tautenhahn, R., Böttcher, C., and Neumann, S. (2008). Highly sensitive feature detection for high resolution LC/MS. *BMC Bioinformatics* 9, 504.
- Tebo, B.M., Scott Linthicum, D., and Nealson, K.H. (1979). Luminous bacteria and light emitting fish: Ultrastructure of the symbiosis. *Biosystems* 11, 269–280.
- Thompson, G.A. (1996). Lipids and membrane function in green algae. *Biochimica et Biophysica Acta (BBA) - Lipids and Lipid Metabolism* 1302, 17–45.
- Thompson, J.N. (2005). *The Geographic Mosaic of Coevolution* (University of Chicago Press).
- Titlyanov, E., Titlyanova, T., Leletkin, V., Tsukahara, J., van Woesik, R., and Yamazato, K. (1996). Degradation of zooxanthellae and regulation of their density in hermatypic corals. *Marine Ecology Progress Series* 139, 167–178.
- Tonooka, Y., and Watanabe, T. (2002). A natural strain of *Paramecium bursaria* lacking symbiotic algae. *European Journal of Protistology* 38, 55–58.
- Touw, W.G., Bayjanov, J.R., Overmars, L., Backus, L., Boekhorst, J., Wels, M., and van Hijum, S.A.F.T. (2013). Data mining in the Life Sciences with Random Forest: a walk in the park or lost in the jungle? *Brief. Bioinformatics* 14, 315–326.
- Tremblay, P., Fine, M., Maguer, J.F., Grover, R., and Ferrier-Pagès, C. (2013). Photosynthate translocation increases in response to low seawater pH in a coral–dinoflagellate symbiosis. *Biogeosciences* 10, 3997–4007.
- Treseder, K.K. (2004). A meta-analysis of mycorrhizal responses to nitrogen, phosphorus, and atmospheric CO<sub>2</sub> in field studies. *New Phytologist* 164, 347–355.

- Tso, G.H.W., Reales-Calderon, J.A., Tan, A.S.M., Sem, X., Le, G.T.T., Tan, T.G., Lai, G.C., Srinivasan, K.G., Yurieva, M., Liao, W., et al. (2018). Experimental evolution of a fungal pathogen into a gut symbiont. *Science* *362*, 589–595.
- Tsuchida, T., Koga, R., Horikawa, M., Tsunoda, T., Maoka, T., Matsumoto, S., Simon, J.-C., and Fukatsu, T. (2010). Symbiotic Bacterium Modifies Aphid Body Color. *Science* *330*, 1102–1104.
- Venn, A.A., Loram, J.E., and Douglas, A.E. (2008). Photosynthetic symbioses in animals. *J Exp Bot* *59*, 1069–1080.
- Vigneron, A., Masson, F., Vallier, A., Balmand, S., Rey, M., Vincent-Monégat, C., Aksoy, E., Aubailly-Giraud, E., Zaidman-Rémy, A., and Heddi, A. (2014). Insects recycle endosymbionts when the benefit is over. *Curr. Biol.* *24*, 2267–2273.
- Visick, K.L., and Ruby, E.G. (2006). *Vibrio fischeri* and its host: it takes two to tango. *Current Opinion in Microbiology* *9*, 632–638.
- Walker, T.L., Purton, S., Becker, D.K., and Collet, C. (2005). Microalgae as bioreactors. *Plant Cell Rep* *24*, 629–641.
- Warnes, G.R., Bolker, B., Bonebakker, L., Gentleman, R., Huber, W., Liaw, A., Lumley, T., Maechler, M., Magnusson, A., and Moeller, S. (2009). *gplots: Various R programming tools for plotting data.* R Package Version 2, 1.
- Weis, D.S. (1978). Correlation of Infectivity and Concanavalin A Agglutinability of Algae Exsymbiotic from *Paramecium bursaria*. *The Journal of Protozoology* *25*, 366–370.
- Weis, V.M. (2008). Cellular mechanisms of Cnidarian bleaching: stress causes the collapse of symbiosis. *Journal of Experimental Biology* *211*, 3059–3066.
- Wendling, C.C., Fabritzek, A.G., and Wegner, K.M. (2017). Population-specific genotype x genotype x environment interactions in bacterial disease of early life stages of Pacific oyster larvae. *Evol Appl* *10*, 338–347.
- Wernegreen, J.J. (2012). Endosymbiosis. *Current Biology* *22*, R555–R561.
- Werner, G.D.A., Cornelissen, J.H.C., Cornwell, W.K., Soudzilovskaia, N.A., Kattge, J., West, S.A., and Kiers, E.T. (2018). Symbiont switching and alternative resource acquisition strategies drive mutualism breakdown. *PNAS* *115*, 5229–5234.
- Werren, J.H., Baldo, L., and Clark, M.E. (2008). *Wolbachia*: master manipulators of invertebrate biology. *Nature Reviews Microbiology* *6*, 741–751.
- West, S.A., Fisher, R.M., Gardner, A., and Kiers, E.T. (2015). Major evolutionary transitions in individuality. *PNAS* *112*, 10112–10119.
- Wichterman, R. (1986). *The Biology of Paramecium* (Springer US).
- Wickham, H. (2016). *ggplot2: Elegant Graphics for Data Analysis*.

- Wilkerson, F.P., Kobayashi, D., and Muscatine, L. (1988). Mitotic index and size of symbiotic algae in Caribbean Reef corals. *Coral Reefs* 7, 29–36.
- Wilkinson, H.H., and Parker, M.A. (1996). Symbiotic specialization and the potential for genotypic coexistence in a plant-bacterial mutualism. *Oecologia* 108, 361–367.
- Wilkinson, T.L., and Ishikawa, H. (2000). Injection of essential amino acids substitutes for bacterial supply in aposymbiotic pea aphids (*Acyrtosiphon pisum*). *Entomologia Experimentalis et Applicata* 94, 85–91.
- Wilson, D.S., and Yoshimura, J. (1994). On the Coexistence of Specialists and Generalists. *The American Naturalist* 144, 692–707.
- Wilson, A.C.C., Ashton, P.D., Calevro, F., Charles, H., Colella, S., Febvay, G., Jander, G., Kushlan, P.F., Macdonald, S.J., Schwartz, J.F., et al. (2010). Genomic insight into the amino acid relations of the pea aphid, *Acyrtosiphon pisum*, with its symbiotic bacterium *Buchnera aphidicola*. *Insect Molecular Biology* 19, 249–258.
- Yakovleva, I.M., Baird, A.H., Yamamoto, H.H., Bhagooli, R., Nonaka, M., and Hidaka, M. (2009). Algal symbionts increase oxidative damage and death in coral larvae at high temperatures. *Marine Ecology Progress Series* 378, 105–112.
- Ye, S., Bhattacharjee, M., and Siemann, E. (2019). Thermal Tolerance in Green Hydra: Identifying the Roles of Algal Endosymbionts and Hosts in a Freshwater Holobiont Under Stress. *Microb Ecol* 77, 537–545.
- Yellowlees, D., Rees, T.A.V., and Leggat, W. (2008). Metabolic interactions between algal symbionts and invertebrate hosts. *Plant, Cell & Environment* 31, 679–694.
- Yoshida, T., Hairston, N.G., and Ellner, S.P. (2004). Evolutionary trade-off between defence against grazing and competitive ability in a simple unicellular alga, *Chlorella vulgaris*. *Proceedings of the Royal Society of London. Series B: Biological Sciences* 271, 1947–1953.
- Zagata, P., Greczek-Stachura, M., Tarcz, S., and Rautian, M. (2016). The Evolutionary Relationships between Endosymbiotic Green Algae of *Paramecium bursaria* Syngens Originating from Different Geographical Locations. *Folia Biologica* 64, 47–54.
- Zhang, M., Kong, F., Shi, X., Xing, P., and Tan, X. (2007). Differences in Responses to Darkness between *Microcystis aeruginosa* and *Chlorella pyrenoidosa*. *Journal of Freshwater Ecology* 22, 93–99.
- Ziesenisz, E., Reisser, W., and Wiessner, W. (1981). Evidence of de novo synthesis of maltose excreted by the endosymbiotic *Chlorella* from *Paramecium bursaria*. *Planta* 153, 481–485.
- Zook, D.P. (2002). Prioritizing Symbiosis to Sustain Biodiversity: Are Symbionts Keystone Species? In *Symbiosis: Mechanisms and Model Systems*, J. Seckbach, ed. (Dordrecht: Springer Netherlands), pp. 3–12.
- Zouache, K., Fontaine, A., Vega-Rua, A., Mousson, L., Thiberge, J.-M., Lourenco-De-Oliveira, R., Caro, V., Lambrechts, L., and Failloux, A.-B. (2014). Three-way interactions

between mosquito population, viral strain and temperature underlying chikungunya virus transmission potential. *Proc. Biol. Sci.* 281.